



UNIVERSITÀ DEGLI STUDI DI PALERMO

D016 - Scienze della Terra e del Mare
DiSTeM - Dipartimento di Scienze della Terra e del Mare
Settore Scientifico Disciplinare – GEO/01

Paleoecological insight into the straight-tusked elephant population from the late Middle Pleistocene site of Poggetti Vecchi

IL DOTTORE

Chiara Capalbo

IL COORDINATORE

Alessandro Aiuppa

IL TUTOR

Federico Masini

CO TUTOR

Paul Mazza

CICLO XXX 2014-2017
ANNO CONSEGUIMENTO TITOLO 2018

To my family

*...the best way out
is always through...*

Robert Frost

*PALEOECOLOGICAL INSIGHT INTO THE
STRAIGHT-TUSKED ELEPHANT POPULATION
FROM THE LATE MIDDLE PLEISTOCENE
SITE OF POGGETTI VECCHI*

Abstract	7
Riassunto	9
Acknowledgements	17
Chapter 1 The late Middle Pleistocene elephant site of Poggetti Vecchi	
1.1 Introduction	19
1.2 Goal and objectives	20
1.3 Geological background	
1.3.1 Geomorphological setting	21
1.3.2 Stratigraphic data	22
1.4 Chronological frame: Radiometric dating	26
1.5 Archeological relevance of the site	28
Chapter 2 Paleodiet proxies in paleoenvironment and paleoclimate reconstruction overview	
2.1 Introduction	
2.1.2 Dental function	33
2.1.3 Tooth wear	33
2.2 Gross methods	34
2.3 Microwear	36
2.4 Isotopic analyses	40
2.5 Methodological approaches for studying elephants diet	42
Chapter 3 Elephants	
3.1 Origin and evolutionary trends in Proboscideans	45
3.1.1 Origin and radiation of Elephantidae	47
3.1.2 Overview of the phylogeny of <i>Palaeoloxodon</i>	49
3.2 <i>Palaeoloxodon antiquus</i>	51
3.2.1 Main morphological features	51
3.3 Geographical distribution and paleoecology insight of straight-tusked elephants	52
3.4 Dental morphology	56
3.4.1 Dental tissues	57
3.5 Elephant's feeding habits	58
Chapter 4 Paleobiological and taphonomical analyses	
4.1 Materials	63
4.2 Methods	63
4.3 Results	
4.3.1 Paleobiology data	65
4.3.2 Taphonomic results	67
4.4 Discussion: Paleobiological and taphonomic inferences on the elephant remains	71
4.5 Paleoenvironment reconstruction	74
4.6 Chronological and paleoclimate implications	75
4.7 Conclusion	78

Chapter 5 Multiproxy-based reconstruction of the Feeding habits of the Poggetti Vecchi straight-tusked elephants

5.1 Paleodietary analysis of the Proboscideans: the state of the art	79
5.2 Dental Microwear Analysis using the Low Magnification approach (LDM)	
5.2.1 Introduction	81
5.2.2 Materials	84
5.2.3 Methods	
5.2.3.1 Casts	85
5.2.3.2 Microwear assessment	86
5.2.4 Results	87
5.2.5 Discussion	94
5.3 Isotopic analyses	
5.3.1 Materials and methods	95
5.3.2 Results	98
5.3.3 Discussion	100
5.4 Mesowear	
5.4.1 Introduction	103
5.4.2 Materials and methods	104
5.4.3 Results	105
5.4.4 Discussion	107
5.5 Texture analysis	
5.5.1 Introduction	108
5.5.2 Materials and methods	112
5.5.3 Results	117
5.5.4 Discussion	130
5.6 Conclusion	130
Chapter 6 Conclusion and remarks	132
References	134
Papers	

Abstract

Poggetti Vecchi is an open air archeo-paleontological site located on the eastern side of Grosseto's plain, in Southern Tuscany (Italy). Excavation for the construction of thermal pools exposed an up to 3-meter-thick succession composed of seven lithostratigraphic units of terrigenous and carbonate sediments. Vertebrate bones mixed up with stone tools and wooden implements were discovered mainly in the lower portion of the succession (Unit 2). Thermal carbonates overlying these remains are radiometrically dated to 171 ± 3 ka. Based on this dating the human artifacts can be assigned to early Neanderthals, which sparks the interest in the site, especially from a geoarcheological perspective. In fact, it provides invaluable information not only on the local environmental conditions at time, but also on the interactions that humans had with the surrounding environment and natural resources. Poggetti Vecchi's macrofaunal assemblage is dominated by large-sized herbivorous, i.e. the straight-tusked elephant and aurochs. Paleobiological inferences indicate the presence of at least seven elephants of different ontogenetic ages and sexes, which were likely the members of a family clan. Our geoarcheological study suggests that the assemblage accumulated in a narrow lacustrine-palustrine embayment, affected by thermal springs and surrounded by extensive open grassland environments. Rapid climatic fluctuations that occurred at the MIS7-6 transition and throughout the MIS6 glacial period caused changes in the lake level and the entire area was repeatedly flooded and exposed to subaerial erosion. During a period of global climate deterioration, the hot thermal springs probably created an attractive recess for the resident faunas and, perhaps, a cold snap during a time of intense seasonal oscillations led to the sudden death of elephants. The carcasses represented an unexpected food resource for the early Neanderthals that lived in this area.

Environmental changes were studied in detail to contribute to the solution of paleoecology issues, with special focus on the paleodietary preferences of local population of elephants. This has been obtained by cross-comparing the results obtained by coupling different methods: low-magnification analysis of microwear (LDM), 2D-roughness parameters and surface geometry assessment (fractal dimensions and isotropy calculations), mesowear and stable isotope analysis. Proboscideans are super keystone species in their ecosystems. They therefore tend to be opportunists, able to feed with equal facility on a wide range of items available locally, whenever they cannot have access to their ideal diet. This improves elephants' ability to respond to climate impacts and environmental fluctuations. Our analyses confirm that *Palaeoloxodon antiquus* was a generalized mixed-feeder, which is here believed to have been especially capable of shifting from its dietary preference according to local vegetation composition and seasonal

changes. In particular, microwear patterns, isotopes and texture results suggest the consumption of a great amount of graminaceae or other plants quite rich in phytoliths. The dietary signal of the last meals confirms the preliminary landscape reconstruction based on multiproxy approach. Conversely, mesowear data that indicate more browse-dominated mixed dietary behavior probably reflect seasonal variations, as well as the environmental scenario of other areas (e.g., the neighboring ones) characterized by more closed canopy woodland. On the whole this study proposes to infer the feeding habits of the group of late Middle Pleistocene individuals of *Palaeoloxodon antiquus* discovered in Poggetti Vecchi and, by doing so, to contribute to the interpretation of the site's landscape at the time. Poggetti Vecchi offers us the fortunate chance to explore new instances of human-animal interaction at the Middle-Late Pleistocene transition, which is still very imperfectly known in Prehistoric Europe.

Riassunto

Il progetto di ricerca s'incentra sullo studio della macrofauna rinvenuta nel sito paleontologico e archeologico di Poggetti Vecchi, scoperto nella località di Roselle situata in provincia di Grosseto. Nello specifico esso è stato focalizzato sulla ricostruzione paleoambientale e paleoecologica dell'area. L'analisi paleobiologica e tafonomica dei resti faunistici è stata perciò inserita all'interno di un progetto multidisciplinare e l'integrazione di tutti i dati paleontologici (relativi a vertebrati, invertebrati, macroresti vegetali e pollini) con quelli stratigrafici ha permesso di ricostruire dettagliatamente l'evoluzione paleoambientale. Nella seconda parte, lo studio paleoecologico è stato completato dalle indagini sugli adattamenti paleodietetici acquisiti dalla popolazione di elefanti della specie *Palaeoloxodon antiquus* che caratterizza questo sito.

Lo scavo, avvenuto nel corso del 2012, ha messo in luce il ritrovamento di un importante sito preistorico, con abbondanti resti di mammiferi associati a manufatti litici e lignei (*digging sticks*). Il sito è situato nella zona orientale della pianura prossimale grossetana. Questa vasta pianura costiera è circondata da rilievi bassi Triassico-neogenici costituiti da depositi clastici e carbonatici. Si tratta di un bacino lacustre-palustre di lungo corso, in cui lo spesso riempimento Quaternario è formato da sedimenti sabbiosi e fangosi. Il substrato carbonatico sottostante è soggetto a fenomeni di carsismo e alla formazione di numerosi sinkhole. L'area è inoltre caratterizzata da numerose risorgive termali, la fratturazione e la foliazione del bedrock favoriscono l'emergenza locale delle acque termali sotterranee.

Lo studio geologico della successione ha evidenziato la presenza di sette unità litostratigrafiche (U1-U7). I resti di vertebrati e gli strumenti sono stati rinvenuti principalmente nell'unità 2, si tratta di una sezione formata in un momento di sedimentazione scarsa o nulla. La sovrastante unità 4 è caratterizzata dalle pisoliti, prodotte per accrezione durante processi di precipitazione biochimica in acque termali calme. Esse sono state sottoposte a datazione radiometrica con il metodo della serie dell'uranio, datando perciò l'unità a 171 ± 3 ka. Una seconda datazione pari a 170 ± 13 ka è stata condotta su un molare inferiore sinistro di *Bos primigenius*, proveniente dalla medesima unità, usando il metodo ESR. Alla luce di questi dati radiometrici, le evidenze umane del sito possono essere attribuite all'uomo di Neanderthal mentre, l'origine e l'evoluzione dell'intera successione sono avvenute nell'intervallo compreso tra l'ultimo interglaciale MIS7 e tutto il glaciale MIS6; un periodo caratterizzato da frequenti fluttuazioni climatiche.

La macrofauna era dominata da erbivori di grande taglia: principalmente *P. antiquus* (almeno 7 individui) e *B. primigenius*. L'insieme dei dati tafonomici e paleobiologici raccolti ha permesso di formulare

alcune ipotesi sull'origine dell'accumulo fossilifero. Il ritrovamento di resti faunistici e manufatti associati pone l'interrogativo sullo sfruttamento umano delle faune, in questo caso degli elefanti, per caccia attiva o come azione di sciaccaggio di animali già morti. Tuttavia, gli altri siti del Pleistocene medio che testimoniano la caccia attiva sono generalmente costituiti da un solo individuo di elefante (e.g., Ficoncella, Notarchirico, Southfleet Road, Ambrona). Al contrario, il ritrovamento di più individui costituisce normalmente accumuli time-averaged generati da trasporto fluviale (e.g., La Polledrara di Cecanibbio). Alla luce di queste considerazioni, appare evidente che gli elefanti di Poggetti Vecchi costituiscano un caso senza precedenti. Diverse caratteristiche concorrono a escludere un'azione di caccia attiva, ad esempio la struttura ontogenetica che suggerisce la presenza di un clan familiare (giovani, subadulti, giovani-adulti e adulti), i contatti osso-osso (il sedimento interposto tra le ossa è scarso o nullo) e l'assenza di segni di taglio e fratture a osso fresco riconducibili ad attività di caccia. Queste evidenze suggeriscono che tutti gli individui siano morti pressoché nello stesso momento a causa di un evento naturale. L'ipotesi di un'azione di caccia attiva e dell'uccisione di un intero clan familiare appare, inoltre, poco plausibile considerando le dimensioni raggiunte da questi animali (oltre 4 m di altezza) e la tecnologia disponibile. Tra le possibili cause naturali sono stati esclusi gli eventi alluvionali, poiché solo una grande alluvione avrebbe potuto trasportare e ridepositare animali di queste dimensioni e le tracce di abrasione e lucidatura dovute al ruscellamento, seppure presenti su alcuni esemplari, non sono tali da giustificare un simile scenario. Inoltre, è stata scartata anche l'ipotesi di una colata fangosa, poiché sono assenti i sedimenti fini che normalmente sono associati a depositi formati in seguito a questo tipo eventi. L'eventualità di degassamento naturale tossico è stata esclusa per almeno due motivi: l'attività termale stabile nell'area è successiva alla deposizione dell'unità 2 e, inoltre, è difficile ipotizzare la morte simultanea nello stesso luogo di individui diversi per età, dimensione corporea e sesso. Alla luce di tutte queste considerazioni è stato ipotizzato che un'ondata di freddo intenso, oltre i limiti di tolleranza termica, abbia determinato la morte degli elefanti. Questa specie era, infatti, tipica delle aree boschive durante le fasi temperate, mentre era rara negli interstadiali più lievi che intervallavano le fasi fredde o nelle condizioni fredde di una fase stadiale; infatti, la sua occorrenza può essere considerata un buon indicatore di condizioni interglaciali. Probabilmente, le condizioni climatiche avverse hanno confinato gli elefanti nelle immediate vicinanze dell'unica fonte di calore, ossia le pozze termali che caratterizzano l'area; poi, una volta esaurito il cibo disponibile, essi sono morti di fame.

Gli strumenti litici associati alle ossa sono ritoccati e le tracce d'uso evidenziano l'azione su tessuti molli; quindi sembra plausibile che le popolazioni locali di neandertaliani abbiano avuto accesso a una grande

quantità di carne messa loro a disposizione dalle circostanze fortunate. Nel complesso: il basso impatto dei carnivori (pochi segni di masticazione, rosicatura e corrosione gastrica), l'assenza di modificazioni di derivazione umana e la bassa incidenza dell'alterazione meteorica suggeriscono che le carcasse fossero in gran parte inaccessibili ai predatori perché presumibilmente parzialmente sommerse dall'acqua. I resti scheletrici non sono in connessione anatomica, ovunque sono evidenti graffi e scalfitture riconducibili al calpestio e fratturazione avvenuta allo stato secco. Calpestio e calci sembrano essere stati prodotti da altri grandi mammiferi, presumibilmente altri elefanti, che hanno determinato la dispersione dei resti. La frequentazione dei luoghi in cui sono morti altri individui della stessa popolazione e il conseguente calpestio e rimescolamento dei resti ossei è stato evidenziato e studiato anche nelle popolazioni attuali di elefanti. Tale comportamento sembra essere connesso al forte psichismo di questi animali. Infine, la selezione di ampie porzioni di carcassa degli elefanti indica che è avvenuta la rimozione di alcuni elementi ossei (vertebre, coste, basipodiali e falangi) che potrebbero essere stati rimossi facilmente dall'acqua quando le carcasse erano già scheletrizzate. Tuttavia, non può essere completamente esclusa la rimozione da parte degli scavengers (carnivori e uomini). Infine, il letto fossilifero è stato colonizzato dalle radici delle piante acquatiche o sepolto da sedimenti pedogenizzati.

L'evoluzione paleoambientale durante la deposizione delle diverse unità stratigrafiche è stata dettagliatamente ricostruita integrando i dati paleontologici (relativi a vertebrati, invertebrati, macroresti vegetali e pollini) con quelli stratigrafici. In sintesi, sono stati identificati quattro diversi eventi alluvionali separati da fasi regressive ed erosive. Durante le fasi alluvionali, i fanghi organici con caratteristiche fisico-chimiche omogenei sono stati depositi sul fondo di un lago poco profondo durante le fasi alluvionali. Al contrario, i resti di vertebrati e gli artefatti umani sono stati accumulati sulle superfici erosive formatesi durante le regressioni. La prima fase alluvionale ha prodotto una baia lacustre-palustre caratterizzata da sedimentazione terrigena (U1). In questa fase il fondo del lago era popolato da molluschi e ostracodi indicatori di acque dolci o leggermente saline (< 4 psu). Il primo episodio di disseccamento ha prodotto la superficie erosiva tra U1/U2; esso è stato sufficientemente lungo e tale da consentire l'accumulo di resti di vertebrati e manufatti. Un nuovo innalzamento tavola d'acqua e la deposizione di fanghi carbonatici che testimoniano l'inizio della risorgenza termale (unità 3). La formazione del deposito pisolitico (unità 4) suggerisce la formazione, durante il tardo MIS6 di pozze termali analoghe a quelle adesso presenti nell'area. Esse erano frequentate dagli elefanti e dagli altri mammiferi. Una nuova caduta del livello lacustre ha determinato la re-incisione dell'impluvio e il riempimento con ghiaia poligenica e clasti calcarei (U5). In seguito, una nuova fase alluvionale ha favorito nuovamente la formazione di una baia lacustre-palustre

caratterizzata da sedimenti terrigeni (U6). Poi, un nuovo evento di abbassamento della tavola d'acqua ha prodotto una nuova fase d'incisione del fondovalle e conseguente formazione di una nuova baia lacustre. Infine, la composizione carbonatica dei fanghi dell'unità 7, testimonia lo sviluppo di attività termale stabile nell'area. Durante le fasi regressive ed erosive il paesaggio era dominato da vaste praterie, boschi radi, corpi d'acqua poco profondi e aree umide formate dalla risalita di acqua sotterranea.

La datazione radiometrica e la stratigrafia dei depositi transgressivi e regressivi hanno permesso di eseguire un tentativo di sincronizzare la successione sedimentaria e i principali eventi climatici quaternari. I depositi transgressivi dell'unità 1 potrebbero essere stati depositi durante il sub-stage temperato MIS7a o durante l'interstadiale successivo alla transizione con il MIS6 (tra 200-191 ka). La formazione della superficie erosiva (unità 2) risalirebbe perciò all'inizio del MIS6. Le unità 3 e 4 testimoniano la transgressione lacustre e l'attivazione del sistema termale durante il primo interstadiale del MIS6 (circa 170 ka). La nuova fase regressiva (unità 5) sarebbe così avvenuta durante lo stadiale successivo; mentre la nuova transgressione lacustre (unità 6) corrisponderebbe al secondo interstadiale. Infine, i depositi dell'unità 7 potrebbero risalire al miglioramento climatico il culminato con il picco dell'interglaciale MIS5e.

L'analisi paleontologica ha evidenziato che nel complesso la fauna a micromammiferi è dominata da *Arvicola amphibius*, un tipico abitante degli ambienti umidi. Tuttavia, mentre nell'unità 6 sono presenti tipici taxa indicatori di habitat temperati (*Crocidura cf. suaveolens*, *Oryctolagus* sp. e *Microtus* (Terricola) *savii*), nell'unità 2 abbonda *Microtus cf. arvalis* che costituisce un chiaro indicatore di come muovendosi verso l'alto nel corso della successione, le temperature siano diminuite. Infatti, le popolazioni italiane moderne di *M. cf. arvalis* sono limitate alle regioni settentrionali della penisola e sono assenti dall'Appennino centrale. Pertanto, la presenza nell'area meridionale della Toscana a quote molto basse è indice di condizioni più fredde rispetto a quelle oggi esistenti. Inoltre, in quest'unità diminuisce l'abbondanza relativa di *M. (Terricola) ex gr. savii* e sono assenti *Crocidura* e *Oryctolagus*. La macrofauna e l'erpetofauna rinvenute nell'unità 2, sono costituite da taxa termofili che ben si adattano alle oscillazioni climatiche avvenute tra l'inizio del MIS7a (regressione lago ed erosione sommità di U1) e l'interstadiale successivo (regressione del lago e deposizione U3-4). Anche il record della fauna a molluschi è compatibile con la tendenza al raffreddamento culminata con il massimo glaciale del MIS6, così come le specie di ostracodi che indicano chiaramente temperature inferiori di 6°C rispetto a quelle attuali. Oscillazioni stagionali, talvolta molto intense, possono ragionevolmente aver interessato l'area nel corso dell'intera successione; ciò suggerisce che un'ondata di freddo intenso, nel corso del periodo in cui si è depositata l'unità 2, potrebbe aver portato allo stremo la famiglia di elefanti poi morti di stenti. In conclusione,

il periodo umido registrato intorno a 171 ka, cui si riferisce la datazione radiometrica assoluta calcolata sulla base dei sedimenti e dei resti fossili dell'unità 4, potrebbe ragionevolmente corrispondere al primo interstadiale glaciale del MIS6.

Gli studi di paleodieta nei proboscidi presentano intrinseche difficoltà logistiche che possono essere facilmente intuibili considerando la complessa anatomia dei molari (con struttura modulare), la morfologia funzionale (ossia la meccanica di masticazione che modella costantemente la superficie occlusale) e, infine, il peculiare meccanismo di sostituzione per scorrimento orizzontale. Altre difficoltà riguardano l'interpretazione degli adattamenti dietetici, soprattutto quando si utilizza un solo metodo analitico; perciò l'analisi paleodietetica della popolazione di elefanti di Poggetti Vecchi e le derivanti speculazioni sulla ricostruzione paleoambientale sono state eseguite con un approccio multiproxy. Esso è stato basato sulla valutazione incrociata dei dati prodotti da: 1) analisi delle micro-tracce (microwear) presenti sulla superficie dello smalto dentario mediante basso ingrandimento (LDM); 2) determinazione del contenuto isotopico ($\delta^{13}\text{C}$ e $\delta^{18}\text{O}$) nella bioapatite (smalto) e relativo calcolo del contenuto isotopico della paleodieta ($\delta^{13}\text{C}_{\text{diet}}$) e dell'acqua ambientale ($\delta^{18}\text{O}_{\text{w}}$); 3) mesowear e 4) valutazione della tessitura superficiale attraverso i criteri della rugosità 2D, la valutazione statistica della complessità superficiale (mediante il calcolo della dimensione frattale che descrive i pattern geometrici complessi sfruttando la geometria non-euclidea) e l'identificazione della direzionalità delle micro-tracce superficiali.

Il campione analizzato è costituito da 15 denti molari e include denti inferiori, superiori, appartenenti ad individui di entrambi i sessi e diverse classi di età. Poiché lo smalto è un materiale riflettente, l'osservazione delle tracce di microwear e della tessitura superficiale è eseguita su superfici replicate, generalmente prodotte in resina epossidica. Per quanto riguarda la tecnica di microwear mediante basso ingrandimento (LDM), i calchi della regione centrale di ogni lamella funzionale sono analizzati mediante stereomicroscopio con ingrandimento a 40 e 100x e illuminazione unidirezionale esterna. Le osservazioni qualitative e quantitative sono state compiute su microfotografie, mediante l'ausilio del software di grafica vettoriale ImageJ. Il pattern di microwear ottenuto è omogeneo ed evidenzia l'assenza di sostanziali differenze fra i molari superiori e inferiori, nelle diverse classi d'età così come nei due sessi. Al contrario, una maggiore eterogeneità caratterizza le estremità (laterale e buccale) di ogni lamella. I dati emersi da quest'analisi confermano che le lamelle centrali (e in particolare la regione mediana dei loop funzionali) registrano in modo più efficiente il segnale dietetico. Le lamelle più intensamente danneggiate mostrano il maggior impatto dell'usura, confermando l'esistenza di una forte correlazione tra l'usura attrizionale e le frequenze/densità delle microusure. Il pattern di microwear, soprattutto nelle lamelle centrali, è

dominato dalla presenza di graffi (sia grossolani sia fini) associati ad aree di micro-abrasione; mentre i buchi sono molto scarsi. I graffi più grossi e quelli incrociati sono più frequenti nella porzione mesiale (più usurata) e distale (meno usurata). I dati ottenuti suggeriscono l'adattamento a una dieta mista dominata dal pascolo. L'analisi isotopica è stata condotta su un singolo campione di smalto. Un frammento della lamella centrale di un dente molare è stato prelevato dalla porzione basale. Il campione di smalto è stato separato meccanicamente dalla dentina e dal cemento. Dopo essere stato finemente macinato, è stato prima sottoposto a diffrazione ai raggi x per verificarne l'integrità strutturale; infine, la composizione isotopica (carbonio e ossigeno) del carbonato strutturale della bioapatite è stata analizzata allo spettrometro di massa. I valori del $\delta^{13}\text{C}$ e $\delta^{18}\text{O}$ ottenuti suggeriscono che nel momento di formazione dei livelli fossiliferi, la valle di Poggetti Vecchi era dominata da praterie boscoso e condizioni climatiche freddo-umide. Gli attuali elefanti della savana africana hanno acquisito adattamenti alimentari da pascolatori e, soprattutto, nei periodi più umidi aumentano la quantità di erba ingerita; mentre in condizioni di maggiore aridità (quando l'erba declina) cambiano opportunisticamente abitudini alimentari prediligendo il consumo di foglie e arbusti (acquisendo perciò adattamenti alimentari tipici dei brucatori). I dati isotopici e il pattern di microwear confermano che un simile comportamento caratterizzava anche le specie estinte. Due campioni rappresentativi della popolazione, un cucciolo e un individuo adulto, sono stati selezionati per eseguire la caratterizzazione della tessitura superficiale. I calchi delle lamelle centrali sono stati quindi scansionati con un microscopio digitale a 500x in grado di generare immagini 3D componendo una serie di piani presi a vari livelli. Varie aree d'interesse sono state selezionate dalla porzione centrale delle lamelle di smalto mediane. Le foto sono state poi processate con i software MountainsMap® e ImageJ. I vari strumenti presenti nel primo software hanno permesso di ottenere immagini 2D e di estrarre 10 profili di rugosità 2D per ogni area selezionata; così come di calcolare alcuni parametri di rugosità industriale 2D (secondo lo standard ISO 4287) utili nel discriminare il comportamento alimentare. Il calcolo della dimensione frattale (Df), ha fornito una stima della complessità superficiale, mentre l'orientamento delle caratteristiche tessiturali (espresso come percentuale d'isotropia e direzioni dominanti, in gradi) è espresso graficamente da un diagramma polare. Infine, sono state ricostruite le immagini 3D delle superfici di smalto montando i singoli profili bidimensionali. I risultati emersi da questa procedura sembrano confermare il pattern di microwear emerso dall'analisi a basso ingrandimento; suggerendo, inoltre l'assenza di distribuzione marcatamente anisotropa delle micro-scalfitture e tessitura superficiale generalmente complessa. Tutti gli indizi raccolti dall'analisi multiproxy avvalorano l'ipotesi che questa specie di elefanti avesse un comportamento alimentare non specializzato di tipo intermedio, basato sul

pascolo di un notevole quantitativo di piante ricche di fitoliti, quali le graminacee. Infine, le misure di mesowear, sebbene concordino nell'individuare l'adattamento a una dieta mista, suggeriscono un comportamento più spiccatamente da brucatore. La discordanza nei risultati, emersi da microwear e mesowear, potrebbe essere spiegata considerando le differenze nella risoluzione temporale dei due metodi. Infatti, l'analisi di microwear rivela il comportamento alimentare negli ultimi giorni della vita dell'animale, mentre il mesowear registra i segnali alimentari corrispondenti a un periodo più lungo, dagli ultimi mesi di vita fino a qualche anno prima della morte. Inoltre, poiché *P. antiquus* cambiava opportunisticamente comportamento alimentare secondo le diverse condizioni ambientali locali, è plausibile pensare che le misure di mesowear catturino anche le possibili variazioni dietetiche stagionali. Tuttavia, così come per altre specie di proboscidi, anche l'elefante dalle zanne dritte era prevalentemente un pascolatore negli ambienti aperti e dominati dall'erba. Le misure di mesowear ottenute potrebbero così indicare anche lo spostamento degli elefanti da altre aree (e.g., quelle limitrofe), in cui il paesaggio era invece dominato da boschi, verso la vallata. Alla luce di queste considerazioni, la ricostruzione paleoambientale emersa dall'analisi mediante l'approccio geoarcheologico sembra essere confermata anche dal pattern di microwear. Le evidenze paleobiologiche e tafonomiche che suggeriscono il confinamento degli elefanti in un'area ben limitata, l'impossibilità di lasciare la valle con conseguente consumo di tutto il cibo presente nelle immediate vicinanze delle pozze termali e, infine, la morte per stenti, sembrano trovare riscontro nel segnale dietetico degli ultimi pasti che tipicamente descrive il pascolo di erbe e graminacee che dominavano la vallata di Poggetti Vecchi.

Acknowledgements

Firstly, I want to express my gratitude to the Earth and Sea Science department of the University of Palermo to give me the opportunity to carry on my doctoral project in a permanent off-site condition. Special thanks go to Alessandro Aiuppa, who was an exceptional coordinator always available with clarifications; and, to my supervisor Federico Masini.

Secondly, I want to provide my heartfelt thanks to the department of Earth Science of the University of Florence that has welcomed and endorsed my constant visiting presence over these three years. About that I am indebted to several people that contributes practically and mentally to the realization of this thesis. I owe my deepest gratitude to my co-supervisor Paul Mazza. Thanks for all you taught me and for having offered constant support, encouragement and advice; as well as for believing in me throughout this whole process and having left me free to seek my ideas. I appreciate more than I could say in words. Special thanks go to Francesco Landucci for supporting me during lab work, to Adele Bertini and Gigliola Valleri for having shared some equipment with me. I am grateful to Orlando Vaselli for logistics support and for providing me the geochemistry lab, thanks to Simone Tommasini, Andrea Orlando and Elena Pecchioni.

I cannot forget Maria Rita Palombo, from the University of Rome (Sapienza), who introduced me to paleodietary analysis. I really appreciate Simona Raneri (University of Pisa), Jacopo Crezzini and Francesco Boschini (University of Siena) for having agreed to collaborate by providing instruments and sharing expertise in a research field until recently for them, as well as for me, completely unknown. I wish to thank the whole team involved in the multidisciplinary project and all the coauthors.

Thanks to the few but precious, friends and acquaintances associated with the Department of Earth Science in Florence, who have helped and contributed with important suggestions: Andrea Savorelli and Ezher Tagliasacchi. Chatting and spending time together have enriched me beyond the professional sphere.

Last but not the least, I would like to thank my parents Antonella and Giorgio, because whatever happens, without you I would have done nothing of this. Thanks to my lovely sisters Annarita and Margherita and my nephew Niccolò. Gianfranco, I am indebted to your endurance in everyday life and for always trusting me.

Chapter 1 The late Middle Pleistocene elephant site of Poggetti Vecchi

1.1 Introduction

Poggetti Vecchi is an open-air archeo-paleontological site located in southern Tuscany (central Italy), some 5,5 km WNW of Roselle and 7 km NW of Grosseto ($42^{\circ}49'8.92''$ N, $11^{\circ} 4'19.41''$ E, **Figure 1**). This area is celebrated for its Etruscan and Roman archeological treasures, but no paleontological site had ever been reported before.

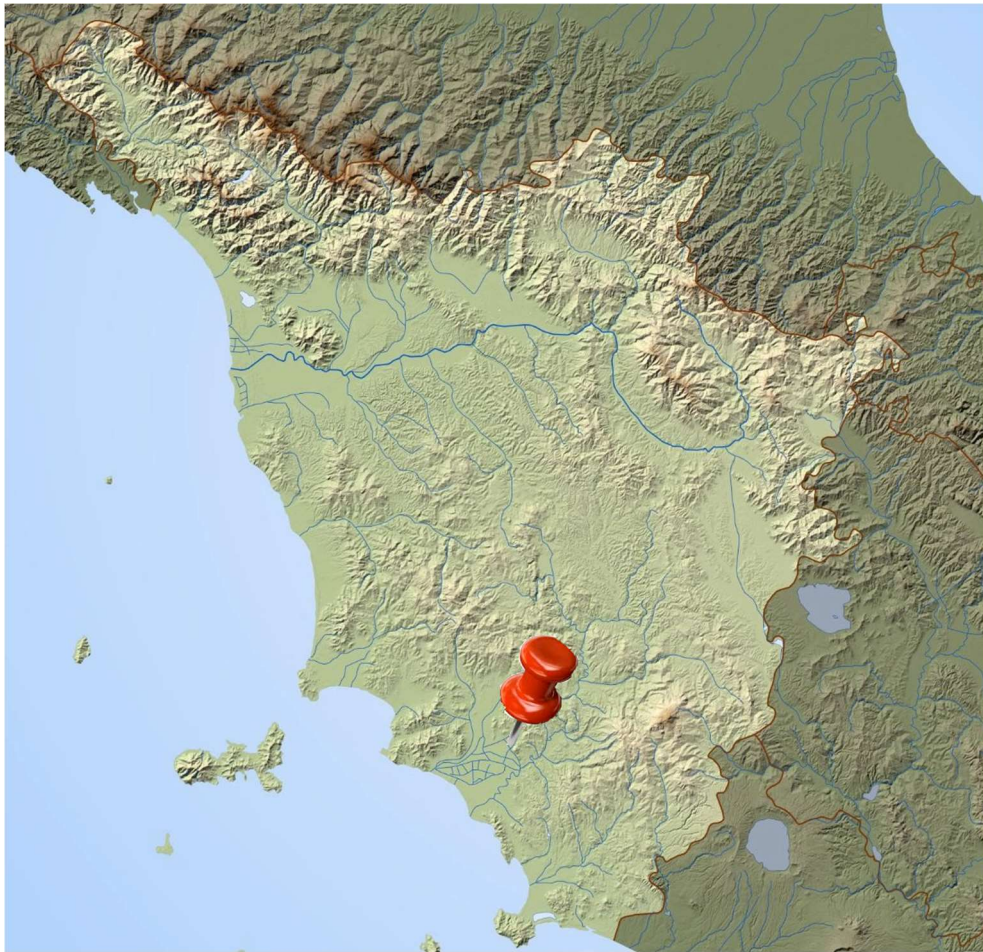


Figure 1 Geographical map of Tuscany highlighting the position of Roselle.

Recently, in the spring of 2012, works for thermal pools unearthed fossil bones associated with lithic artifacts and wooden tools. At the beginning the excavation was carried out mechanically and involved an area of about 160 m^2 , then divided into a northern and southern portion by a narrow artificial canal that allow to drain thermal water. Moreover, the abundant discharge of thermal water that affected the bottom of the excavation required the use of pumps to keep the area drained and facilitate the recovery of specimens. Then, under the supervision of the

Superintendence for the Archaeological Heritage of the Tuscany Region, the area studied has been reduced to 60 m² and the excavation proceeded stratigraphically. The excavation grid was subdivided into squares of 1 x 1 m². The quarry (i.e., stratigraphic unit, square, plane, cut, depth and original plan), assemblage (identification number and typology of findings) and modification data of the site were recorded to produce GIS map outputs for each archeological level.

Most of the bones belong to different individuals of the same species, the straight-tusked elephant *Palaeoloxodon antiquus*. The faunal list also includes *Bos primigenius*, *Cervus elaphus*, *Capreolus capreolus*, an advanced form of *Ursus deningeri*, transitional to *U. spelaeus*, rodents, avifauna, erpetofauna (Chelonia, Ofidia and Anura) and a rich malacofauna and ostracofauna.

The site yielded also numerous plant macroremains, alongside stone and wooden implements. Radiometric dating (171 ± 3 ka) indicates that the fossil accumulation originated during the final stages of Middle Pleistocene. Hence, the artifacts can be likely assigned to early Neanderthals.

1.2 Goals, methods and Objectives

The overall richness of findings sparks the interest in the site, which offers the opportunity for a most valuable geoarcheological study. Geoarcheology is a discipline that bridges the existing conceptual and methodological gap between archeology and human sciences, on one hand, and natural and geological sciences, on the other (Butzer, 1982). It is also the most effective way to disclose information from the stratified archeo-sedimentary archives (Rapp and Hill, 1988; Ghilardi and Desruelles, 2008). More generally, geoarcheology affords to study local relationships between past human populations and ecosystems, whose dynamics were influenced by geological, climatic and biological factors, and identify man-made strategies for addressing climatic and environmental changes that occurred in the past. At Poggetti Vecchi, this multidisciplinary approach provides new insight into the human and animal life in this period of time and in this part of Italy where paleontological and prehistoric discoveries had never been reported before. In particular, geoarcheology permits us to understand how and how much local environmental conditions affected local living communities, and to improve our knowledge of the interactions between early Neanderthal populations, local faunas, and their natural surroundings. The environmental changes inferred from paleobiological and taphonomic information collected at the site contribute to the solving of significant paleoecological issues, as well as to provide new insights into how local populations of elephants reacted to them.

Dental microwear has the ability to tell us much about diet and dental function of mammalian teeth. It therefore is one of the most effective

tools with which to record ecological interactions; hence much attention has been placed on comparing results obtained coupling low magnification with dental microwear texture methods, which can be used as a proxy for paleoenvironment reconstruction. To avoid biases and distortions caused by counting and describing both single scars and overall textural features, produced by food acquisition and processing, ecological signals that result from different sources need to be teased apart. By cross-comparing results obtained using microwear, mesowear and stable isotope approaches food habits and processing traits can be distinguished from the effects of other factors.

Integrated multiproxy study and interdisciplinary research can tackle complex paleoethological and paleoecological issues yielding some of the most detailed and reliable understandings of animals' biological requirements. These results clarify the population dynamics of Pleistocene faunal communities and are useful for reconstructing the evolution of the paleoenvironments and understanding how it correlates with the European Quaternary climatic cyclicality.

1.3 Geological background

1.3.1 Geomorphological setting

The whole area (**Figure 2**) constitutes a wide coastal plain and a long-lasting lacustrine-palustrine system, known as *Lacus Prilis* in Etruscan and Roman times and still existing in the 19th century (Stea and Tenerini, 1996). Quaternary filling of this coastal basin is made up of sandy and muddy surface sediments that continue few hundred meters underground (Bravetti and Pranzini, 1987; Censini and Costantini, 2002). The Poggetti Vecchi site stands in a geographically confined, depressed plain at the feet of an about 11 m-high hill. The bedrock outlier, buried by alluvial Quaternary sediments, is made of Mesozoic limestones, which crop out extensively in the slopes bounding Roselle to the east (**Figure 2B**). The topmost portion of the bedrock appears fractured and is affected by diffuse karstification responsible for catastrophic subsoil collapses known as sinkholes. A sinkhole formed in January 1999 at Bottegone, a locality situated about 2 km north of the site (Censini and Costantini, 2002). These carbonates also include a secondary porosity, generated by thermal circulation related to the intense local geothermal gradient. Similarly, to the rest of southern Tuscany, small Neogene-Quaternary magmatic intrusions originated a high overall geothermal gradient in the Roselle area (Baldi et al., 1995) and faults and fractures through the bedrock facilitated the rise of underground thermal water and consequently the formation of local thermal pools such as those still present in Poggetti Vecchi (Censini and Costantini, 2002).

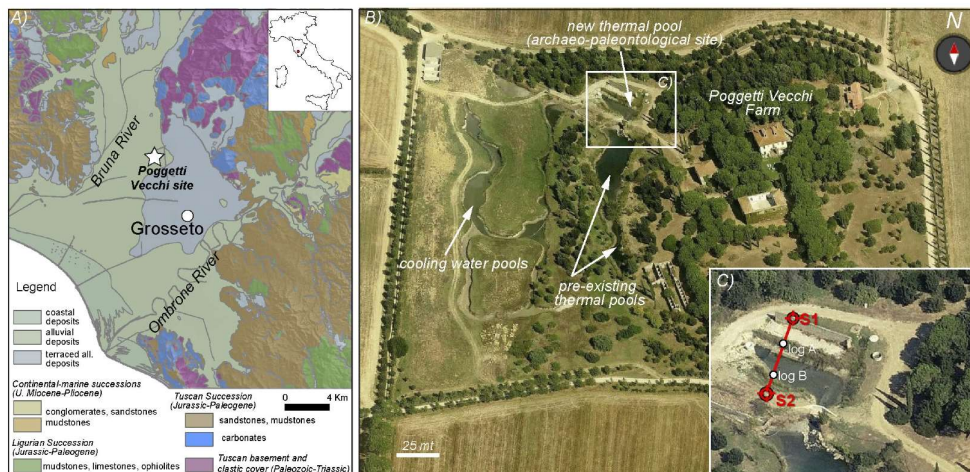


Figure 2 A) Location of the Poggetti Vecchi site and schematic geological map of the Grosseto plain and surrounding elevations. B) Aerial view from Bing Map (<https://www.bing.com/maps/?cc=it>). C) Detailed oblique view of the excavation area, with annotated location of cores S1 and S2 and logs A and B reported in **Figure 3**.

1.3.2 Stratigraphic data

The excavation exposed an about 3 m thick sedimentary succession, deposited in a very narrow bay through alternating phases of accumulation and erosion. The succession was disturbed at the beginning of the thermal activity, which complicated the identification of the layers and interpretation of the deposition processes. All in all, seven lithostratigraphic units have been recognized (**Figure 3** and **4**), of either terrigenous or carbonate nature; they have been called, from the bottom upwards, Unit 1 to Unit 7 (U1-U7).

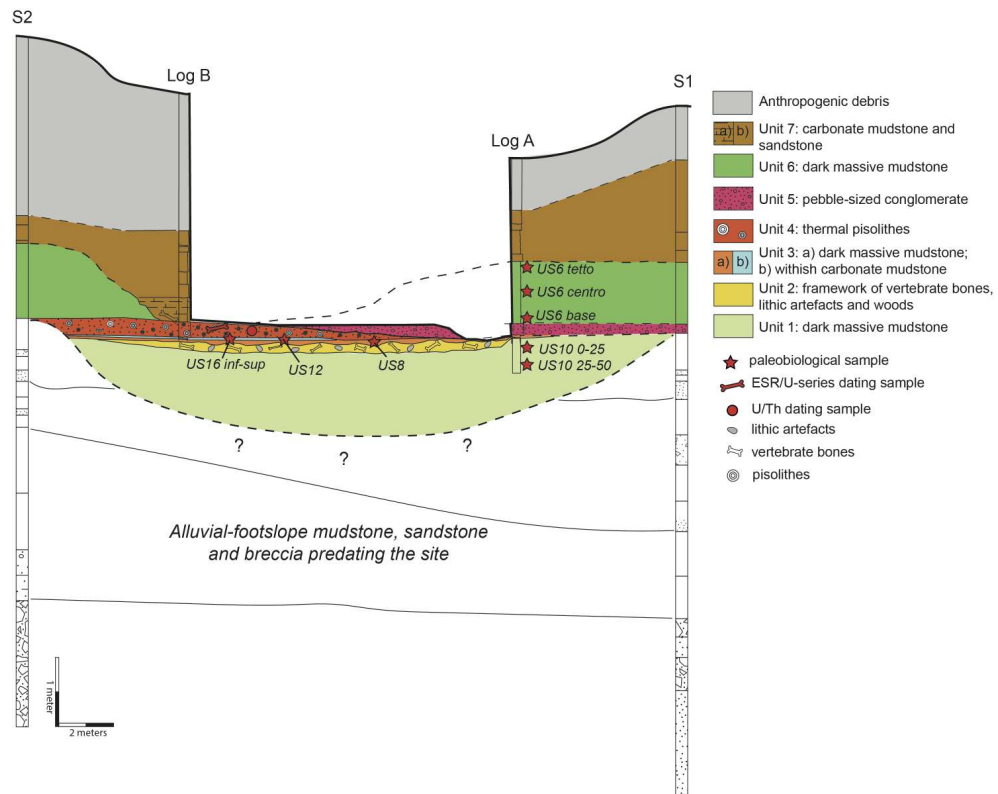


Figure 3 Correlation of stratigraphic data along the cross section showed in **Figure 2C**.

Unit 1 is the lowermost layer of the succession; it consists of 50 cm of dark gray mudstone. It contains abundant remains of mollusks, ostracods, micro-vertebrates (mammals, amphibians and fish), plant residues (both unaltered, such as seeds, carophytes, and pollen, and carbonized grains) homogeneously dispersed in the sediment matrix. The upper erosive surface is buried by the overlying Unit 2, which includes 20 to 40 cm of dark gray mudstone. Most of the vertebrate remains, largely represented by bones of *Palaeoloxodon antiquus*, come from this unit; they are associated with stone and wooden implements (**Figure 4A**). Unit 2 can be considered as a condensed section, whose sediments have been deposited at a very low to extremely low rate of sedimentation. Some of the largest vertebrate remains had accumulated at the top of the unit.

Unit 3 is lithologically mixed and is at most 20-cm thick. The lower portion (3A **Figure 3**) starts with an irregular, wavy erosive base. It consists of gray mudstone containing numerous gastropod shells. The upper portion (3B) is a thin layer of whitish, muddy carbonate that heralds the beginning of thermal activity in the area.

The overlying Unit 4 has a discontinuous erosive base. It is formed by a framework of mm-cm sized, clast-supported, coated carbonate particles, known as pisoliths with dispersed microfossils, mainly gastropod shells. Pisoliths are usually produced by bio-chemical precipitation in quiet hot springs and grow by accretion; they still form today in the Poggetti

Vecchi artificial thermal pools. This layer yielded isolated bones of *P. antiquus*, associated with stone tools. The unit is a lenticular sedimentary deposit with a maximum thickness of 30 cm, which tapers progressively towards the northern end of the excavated area.

Unit 5 lies on an erosive surface and is an about 25-30 cm lens of conglomerates, enclosed in muddy and sandy matrix. The clasts, either sub-rounded or sub-angular, are mostly composed of micritic grayish limestone with subordinate pisoliths and gastropod shells. Isolated remains of macrovertebrates were found mixed with both unretouched and polished stone implements. Unit 5 is sometimes in direct contact with unit 2 in the northernmost portion of the excavation (**Figure 3**).

Unit 6 is up to 90 cm thick and lithologically similar to Unit 1 (**Figure 3** and **4B**). It contains abundant Gastropod shells and plant residues; rare stone tools have been found in the lower portion of the unit, associated with few and doubtful wooden tools.

Unit 7 is up to 2 m thick, but includes two distinct levels; the lower portion, 7A, consists of 40 cm whitish, massive calcareous mudstones, which cover and fill the basal erosive surface (**Figure 4C**); it yielded the skull of a young individual of *P. antiquus*; the upper portion (7B) is composed of individual beds of homogeneous and graded sandstone, separated from one another by erosive surfaces (**Figure 4B**). At the top the succession is capped by layers of light-colored calcareous muds, which are separated by erosive contacts. The unit is covered by an anthropic deposit up to 2 meters thick, containing residues of the Roman Age.

Two shallow cores, S1 and S2, each drilled down to about 10 m from the surface, have been collected outside the excavated area, just beyond its southern and northern margins. The correlation of the stratigraphic logs (**Figure 2C** and **3**) shows that the site is located in a small valley, extending from the slopes of a modest hill down to the plain. The seven Units are all confined within a section between the cores S1 and S2. The calcareous breccia is the bottom-most layer of the cores; this term is followed by reddish mudstone and then, with abrupt transition, by homogeneous mudstone with subordinate sandstone. The deposits of Units 7 and 6 are the top-most deposits of the cores. To summarize, the site included deposits accumulated in a small valley cut at the side of a wide lacustrine area with a fluctuation water table, which was ultimately affected by the geothermal heat flux.

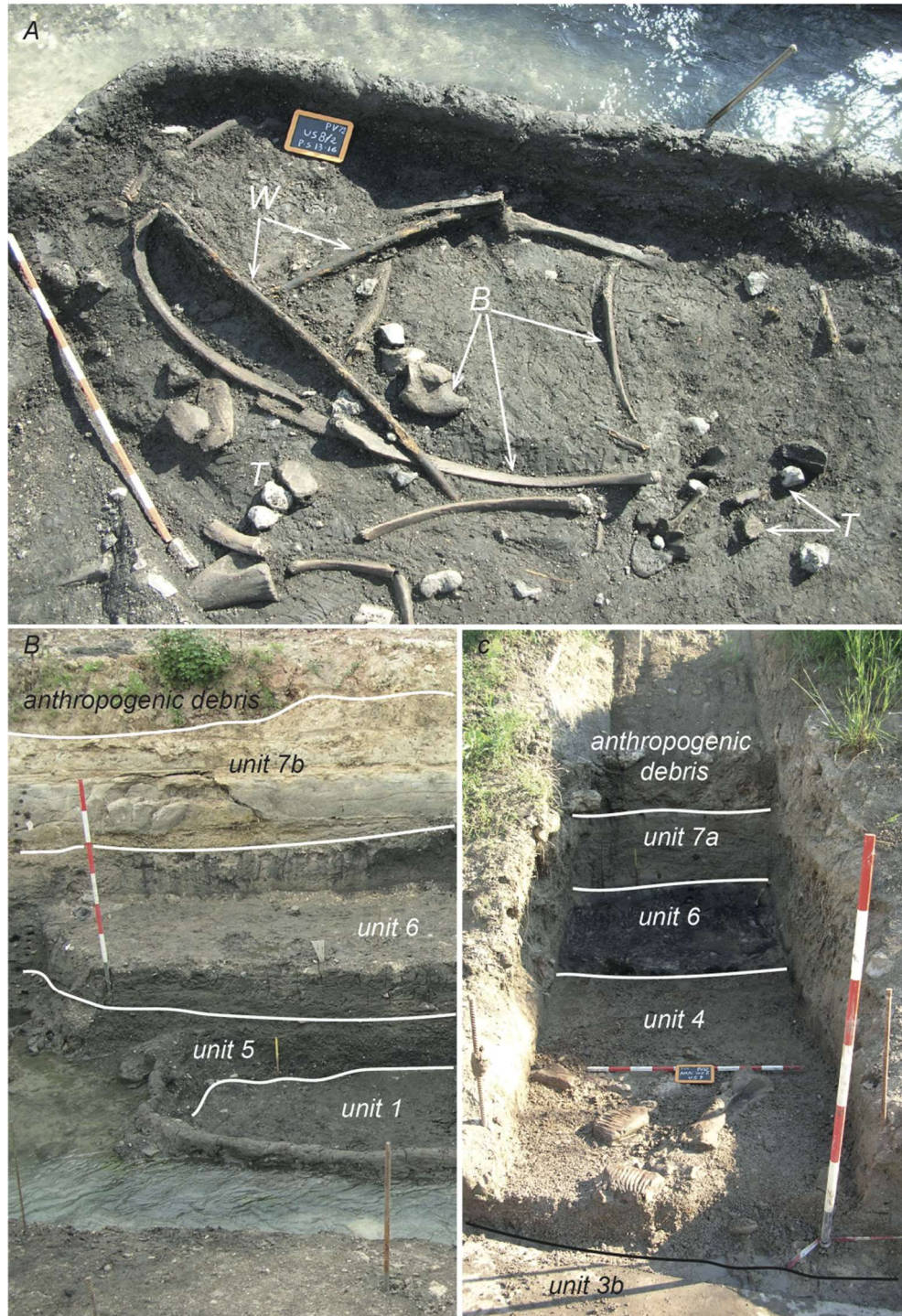


Figure 4 A) Plan view of the Unit 2 during excavation step showing the framework of bones (indicated by letter B), stones (most of which artifacts, letter T) and wooden rods (indicated by letter W). B) Part of the section excavated along the northern side of the site where log A was measured. C) The section excavated on the southern side (log B); note two molars and bones of *Palaeoloxodon antiquus* on top of Unit 4. Ten centimeters divisions for scale in all photographs.

1.4 Chronological frame: Radiometric dating

Vertebrate fossil remains and pisoliths from Unit 4 were suitable for ESR / U-series radiometric dating. They gave two separate and complementary results (Table 1). A lower third molar of adult *Bos primigenius* (No. 5485) was selected and dated at the Department of Prehistory of the Museum of Natural History (UMR 7194 of CNRS) in Paris. It provided a date of 170 ± 13 ka. The pisolith was selected from a 220-g sample and dated with the uranium method at the CNR -IGAG in Rome. It gave a date of 171 ± 3 ka. Both results suggest that the sedimentary sequence started during the final stages of the interglacial MIS7 and continued throughout the glacial MIS6; this period of time is imperfectly known both paleontologically and archeologically. In addition, absolute dating at about 171 ka also provides a *terminus ante quem* for Unit 2 and consequently the human artifacts from it may likely be attributed to early populations of *Homo neanderthalensis*.

A

$^{234}\text{U}/^{238}\text{U}$ (activity ratio)	$^{230}\text{Th}/^{234}\text{U}$ (activity ratio)	$^{230}\text{Th}/^{232}\text{Th}$ (activity ratio)	^{238}U (ppm)	^{232}Th (ppm)	Age (ka)
1.414 ± 0.014	0.841 ± 0.008	77 ± 5	1.48 ± 0.01	0.049 ± 0.003	171 ± 3

B

Sample	Tissue	U (ppm)	Paleodose D_E (Gy)	U uptake p-parameter (ppm)	$D_{a\alpha}$ Internal ($\mu\text{Gy/a}$)	$D_{a\beta}$ ($\mu\text{Gy/a}$)	D_a total ($\mu\text{Gy/a}$)	D_a total ($\mu\text{Gy/a}$)	D_a total (US) (ka)	ESR/U-series ages (ka)
PGV1502 (c n°5485)	dentine	1.84 ± 0.12	91.41 ± 3.03	-0.84 ± 0.06	36 ± 37	69 ± 16	433 ± 20	538 ± 45	170 ± 13	
		0.11 ± 0.01		-0.53 ± 0.08						

Table 1 A) Activity ratios and age of the pisolith carbonatic fraction from Unit 4. All errors reported as 1σ . B) ESR/U dating of the Auroch's tooth from Unit 4.

1.5 Archeological relevance of the site

Unit 2 is Poggetti Vecchi oldest anthropic layer. As explained above, it accumulated during one of the lake's lowstands and in a moment of sub-aerial erosion. In fact, Units 1 and 2 likely deposited at the onset of MIS6. During this period, the short-lived valley was part of a landscape inhabited by large animals, especially elephants and groups of human hunter-gatherers, as suggested by the many artifacts broadly referable to an early-middle Paleolithic age. The stone implements were obtained from local siliceous fluvial pebbles and cobbles, deriving from the erosion of Northern Apennine Mountain rocks. The most common raw materials are different types of chert, radiolarite and quartzite.

All in all, about 200 stone objects (including cores, flakes, unworked raw material) and several wastes (i.e., debris and fragments) were recovered. Scrapers, notches and choppers are generally retouched and were associated with several tens of tiny flakes that are interpreted as by-products of a retouching activity, which took place on site. They show evidence of longitudinal actions on soft animal tissues, as well as of scraping or shaving wood.

Wooden rods have also been found. Wood is one of the most popular, available and versatile raw material (Coles et al., 1978; Smith, 2003; Waguespack et al., 2009) but is rarely recovered because of its very low durability. Wooden artifacts are reported from two more sites: the Clacton (Oakley et al., 1977) and Lehringen spears (Weber, 2000; Bigga et al., 2015; Thieme and Veil 1985), and the 300 ka-old Schöningen spears (e.g. Schoch et al., 2015), which seem to be connected with horse hunting. These spears have been made of soft wood, such as spruce (*Picea* sp.) and pine (*Pinus* sp.), and most of them are sharpened only at one end.

Unlike these specimens, the sticks from Poggetti Vecchi were obtained from boxwood (*Buxus sempervirens*); pollen evidence actually indicates the presence of boxwood in the surroundings of the site. Boxwood is one of the heaviest, hardest, strongest and most compact but also most flexible woods in Europe. The Poggetti Vecchi sticks were worked to obtain a handle and point at the two extremities, using a technique with no other equivalent at the time. Some rods bear a thin, black layer, about 1 mm thick. Microscopic analysis indicates that it was generated by partial charring, likely to lessen the labour of scraping off the bark and working the two ends of the sticks. This labour- and time-saving approach proves to be particularly profitable, especially when dealing with hard boxwood. The Hazda people, in Tanzania (Woodburn 1990), and the Californian Indians (Oakley et al., 1997) are accustomed to using fire as an engineering tool to manufacture wooden tools. This technology is an early evidence of the control and manipulation of fire, which started when Neanderthals arose

towards the end of the Middle Pleistocene (Mazza 2006; Roebroeks and Villa 2011).

The wooden rods from Poggetti Vecchi were not weapons, employed to kill the elephants. In contrast, they were multipurpose tools, which differed from the other wooden tools listed above both in shape and craftsmanship. With their point and rounded handle, the Poggetti Vecchi sticks were likely driven into very tough material and probably used as skewers to carry large pieces of meat, similar to those described by Toth and Schick 2007.

Virtually all the Middle Pleistocene European sites that yielded remains of *P. antiquus* associated with human artifacts are believed to attest to active human hunting, butchering or scavenging of already dead carcasses (e.g., Conybeare and Haynes, 1984; Haynes and Klimowicz, 2015; Konidaris et al., 2017). Hunting and carcass processing are normally supposed when only a single elephant individual is involved (e.g., Santucci et al., 2015; Aureli et al., 2015; Weban-Smith et al., 2006; Villa et al., 2005; Weber 2000; Yravedra et al., 2010). A notable exception is the site of La Cotte de St. Brelade, where heaps of bones of mammoths are supposed to be the result of several intentional hunting drives (Scott 1980; Scott et al., 2014).

Non-accidental association of animal remains, and human implements is usually interpreted as evidence of different human actions, including hunting, butchering or scavenging (Bindford 1987; Weber 2000; Surovel and Waguespack 2008; Yravedra et al., 2010; Rabinovich et al., 2012; Scott et al., 2014). Concentrations of bones of several individuals are generally believed to be time-averaged accumulations produced by some natural, abiotic agent, like fluvial transport (Villa et al., 2005, Santucci et al., 2015, Boschian and Sacca, 2014, Gaudzinski, 1996).

Poggetti Vecchi seems to differ in many respects (e.g., stratigraphic age, number of elephants involved, kind of artifacts) from the other European sites where artifacts are associated with remains of *P. antiquus* [i.e., Fontana Ranuccio, Torre in Pietra, La Polledrara (Anzidei et al., 1999, 2012), Castel di Guido (Radmilli and Boschian 1996; Boschian and Sacca 2014), Ficoncella (Aureli et al., 2015), Atella and Notarchirico (Piperno 1999; Piperno and Tagliacozzo 2001), and Isernia La Pineta (Sala, 1983, 1996), Boxgrove (Weban-Smith et al., 2006), Ealing (UK), Bilzingsleben (Mania and Mania, 1988), Kärlich–Seeufer (Gaudzinski 1995a, b), and Lehringen (Weber 2000) (Germany), Aridos I-II (Yravedra et al., 2010), Ambrona (Villa et al. 2005; Yravedra et al., 2010) and Torralba (Haynes 2005; Villa et al., 2005) (Spain), Marathousa I (Greece) (Panagopoulou et al., 2015)].

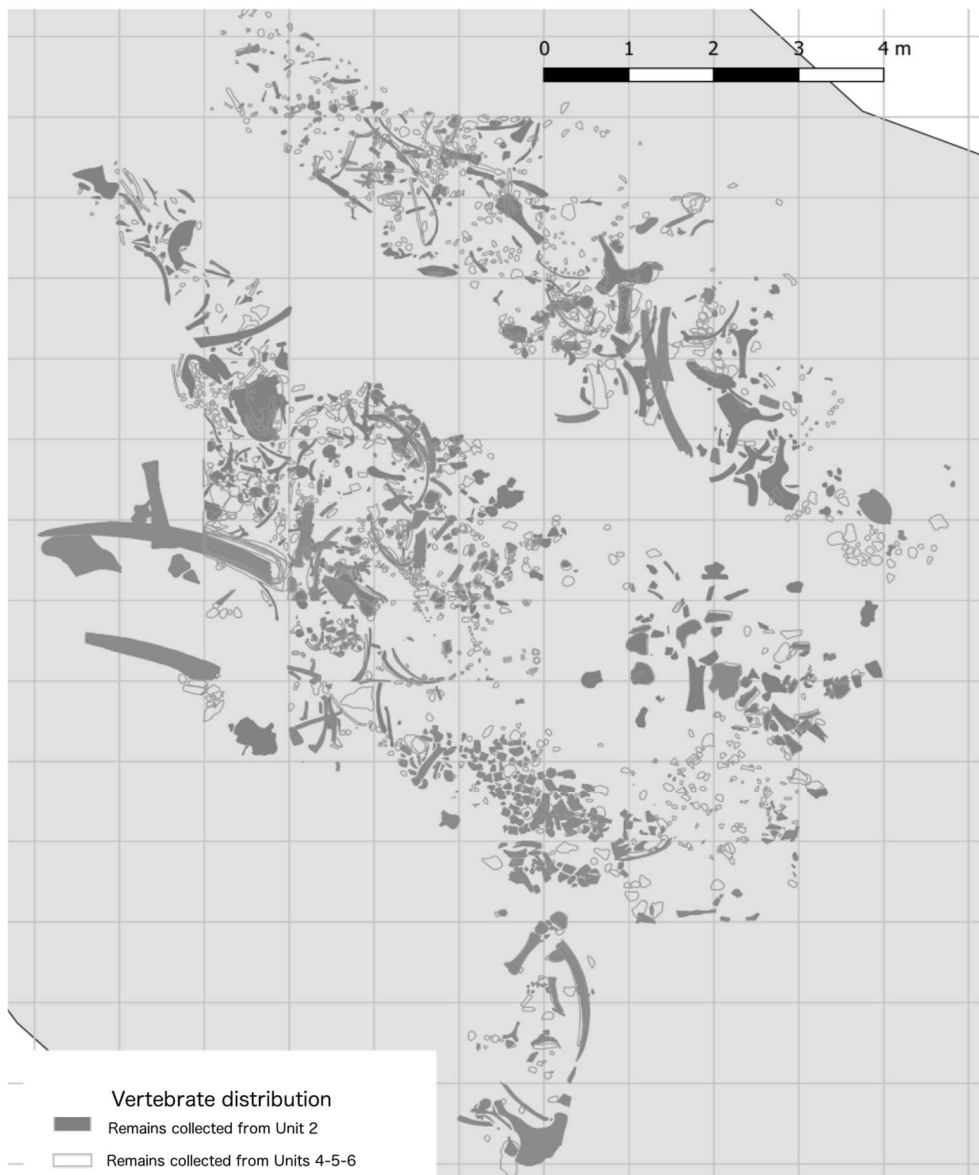


Figure 5 Archeo-paleontological plan highlighting all vertebrate remains.

Poggetti Vecchi is certainly one of the few sites that date back to the MIS7-6 transition, which is a time period affected by an intense climate deterioration (Sanchez Yustos and Diez Martin, 2015). The only prehistoric evidence of this period in Italy is the human skeleton from Altamura (Lari et al., 2015). Poggetti Vecchi yielded remains of several individuals of *P. antiquus* of different ontogenetic ages. The bones were mostly concentrated in a relatively small area, they lied horizontally, in contact with one another and interspersed with the tools (**Figure 5**). This association is recurrent in the various layers (U2-4-5-6), which suggests that local human hunters frequented the area regularly, exploiting the megafauna. The hot thermal springs of Poggetti Vecchi may have created a favorable microenvironment at a time when global climate was worsening, which likely attracted both the local faunas and their human pursuers. These fortunate circumstances

possibly explain the association of bones and human implements. The site therefore offers the chance to gain new insights into early Neanderthals' behavioral plasticity and food procurement strategies (Binford, 1987; Weber, 2000; Surovel and Waguespack, 2008; Yravedra et al., 2014; Rabinovich et al., 2012; Scott et al., 2014).

Chapter 2 Paleodiet proxies in paleoenvironment and paleoclimate reconstruction

2.1 Introduction

2.1.2 Dental function

George G. Simpson was a pioneer of paleobiological research. Early studies focused on the reconstruction of chewing movements by examining the shapes of fossil teeth and the directions of scratches between wear facets. He believed that teeth are the most efficient tool for processing tough vegetation (Simpson, 1926). To explain chewing movements, Simpson (1926) devised a model involving horizontal and vertical movements, but also two types of tooth crown structure, i.e., crests and cusps. Simpson (1933) thus defined three actions of food processing: 1) shearing, where vertical jaw movements force opposite crests to slide past one another; 2) crushing, in which cusps are vertically pressed into basins; 3) horizontal grinding movement, wherein cusps slide across basins. During most of the middle 20th century, Simpson and several other researchers studied how wear facets match on opposing teeth and assessed relative tooth movements based on occlusal surface scars. Mills' (1963) critics of Butler's (1925) conclusions fruitfully generated important insights. Both authors agreed that most mammals chew on one side at a time, but had different ideas concerning the chewing function and how to interpret wear facets. The former observed that each mammalian molar shows two separate wear facets, one on the buccal side, the other on the lingual; he believed that the two form when upper and lower teeth come together (“Phase I”) and then separate (“Phase II”) during the chewing process. In contrast to Butler (1925), Mills (1963) was convinced that there is contact between upper and lower teeth not only on the working side but also on the balancing (i.e., non-working) side, due to the balanced stresses along the dental arch. Hence, according to Mills' (1963) view, the two facet types are connected both with the chewing and balancing processes. These pioneer studies provided the basis for our improved understanding of tooth matching, chewing movements and wear.

2.1.3 Tooth wear

Paleodiet studies allow tracking environmental changes and contribute to solve paleoecological issues, since food creates a strong bond between animals and their surroundings. The size, shape and structure of mammalian teeth provide important clues for paleodietary inferences, but are under genetic control and reflect only ancestral relationships. Moreover, some species with highly specialized teeth often avoid foods to which they

are most adapted. This is the so-called "Liem's paradox": dental morphology provides information on potential feeding choices and not on the actual consumption of specific food items (Ungar, 2015). In contrast, wear patterns are not inherited and show real feeding habits, which can be analyzed at both macro- and microscopic scales. Wear sculpts secondary morphologies on teeth providing the most suitable shapes for the best food processing performances required by each species.

2.2 Gross methods

The estimation of wear rate is a basic gross method that allows determining abrasiveness or fiber intake with food. Wear rate can be inferred on fossil teeth by comparing differences in the degree of wear between teeth in a row (Ungar, 2015). Moreover, it provides information on chewing mechanics: e.g., tougher foods tend to require more chewing cycles per volume of food. Wear gradients can be defined based on the fact that dental eruption follows a predictable schedule; nonetheless, the abrasiveness of the foods not necessarily accounts for steep wear gradients.

Other methods help address this issue. Mesowear is a fast, reliable and simple method proposed by Fortelius and Solounias (2000). The theoretical principle of mesowear is based on the development of relative tooth facets: tooth-to-tooth contact causes attrition and forms dental facets; in contrast, abrasion, which is caused by tooth-to-food interactions, tends to obliterate them. Mesowear scoring is obtained by analyzing angled surfaces, such as those at the leading edges of facets. Attrition forces are developed when the teeth slide one against each other; they should preserve sharp surfaces, whereas abrasion tends to produce blunt surfaces. Consequently, cusps and cuspids appear sharp, rounded, or blunt and the valleys between them either high or low.

Mesowear is an appropriate method for analyzing the average dietary signal of herbivorous mammals, because it represents a long-term signature due to prolonged wear over the whole lifespan of an individual (Fortelius and Solounias, 2000). The mechanisms of tooth wear are not yet fully understood; whether it is produced only by phytoliths, or even by exogenous grit remains unclear (Lucas and Omar, 2012). Empirical evidence confirms that the physical properties of food are directly reflected by the relative amount of attritional and abrasive damage; grasses are abrasive and thus accelerate and balance the wear rates of enamel and dentin, causing flatter occlusal surfaces. Conversely, soft dicotyledonous plants are less abrasive and, as dental wear progresses, the attritional component becomes dominant: the wear-resistant enamel ridges thus create deeper valleys into the softer dentin of opposing teeth, thereby contributing to the formation of higher reliefs.

Several pioneering paleodietary studies on ungulates were based

on the crown height of molars, which represents a morphological predictor of diet by reflecting tooth durability against wear (Janis and Fortelius, 1988). Hypsodonty is measured by various indices, e.g., the height/width of enamel ratio. Yet, it assesses only overall wear rate and is not a sensitive dietary indicator, due to its non-specific relationship with food properties (Solounias et al., 1994). Alternative proxies, such as microwear and mesowear, can be considered more specific. Moreover, it is becoming increasingly clear that crown height is the result of numerous factors: attrition, abrasion and grit intake of food items. It is therefore related to feeding habits of a species in deep time (Solounias and Semprebon, 2002). Fortelius and Solounias (2000) suggest that mesowear variables produce robust dietary clusterization of ungulates into different classes, which are independent of hypsodonty indices. Furthermore, clusters derived from mesowear variables appear biologically more accurate than those based on hypsodonty factors. All in all, measurements of hypsodonty and sharpness can at most be used for distinguishing grazers from browsers within several mammalian families.

Another approach is topographic analysis, which consists of the comparison of ongoing tooth wear, considering the static and dynamic aspects of the gross occlusal pattern. Wear, therefore, affects tooth shape modifying the heights of the cusps and the slopes but several features such as surface, angularity as well as the boundary between enamel and underlying dentin, remain constant (Buun and Ungar 2009).

Dental topographic analysis is a whole-surface characterization (measured as surface complexity or jaggedness). Measurements are taken freely and not from or between specific points and provide a shearing quotient (computed as the sum of the lengths of shearing crests against the tooth length). This method was developed to distinguish primates as folivores or insectivores. It involves the collection of laser scanner-generated three-dimensional point clouds, which are imported into a geographic information system (GIS) where the surfaces are interpolated using inverse-distance weighting. Tools available in the GIS software are devised to measure landscapes (i.e., average surface slope and relief) and angularity; by comparing the patterns of different specimens the device can reveal gross surface morphologies. Results to date show that the teeth of leaf eaters have occlusal surfaces with steeper slopes and higher elevations, at a given stage, than have those of fruit eaters; furthermore, observation confirmed that, as wear progresses, occlusal surfaces become flatter (Ungar, 2015). Feeding habits can therefore be inferred by comparing gross dental features of the different species as long as the degree of tooth wear is constantly monitored.

2.3 Microwear

Dietary adaptation can be based on the analysis and detection of microscopic scars on tooth enamel. Scratches, pits and gauges are produced during chewing by abrasion and attrition **Figure 6**. Microwear analysis is one the methods used to infer animal feeding habits and food availability. As mentioned above, the orientations of microscopic scratches visible on molar facets have first been used to infer the directions of jaw movement (Simpson, 1926-1933). Later on, Butler (1952) and Mills (1955) focused on specific details of masticatory behavior in various living and fossil species, and Baker (1959) analyzed the etiology of microwear.

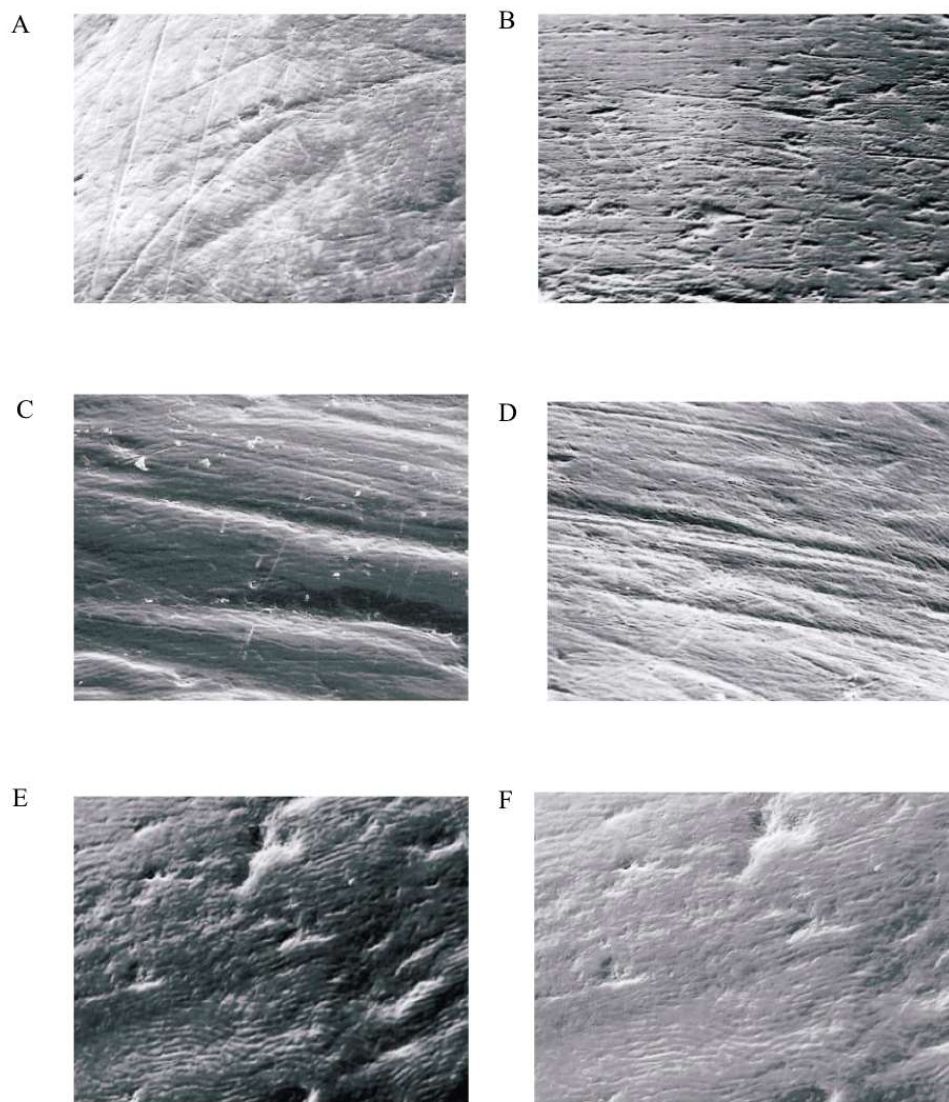


Figure 6 Photomicrographs on enamel facets obtained by SEM scanning at 500x. A) Polished surface with many fine and coarse scratches; B) microwear pattern with several small pits that suggest mixed feeding behavior; C) wide and coarse scratches; D) several fine scratches and few pits on polished surface where are visible enamel prisms, this microwear pattern is indicative of graze feeding habits;

E) unscratched pattern with several pits; F) enamel prism with several pits. (Modified from Solounias and Semprebon, 2002).

Pioneering studies on a variety of taxa, from both archeological and paleontological contexts, had been stimulated by the widespread adoption of scanning electron microscope technology, already since the late 1970s (Solounias et al., 1988; Solounias and Moelleken 1992a,b, 1993a,b; Solounias and Semprebon 2002). Scratches and pits are likely proxies of the last meal consumed by the individuals. This laser scanning approach is not only able to differentiate browsers, grazers and mixed feeders, but it also provides direct evidence on feeding behaviors, thus contributing to determine ecomorphological traits and, ultimately, the trophic scenario. Early studies were largely based on the qualitative degree of morphological similarity among photomicrographs of teeth of fossil and living species (Ungar, 2015). Furthermore, past studies examined enamel surfaces at high magnification (e.g. Grine, 1977, 1986; Gordon, 1982; Teaford, 1988; Ungar, 1990). Scanning electron microscopy (SEM) offers resolution and depth of field capable to produce very detailed images of superficial scars. During the 1980s analytical techniques have been refined; tooth surface parameters and amount of magnification have been standardized; moreover, counting and measuring procedures for the quantification of scratches and pits were defined, thus allowing the acquisition of more uniform and comparable data on lengths, breadths and orientations of these marks. Special attention has been given to the facet types (singling out those produced during each of the two phases described above) present on the different teeth as well as to the instrumental setting.

SEM methodology has the inconvenience of being expensive and time-consuming for the acquisition of photomicrographs. Another inherent drawback is due to the interaction between the electron beam and sample surfaces: changes in the technical parameters (e.g., type and relative position of the detector, specimen geometry, types of electrons, voltage, working distance, surface tilt) may affect the observations, often producing different pictures of the same surface (Gordon, 1988; Pastor, 1993), which can strongly bias results and interpretations. The attempt to represent a tridimensional object using two-dimensional images probably causes a loss of data: e.g., a scratch becomes a relief by changing the electron beam intensity and fine scratches disappear if the beam is oriented parallel to the feature. All these difficulties may impair the comparison between studies.

In order to reduce time and expenses of analysis some scholars proposed to return to low-magnification observations, which also guarantees reproducible, robust and reliable cross-order comparisons (Solounias and Semprebon, 2002; Godfrey et al., 2004; Semprebon et al., 2004; Merceron et al., 2004a,b, 2005a,b; Nelson et al., 2005; Green et al., 2005). Microwear features are identified by their differential light refractive properties when

the occlusal surface of tooth casts is illuminated by an external optical fiber light source. Qualitative assessment, morphological description, and semi-quantitative analysis (proportion of scratches to pits, length and orientation of scratches and size of pits) are essential to making diet inferences for the reason that different foods produce various kinds of scars. As mentioned above, since the late 1980s researchers sought to improve repeatability and objectivity of observations. A computer-based, semi-automated counting method introduced by Ungar (1990) was unable to solve completely all the intrinsic problems because it still strongly relied on human intervention for the identification of the scars. This implied a considerable amount of subjectivity and of intra- and inter-observer errors (Grine et al., 2002). The need for three-dimensional scans uncontaminated by subjectivity led to the development of an alternative method. Dental Microwear Texture Analysis (DMTA) is a relative new approach that was developed in 2003 and used since that time (Ungar et al. 2003, Scott et al. 2005, 2006). It works by acquisition of three-dimensional surface scans which allows analyzing the texture of the whole tooth surface as a single unit, and obtaining a truly automatic count of microwear scars **Figure 7**.

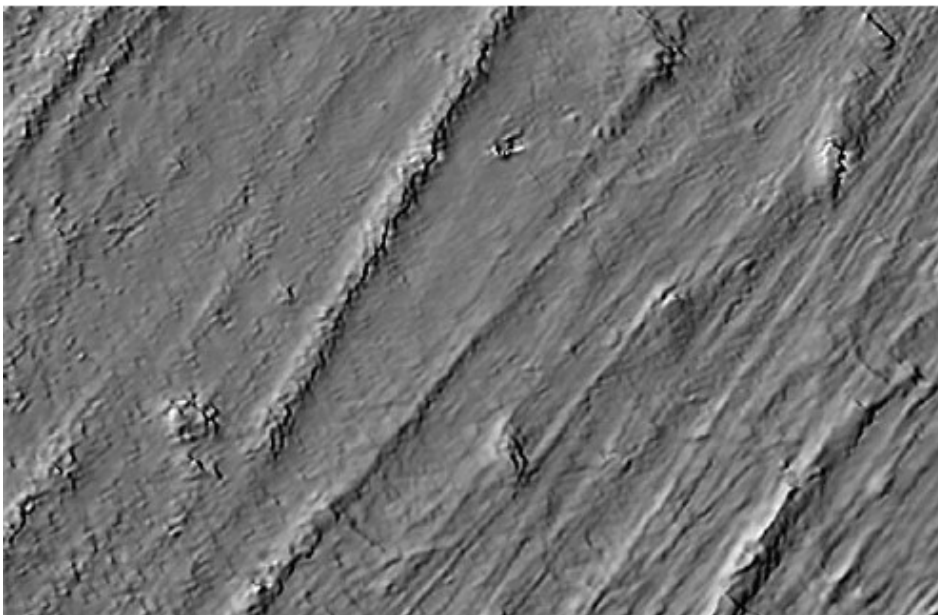


Figure 7 Photosimulation of an enamel surface obtained using non-contact profilometer with oriented striations (modified from Scott et al., 2006).

Contact sensors (diamond or ruby stylus) and non-contact systems (interferometry, optical profiler and confocal microscope) that are based on light refraction and diffraction methods can be used to collect 3D surface data at the microscopic scale (Kaiser and Katterwe, 2001; Evans et al., 2001; Ungar et al., 2003). These instruments only scan tooth surfaces, without penetrating them, and yield 3D models **Figure 8**. Resolution and work envelope size can be selected to compare three-dimensional data with those obtained with SEM. Each scan represents a specific area (usually

104x138 μm^2 wide) with a fixed lateral point spacing (i.e. 0.18 μm) and vertical resolution (i.e. 0.05 μm). The resulting point clouds can be analyzed using two alternative systems: Scale Sensitive Fractal Analysis (SSFA; Ungar et al. 2003, Scott et al. 2006), or Surface Texture Analysis (STA), which is based on industrial standardized parameters (ISO standard).

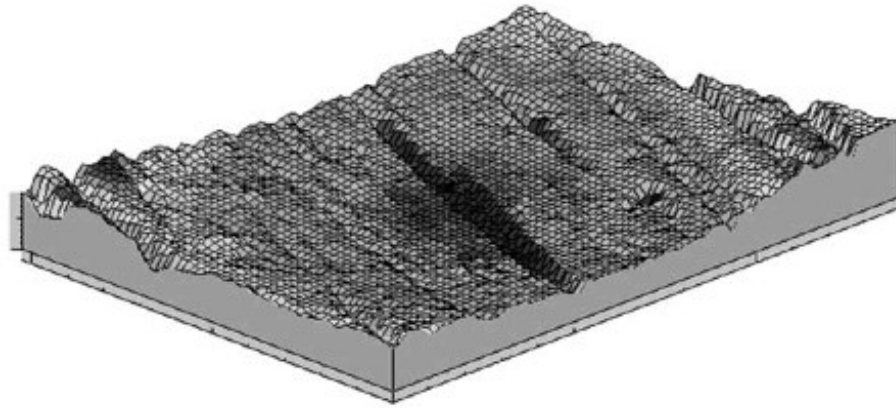


Figure 8 3D-model of a striated enamel surface obtained with DMTA method (modified from Scott et al., 2006).

This approach recognizes tooth function at multiple levels; surface scars are seen as “scale sensitive”, because different features, such as apparent length, area and volume, of a rough surface change based on the scale of observation. Fractal Analysis uses different superficial parameters “to describe” the tooth that reflect an assembly of attributes correlatable with feeding habits. These include complexity (Asfc); heterogeneity of complexity (HASfc); scale of maximum complexity (Smc); anisotropy (epLsar) and textural fill volume [(Tfv); Ungar et al. 2003, Scott et al. 2005, 2006]. For example, a heavily pitted surface with variable size and shape patterns tends to give a higher value of complexity compared to an enamel area with more uniformly-sized scratches. Higher texture complexity is often related to mammals that feed on hard and brittle foods. Texture direction or anisotropy varies between 0-1 and, hence, high anisotropy values are typically associated with surfaces dominated by striations that are well-aligned and oriented in the same direction, generated by shear or by slicing through tough matters. Surfaces dominated by pits and/or with a few scratches without preferred orientation give values close to zero. Other parameters (i.e., the scale of maximum complexity, the fine-scale limit of the Asfc line, and textural fill volume) provide a measure of surface feature sizes; the heterogeneity of surface complexity is given by fluctuations in heterogeneity values across sub-sampled areas (i.e., 3x3 and 9x9 cells).

Both Scale Fractal and Standard systems are based on algorithms and thus allow automatic computation and ensure analytical repeatability minimizing intra- and inter-observer errors. However, possible biases due to subjective choices are still present but are limited to preliminary steps, such

as the selection of the tooth facet, the type of impression material to use, researcher know-how and the precision of molding and of casting preparation.

2.4 Isotopic analyses

Dietary habits, paleoclimate and paleoenvironmental reconstruction should also be based on the analysis of the stable isotopic composition of the bioapatite of teeth and of the collagen of bones. Carbon, nitrogen and oxygen isotopic compositions are assumed to be a direct and constant function of the food and water consumed by the animals. Changes in dietary habits, large modifications in the vegetation structure (i.e., the switch from C3 to C4) and/or smaller variations in local climate, should be reflected by the isotopic fractionations of animal tissues and diet.

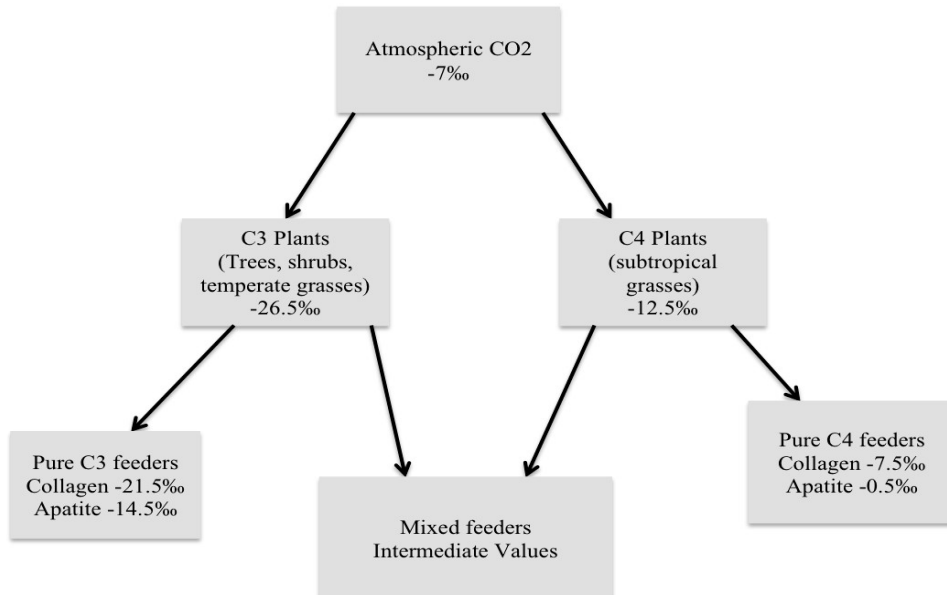


Figure 9 Carbon fractionation in terrestrial food webs (drawn from Tykot, 2004).

The highest carbon fractionation (**Figure 9**) is detected in photosynthetic plants. Plants are located at the base of the trophic webs and can have different metabolic pathways (C3, C4 and Cam) with different carbon isotopic composition. For example, in temperate and cold environments, the vast majority of terrestrial plants (trees, fruits, shrubs and temperate grasses) use C3 photosynthetic pathway to convert atmospheric CO₂ into organic compounds. Carbon dioxide in Earth's atmosphere has a $\delta^{13}\text{C}$ value of about -7‰. C3 plants show lower $\delta^{13}\text{C}$ values than their carbon source (mean value -26.5‰; O'Leary, 1988); conversely, a mean amount around -12.5‰ is typical of tropical grasses that use C4 photosynthetic pathway. Terrestrial C3 and C4 plants do not have

overlapping $\delta^{13}\text{C}$ values but CAM plants (cacti and succulents that are typically restricted to tropical deserts) show a wide range of $\delta^{13}\text{C}$ values, which overlap those of both C3 and C4 plants. Small variations in the $\delta^{13}\text{C}$ signatures of plants are due to variations in water availability, salinity, lighting levels and degree of canopy cover (Kohn and Cerling, 2002). In particular $\delta^{13}\text{C}$ depletion is related to lower levels of light, higher canopy cover and lower salinity (Farquhar et al., 1989); in contrast, drought tends to cause variable degrees of isotopic enrichment (Farquhar et al., 1989; Peuke et al., 2006).

When food is ingested, the isotope content is transferred from producers to consumers through the food chain and undergoes fractionation (DeNiro, 1987). The enrichment factors (ϵ) are determined by environmental circumstances (mesic or xeric conditions), on the type of species that are involved, but also on the body sizes (either medium or large) of the various plant eaters. In large-sized species, the enamel structural carbonate ($\delta^{13}\text{C}_{\text{sc}}$) ranges from about 9 to 14.5‰, whereas in collagen it reaches 5.5‰. A large proportion of carbon in collagen derives directly from the protein intake from food rather than from bulk diet, and this probably originates the differences in the carbon isotopic values (Cerling, 1999).

The oxygen isotopic composition of bioapatite reflects the $\delta^{18}\text{O}$ value of environmental water ($\delta^{18}\text{O}_{\text{w}}$) that an individual ingests over its lifetime. The oxygen isotope contents in different water sources (rain, rivers, lakes, springs and ponds) are in turn related to the physical environmental and biological conditions. $\delta^{18}\text{O}$ values have been observed to grow, in both plant and surface water, with falling temperatures, increasing distance from the sea, elevation, higher precipitation and low rate of evaporation and evapotranspiration (Dongman et al. 1974; Burk and Stuiver 1981). Oxygen fractionation steps are showed in **Figure 10**.

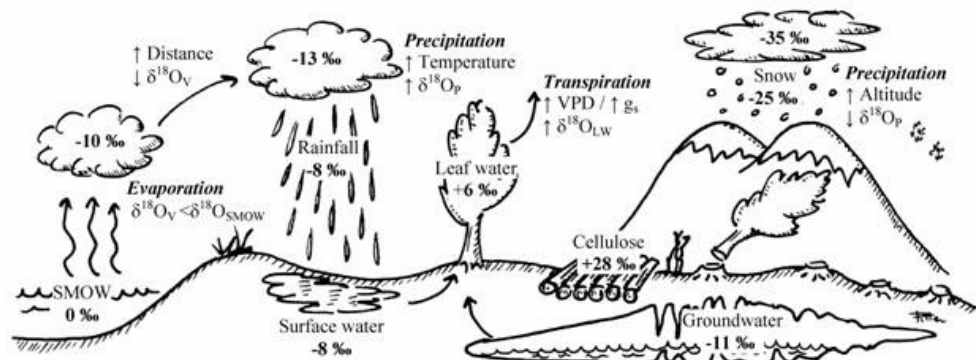


Figure 10 Main fractionation steps and typical values of oxygen isotope composition in a temperate climate. $\delta^{18}\text{O}$ SMOW, standard mean $\delta^{18}\text{O}$ in ocean water. $\delta^{18}\text{O}_{\text{v}}$, $\delta^{18}\text{O}_{\text{p}}$, $\delta^{18}\text{O}_{\text{LW}} = \delta^{18}\text{O}$ in water vapor, precipitation (either rainfall or snow) and leaf water, respectively; VPD (vapor pressure deficit); gs (stomatal conductance). Drawn from Ferrio et al., 2005.

The oxygen isotopic signature can be measured using both phosphate and carbonate, which are the major and minor anionic compounds of the mineral components of bones and teeth, respectively. The isotopic compositions of the water of each mammal's body and of each water source in the environment are directly related to one another; similar connections exist even between the mineral oxygen of organic tissues and environmental water. Consequently, scholars calibrated isotopic scales on modern species from different geographic and climatic areas for the transformation of phosphate $\delta^{18}\text{O}$ values into those of environmental water (Longinelli, 1995). Bone phosphate and carbonate are interrelated, and this enables the conversion of the amount of carbonate oxygen isotope into the isotopic values of phosphate (Iacumin et al., 1996).

Despite Earth's atmosphere is largely composed of nitrogen (about 78%) most organisms cannot use this gas. Organisms can access atmospheric nitrogen only through the mediation of particular biochemical processes. Metabolically-induced fractionation of nitrogen affects the $\delta^{15}\text{N}$ signals in different environmental contexts. Terrestrial plants can be distinguished into two groups based on the different kind of nitrogen source. Nitrogen-fixing plants have a symbiotic relationship with Rhizobium-type bacteria that convert nitrogen into ammonium; their $\delta^{15}\text{N}$ values are very low, with average values around 1‰. In all other plants values range at about 6‰. The trophic chains in marine environments are longer than in terrestrial ecosystems and marine organisms exhibit higher $\delta^{15}\text{N}$ values than terrestrial ones. Isotopic ratios in freshwater environments are enriched in ^{15}N like in marine settings; concentrations vary considerably where there is mixing of water and soil. Therefore, similarly to stable carbon isotopes, stable nitrogen isotopes are useful in differentiating terrestrial and aquatic (marine and freshwater) food sources. However, nitrogen is most effective in detecting trophic relationships. Moving up the food chain, there is a steady increase in $\delta^{15}\text{N}$ by a factor of about 3-5‰ which is probably associated with the preferential use of ^{15}N during the synthesis of tissue proteins and consequently with its excretion as urea (in terrestrial environments) or ammonium [in the marine contexts; (Tykot, 2004)].

2.5 Methodological approaches in the study of elephants' diet

Despite the large availability of elephants remains, of both extinct and living species, relatively few studies focused on the role played by the feeding habits of these pachyderms as ecological proxy indicators (i.e., Palombo et al. 2005; Todd et al. 2007; Calandra et al., 2008; Grube et al., 2010; Konidaris et al., 2016). Studies have generally been based on the 2D microwear method as well as on stable isotopic determination. Only recently (Saarinen et al., 2015; Saarinen and Lister, 2016) a mesowear experimental

protocol was devised with new, spectacular results i.e., it gives a robust signal concerning the amount of abrasive foods (principally grass) independently of plant photosynthesis mechanisms as well as it has allowed to properly investigate the feeding adaptations of sympatric species.

The lack of specific studies on the diet of elephants is probably due to the difficulties in approaching the complex morphological and biomechanical features of these animals, as well as the peculiar processes of tooth substitution. Elephantidae molars are very large and composed of several plates, each formed by an individual enamel loop. The functional chewing surface of these oddly structured molars is very wide, and the shape and orientation of each plate are progressively sculpted by wear. The peculiarly built molars and the horizontal tooth substitution are adaptive solutions that significantly increased elephants' life expectancy. The large size of the molars and their horizontal substitution, associated with the animal's enhanced longevity, generate particular patterns of development and wear. In each of the last three molars, while the front lamellae start to be used and hence are affected by wear, the rear ones are not yet completely developed and fused within the main body of molar, and are still situated inside the tooth socket. The microwear pattern is conditioned by the different degree of attrition occurring from the front to the rear end of the teeth; it is quite expectable that the most worn plates show the highest wear damages. Microwear analyses have suggested strong positive correlation between attritional wear and concentration of scars (Palombo et al., 2005). In general, enamel loops on central plates show large amounts of coarse scratches and a certain number of gouges, whereas cross scratches are sometimes more frequent on anterior (more worn) and rear (less worn) plates. Scar patterns on both lateral and buccal sides are the most variable, whereas the central portion is subject to the greatest attrition/abrasion stresses. The central areas of the molars are therefore the most representative of the overall average microwear patterns present on the teeth.

Based on current knowledge, elephants are mixed-feeders, which can be considered a super-keystone species in their ecosystem (Fritz et al., 2002). Their feeding habits reflect local environmental conditions more than their "adaptive optimal" diet (Rivals et al., 2012, 2015; Lister, 2013); their food selection may therefore change frequently (Haynes, 1991). Consequently, in order to establish the major representative dietary behavior in extinct elephant populations, paleodiet analyses have to be performed on fairly large samples belonging to the same site including individuals of different sex and ontogenetic classes; moreover, data must be collected in different points for each enamel loop.

Chapter 3 Elephants

3.1 Origin and evolutionary trends in Proboscidea

Proboscidea is one of the least diverse placental mammal orders, represented by only three living species of elephants. However, this group counts about 180 extinct species and has a long-lasting evolutionary history spanning 55 Ma (Shoshani and Tassy, 2005). Therefore, Proboscidea has one of the longest known histories among living mammals. Moreover, its complex evolutionary history includes several examples of evolutionary parallelism and convergence.

The group arose in Africa at Paleocene–Eocene transition and evolved as member of the endemic African fauna for over half of its evolutionary history (Gheerbrant and Tassy, 2009). Then, during the Oligo-Miocene transition (24-23 Ma), after the closure of the Tethys Ocean, proboscideans spread and diversified in the Old World and finally colonized both New World continents (Gheerbrant and Tassy, 2009).

Recent morphological- and molecular-based reviews of interordinal relationships within Placentalia (e.g., Eizirik et al., 2001; Murphy et al., 2001; Shoshani and McKenna, 1998; Springer and de Jong, 2001) support the close relationships of Proboscidea and Sirenia, which had already been supposed during the XIX century (Blainville, 1936). Various osteological and dental characters understood as synapomorphies support a sister group relation between Sirenia and Proboscidea: i.e., the processus zygomaticus of the squamosal expanded laterally, the anterior position of the orbit, above the premolars, in both orders with infraorbital canal under the orbit. The affinity is furthermore revealed by the reduction of the mastoid process, and bilophodont bunolophodont molars (Tassy and Shoshani, 1998); meanwhile the petrosal bones affinity might be caused by homoplasy (Fischer, 1990). Moreover, their common ancestor was likely adapted to a semiaquatic life (Gheerbrant and Tassy, 2009; Mirceta et al., 2013); proboscideans became secondarily terrestrial, while manatee and dugong evolved independently into fully aquatic mammals (Sukumar, 2003).

The phylogeny of proboscideans includes a number of dominant trends, the most notable being that which led to size increase. Other tendencies were those leading to the lengthening of limb bones and to the development of short and broad feet. The order experienced three successive radiations: 1) the Eocene one of primitive lophodont taxa; 2) the Miocene one of gomphotheres and stegodonts; 3) the Mio-Pliocene one of the modern family Elephantidae (Shoshani and Tassy, 1996). Peculiar proboscideans features (i.e., trunk, tusk, horizontal displacement of the molars, graviportal gait) were absent in the earliest members (Gheerbrant and Tassy, 2009). *Eritherium azzouzorum* (60 Ma) is the first known proboscidean (Gheerbrant, 2009); it stood 20 cm at the shoulder and

weighed about 5-6 kg (Larramendi, 2016). The tallest proboscideans, of Middle Pleistocene age, were 4.5 m high at the withers (Shoshani and Tassy, 1996). On the other hand, dwarfism is also observed in certain lineages, caused mainly by allopatric speciation in insular settings (Orlando et al., 2007).

According to recent cladistics, *Phosphatherium* and other primitive Proboscidea were lophodont and folivores (Gheerbrant and Tassy, 2009); bunolophodont and more crushing molars, which are typical of Elephantiformes, appeared only later on during the Late Eocene (Gheerbrant and Tassy, 2009). At the same time several taxa developed enlarged and pneumatic cranial bones which warranted wider surfaces for muscle attachment externally, while internally increased diploes probably offered protection and thermic insulation to the brain tissues against extreme environmental temperature fluctuations (Shoshani, 1998). The shortening of the neck counterbalanced the growing weight of the skull caused by the elongation of the tusks and, in early evolutionary phases, of the lower jaw (Shoshani, 1998). Early Elephantiformes (*Palaeomastodon*, *Phiomia* and *Hemimastodon*), which date back to the Oligocene, had a short trunk and long snout with the whole set of lower premolars, and also the last molars in adults (Gheerbrant and Tassy, 2009). Nonetheless, these early representatives already possessed a few elephantine-like features, such as graviportally-built columnar limbs and the typical horizontal dental replacement mechanism, which was probably present also in other Oligocene taxa, among which *Eritherium* (Gheerbrant and Tassy, 2009).

The reduction of the dental formula, from the basic eutherian one, had already started since the earliest Eocene and continued throughout the Miocene (Shoshani, 1998). During this time period, the order underwent the highest taxonomic diversification, with the appearance of 7 new genera attested to in the rich fossil records from African deposits (Gheerbrant and Tassy, 2009).

In the course of the Neogene other elephantine features had been attained independently in different lineages with impressive examples of parallelism. The secondary shortening of the lower jaw, which was especially conspicuous in symphyseal portion, was coupled by the backward shift of the center of gravity in the head (Shoshani, 1998). This trend was associated with the parallel development of the trunk, as testified by several anatomic features (elevated position of naris, enlargement of the infraorbital canal, shape and size of the nasal and premaxillary bones which joined the frontal bones), which furthermore became very mobile. The combination of these characters is believed to have been correlated with the increase in size and in the lifting of the head from the ground (Shoshani, 1998).

Proboscidean tusks represent an evolutionary epitome. They are continuously growing hypertrophic, second incisors and the largest known teeth among both living and extinct animals (Shoshani, 1998). Their

morphology is highly variable, ranging from straight to curved downward, upward, or twisted helicoidally along the length. They are used to gather food, as offence/defense weapons in inter-individual confrontations or against predators and for sexual display. The enlargement and specialization of the molars, which began already in early evolutionary stages, involved the increasing height of the crown (hypsodonty), the molarizing of the deciduous pre-molars and the thinning of enamel (Shoshani, 1998).

All in all, the spectacular Neogene radiation of the clade Elephantimorpha led to the appearance of real mastodons (Mammutidae) as well as to the onset of the para-polyphyletic group of the gomphotherids. Gomphotheres had four tusks (two upper and two lower ones); the upper were curved both downwards and outwards; the lower ones were progressively spatulate-shaped and had no enamel. Gomphotheres possessed bundont trilophodont or even tetralophodont (with a fourth loph on the last deciduous molar, as well as on the two permanent anterior ones) molars; the enamel prisms had a fan-shaped, transversally enlarged section, similar to the leaves of the ginkgo. Despite gomphotheres with trilophodont molars became widely distributed during the Miocene, they were not the ancestors of the Elephantidae family. In contrast, tetralophodont gomphotherids were ancestral to lamellar-toothed proboscideans. Hence, during the Miocene lamellar molars were developed in parallel by both stegodonts and elephantids through a multiplication of cusps (i.e., addition of central conules/conelets, then transformed into lamellae (Gheerbrant and Tassy, 2009).

3.1.1 Origin and radiation of Elephantidae

During the Late Miocene, in Africa, several early primitive Elephantidae (such as *Primelephas*) coexisted with the first representatives of modern elephants (*Loxodonta* and *Elephas*) as well as with extinct genera (*Palaeoloxodon* and *Mammuthus*) (e.g., Maglio, 1973; Kalb et al., 1996; Mackaye et al., 2005; Shoshani and Tassy, 2005; Tassy, 2003, Mol, 2006; Sanders, 2006). Then, some time between 3.5 and 3 Ma, elephants dispersed through Levantine corridor into Europe and Asia, i.e., the fossils from Bethlehem represent the most primitive known elephantines out of Africa (Rabinovich and Lister, 2016). Early mammoths, *M. rumanus*, arrived in Eurasia around 3 Ma (Markov, 2012; Lister and Sher, 2015) and, then, evolved independently in the Old and New World, where reached large sizes (Lister and Sher, 2015). Turkey occupies an important position for the migration of mammals, such as early migration of elephantids from Africa and subsequently dispersion from Asia to Europe (Albayrak and Lister, 2012). For example in sum the Turkish specimens of *M. meridionalis* have some primitive features. *M. trogontherii* originated in Asia 2.0 - 1.5 and the remains from southern Russia and Turkey might be the evidence for the

migration through Siberia and Europe, and/or may represent an important step in *meridionalis/trogontherii* evolution in Europe (Lister et al., 2005; Albayrak and Lister, 2012). *Palaeoloxodon* representatives dispersed to Europe during the latest Early Pleistocene from the Levant (Palombo, 2017) and the earliest immigration into Europe are recorded at Gesher B'Not Ya'aqov (GBY; Israel), Slivia (Italy), and Pakefield (England), which all relate to the interval 800-700 Ka (Lister, 2004). Therefore Turkish remains at Dursunlu represent potentially one of the earliest records of the genus out of Africa, which thereby strengthening its presumed migration route (Albayrak and Lister, 2012). The Asian elephants' lineage dispersed out of Africa around 3 Ma (Todd, 2010). The most numerous fossil remains came from the Plio-Pleistocene (2.7-0.6 Ma) Pinjor Formation of Siwalik sequence of India and Pakistan (Nanda, 2002 and 2008). The morphology of Pleistocene species *E. hysudricus* of the Indian subcontinent and *E. hysudrindicus* of SE Asia are clearly close to living species. However, the history of these species, their temporal and geographical extent, and the transition to modern species, are poorly known (Lister et al., 2013). The earliest known *Elephas* in the Levant from Evron Quarry (Tchernov et al., 1994) dated to ca. 1.0-0.78 Ma (Ron et al., 2003); new radiocarbon dates suggested that approximately 3500 BP, the range of Asian elephants included Southern Turkey and, hence, *E. maximus* remains from Gavur Lake Swamp represent the westernmost population (Albayrak and Lister, 2012).

Relationships within Elephantinae and the systematics of modern African elephants have been investigated based on morphological and molecular (both mitochondrial and nuclear DNA) evidence. Despite the great variability and the occurrence of convergence, several well-known morphological traits support the existence of an *Elephas-Mammuthus* clade (Tassy and Shoshani, 1988). Over time, these hypothetical relationships had been either supported or questioned by molecular studies (e.g., the possible links between *Mammuthus* and *Loxodonta* within Elephantidae: Noro et al., 1998; Thomas et al., 2000; Debruyne et al., 2003). In particular, Thomas et al. (2000) criticized the traits affected by convergence (i.e., the large dorsal parietal bulges and concave fronto-parietal region); which, however, are symplesiomorphic traits present in early *Mammuthus* and *Elephas* species; as well as in tetralophodont gomphotheres. Nevertheless, these traits are connected with the globular skull, which is considered an autapomorphic character of *Loxodonta*; hence, they can alternatively support the existence of *Mammuthus-Loxodonta* clade.

However, the latest cladistic analysis (based on hyoid characters) confirmed that *Mammuthus* is more closely related to *Elephas* than to *Loxodonta* (Shoshani et al., 2007). In addition, formerly conflicting results, from molecular data, appear to have been resolved based primarily on morphological evidence (Krause et al., 2006; Poinar et al., 2006; Rogaev et

al., 2006, Rohland et al., 2007). Today we recognize the Asian elephant, which includes three subspecies: the Sumatran Asian elephant (*Elephas maximus sumatranus*), the mainland Asian elephant (*E. m. indicus*), and the Sri Lankan Asian elephant (*E. m. maximus*). African elephants include two separate species, the bush African elephant (*Loxodonta africana*) and the forest African elephant (*L. cyclotis*). The taxonomic position of the latter, which has been elevated to the species level, was cleared based on both morphological (Grubb et al., 2000) and molecular evidence (Roca et al., 2001). Molecular evidence indicated that also the so-called pigmy elephants of Central Africa are a subspecies of *L. cyclotis* (Debruyne et al., 2003). In addition, genetic data showed that the West African populations (which live in both forest and savannah habitats) have been isolated from other elephant populations for as long as 2.4 million years; hence, they could rightfully be interpreted as a possible third African species (Eggert et al., 2002).

3.1.2 Overview of the phylogeny of *Palaeoloxodon*

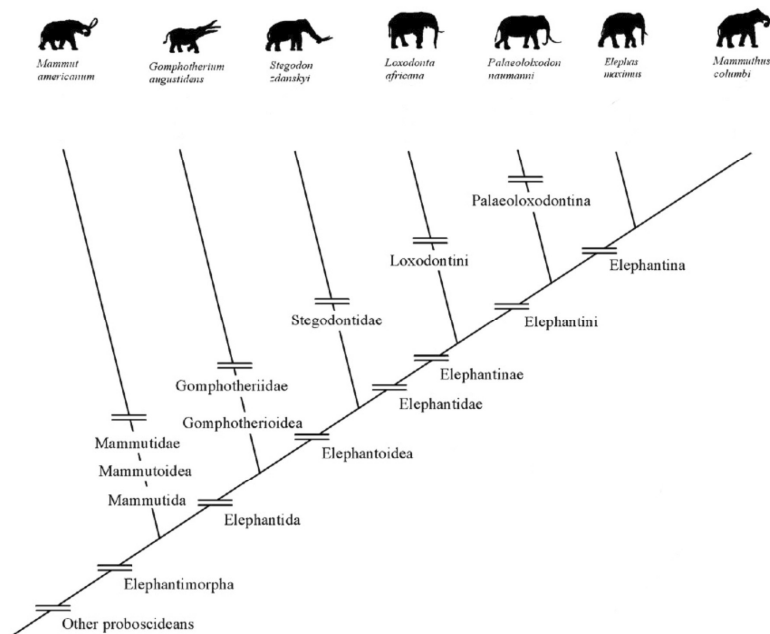


Figure 11 Cladogram of proboscidean taxa based on the available hyoid characters (drawn from Shoshani et al., 2007).

The taxonomic position of *Palaeoloxodon* (Matsumoto, 1924) was not established until about twenty years ago and was the subject of numerous studies. Some scholars considered *Palaeoloxodon* as a distinct genus from *Elephas* (i.e., Inuzuka, 1977 a and b; Takahashi et al., 1991). Matsumoto (1924), Osborn (1942) and Shikama (1975) related *Palaeoloxodon* to *Loxodonta*, whereas Poulakakis et al. (2002, 2006) asserted, based on molecular evidence, a closer relationship with *Elephas*. While *Palaeoloxodon* was later lowered to the subgenus level and included

in *Elephas* (Maglio, 1973; Caloi et al., 1996), Aguirre (1969) raised *Palaeoloxodon* to the rank of species. Recently, based on several morphological traits of the hyoid bone and skull, *Palaeoloxodon* has been more closely related to the extant Asian elephant than to mammoths or the modern African elephant (Shoshani et al., 2007; Todd, 2010). These reviewed phylogenetic relationships (**Figure 11**) support Palaeoloxodontina (Zhang and Zong, 1983) and Elephantina (Gray, 1821) as new sister subtribes.

Pioneering molecular studies on proboscideans induced contradictory results; criticism often focused primarily on methodological issues (i.e. Orlando et al., 2007). Paleogenomic studies have benefitted considerably of the recent technological advances in the analysis of ancient and degraded DNA extraction (which permitted the progressive back-dating of ancient DNA records), as well as in high-throughput sequencing methods (Orlando et al., 2013; Dabney et al., 2013; Meyer et al., 2016). A recent study devoted to the phylogeny of *Palaeoloxodon antiquus* and based on new mitochondrial and nuclear genomic evidence (Meyer et al., 2017) overturn widespread belief, grounded on morphological evidence, that *P. antiquus* and *E. maximus* are closely related to one another. Surprisingly, mito-genetic diversity suggests that straight-tusked elephants were closely related to the extant forest African elephant *Loxodonta cyclotis* (Meyer et al., 2017). Results also indicate that *Elephas antiquus* should not be used as synonym of *Palaeoloxodon antiquus* (Meyer et al., 2017). Osborn, in 1942, had actually placed *Palaeoloxodon* in the Loxodontinae on the basis of several skull traits. Evolutionary transformations, from an ancestor with morphological traits (in the skull and teeth) typical of *Loxodonta* to a descendant characterized by several *Elephas*-like features, may have involved gene flows between the two genera (Maglio, 1973; Sanders et al., 2010). *Loxodonta africana* and *L. cyclotis* are demonstrably linked to one another genetically (Roca et al., 2005). Conversely, Rohland et al. (2010) showed that incomplete lineage sorting could have allowed the retention of ancestral traits in forest elephants. In addition, Meyer et al. (2017) reveal that two specimens of straight-tusked elephant, one from Weimar-Ehringsdorf (WE), the other from Neumark-Nord 1 (NN1), are separated from one another based on mitochondrial evidence, but the analyses show that both have a sister group relationship with *L. cyclotis*. Mitochondrial DNA does not reflect the full evolutionary history of populations or species because it represents a single, maternally inherited locus; in addition, the transfer of mitochondrial DNA between hybridizing species is not unusual when gene flow is strongly male-mediated (Cahill et al., 2013; Petit and Excoffier, 2009; Li et al., 2016; Meyer et al., 2017), as is the case with elephants. Despite their geographical proximity, the WE and NN1 specimens analyzed by Meyer et al. (2017) occupy different positions in the mitochondrial tree. Electron Spin Resonance dating suggests an Eemian age

for the NN1 specimen (Schüler, 2010; Penkman et al., 2011, Sier et al., 2011) and a late Middle Pleistocene age for the one from WE (Schüler, 2003), which dates it to the previous interglacial (MIS7; Mallick and Frank, 2002). Hence, the very different mitogenomes between WE and NN1 might reflect fluctuations in home range of *P. antiquus* across glacial cycles (Meyer et al., 2017).

Meyer et al.'s (2017) phylogenetic reconstruction shows that *P. antiquus* is to be included into the *Loxodonta* lineage. This deeply modifies previous interpretations based on fossil remains and calls for a thorough revision of the taxonomic status of African elephantids. It also shows that, similarly to *Mammuthus* and *Elephas*, the evolutionary history *Loxodonta* is not confined to Africa. Finally, the genetic distance between *L. africana* and *L. cyclotis* justifies their separation as two different species, complementing the results of earlier studies based on morphological and genetic evidence.

3.2 *Palaeoloxodon antiquus*

The type specimen of *Palaeoloxodon antiquus* (Falconer and Cautley, 1847) is an incomplete mandible retrieved from upper Middle Pleistocene terrace deposits of the River Thames at Grays (England; Palombo and Ferretti, 2005). The anatomical features, variability, and ontogenetic modifications of the species are well-known thanks the abundant fossils from European deposits.

3.2.1 Main morphological features

The skull is typically high and short, with a flat frontal profile and a double-domed vertex. The shape of the forehead, more precisely that of the parieto-frontal ridge, is highly variable (Palombo and Ferretti, 2005). The different Eurasian populations of straight-tusked elephant can be distinguished based on forehead morphology (Saegusa and Gilbert 2008). German populations present the so-called “Stuttgart morph” which is mainly characterized by the weak development of the parieto-frontal crest. Conversely, the Italian ones, both from the continent and from the islands (Ferretti, 2008; Anzidei et al., 2010), show the “namadicus morph” which is characterized by having a strong parieto-frontal crest. The premaxillaries are fan-shaped and form a wide apron distally. The tusk curvature and size (robustness) vary greatly during ontogenetic growth, in the two sexes and also among the various populations from different geographic areas: e.g., the tusks of Italian adult males seem to be definitely stouter and less curved than those of German males, such as those from Neumark-Nord 1, of equivalent ontogenetic age (Palombo et al., 2010). In general, the tusks are large and divergent proximally, slightly curved downwards and towards the sagittal plane at approximately mid-length, and moderately upwards at the

distal end. Moreover, the transversal cross-section shows a typical Schröger line pattern, consisting of intersecting lines forming minute, diamond-shaped partitions. The outer Schröger angles range from about 60° (near the pulpal cavity) to 120° (near the cementum), and are therefore wider than in *Mammuthus* (Palombo and Villa, 2001 - 2003). The skull encloses other distinctive features, such as fairly slender zygomatic bones; a short mandible with moderately-developed symphyseal hook. The molars are hypsodont (i.e., HI 1.8–2.0 in M3) and the crown is relatively narrower bucco-lingually compared to modern species and mammoths. The enamel ridges are peculiarly wrinkled and the mean enamel thickness on third molars is 2.6–2.7 mm, with a maximum of 19–20 plates and 16 on average (Palombo and Ferretti, 2005). In general, occlusally, each plate, at an incipient wear stage, shows a large, oval, central loop and two smaller ones, symmetrically placed at its sides. At an intermediate wear stage, complete enamel loops are usually of either convex–convex or convex–concave type (Kalb and Mebrate, 1993); however, these morphologies are highly variable. One or two enamel folds are often present on the mesial and distal side of each enamel loop.

3.3 Geographical distribution and paleoecology of straight-tusked elephants

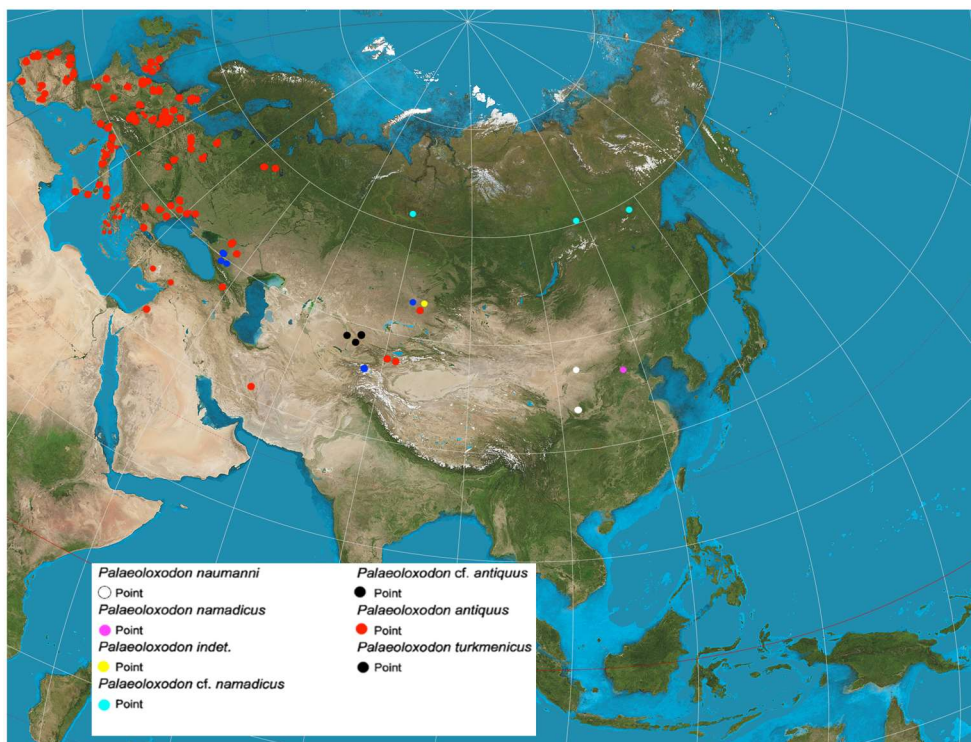


Figure 12 Geographical distribution of *Palaeoloxodon antiquus* and related species.

Palaeoloxodon antiquus is the second most represented elephant in the Eurasian fossil record after the woolly mammoth, *Mammuthus primigenius*. The species appeared in Europe around 750 Ka (Lister, 2017). Its name typifies the so-called Cromerian/Galerian *Palaeoloxodon*-faunal assemblage, which comprises also the Merck's rhinoceros *Stephanorhinus kirchbergensis*, the narrow-nosed rhinoceros *Stephanorhinus hemitoechus*, the hippopotamus *Hippopotamus amphibius*, the water buffalo *Bubalus murrensis*, the aurochs *Bos primigenius*, the giant deer *Megaloceros giganteus*, the fallow deer *Dama dama*, the roe deer *Capreolus capreolus*, and the European wild boar *Sus scrofa ferus* (Kahlke, 1986; Azzaroli et al., 1988; Stuart, 1991; Lister, 2004).

Large sized species are less sensitive to the harshness of living under severe and unstable climatic conditions than smaller taxa; consequently, they spread more widely. This is probably why the area of distribution of *Palaeoloxodon* ranged from Western Europe to Japan (**Figure 12**), which favored local speciation events along the way (Shoshani et al., 2007). Most of the fossil remains of *P. antiquus* found south of 55°N and west of 50°E (Pushkina, 2007); the species, therefore, can rightfully be considered a strictly European taxon. It was replaced by related species in eastern Siberia, China and Japan. Sound comparative analyses indicate that *Palaeoloxodon antiquus* indisputably derived from *Palaeoloxodon recki* (Maglio, 1973; Saegusa and Gilbert, 2008), which was dominant in Africa during Pliocene and the Early-Middle Pleistocene; then *P. recki* disappeared around 100 Ka (Owen-Smith, 2013).

Palaeoloxodon antiquus was adapted to woodland habitats and mild, humid climate and therefore was a typical component of interglacial faunas (Stuart, 1991), although it persisted also in cooler contexts (Mazza et al., 2006). Straight-tusked elephants were widely distributed over most of Eurasia during interglacial/interstadial phases. Populations of this elephant moved northward along alluvial plains and through broad-leaf woodlands (Stuart, 1991). In contrast, during glacial/stadial oscillations, it persisted in Mediterranean enclaves, and was replaced by the cold-adapted woolly mammoth elsewhere throughout Europe (Stuart, 1991; von Koenigswald, 2003). At the onset of the Last Glacial Stage (MIS5d–2), when steppe-tundra vegetation spread over most of Europe, its distribution contracted drastically; the species persisted only in relict, temperate forests of southern Europe (Stuart and Lister, 2007). Also, Caucasus (Baryshnikov, 1987), Urals (Stuart, 2005) and southern Russia probably were temperate refuges for straight-tusked elephants, thanks to the local warming effect of the Baikal Lake.

Palaeoloxodon assemblages are more difficult to recognize in eastern areas, because mammalian communities were usually more fragmented, which led to the formation of several regional communities and to enhanced heterogeneity (Pushkina, 2007). Under these circumstances,

local subspecies could form, albeit in the absence of physical and biological barriers (i.e., sympatric speciation and other non-allopatric pathways). When climatic oscillations were less severe, habitats turned less patchy in Eastern Europe and Siberia than in the rest of Europe and the distribution of the straight-tusked elephants often overlapped that of glacial-steppe fauna (Pushkina, 2007). All in all, in eastern areas local mammalian communities tended to respond differently from one another to climatic changes, in the smaller biogeographical contexts of central and western Europe faunal communities responded more evenly (Pushkina, 2007). Notable is that after the MIS5e interglacial *Palaeoloxodon*-faunal assemblage never spread again beyond the steppe barrier in Central Asia (Garut, 1986). Thereafter, the straight-tusked elephants were confined to Europe, probably because of the local, mitigating effects of the Atlantic Ocean and Mediterranean Sea, until their final extinction (Zagwijn, 1996).

Worth noting is that the central European fossil records indicate that warm- and cold-adapted species could sympatrically coexist, creating assemblages “non-analogous” to any modern ones (Guthrie, 1984; Aaris-Sørensen, 2009). Such kind of assemblages was atypical for both interglacial and glacial environments and included species that apparently should not coexist (Guthrie, 1984; Aaris-Sørensen, 2009). Sampling biases or extended time averaging over periods of rapid climatic fluctuations could explain these oddities (e.g., Stewart, 2008). Alternatively, and growing amounts of fossil remains seem supporting this hypothesis, the species might have had greater ecological flexibility than expected which enabled these species to coexist (Rivals et al., 2008; Pushkina et al., 2010). These issues could be addressed by accurate dating, careful verification of the ecological preferences of the species, as well as sound taphonomic analysis. Moreover, stable isotopic analyses of tooth enamel are another reliable proxy for accurate reconstructions terrestrial paleoenvironmental changes (e.g., Bocherens, 2011).

The history of the latest populations of *Palaeoloxodon antiquus* is still shrouded with uncertainty, mainly due to a very imperfect fossil record, as well as to stratigraphic issues. For long time it was accepted that *P. antiquus* became extinct in North Western Europe at the end of the Eemian. Only scanty remains were found associated with Mousterian and/or Aurignacian artifacts in Iberian and Italian cave successions (Stuart, 2005). Often these finds are difficult or even impossible to date because their ages are at or even beyond the limits of radiocarbon dating. Nevertheless post-Eemian records in Iberia, Italy and probably the Balkans suggested the hypothesis of *P. antiquus* surviving in Southern Europe into the early part of the Last Cold Stage (Stuart, 2005). New radiocarbon dates from remains of the straight-tusked elephant from the Netherlands point towards *P. antiquus* becoming extinct later than the Eemian also in Western and Northern

Europe. The youngest remains of *P. antiquus* are referred to 37,440 (+350, - 310) BP (Mol et al., 2007).

During the Plio-Pleistocene, new elephant taxa migrated into central and western Europe from Eastern Europe and Asia. Several fossil remains of elephants, including *Palaeoloxodon*, were discovered throughout continental and insular Italy, owing to the peninsula's southern geographical location, which offered a refuge for several species, including many elephant taxa, whose range was restricted by climate deterioration (Stuart, 2005). These dispersion events are fundamental references not only for local biochronological schemes, but also for wider scale correlations.

Important Italian findings are complete skeletons found at Riano (Maccagno, 1962b) and at Grotte S. Stefano-Fonte Campanile (Viterbo; Trevisan, 1948; Palombo and Villa, 2003). Skeletons in partial anatomical connection were retrieved from La Polledrara di Cecanibbio (Rome; Palombo et al., 2003); Casal de'Pazzi (Rome; Filippi et al., 2001). Both juvenile and adult skull remains were found at Pignataro Interamna (Cassino; D'Erasmus and Montcharmon Zei, 1955; De Lorenzo and D'Erasmus, 1927; Osborn, 1942). Isolated teeth and skeletal elements were discovered at Isernia (Sala, 1983), Venosa Notarchirico (Potenza; Piperno and Tagliacozzo, 2001; Lefèvre et al., 1998), Fontana Ranuccio (Anagni; Biddittu et al., 1979), Castel di Guido (Rome; Sala and Barbi, 1996), Pian dell'Olmo (Fiano Romano; Maccagno, 1962), Archi (Reggio Calabria; Bonfiglio and Berdar, 1983). Bones of a young adult female individual have been discovered at Campitello Quarry, in the outskirts of Bucine (Arezzo; Mazza et al., 2006). Other fossils were retrieved from various sites near Arezzo and Rome (Palombo, 1986, 1994). The straight-tusked elephant reached also Sicily, where it underwent dwarfism, in line with Van Valen's (1973) "Island Rule"; remains of its endemic, dwarf offspring, *Palaeoloxodon falconeri*, are known from Luparello (Palermo; Vaufray, 1929; Imbesi, 1956), Spinagallo Cave (Siracusa; Ambrosetti, 1968), and Alcamo (Burgio and Cani, 1988). Many specimens commonly ascribed to *P. mnaidriensis* based on their dimensional equivalence with dwarf elephants from Malta, are reported from several Sicilian localities; the richest collections of bones of *P. mnaidriensis* come from the lower Upper Pleistocene deposits of Puntali cave (Carini, Palermo). Many molars, mandible and postcranial remains of the dwarf *P. mnaidriensis* were also found, Grotta di Za' Minica (Capaci, Palermo), Cava di Asfalto (Ragusa) and Contrada Fusco (Siracusa; Chilardi, 1996). Conversely the specimens found in Via Libertà (Palermo) are similar morphologically to the remains of *P. antiquus* from continental Italy, but their size is somewhat smaller (Masini et al., 2008; Ferretti, 2008); which suggests that they might belong to populations genetically isolated from their mainland counterparts (Aguirre, 1968–1969).

3.4 Dental morphology

Elephants' molars are made of a pleated sheet of enamel, shaped like the bellows of an accordion, resulting in series of plates, transverse to the axis of the tooth, individually containing a pulp cavity coated with dentine and enamel, and covered externally by cementum (**Figure 13**). The plates originate from deep folds in the dental epithelium of a single germ. The development of each lamella is oriented, starting from the apical area, which is divided into several tubercles, and proceeds to the basal end. During the ontogenesis the dental pulp is covered with sheets of dentin, secreted from odontoblasts that progressively transgress inwards towards the pulp, and enamel, produced by ameloblasts that move outwards towards the oral cavity (Osborn, 1970). The enamel sheaths are completely embedded and covered with cementum secreted by mesenchymal cementoblasts of the dental follicle. Growth stops when the plates merge together, are embedded in cementum and roots are formed (Anthony and Fraiant, 1941). The latter are arranged in a "front complex", where the roots of the first 3/4 plates are clustered together, and a "rear complex", which includes the roots of all the other plates (Sikes, 1966). Both upper and lower molars are tilted downwards within the alveolus due to the lack of space longitudinally. Consequently, as they erupt, teeth rotate and emerge obliquely.

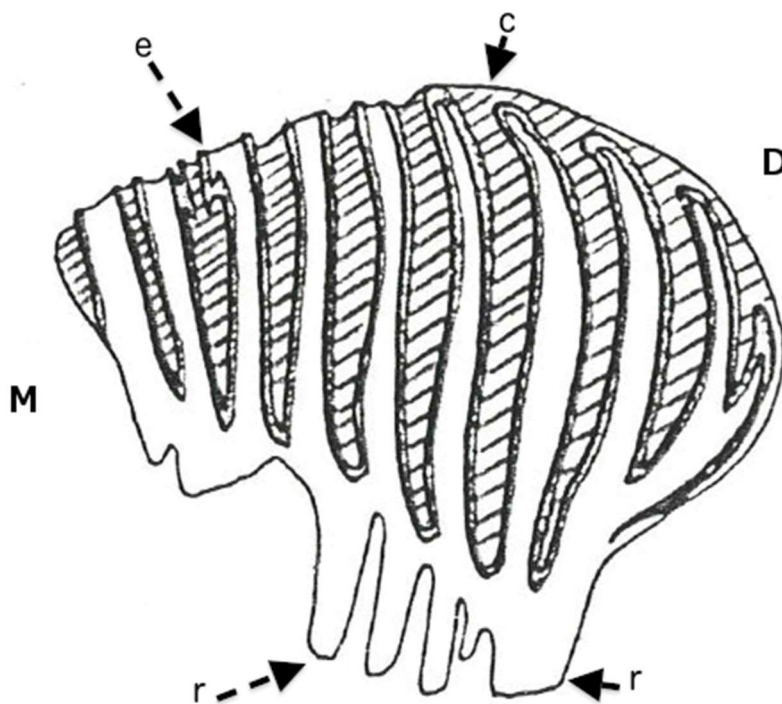


Figure 13 A molar of elephant along the parasagittal section view. (M = mesial, D = distal, r = roots, e = enamel, c = cement).

Dental ontogenesis is a lifelong process. Hence, molar replacement in elephants is in dynamic equilibrium with the chewing function (Roth, 1989). The molars are continually remodeled as they move progressively forward and are consumed. The plates are tilted with respect to the chewing plane. Wear starts at the mesial end of the first plate and gradually extends to the following plates, so that the front plates are completely consumed when wear reaches the rearest ones and starts affecting the following molar.

The shape of the plates is variable. Generally, the first ones are irregularly shaped, on account of the mechanical stresses they are exposed to at the contact with the preceding tooth, but also of genetic atavism (Aguirre, 1969). In fact, the presence of a median groove, with variable depth, separating the plate into a vestibular and a lingual portion and the retention of a rear/front median pillar in the first plates, are valuable examples of the preservation of vestigial traits in elephants' molars. The wear pattern consists of a series of enamel ridges with dentine cores, transverse to the main longitudinal axis of the teeth and alternating with valleys filled with cementum. Elephants' propalinal mastication causes the enamel ridges of the upper and lower molars to come in contact obliquely. The enamel ridges form the functional unit of the tooth and grind the food acting like scissor blades.

3.4.1 Dental tissues

Teeth and bones include both organic and inorganic components, plus water; in fresh enamel the ratio of organic to inorganic matter to water (by weight) is 2:96:2 (LeGeros, 1991). The organic components are made of collagen fibrils and non-collagenous structural matrix proteins. The main inorganic component of teeth (as well as of bones) is biological apatite, which is a nanocrystalline, non-stoichiometric and non-homogeneous calcium phosphate. It can be represented by the idealized chemical formula $[\text{Ca}_{10}(\text{PO}_4)_6(\text{OH})_2]$. However, the exact composition of bioapatite is not fully understood, because it changes in the different calcified tissues. It contains several minor and trace elements, which are substituted into the structure, absorbed onto the surface and/or present in inclusions of non-apatite phases (LeGeros, 1991; Wopenka and Pasteris, 2005). The carbonate ion (CO_3^{2-}) is the most important substitution for stable isotope analysis; it comprises about 3.5% by weight in enamel, 5.6% in dentin, and 7.4% in bone (LeGeros, 1991). Most carbonate ions are substituted in the phosphate site (B-type substitution), but can also be present in the hydroxyl site (A-type substitution) or be adsorbed onto the crystal surface (Elliott, 2002). In bone, specialized cells destroy and reconstitute the organic and inorganic components, to maintain functional efficiency. Hence, bone provides isotopic records relative to the last period of an individual's life (Manolagas, 2000).

Dentine is similar to bone in both structure and composition; nonetheless, it is harder and not continuously remodeled, so that its isotopic composition reflects the conditions at the time of the formation of the tooth. Collagen fibrils provide the matrix for bioapatite deposition. Dentin is permeated by several dentinal tubules, wherein odontoblasts diffuse nutrients and precipitate new dentin in response to injury (Nanci, 2003a).

The organic fraction in fully mature enamel is entirely made of non-collagenous proteins. Its formation is a two-step process. First, an organic-rich, partially (~30%) mineralized enamel is formed. Then, further mineral is deposited, and at the same time organic matter and water are removed, producing a mature tissue, which comprises 96% of bioapatite by weight (Nanci, 2003b). The enamel mineralization involves a vertical (occlusal to basal) and horizontal (enamel-dentin junction to outer surface) gradient (Kohn et al., 2002; Suga, 1982; Zazzo et al., 2005).

3.5 Elephants' feeding habits

During the Neogene, aridification and replacement of C3-dominated woodland with C4-dominated grassland, led to the development of high-crowned molars and to the lamellar structure of the teeth in different proboscidean lineages (Uno et al., 2011, Levin et al., 2011). Both are adaptations to increased dietary wear and possibly to the mechanics of masticating grass. The development of high-crown teeth imposed a substantial reorganization of cranial anatomy. More broadly, cross-taxon and vegetation studies interpret C3 or C4 feeding in Neogene ungulates of Africa, but also of other areas, as largely indicating browse or graze behavior.

Carbon isotope signature in paleosol evidences that the spread of C4 vegetation, in East Africa, started around 10Ma and accelerated after 4 Ma (Cerling et al., 2011; Levin et al., 2011). In elephants, enamel $\delta^{13}\text{C}$ data show that the switch to a C4-dominated mixed-feeding strategy began around 8 Ma and persisted little-changed through their subsequent history (Lister, 2013). Elephants underwent a threefold transformation. It started some 10 Ma, with small increases in the number of lamellae, followed by the second one during the 8–6 Ma interval, marked by moderate hypsodonty growth. It is only after 5 Ma that the number of enamel plates significantly increased and so did also hypsodonty. Nonetheless, it cannot be ruled out that some proboscideans fed on C3 grasses before 8 Ma ago, like modern Asian elephants that feed on bamboo (Cerling et al., 1999). The isotopic results do not fully clarify if the morphological changes triggered these behavioral modifications. Before 5 Ma gomphotheres, early elephants and stegodonts, whose tooth morphology is generally associated with soft-leaf browsing, showed limited dental changes; yet, isotopic signals indicate that

they had already switched to a more grazing behavior (Zazzo et al., 2000). Environmental changes probably offered new ecological niches favoring behavioral prior to morphological adaptations, which led to the selection for enhanced dental resistance to abrasion. Grasses not only contain more biogenic silica (phytoliths) than leaves and shrubs, but grazing ungulates are low-feeders and, thus, ingest a greater amount of soil-derived grit than tree-feeding browsers. Before 5 Ma, the dental morphology of elephants did not change substantially because of the low phytolith concentrations contained in the C3 grasses they fed on and of the limited airborne dust present in the semi-wooded landscapes where they lived. The dental changes connected with the transition to grass feeding was observed in several mammal lineages (e.g., in horses, Mihlbachler et al., 2011). The “evolutionary lag” due to behavioral shift to grazing is often considered implausible because of the implied period of “maladaptation” (Janis, 2008); however, both these functional and morphological modifications led to a higher selective advantage to exploit new resources. In fact, during the 8–5 Ma interval, elephants had their molars exposed to enhanced wear as a result of their grazing behavior, but the advantage offered by exploiting a new ecological niche imposed modifications to their life-history, such as, for instance, earlier reproduction. Another modification connected with the adaptation to graze was the development of the peculiar system of horizontal replacement of the molars, which had been achieved before 8 Ma. The appearance of a long series of molars with transverse lamellae held together by cementum, followed by the multiplication of plates and eventually by increased hypsodonty were crucial acquisition. The lag between the onset of grass-eating and the associated morphological adjustments (hypsodonty and lamellar number) could be explained supposing that the amount of environmental grit that was ingested with the food increased progressively reaching relevant levels only after 3.5 Ma, in parallel with the increasing aridity strongly correlated with the opening of landscapes and with augmented airborne particulate matter. By and large, growing competition by encroaching short grass feeders (typical of more arid grasslands) and increased dust and soil uptake might have expanded considerably the guild of grazing elephants.

Several evolutionary trends are apparent in the various proboscidean lineages. The *Palaeoloxodon recki/iolensis* lineage reached the highest values of lamellar number and hypsodonty only after 0.5 Ma, at least 7 Ma after the onset of a grazing-dominated diet. *Elephas* and *Mammuthus* showed similar morphological changes approximately during the same time period, which might reflect common limits of the rate of adaptation, or their being exposed to similar environmental pressure, in southern and northern Eurasia (Lister and Sher, 2001; Lister et al., 2013). Conversely, the two late elephantoid lineages *Stegodon kaisensis* and *Anancus kenyensis/ultimus* that had survived the first behavioral switch to grazing, failed to develop the

necessary morphological adaptations and went regionally extinct soon after 4 Ma (Lister, 2013).

Loxodonta cyclotis and *L. africana* have similar hypsodonty index, typically ranging from 1.7 to 2.1 (Aguirre, 1969; Cerling, 2011), and number of lamellae, i.e., 10–12 plates (Debruyne, 2003; Laws, 1966). Fossils show that the current lamellar count was reached about 3,5 Ma; in contrast, the present hypsodonty index was attained after 2 Ma (Sanders, 2011). Despite its current forest habitat and browsing diet, *L. cyclotis* evolved from mixed-feeders as indicated by its lamellar counts and hypsodonty index which could not be attained living in canopy forest. This hypothesis cannot be tested due to the paucity of fossils from tropical forests (Lister, 2013). However, the wide range of $\delta^{13}\text{C}$ values in enamel, typically detected in mixed-feeding to grazing diets, actually indicates an expansion of open habitat (Lister, 2013). Around 2 Ma savannah and forest *Loxodonta* elephants may have entered Central African forests; no fossil remains of *Loxodonta* have been found in savannah contexts, where *Palaeoloxodon recki* became ecologically dominant, after this time period (Sanders and Haile-Selassie, 2012). It is still unclear if the first populations of modern *L. africana* persisted in savannah grasslands, or returned to them from the forest (Lister, 2013).

Multiproxy analyses suggest that modern elephants show significant dietary flexibility and fall within the so-called “browsing-grazing transitional phase”, which includes taxa that are situated between the ranges typical for browsers and grazers, i.e., seasonal, regional and meal-by-meal mixed feeders (Cerling et al., 1999; Codron et al., 2006; Sukumar, 1989). Based on conventional microwear scars, both Asian and African elephants display average numbers of scratches typical of grazers (Solounias and Semprebon, 2001). In general, enamel surfaces show high numbers of scratches and very high percentages of purely coarse scratches and cross scratches. Moreover, few pits can be observed on average, although all the individuals show high percentage of very large pits and gouges which are suggestive of the consumption of tree branches and bark. *Loxodonta africana* differs from *Elephas maximus* by displaying a higher number of pits, gouges, and cross scratches, which are, usually, produced by coarse food, such as tough bark. In addition, Asian elephants that subsist on softer food are closer to the morphospace of grazers than *Loxodonta* (Solounias and Semprebon, 2001).

Elephant’s diet may include grasses, herbs, bark, fruits and tree foliage. In savannahs, grasses may make up to 70% of elephants’ diet, in the wet season; during dry period of the year, the contribution of browse grows progressively. Trees represent up to three-quarters of the species fed upon (White et al. 1993) and in tropical forest environment leaves, twigs, bark and fruit reached 90% of total bulk eaten (White et al. 1993). Mean daily intake ranges from 4% (Laws et al., 1970) to 7% (Ruggiero, 1992) of body

weight, with lactating females consuming proportionately higher quantities of foods (Laws et al., 1970). Elephants are long-lived animals, reproduce at low rate and have low mortality rates; and, achieving a complete understanding of the interactive processes would be time consuming and would require using proxies for describing and understanding the complex system that operates on a scale much longer than human lifespan. Elephants affect greatly the structure of vegetation and, perhaps, also the animal communities living in it. The study of elephant-environment interactions includes: elephants' population dynamics, density, distribution and food selection, but also the population dynamics and responses to environmental stresses on the plant communities. Vegetation dynamics, however, are not only by elephants affected by elephants, but also by other environmental factors, such as fire, climatic extremes such as drought, high rainfall and flooding, frost, high wind, browsing by other herbivores and human activities.

Chapter 4 Paleobiological and taphonomical analyses

4.1 Materials

Most of the fossil vertebrate remains have been collected from Unit 2 but scattered bones were also found in Units 4 and 6. A total of 634 specimens were retrieved from Unit 2.

4.2 Methods

Paleobiological and taphonomic analyses started with the anatomical and taxonomic (class/gene/species) identification of the fossil remains. This was performed using atlases but also, and above all, the collections of fossils of the section of Paleontology of the Museum of Natural History of the University of Florence, as well as the osteological collections of the Zoological section and of the Borzatti von Löwerstern Comparative Collection of Recent Specimens, which are both kept in the same museum.

A computer archive was produced based on the data collected for both the paleobiological and taphonomic studies. The relative abundances of the taxa from the different layers were expressed in NISP (number of identified specimens) and in MNI (minimum number of individuals) counts. Specimens have been attributed to single individual by side matching, taking into account several characteristics, such as size, relative proportions, the degree of ossification, age and state of preservation. To avoid biases induced by different fragmentation potential, the NISP was calculated separately for each of three distinct size classes. The first includes animals of small size with a weight between 10 and 100 kg, the second one animals of medium to large size, up to 300 kg; and the last one involves very large animals weighing over 300 kg.

Most of the remains were concentrated in a relatively small area of the depositional Unit 2; for this reason, the archeological context had no influence on the estimation of the MNI. In addition, possible analytic deviations caused by the aggregation on the MNI counts were avoided by analyzing the entire faunal assemblage from Poggetti Vecchi (Brewer, 1992; Grayson, 1978, 1984).

Bones can be fractured by both abiotic and biotic agents; the former include sediment load, physical and mechanical stresses associated with many ways of transport, and chemical alterations; the latter involve a whole range of organisms, from microbes to plants, invertebrates and vertebrates (humans included). Haynes (1983), and Villa and Mahieu's (1991) studies focused on bone fragmentation and provided the criteria for distinguishing between bones broken in fresh or dry state. These papers were therefore used precisely for this purpose. If green bone fractures can be related to intentional butchery they can provide insights into human carcass-

processing behaviors, as well as into the existence of possible rituals. The relative frequency of the different fracture features are presented in NISP counts.

The Poggetti Vecchi fauna comes from a lacustrine marginal deposit; the susceptibility of the specimens to hydraulic transport had to be estimated. This was obtained by adopting Voorhies' approach (Behrensmeyer, 1975; Villa and Mahieu 1991; Voorhies, 1969), which assesses the susceptibility of individual, isolated specimens to winnowing (fluvial scattering).

Bone surface modifications (pre- and post-depositional) were sought for using lens at 10x magnification under oblique illumination. Human- and non-human-derived modifications can be distinguished only after careful inspection: e.g. human-derived alterations (intentional fracturing, skinning, defleshing, butchering) are tell-tale carcass processing marks. Non-human-derived damage may include cortical-surface degradation (e.g., weathering, mechanical wear by water transport resulting in polishing or abrasion), biochemical corrosion (e.g., digestive fluid corrosion, root or humic-acid etching), biomechanical modifications (e.g., bites, punctures, scorings, gnawing marks, trampling), post-burial physical and chemical alterations (diagenetic modification, the major being the transformation of hydroxyapatite into fluorapatite/frankolite). Tallying these pre-depositional, post-depositional and post-burial alterations over all the specimens permitted to trace to which the fauna was subjected at Poggetti Vecchi. Particular attention has been paid to possible evidence of scavenging.

The relative degree of weathering can be roughly correlated with the time elapsed since the death of the animal (Behrensmeyer, 1978). Nevertheless, it depends on bone compactness and porosity, and thus on the size of the elements, as well as, on the relative anatomical district they belong to: the cortical layers of the short bones and of the diaphyses of the long bones of large animals are generally far more resistant to weathering than the external layers of flat bones of smaller-sized taxa. However, the resistance to weathering is strongly dependent also on the environmental conditions, such as temperature, humidity, vegetation, exposure, shading, nature of substrate which can either accelerate, slow down, or even inhibit this kind of alteration.

The degree of weathering was evaluated following Behrensmeyer's (1978) weathering stages (from stage 0 – non-altered to stage 5 – heavily altered). The paleobiology of the Poggetti Vecchi mammals (age and sex) have been assessed based on different proxies. Ontogenetic ages were calculated from the degree of ossification and epiphyseal fusions (Roth, 1984; Kangwana, 1996; Lister, 1999; Reitz and Wing 2010; Speth, 2000; Herridge, 2010), as well as from tooth eruption and wear (Laws, 1966; Krumrey and Buss 1968; Brown and Chapman 1991; Haynes, 1991; Hillson, 2005; Rasmussen et al., 2005). Although the timing of tooth

eruption and bone development are subject to modification by sex, health, nutrition, and individual variability, the stages of these ontogenetic processes are under genetical control; thereby, individual ages can be reliably defined based on tooth emplacement and bone development. Teeth, however, have the advantage of being more durable than bones, and therefore most of the ages of death are actually inferred from teeth. In this study, the capital letters represent upper cheek teeth (e.g., M1), while lower case letters indicate lower teeth (e.g., m3).

Some of Poggetti Vecchi's mammal remains have been tentatively sexed, aiming at assessing the relative frequencies of males and females. Distinguishing the bones of the two sexes, especially in the case of dimorphic species, is somewhat easier dealing with coxal bones, metapodials, teeth, skulls and cranial appendages. Palombo and Villa (2003) was followed to sex the remains of *Palaeoloxodon antiquus*.

4.3 Results

4.3.1 Paleobiological data

The macromammal assemblage from Unit 2 is dominated by very large herbivores: the straight-tusked elephant (*Palaeoloxodon antiquus*) and the aurochs (*Bos primigenius*), which represent 67% and 32,6%, respectively, of the total remains based on NISP counts. Red deer (*Cervus elaphus*), roe deer (*Capreolus capreolus*) and fallow deer (*Dama dama*), are quite less frequent; the red deer is the only middle-sized species from this Unit. Small-sized species include the roe deer and fallow deer, which are represented by 1,4% and 1,2% of the bone fragments, respectively. A right upper canine and a left m2 attest the occurrence of a very advanced *Ursus deningeri* transitional to *U. spelaeus* (*Ursus deningeri-spelaeus*: Auguste, 1992; García et al., 1997; Pacher and Stuart, 2008). This Unit gave also sparse remains of the European pond turtle *Emys orbicularis*, a vertebra of the European whip snake *Hierophis viridiflavus*, and two fragmental bones of birds (belonging to the Anatidae family). The list of the species, their frequencies and relative abundances in NISP counts, are reported in table (Table 2) and shown in Figure 14.

Taxa	NISP	NISP %
<i>Palaeoloxodon antiquus</i>	283	39.70
<i>Bos primigenius</i>	138	19.35
<i>Capreolus capreolus</i>	12	1.70
<i>Dama dama</i>	1	0.14
<i>Cervus elaphus</i>	38	5.80
<i>Ursus deningeri-spelaeus</i>	2	0.28
<i>Arvicola terrestris</i>	62	8.70
<i>Terricola</i> sp.	2	0.28
<i>Microtus</i> cf. <i>arvalis</i>	1	0.14
Aves	2	0.28
<i>Emys orbicularis</i>	4	0.56
<i>Hierophis viridiflavus</i>	1	0.14
Doubtful attribution	74	10.37
Indetermined	93	13.04
Total	713	

Table 2 Vertebrate taxa from Poggetti Vecchi with relative frequencies expressed in Number of Identified Specimens (NISP) counts.

Based on the developmental stages of different skeletal remains (skull, mandible, molar, and tusk) from Unit 2, *Palaeoloxodon antiquus* is represented by a total of 7 individuals: 3 juveniles of 1-8 years, one 14-15-year-old sub-adult, two 20-30-year-old adults, and one individual older than 40 years. The skulls are crushed into splinters; a fairly complete, but poorly preserved, tusk (n.162) belongs to one of the young-adult individuals. Based on the criteria proposed by Palombo and Villa (2003) and Lister (1996), the assemblage from Poggetti Vecchi's Unit 2 includes elements of both males (i.e., the right pyramidal 987, which has the articular surface for the unciform largely overlapping the hooked process; the right uncinat 295 which bears an elongated and straight joint surface for metacarpal V) and females (i.e., the right coxal bone 5245 with the wing of the ileum shaped like that of female individuals of *Mammuthus*). Unit 2 yielded the remains of at least 4 individuals of *Cervus elaphus*, ranging in age from 3 to 12/13 years. Notable is the occurrence of at least 9 left and 3 right fragmental cranial appendages of this species: surprising is that they all belong to shed antlers. *Capreolus capreolus* is present with only a single adult individual; in contrast, *Bos primigenius* includes a fetus, a juvenile and an adult. All the other taxa include one individual each.

The watervole *Arvicola amphibius* approximates 95% of the small mammal counts. It is represented by individuals with undifferentiated dental enamel (*sensu* Heinrich, 1978). The species commonly inhabits waterside habitats. The genus *Microtus* includes only 3 specimens (a fragmental left m1, attributed to *Microtus* cf. *arvalis*, a left m1 of *Microtus* (*Terricola*) ex gr. *savii*, and a right M1 referred to *Microtus* sp.). The first lower molars of

Terricola show a relatively short and wide anteroconid and wide anterior cap, which are features suggestive of *Terricola* species of the *savii* group. Altogether, the small mammal fossil assemblage from Units 4 and 6 are very similar to that found in Unit 2; Unit 4, in particular, gave virtually the same relative frequencies. From Unit 2 to Unit 6 *Arvicola amphibius* drops to 88%, and decreasing abundances are recorded also for *Microtus* spp.; its undetected presence cannot be ruled out in either units. Worth noting is the occurrence, in Unit 6, of a fragmental mandible of *Crociodura* cf. *suaveolens* and of a fragmental maxillary bone of *Oryctolagus* sp.

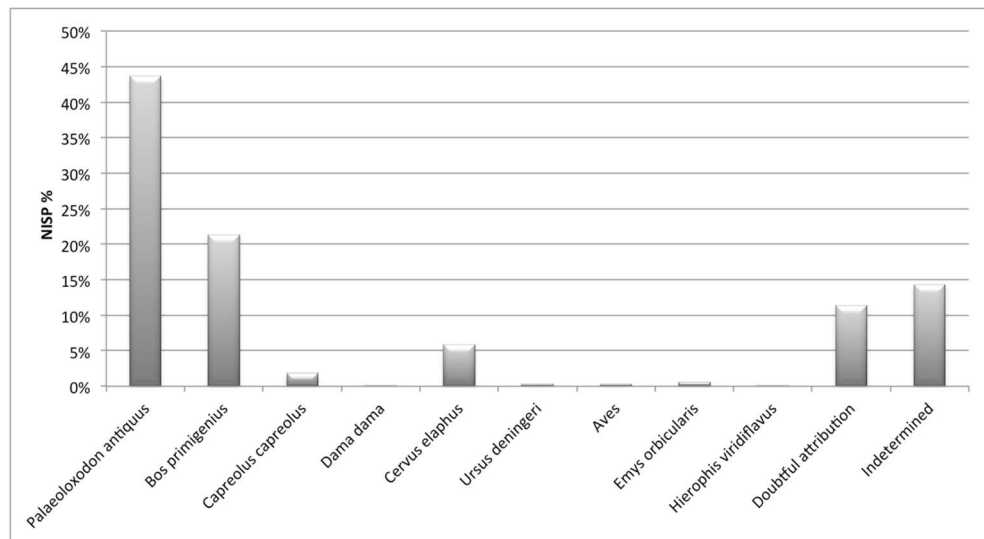


Figure 14 Relative frequencies of the vertebrate taxa expressed in Number of Identified Specimens (NISP) counts (data are reported in **Table 2**).

4.3.2 Taphonomic results

The 634 vertebrate specimens retrieved from the dark clay sediments of Unit 2 had subhorizontal orientation, and were concentrated in a NE-SW-trending strip. Several long bones were bimodally oriented NW-SE and N-S. They were found juxtaposed with little or no sediment in between them (**Figure 5** in Chapter 1). The general state of preservation of the bones is good; almost all, however, are broken and have severely scratched surfaces (**Figure 15 and 16**). The relative skeletal frequencies of the site's best represented species, i.e., *Palaeoloxodon antiquus* and *Bos primigenius*, gave revealing results. The vertebrae, basipodial bones, and phalanges of *P. antiquus* are unexpectedly under-represented (**Figure 17A and B**), whereas the opposite occurs for *B. primigenius*. Due to their high fragmentation, ribs are generally overestimated in the NISP counts.

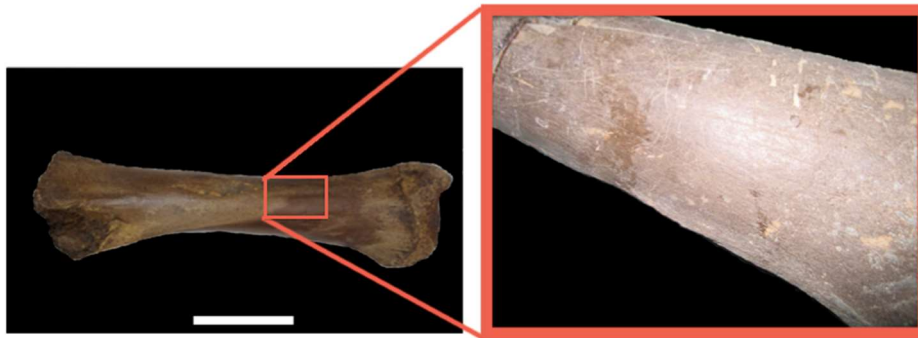


Figure 15 Right tibia of *P. antiquus* with proximal epiphysis unfused and distal in fusion. White bar = 10 cm. The red box shows a detail of the scratches due to trampling.

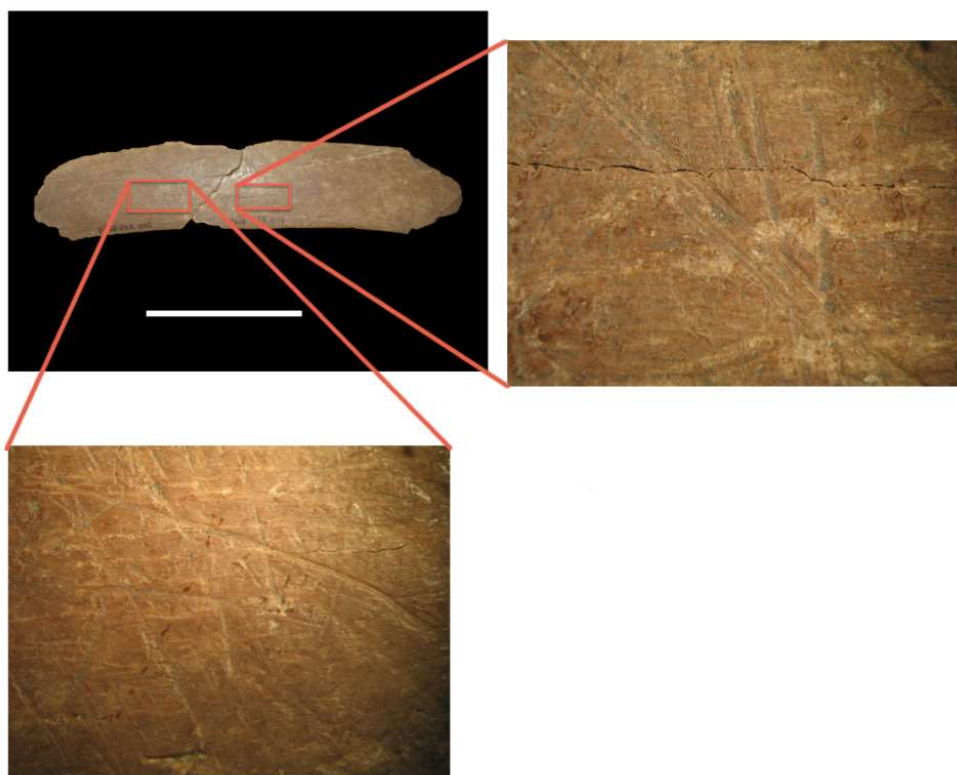


Figure 16 Rib fragment of *P. antiquus* with extensive trampling marks (red box). White bar = 10 cm.

The analysis of the collection of remains of *Palaeoloxodon antiquus* reveals that easily winnowed bones of the Voorhies Groups I (i.e., ribs and vertebrae) and I & II (i.e., phalanges) are under-represented; in contrast, the modestly transportable ones, belonging to Voorhies Group II (i.e., humerus, radius, pelvis, femur, tibia, metapodial) and the lag elements of Voorhies Group III (i.e., skull, mandible), are quite more numerous. Moreover, the elephant bones show relatively low incidence of abrasion/polishing (18.63%). *Bos primigenius*, *Cervus elaphus* and *Capreolus capreolus* are largely represented by bones that are susceptible to hydraulic transport. In

fact, most of them are polished and show evidence of abrasion (28.43% of these belong to *Cervus elaphus*, 27.45% to *Bos primigenius*, and 5% to *Capreolus capreolus*).

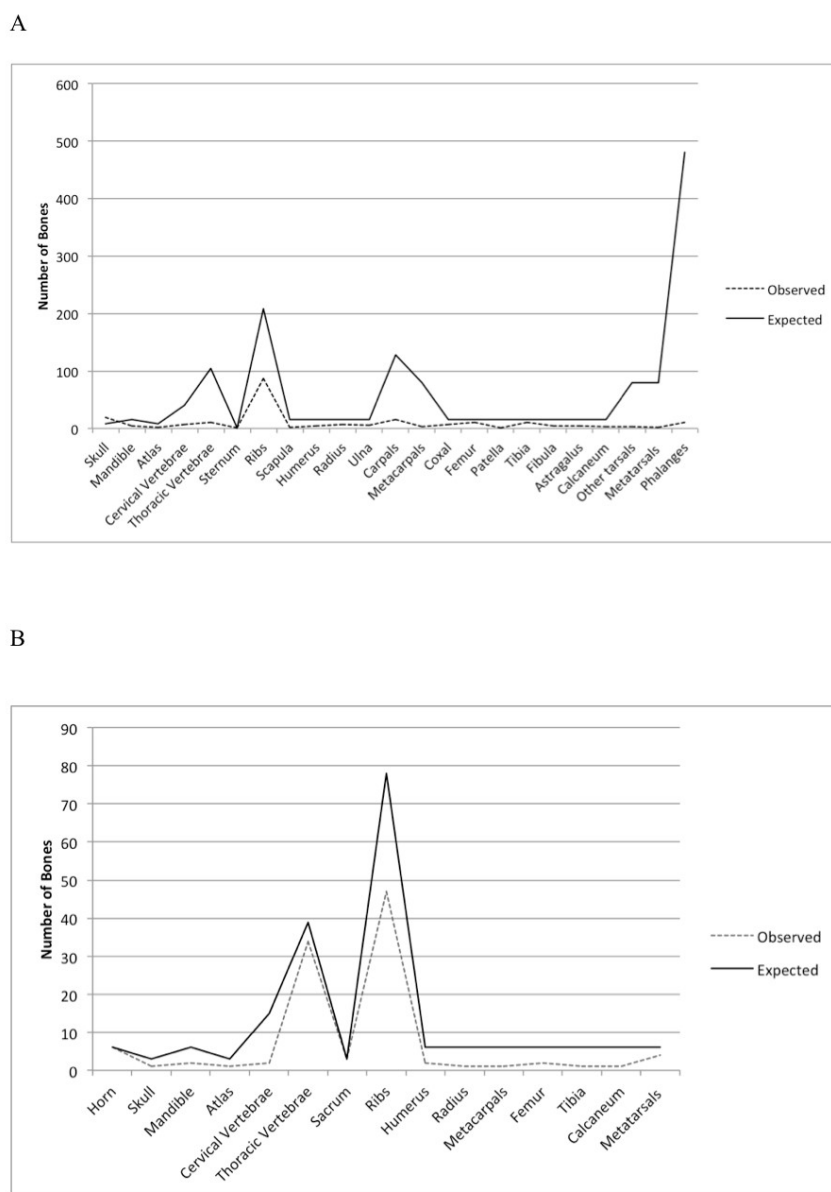


Figure 17 Frequencies of skeletal parts (Observed versus MNI-based expected amounts of bones). A) *Palaeoloxodon antiquus*; with a marked under-representation of axial bones, basipodial bones and phalanges. B) *Bos primigenius*.

Based on NISP counts, virtually all the hardparts are broken (91.75%). Most (23.91%) were fractured in dry state and only 7% in fresh state. Scratches have been observed on many bones (56.1%) belonging to *P. antiquus*, *B. primigenius*, *C. elaphus*, *C. capreolus*, and *U. deningerispelaeus*.

Very few bones (3.5%) have undergone modest weathering (1.8% are in weathering stage 1, and 1.5% in weathering stage 1/2-2:

Behrensmeyer 1978). Root etching (2.7%) was observed on the bone surfaces and, sometimes, also on the fractures. Humic corrosion evidence is very low (1.4%).

A few bones (4.53%) show evidence of scavenging. The size of the scoring marks, pits and bites are suggestive of a predator or scavenger with blunt pointed teeth (**Figure 18, 19 A and B**). The occurrence of rare hyena coprolites and of an erratic left second lower premolar of the spotted hyena *Crocuta crocuta* attest to the presence of these carnivores at the site. The damages were mostly observed on bones of *Bos primigenius* (femur, calcaneum, vertebrae and ribs), and *Palaeoloxodon antiquus* (proximal margin of ascending ramus of juvenile mandible n.5546, transverse processes of thoracic and cervical vertebra, end of a rib, both ends of ulnae and humerus, as well as, on individual fragments of long and flat bones). Finally, only three specimens show evidence of human-derived modification: the lateral portion of the diaphysis of a left humerus of *Bos primigenius*, the basal portion of a shed right antler and a fragmental diaphysis of a tibia of *Cervus elaphus*. Both humerus and tibia are very polished.

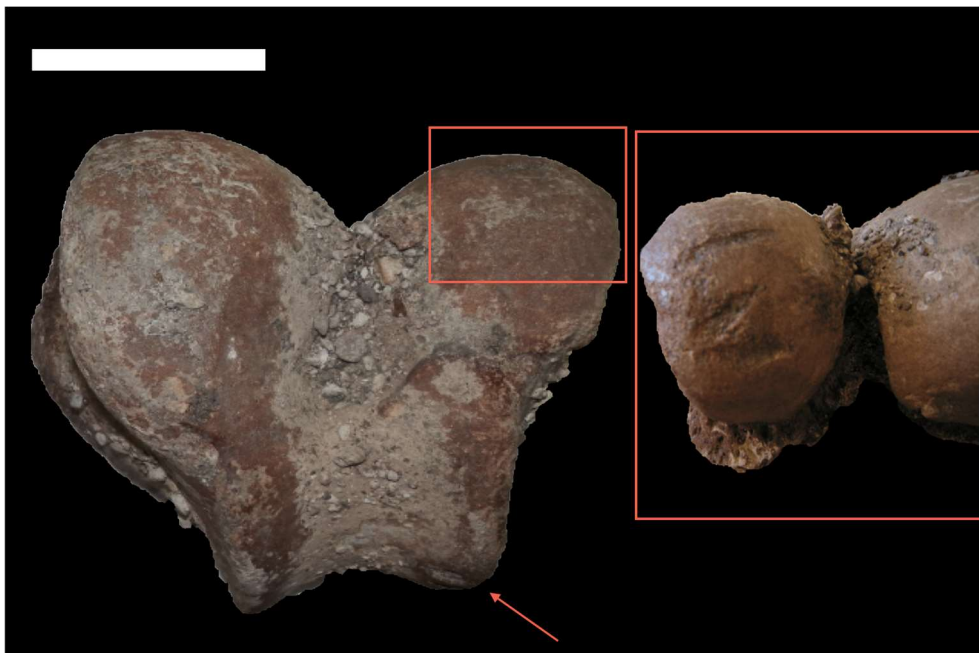


Figure 18 Unfused distal epiphysis of a right femur of *P. antiquus* with bites probably made by spotted hyena. The bites are transversal to the trochlear axis and of the intercondyloid fossa, on the lateral lip of the trochlea (red arrow) as well as on the lateral condyle (as shown in red box). White bar = 10 cm.

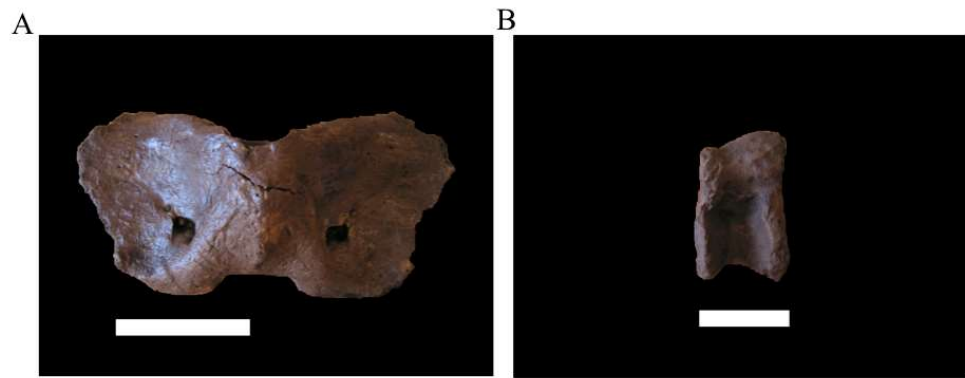


Figure 19 **A** Atlas of *B. primigenius* with bites on the margin of the wigs. White bar = 10 cm. **B** Astragalus of *B. primigenius* with extensive occurrence of bites and gnawing marks. White bar = 5 cm.

4.4 Discussion: Paleobiological and taphonomic inferences on the elephant remains

As mentioned in chapter one, Poggetti Vecchi differs from other similar sites in many respects (e.g. stratigraphic age, number of elephants involved, kind of artifacts). The Poggetti Vecchi sticks are short wooden tools, probably multipurpose digging sticks used for harvesting, or hunting small game, which are common among all primitive populations (D’Errico et al., 2012; Nugent, 2006). Probably both stone tools and sticks formed a tool-kit that (local?) early Neanderthals normally carried along with them. It can be alternatively speculated that the wooden tools were somehow involved with the scavenging of the elephant carcasses, or employed as skewers for carrying away chunks of meat. Consequently, the lack of paleobiological and taphonomic evidence for active hunting suggests that the Poggetti Vecchi elephants probably died from some natural, catastrophic event.

The presence of females and males coupled with the wide age spectrum of the different individuals (cubs, sub-adults and one adult) and the bone-to-bone contact of their remains (that were all piled up with virtually no interposed sediment) suggest that the straight tusked elephants of Poggetti Vecchi were components of a family group, which likely died at the same time. Different hypotheses can be formulated to account for the simultaneous deaths and, a plausible scenario could be a very intense cold snap, beyond the elephants’ thermal tolerance limits and too sudden to flee from. *P. antiquus* typified the wooded, temperate phases of the odd-numbered marine oxygen isotope stages (Stuart, 1982) and it is therefore normally considered a distinctive interglacial marker in both central and northern Europe. Nonetheless, it can occasionally be encountered during milder interstadials of intervening cold phases (Lister et al., 1990), as well as, under the cool conditions of a stadial phase (Mazza et al., 2006). It is

anyhow unlikely that this specie could survive prolonged and intense winter frosts.

Based on these insights, the lowland plain of Poggetti Vecchi, with its geothermal hot springs, might have offered a shelter to the elephant clan during a particularly cold season, during a time period spanning the MIS7-6 transition. By being forced to stay near the only heat source, they consumed all the vegetation in the surrounding area and finally died of starvation.

Another possible option is that the elephants were killed by emissions of poisonous gases from the geothermal springs, or died from drinking contaminated water. Geothermal fluids contain dissolved gases, such as carbon dioxide (CO₂) and hydrogen sulfide (H₂S), as well as high levels of toxic elements, such as arsenic, mercury, lithium and boron. Furthermore, both carbon dioxide and hydrogen sulfide are denser than air and tend to accumulate in depressed or confined areas. High concentrations of carbon dioxide can saturate blood in a matter of minutes, and quickly lead to respiratory arrest and death (Ikeda et al., 1989). Hydrogen sulfide is even more lethal already at relatively low concentrations (Adelson, 1966). Exposure to concentrations of only 300 ppm for 30 minutes renders humans unconscious, and exposure to a 1.000 ppm concentration causes rapid paralysis of the respiratory system, cardiac arrest and death within minutes. Elephants with the size of *Palaeoloxodon* may have taken longer to collapse, but in time they too would have succumbed. Conversely, it seems highly unlikely that drinking toxic water would have caused the simultaneous death at the same place of several individuals, of different ages, sexes and sizes.

Another possibility is that the elephants were caught by a flood. Several lines of evidence, however, rule out that they were caught by flash floods, drowned, and that their carcasses were carried downstream and eventually deposited. Elephants are notoriously good swimmers (Johnson, 1980) and are favored by their unique lung anatomy, but also by their capability to use their trunks for snorkeling (West, 2001). Moreover, only a major flood would be capable of carrying off animals of these sizes. The site's fine-grained entombing sediments do not show the unequivocal features of this kind of event.

The accumulated evidence indicates that the carcasses lied largely unexposed and inaccessible to predators, presumably at least partially immersed in water. In fact, there is very low impact of carnivore ravaging and very low incidence of weathering, but also no evidence of human-derived modifications. The few bites and gnawing marks suggest that carnivores had access only to very few parts of the carcasses. Decomposition then progressed in the conservative environment until complete skeletonization. After this, the skeletons were disarticulated, and the bones scattered nearby, presumably by occasional streams of water.

Although the death of elephants cannot be associated with active hunting, the high amount of stone and wooden implements found closely interspersed among the bones suggests that humans managed to access the great amount of flesh that the lucky circumstances made available. The great abundance and variability of the tools and their association with bones may also be due to coincidence, however it seems more plausible to assume that these aspects are not due to chance but a sign of the close interactions between the accumulation of carcasses and the evidence of human presence. Furthermore the wear patterns on the edges of stone tools indicate butchering actions on soft animal tissues but also of scraping or shaving wood, which suggests that the wooden rods were probably at least partially manufactured directly at the site. It is also likely that they removed only small amounts of flesh, without reaching the bones. Hafted axes usually produce chop-marks and not simple cut marks on bone surface (Haynes, 1991; Haynes and Klimowicz, 2015). The absence of stone axes at Poggetti Vecchi may account for the lack of chop-marks. These tools are heavy-duty implements capable to detach large portions of meat from the bones. In contrast, knives require much greater effort to reach muscle origins and cut strong, tough tendons. Hence, if knives were used to butcher the Poggetti Vecchi elephant carcasses it is likely that they would have left no cut marks on the cortical surfaces of the bones. It has been experimentally demonstrated that knife-edges are dulled by slicing against hard surfaces (Haynes and Klimowicz, 2015). In case, new tools have to be procured or manufactured directly at the site, or otherwise the original knives need to be resharpened by frequent retouching.

The scattering of bones in a fairly small area, the total lack of anatomical connection between different bone elements and the virtual absence of specific kinds of bones such vertebrae, basipodial and metapodial bones, and phalanges account for some kind of skeletal selection. Whether this occurred before or after the skeletonization and dismembering of the carcasses is unclear. The behavior of extant African hunters (Crader, 1983; Fisher, 1992) may provide insights into the possible patterns of processing and preferential selection of the elephant carcass parts at Poggetti Vecchi. In general, the proximal parts of the limb bones and the extremities are removed from the carcasses and transported to the villages, where the flesh can be stripped off more accurately and marrow extracted if necessary. A similar behavior could explain the underrepresentation of basipodial and metapodial bones and phalanges in the Poggetti Vecchi elephant samples. Nonetheless, the Voorhies (1969) categories of bones represented at the site indicates that the winnowing action of streaming water could also well explain the very low frequencies of easily transportable elements. At the same time, streaming water may account for the occurrence of the remains of other taxa (*Bos*, *Cervus*, *Capreolus*): these bones, which are quite susceptible to hydraulic transport, are largely

abraded or polished. They were therefore likely reworked from uphill areas and are allochthonous for the site.

The final steps of the story are suggested by the extensive scratching of the bone and tusk surfaces, as well as by the dry bone breakage. This evidence is highly suggestive of trampling by bypassing animals, elephants included. Hence, trampling and kicking can account for the disarticulation and scattering of the skeletons when the bones were already in dry state. Finally, the root etching and humic corrosion on many bones are probably associated with the temporary formation of a soil. Therefore, the bone-bed was either reached by the roots of aquatic plants or buried in pedogenized sediments colonized by plants.

4.5 Paleoenvironmental reconstruction

The integrated multiproxy approach used in the analysis of Poggetti Vecchi offered an effective tool for deconvolving the succession of events that occurred during the deposition of Units 1-6. Four different flooding events were detected, separated by regressions. During the flooding episodes homogeneous organic muds deposited in shallow, protected lacustrine settings; in contrast, vertebrate remains, and human artifacts accumulated on the erosive surfaces that formed during the regressions.

The accumulated evidence first indicates the presence of a narrow valley, in which the sediments of the oldest deposits met by cores S1-2S, drilled at the margins of the lake, were deposited. Then the lake inundated the valley and a very shallow bay formed at Poggetti Vecchi. The previously deposited beds were covered with the lacustrine sediments of Unit 1. The poorly-oxygenated lake bottom favored the preservation of organic matter. The abundant and diversified mollusk and ostracod assemblages, dominated by *P. moussonii* and *H. salina*, from the bottom portion of Unit 1, indicate fresh or slightly saline waters (< 4 psu). A first complete desiccation of the lake led to the formation of a valley, roamed by animals and human hunters. The erosive surface separating Unit 1 from Unit 2 formed at this time, when several carcasses of elephants and human artifacts accumulated on the exposed banks of the former lacustrine bay. The return to a marginal lacustrine environment first created a shallow, mud-dominated pool (Unit 3a), possibly affected by seasonal fluctuations of the water level, and inhabited by mollusk and ostracod communities, similar to the ones that lived there before, and dominated by the ostracod *Candona (Candona) improvisa*. Then, the topmost carbonate muds of Unit 3b accumulated; these are connected with the start of the thermal activity at the site. Later on, during the late Middle Pleistocene (MIS6), the valley was the site of thermal pools, where pisoliths formed. Humans and large mammals, such as elephants, visited the pools. Invertebrate assemblages were still dominated by taxa with strong affinity to waterbody's thermal conditions (i.e.,

Pseudamnicola moussonii and *Heterocypris salina*, *Belgrandia thermalis* and *Melanopsis etrusca*), which are present still today and typical of the thermal settings of southern Tuscany (Cianfanelli, 2010; Cianfanelli et al., 2010). After this, the lake level dropped again, and the second lacustrine phase thus came to an end, followed by a new episode of erosion, which carved through the older deposits during a time of fluvial downcutting (Unit 5). A short creek started flowing down from the Poggetti Vecchi hill through the narrow depression; the run-off flow over the valley floor was of sufficient energy to transport and deposit the calcareous pebbles that formed the channel lag of Unit 5. The third flooding phase restored the lake embayment once again. Organic-rich mudstones (Unit 6) deposited, suggesting depositional and ecological conditions virtually identical to those when unit 1 was formed. The last terms of the sedimentary succession record a further lake-level drop, followed by a new, deep incision of the valley floor. The erosive surface at the base of Unit 7 provided abundant remains of terrestrial gastropods, alongside an isolated skull of elephant, indicating a certain length of time of exposure. Finally, the valley floor was once again carved and infilled with carbonate sediments, originated from the reworking of thermogenic travertines that had accumulated in neighboring pools and that were dispersed as calcareous sands and mudstones (Unit 7) by flowing water. The hot springs recreated the lake bay and produced a stable thermal activity in the area.

The fossil records from the various Units also tell us much about the overall paleoenvironmental conditions in the surroundings of Poggetti Vecchi. At the time when the fossiliferous site was formed, the area was dominated by extensive open grassland inhabited by large grazers, among which *Palaeoloxodon antiquus* and *Bos primigenius*, whereas the red and roe deer probably browsed in sparse groves. This outline is confirmed by the abundant herbaceous plant pollen, especially of Poaceae, which dominates the spectra along all the stratigraphy.

The abundant frequency of freshwater fens, together with the high variety of wetland plants recorded along the whole sedimentary succession, confirm periodic fluctuations of groundwater seeps and freshwater bodies, attested to by the mollusk and ostracod assemblages. Tree pollen is scanty; it indicates the occurrence of deciduous *Quercus* probably on the elevations around the site, and of less frequent *Buxus*, which prefers well-drained and calcareous soils, often associated with travertines.

4.6 Chronological and paleoclimatic implications

The paleontological insights from Poggetti Vecchi and the radiometric dating from Unit 4 indicate that the sedimentary succession deposited at a time of climatic instability. As already mentioned above, the stratigraphic sequence is bracketed between the latest MIS7 interglacial and

the late MIS6 glacial. Pollen data report the presence of Tertiary taxa in the lowermost levels of Unit 1. These plants disappeared from Central Italy during the Early-Middle Pleistocene. Their presence is not rare, but they are likely allochthonous elements reworked from older levels and migrated into higher beds via capillary rise of mud. In particular, the spread of *Tsuga* and *Carya* declined in both Northern and Central Italy during the Early-Middle Pleistocene transition and disappeared completely between 0.75 and 0.45 Ma (Corrado and Magri, 2011; Orain et al., 2013). Under the drive of strong climatic oscillations, the area of distribution of *Zelkova* shrank during cold-arid periods and expanded again in warm-moist phases; it finally became extinct in peninsular Italy before the latest glacial maximum (Follieri et al., 1986). In the light of all this, the lower portion of Unit 1 cannot be younger than 0,4 Ma.

The physical stratigraphy of the transgressive and regressive deposits that accumulated during the time period indicated by the radiometric dates from Unit 4 suggests the following tentative calibration (**Figure 20**):

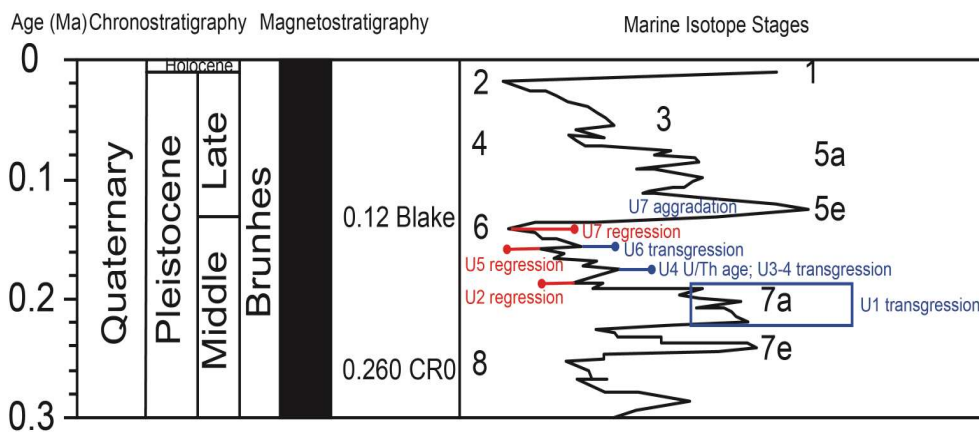


Figure 20 Tentative of correlation of the Poggetti Vecchi stratigraphy, calibrated for Unit 4 with radiometric datings to the Late Quaternary Marine Isotope Stages. The curve was drawn based on Lisiecki and Raymo (2005) and the Global chronostratigraphical correlation table for the last 2.7 million years (v. 2016a).

1. The sediments of Unit 1 correlate with a transgressive phase, when the lake reached its highstand during the warm sub-stage MIS7a or during the following interstadial at the transition to MIS6 (between 200-191 ka). If this is correct, Poggetti Vecchi would have been a refuge for Tertiary flora, which survived in this area later than 0.4 Ma.

2. The subsequent regression phase (Unit 2) occurred at the onset of MIS6, when the lake reached its first lowstand and there was subaerial exposition of the erosive surface.

3. The deposits of both Units 3 and 4 reveal a new transgressive phase plus the activation of the thermal system at around 170 ka, i.e., during

the first interstadial of MIS6. Based on Ayalon et al.'s (2002) study, the humid period radiometrically dated at 171 ka (Unit 4) was likely the first interstadial of the glacial interval MIS6.

4. The new fall of the lake level occurred during the next stadial stage (Unit 5 regression).

5. Unit 6 testifies a new transgression, during the second interstadial; the lake level reached a new highstand.

6. Unit 7 reports the final regression at the site. The lake lowstand was reached around 130 ka, i.e., during the MIS6. This was perhaps the time of climatic amelioration, which peaked during the interglacial interval of MIS5e.

Paleoecological insights indicate that the Unit 2 fauna was well-tuned with the climatic and environmental fluctuations that occurred within the short time period between the onset of MIS6 (lake regression and erosion at the top of Unit 1) and the next interstadial (lake transgression phase and deposition of sedimentary Units 3-4). The paleobiological inferences from the small and large mammal assemblages are coherent with the succession of paleoenvironmental signals and sedimentary events and their tuning with the main climatic fluctuations.

As expected, the small mammal fauna was dominated by *Arvicola amphibius*, which is a typical inhabitant of moist environments. Unit 2 yielded remains of *Microtus* cf. *arvalis*; modern Italian populations of this taxon are confined to the northern regions of the peninsula and are absent from the central Apennine. Therefore, its presence in southern Tuscany at very low altitudes is indicative of colder conditions than those existing today. The occurrence of *Microtus* cf. *arvalis* is not in contrast with the hypothesis that a cold snap may have occurred at the time of deposition of Unit 2, causing the sudden death of the elephant clan. Intense seasonal oscillations likely occurred during the whole-time span recorded by the Poggetti Vecchi succession.

The decreasing abundances of *Microtus (Terricola) ex gr. savii* and the absence of *Crocidura* and *Oryctolagus* in the following units, might indicate cooler conditions moving upwards in the succession. Conversely, these taxa occur from Unit 6 on, suggesting climate amelioration and warmer conditions.

Unit 2 includes warm-adapted mammals, such as the roe deer *Capreolus capreolus*, and thermophilic herpetofauna; the latter include the European pond turtle *Emys orbicularis* and the European whip snake *Hierophis viridiflavus*, which distribute widely from the warm peri-Mediterranean area to much cooler northern European contexts (Lelièvre et

al., 2010a, b). The European pond turtles are active above 5°C (Novotný et al., 2004). Also, *Palaeoloxodon antiquus*, which is a typical member of temperate contexts, can occur in cooler conditions (Mazza et al., 2006), as mentioned above.

The molluscan fauna includes typical open-landscape species, such as *Pupilla muscorum* and *Vallonia pulchella* from Unit 6, which suggest under cool climatic conditions (Rousseau, 1989; D'Amico et al., 2014), compatible with the global cooling trend that culminated in the glacial maximum of MIS6. Also, the whole ostracod fauna, proceeding from Unit 1 to 6, indicates average temperature values about 6°C lower than today. The accumulated data therefore confirm mean temperature values typical of the onset of MIS6, which were about 7.5°C lower than current values, as indicated by Vostok Ice core in Antarctica (Petit et al., 1999).

4.7 Conclusion

The radiometric datings from Unit 4 locates the Poggetti Vecchi section at a time period between late MIS7 and late MIS6. The lake lowstand and subaerial erosion at the transition from Unit 1 to Unit 2, likely occurred at the onset of MIS6. Hence, the Poggetti Vecchi archeo-paleontological site deposited during the Middle-Late Pleistocene transition, which is a time period imperfectly documented by the European fossil records. This crucial chronological information indicates that the stone and wooden implements from the site were produced by early Neanderthals. Poggetti Vecchi, therefore, offers the chance to obtain an unprecedented amount of information on how local early Neanderthals interacted with the animals of the time, as well as on how they managed to deal with the environmental and climatic challenges at the MIS7-6 transition.

Based on the collected evidence, local human hunters benefited from the large accessibility to concentrated resources unexpectedly made available by the fortunate interplay of paleobiological, geologic and climatic factors. The site thus offers critical information on the behavior of early Neanderthals, which is still very imperfectly known. Contrary to previous belief, early Neanderthals appear to have been particularly skilled to deal opportunistically with environmental and climatic adversities, and able to modify over time the scheduling of their exploiting strategies.

Chapter 5 Multiproxy-based reconstruction of the feeding habits of the Poggetti Vecchi straight-tusked elephants

5.1 Paleodietary analysis of the Proboscideans: the state of the art

To date relatively few studies focused on the paleodiet of elephants, especially because of the logistical difficulties in developing analytical protocols for the study of proboscideans. Microwear analysis, in general, requires the use of high magnification scanning by SEM of only small portions of the total enamel surface. In his pioneering study, Capozza (2001) examined a well-preserved upper third molar of *Mammuthus meridionalis* from Campo del Conte (Frosinone, Italy) at different magnifications (25x, 200x and 500x). According to Capozza's (2001) conclusions the significantly higher frequency of scratches than pits (most worn plates show higher percentage of scratches; in contrast, unworn plates have lower incidence of pits) and the peculiar distribution of scars suggest preferential consumption of grasses (Capozza, 2001). Another leading study of dental Microwear Analysis by Low Magnification (LDM) was performed by Solounias and Semprebon (2002). This analysis contains a comprehensive comparative database built using an innovative method of microwear detection, which the authors extended also to modern elephants. Solounias and Semprebon (2002) first identified and counted the different scar patterns of living elephants at 35x magnification. Then Green et al. (2005) examined several molars of *Mammuth americanum*, from the Pleistocene of Florida. The results not only indicate that American mastodons had browsing habits but also that a significant amount of bark and twigs was included in their diet, with the supplementary consumption of fruit. Meaningful insights were obtained from comparative, high and low magnification microwear and isotope analysis of several Italian specimens of *Palaeoloxodon antiquus* (Palombo et al., 2005). The results of these studies indicate that the Middle Pleistocene *Palaeoloxodon antiquus* populations of "Campagna Romana" were characterized by prevalent browser/mixed feeder adaptation. Microwear patterns and isotope records suggest that during the late Middle Pleistocene the central Italian landscape was dominated by wooded grassland, under moderately humid and temperate climatic conditions. These straight-tusked elephant populations consumed grasses, leaves, bark and coarse stem and, in general, their diet was rich in graminaceae or plants with rather high phytolith-content (Palombo et al., 2005). In a later study, Todd et al. (2006) used the low-magnification method to verify if there were possible changes in the microwear pattern over the occlusal surfaces of a single molar. Todd et al. (2006) concluded that a larger amount of data is needed to detect the existence of possible intraspecific and interspecific variations in microwear patterns.

Paleodietary methods can solve important ecological issues related to sympatry, niche partitioning and dietary overlap; i.e., assessing how mammals modify the structure and composition of a plant paleocommunity in a given environment. The separation of dietary niches was shown to permit the coexistence of sympatric species of proboscideans (e.g., Calandra et al., 2010; Rivals et al., 2015). Low magnification microwear analysis proved that the Channel Island pygmy mammoths (*Mammuthus exilis*) narrowed their dietary niche space after the colonization of mainland mammoths (Semprebon et al., 2016). Competition-induced diet shift likely led *Mammuthus exilis* to browse on leaves and twigs, as opposed to Columbian mammoths. Pleistocene vegetation history of Channel Islands supports the environmental reconstruction based on the analysis of the microwear patterns: during the last glacial, when *Mammuthus exilis* flourished, the landscape was dominated by extensive conifer forests. Then, ecological disruptions and replacement of woodlands by grasslands indicates that climatic factors might have been the main factor contributing to the extinction of Channel Island pygmy mammoths during the Late Pleistocene.

To date, Zhang et al. (2016) is one of the few published studies reporting empirical textural data (DMTA). According to these researches, turnovers in faunal assemblages, such as that from bunolophodont to lophodont proboscideans during the Pleistocene in Southern China, could have been more complex than it has been hypothesized so far. Contrary to traditional view, which supports the unidirectional transition from forested to more open areas driven by climate deterioration biotic factors could also have had an important role to play. Repeated environmental perturbations, over this period, could have created dynamic and non-directional conditions of equilibrium. Both *Sinomastodon* and *Stegodon* had a typical textural profile related to browsing behavior, which in the latter is associated with the acquisition of derived morphological traits (i.e., lophodont molars) connected with a masticatory mechanism more apt for processing plants. Competition for access to the same food resource may have allowed *Stegodon* to outcompete *Sinomastodon*. The former therefore became the dominant proboscidean in the Pleistocene of Southern China, leading *Sinomastodon* ultimately to become extinct. *Elephas* species have higher hypsodonty than stegodonts; the dental textures of the Middle and Late Pleistocene representatives are heterogeneous, indicating that the various species exhibited different feeding habits. Therefore, the coexistence of *Stegodon* and *Elephas*, from the Middle to the latest Pleistocene in Southern China could be explained by possible niche partitioning.

Investigating the trophic relationships in elephants and supposing potential dietary niche separation, Saarinen and Lister (2016) compared the mesowear signals of possible competitors with the environmental proxies coming from the pollen records. Positive correlation of mesowear signals

with local pollen values was thought to reveal the preference for specific components of the local vegetation. The study aimed also to understand if the typical dietary flexibility of elephants is reflected by niche separation or if it is a response to changes in the local vegetation community. Intra- and inter-specific mesowear variability confirms that, despite their different dietary adaptations, British Pleistocene proboscideans had relatively flexible feeding behaviors. Thanks to their different dietary preferences, the species could occasionally coexist, without outcompeting each other (Saarinen and Lister, 2016).

5.2 Dental Microwear Analysis using the Low Magnification approach (LDM)

5.2.1 Introduction

Strictly speaking, the term microwear analysis consists of the qualitative assessment, measurement and quantification of the relative abundances of enamel scars (i.e., pits, scratches) considered as discrete entities. Microwear analysis therefore excludes the tridimensional texture approach. There is growing use of this approach to address ecology and paleoecology issues in the study of past and present-day vertebrates. Despite early studies were based on high magnification inspection using SEM-generated photomicrographs, in more recent years scholars have increasingly performed dental microwear analysis using low-magnification (30x to 100x) refractive light microscopy (LDM). The magnification is imposed by the resolution limits of the instruments, but depends also on the size of the objects to be studied. Lower magnification is normally used for medium/large-sized animals, and a higher one for smaller subjects. Qualitative description criteria were defined by Solounias and Semperebon (2002, pp.11-18); they are the following:

1. Pits are cavities in the enamel with circular or sub-circular outline and approximately similar widths and lengths. Their refractive power varies according to the size: small pits are relatively shallow and refract light easily and consequently appear bright and shiny. Large pits, which are generally at least twice the diameter of small pits, are deeper, wider and less refractive. Exceptionally large pits are called puncture pits; are very deep, especially in the central portion and their outline is symmetrical with regular edges and craterlike features. Under light microscopy they appear dark due to their low refractivity; puncture pits appear darker than large, fairly shallow, ordinary pits.

2. Gouges are particularly large, irregularly-shaped depressions, wider than ordinary and puncture pits.
3. Scratches are elongated, straight marks; they can be distinguished as fine, coarse, or hypercoarse. Fine scratches are narrower than the coarse ones and barely etched into the enamel surfaces. Neither is deep and, in general, refracts light well; hence, they generally appear shiny and white; nonetheless, very narrow fine scratches are fainter. Fine scratches are usually V-shaped in cross section, and coarse ones U-shaped. Hypercoarse scratches are very deep and wider than coarser and finer scratches; consequently, they have low refractive power and always appear dark. Sometimes hypercoarse scratches bear puncture pits at one of their ends.

Two alternative approaches are widely adopted. The first prescribes that samples be analyzed directly through the eyepieces of the microscope with a micrometric ocular reticle (i.e., Solounias and Semprebon, 2002). With this methodology microwear features are subjectively categorized without standardized size criteria. Direct analysis is often not repeatable; moreover, interpretive errors are hard to detect this way, and can also potentially build up through time. The second approach is based on computer-analyzed digital images, following the methodology proposed by Merceron et al. (2005a, 2005b).

The main goal of the LDM method is grouping animals into major dietary categories: grazers, browsers, and frugivore-hard object feeders (Solounias and Semprebon, 2002). High densities of scratches and low densities of pits are usually associated with grazers, the opposite with browsers. Intermediate amounts of scratches and higher frequencies of pits (especially large pits) are commonly related to frugivore-hard object feeders (Solounias and Semprebon, 2002; Semprebon et al., 2004b). Solounias and Semprebon (2002) sort species in three categories based on the spread of scratch numbers observed. The scratch ranges are the following: 0-17; 17.5-29.5; > 30. Leaf browsers are mainly included in the low scratch range category, grazing species fall in the intermediate and/or high scratch range categories; fruit browsers are mainly included in classes of the low and intermediate scratch ranges. The datasets published so far allowed the clustering of average scratch and pit counts in several taxa, i.e., many living ungulates, and a few extinct species and primates (**Figure 21**). This threefold classification of feeding habits is used for comparative assessment purposes; it either provides bivariate spaces where new experimental datasets can be plotted, or discriminating functions that can be used for statistical treatment, where data of various taxa and/or information collected by multiple observers can be combined and compared in many different ways.

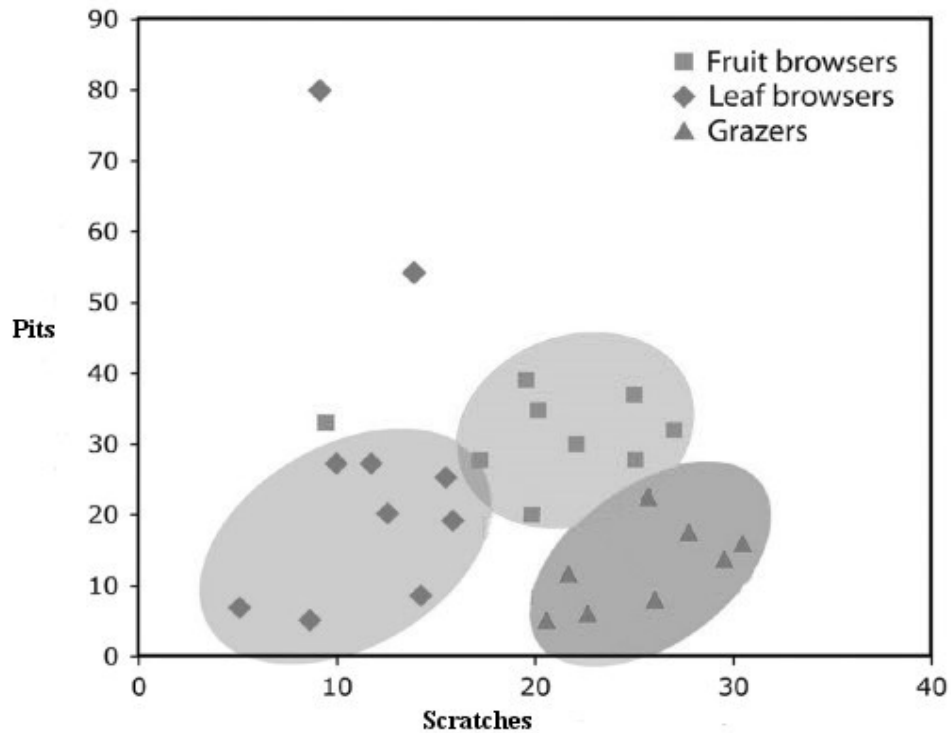


Figure 21 Bivariate plot for average number of scratches versus pits for extant fruit browsers, leaf browsers and grazers (data are taken from Solounias and Semperebon, 2002).

Until recently, scholars have focused relatively little attention on the sensitivity to the resolution at which dental wear surfaces are analyzed, as well as on how resolution relates to magnification (Mihlbachler et al., 2012). Magnification refers to the degree to which a given sample is enlarged using a microscope, or a stereomicroscope; resolution refers to the fineness of observable details. Important requisites for higher resolution are magnification, quality and intensity of light, quality and cleanliness of optical instruments and variations in the human eye. Fundamental is also having a digital camera with sufficient pixel density and adequate number of pixel per area. Until now, the standard parameters for magnification and resolution have not yet been established; however, microwear can be appropriately studied at different resolution based on the size of the scars, which is related to the size of animals. Higher resolution reveals smaller scars because details are more finely resolved. Furthermore, minor variations can be detected by comparing different microwear patterns. In general, all observable microwear features should be scrutinized, also the smallest ones, those that apparently seem to be background noise and not potential paleodiet proxies. Nonetheless, the weaker correlation of small scars with the feeding habits may depend on limited resolution and does not necessarily reflect a lack of effective connection with the diet (Mihlbachler et al., 2012). A reliable quantification of the smallest scars may exceed the capacities of light microscopy, which would thus impose the use SEM or

other instruments capable of investigating three-dimensional surface texture; alternatively, a multiproxy and comparative approach could be used.

Possible interpretative biases may derive from: i.e., morphofunctional variations in the chewing apparatuses, the involvement of food contaminants (such as sand or dust), post-mortem abrasion and erosion of fossil teeth, but also methodological inconsistencies (i.e., the selection of non-informative wear facets, an inaccurate cleaning of the facets or realization of molds and casts). Other flaws may derive from the use of inappropriate instrumentation (e.g., lighting), as well as from potential limitations arising from the analyst's unfamiliarity with the interpretations and measurements. The latest produced and isolated scars with clear-cut, high-contrasted edges are easy to interpret; conversely, when scars are worn, very weakly carved and/or overprinted by more recent marks the interpretation is far more difficult and controversial (Mihlbachler et al., 2012). Many studies show that the low magnification method is more subject to observational biases and to misinterpretation of diet than is SEM scanning. In the light of these concerns, enamel surface replicas (depending on the scale of microwear) should be analyzed at different resolution levels to increase the repeatability of the observations, but also to eliminate potential ambiguities that may arise case-by-case and especially in cases most subject to interpretative biases. Despite all the potential difficulties, traditional dental microwear analysis is still preferable, first of all because LDM (as well as inspection by SEM) is the easiest way to investigate microwear patterns, providing relevant information to functional morphologists. Moreover, it permits to analyze a large number of samples at lower costs and with basic equipment.

5.2.2 Materials

The molar teeth of the elephants selected for microwear analysis have been preliminarily observed with a stereomicroscope to exclude specimens with potential taphonomic alterations of the enamel surface. The specimens are fairly well-preserved and averagely worn; slightly or heavily worn teeth were discarded. With these criteria we selected 15 upper and lower molars of both sides and of a fairly wide spectrum of ontogenetic ages. A list of the selected specimens, together with a summary description of them, is reported in **Table 3**.

Specimens	Tooth	Side	Age (years)
5500	m3	right	40
5546	m2	right	26
265	M2	left	25-30
1609	M2	right	30
1609	M2	left	30
5547	m2	right	25
5547	m2	left	25
98	m1	right	12
98	m1	left	12
219	d3	right	8
219	d3	left	8
219	d4	right	8
219	d4	left	8
5298	D4	right	8
5298	D4	left	8

Table 3 Description of analyzed specimens.

5.2.3 Methods

5.2.3.1 Casts

The high reflectance of the dental enamel surfaces prevents their direct inspection; the microwear analysis must therefore be performed on epoxy or polyurethane resin casts of the enamel surfaces. Both resins are opaque, have low viscosity and can provide high-resolution replicas.

Molds and casts were prepared using the methods described by Solounias and Moelleken (1992a) and Solounias and Semprebon (2002), which are the following:

1. Cleaning step: Nitro anti-fog diluent has been used to remove preservatives and adhesives that had been applied during the recovery of the fossils and, later on, during their restoration. The occlusal surfaces have then been carefully dried with compressed air and subsequently coated with silicone-biphasic rubber prepared by mixing Silical 110 and Silical 115 (catalyst to 3% by weight). Once dry, this first mold has been peeled off to remove possible residual microscopic impurities.
2. Preparation of the molds: the specimens were covered with low-viscous, vinyl polysiloxane (CharmFlex® Light LV) impression material. The two elements of this biphasic substance are added to dispenser with two separated cartridges of equal diameter, from which the two components are pushed through a static mix

nozzle at the correct mix ratio over the target surface. Polysiloxane vinyl shells were finally covered with another layer of silicone rubber (Silical) that forms an external and protective wall, which provides support to the bottom portion of the molds to prevent the loss of resin. The molds take a few minutes to harden; the silicon rubber protective layer takes about 24 hours to dry completely. At last, each mold was peeled off, washed with a little amount of water using a brush and finally dried with compressed air.

3. Preparation of the epoxy resin casts: under a ventilated fume hood, the molds are filled with low viscous epoxy resin Epo 150 and the catalyst K151 (25% by weight). The blended compound was transferred into a tube and centrifuged at about 3.000 rpm for 15 minutes to remove air bubbles and, finally, carefully poured into the molds.

5.2.3.2 Microwear assessment

A correct illumination is crucial in insuring that the scars have the correct amount of contrast. The casts were examined under a Zeiss standard light stereomicroscope at 40x, 80x and 100x magnification using an external oblique light source with a shallow incidence angle, which illuminates the surface from a single direction. External oblique illumination enhances contrast thus improving the visibility of an object against its background. The wear marks (e.g., deep pits, shallow scratches) have different depths and can be observed more effectively by adjusting, whenever possible, the incidence angle of the light source without affecting the degree of resolution. In fact, this is the preferred method of illumination in LDM microwear analysis, because it maximizes the chance of observing all the features. Unidirectional lighting darkens some edges and makes others brighter. This darkness/brightness contrast improves the overall three-dimensional enhanced visualization of the images. With unidirectional lighting overall resolution is somewhat lower; nonetheless, contrast can be improved by partially closing the condenser aperture. In contrast, using axial illumination the specimen is lit from below through a condenser aperture; the object is therefore illuminated from many angles, which confuses the observer. Hence, axial illumination is not recommended for low-magnification dental microwear analysis (Semprebon et al., 2004).

The correct positioning and regulation of the intensity of the illumination can make scars emerge sharply from the background (Foster, 1997). Slight changes in incidence angle are sufficient for achieving the required contrast; intensity is modulated to enable clearer detection of the smallest surface patterns, i.e., small pits. As mentioned above, detecting the

microwear features and interpreting them as paleodiet indicators depends very much on the observer's experience and capabilities.

In the first place, all the enamel plates of the elephant molars were carefully inspected in different areas to verify the range of variability of any possible microwear pattern. Then, investigated the occlusal surfaces from a functional morphological point of view, the analysis was focused on all the functional plates; pits and scratches were thus distinguished following the minimum/maximum axis ratio (Grine, 1986). A digital camera was added to the stereomicroscope and its software selected the areas to be scanned under a 40x and 100x magnification; the latter of these magnifications gave the best resolved images of the elephant teeth, providing a visual field of 2 mm² (Todd et al., 2007). Several microphotographs of all the 15 teeth examined, were downloaded and processed using the open source raster graphic software ImageJ. The qualitative assessment of the microwear features was performed following the protocol proposed by Solounias and Semprebon (2002). The quantitative analysis was performed on 100x photomicrographs. Then, following the indications given by Todd et al. (2007), the scars met in each 2 mm² area were counted and measured. The total number and frequency of scratches and pits were calculated, the average length and width of the scars were measured, and the width/length ratio was used to discriminate fine from coarse scratches and small from large pits. Finally, microwear density was expressed as number of features per analyzed area.

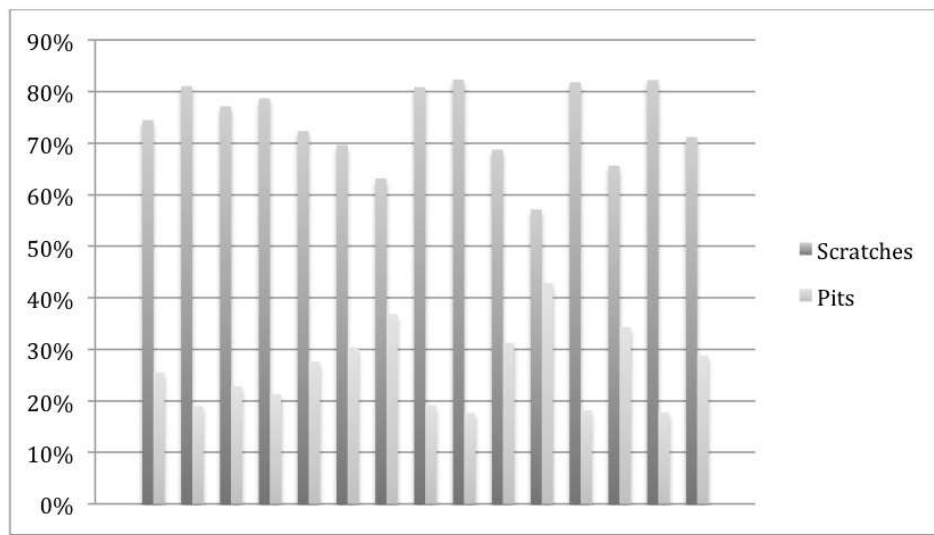
5.2.4 Results

The qualitative assessment of the scars revealed the occurrence of quite similar morphological microwear patterns all over the occlusal surface. The first two plates of each molar were always too worn for the analysis, and were therefore ignored. The greatest variability and density of microwear features was detected on both the lingual and buccal sides of each functional plate. Quite expectedly, the most striking and recurring scar patterns were met not only in the central region of each molar but also, and in particular, at the center of each loop, in line with Solounias and Semprebon's (2002) conclusion that this is the most representative area for inspecting microwear patterns in elephants. Conversely, the frequencies of pits and stretches are much more variable on the distal plates.

Overall, there are more scratches (fine, mixed and coarse) than pits on each plate, with a few exceptions (**Figure 22A** and **B**). Coarse (large, relatively deep, and with a U-shaped bottom) scratches are less frequent than fine and mixed scratches; they are usually more frequent at the center of the enamel loop, whereas fine ones (which are usually longer, narrower and shallower) are mainly observed along the edges of the enamel loops. Deep, V-shaped fine striations are occasionally observed in both central and

lateral (buccal and lingual) portion of each loph. Cross-coarse scratches are particularly present in the middle section, whereas large cavities (gouges) are rare. Pits (either large, mixed or small ones) maybe locally abundant and usually more frequent on buccal and lingual sides. This pattern was confirmed comparing 40x photomicrographs with 100x ones.

A



B

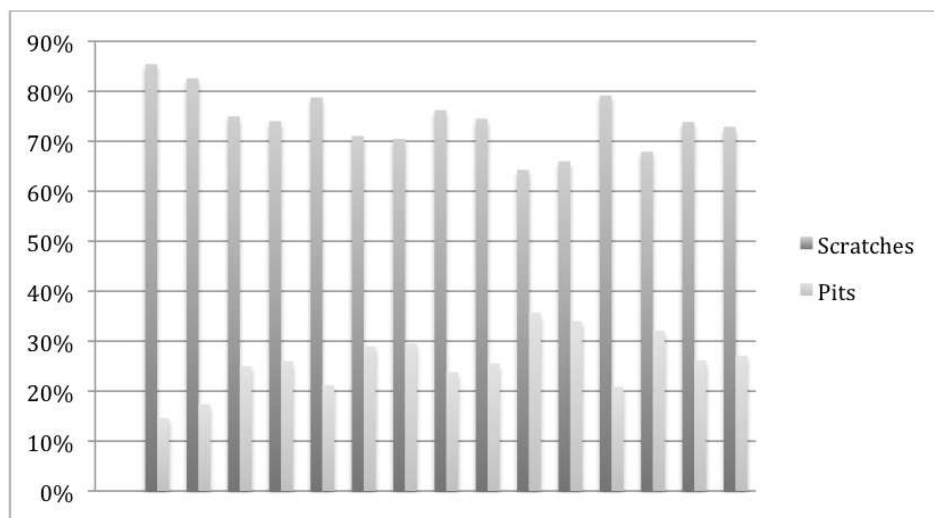
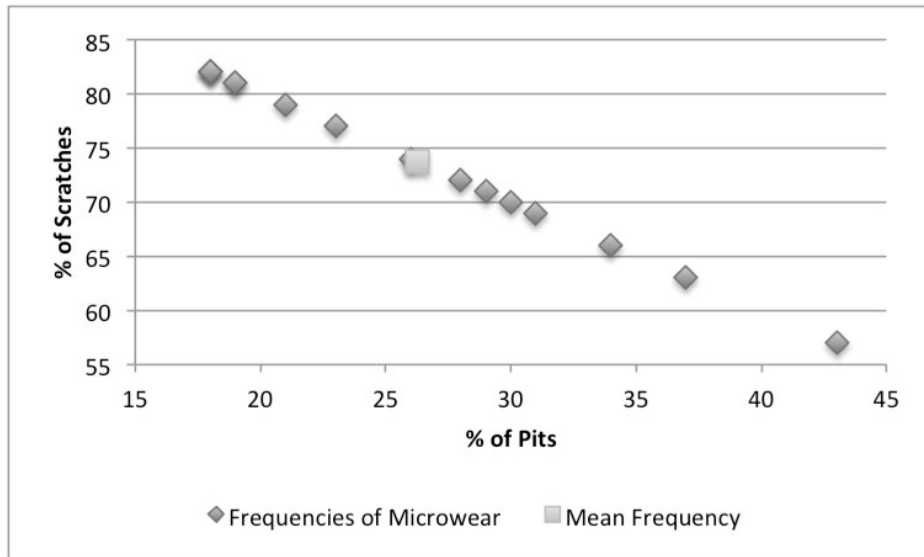


Figure 22 A) Histogram of the average percentage of scratches and pits counted at 40x and B) at 100x magnification.

All measurements are listed in **Table 4**. The average percentage of scratches on each examined tooth always exceeds that of pits (**Figure 23A** and **B**). The microphotographs show that there is higher density of striations

than pits (**Figure 24A and B**). The sizes of scratch and pits are summarized in **Table 5** and the bivariate of these values are shown in **Figure 25A and B**.

A



B

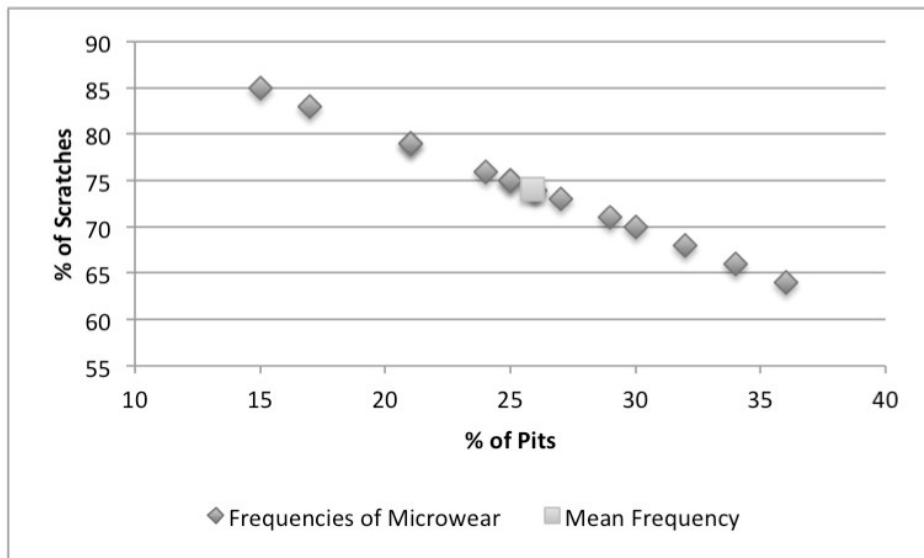
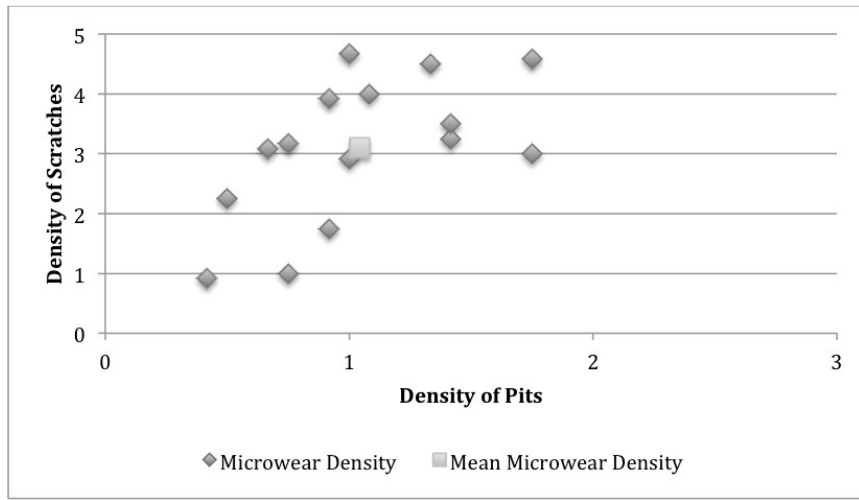


Figure 23 A) Scatter diagram of the average percentage of pits plotted against the average percentage of scratches as obtained from each specimen of the analyzed sample at 40x and B) at 100x magnification.

A



B

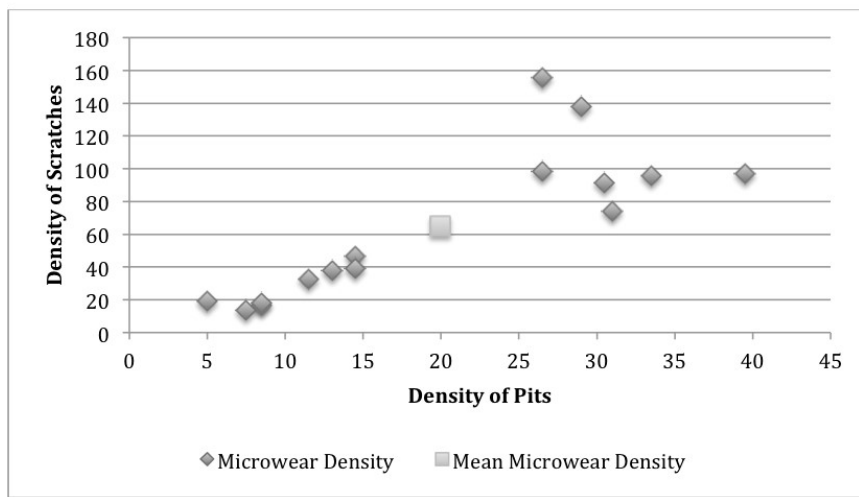
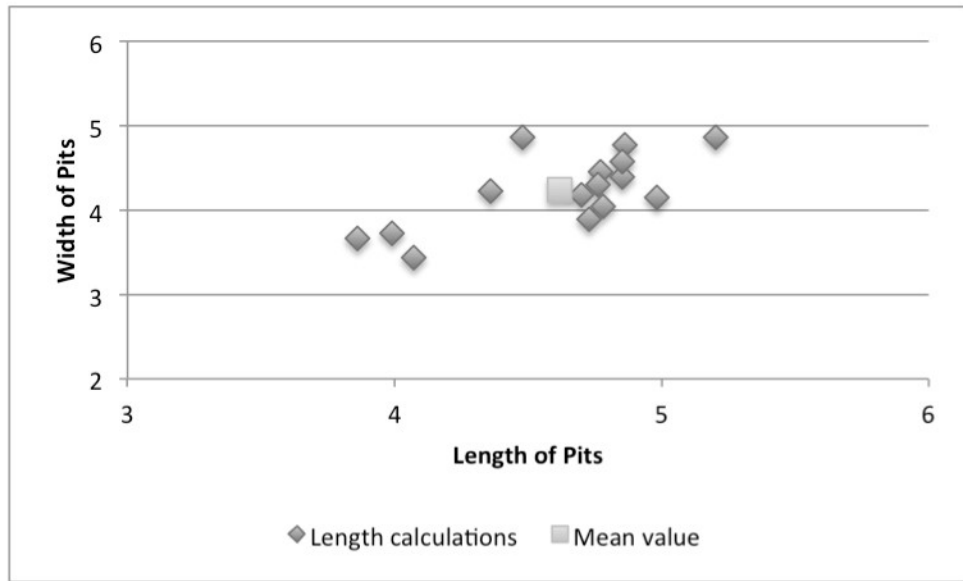


Figure 24 A) Scatter diagram of the average density of pits plotted against the average density of scratches as obtained from each specimen of the analyzed sample at 40x and B) at 100x magnification.

A



B

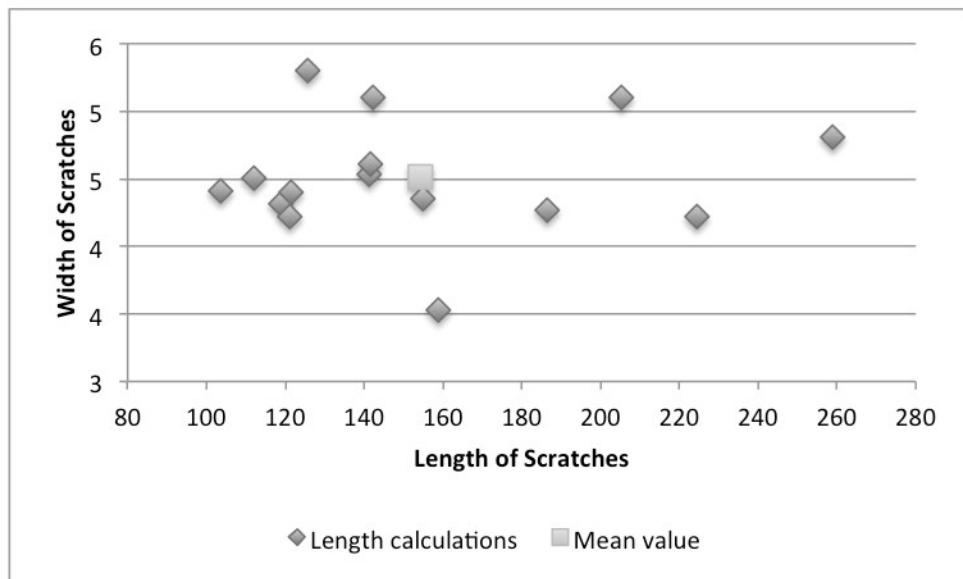


Figure 25 A) Scatter diagram of the average length of scratches plotted against the average width of scratches as obtained from each specimen of the analyzed sample at 40x and B) at 100x magnification.

Tooth	Side	Specimens	Sc.	Pt.	Sc. L. Range	M. Sc.		Sc. W. Range	M. Sc.		Pt. L. Range	M. Pt.		Pt. W. Range	M. Pt.	
						L.	D.S.		L.	D.S.		L.	D.S.		L.	D.S.
m3	R	5500	311	53	50.23-280.75	141.38	18.03	0.92-6.68	4.53	0.92	3.68-6.53	5.20	0.96	3.24-7.82	4.86	1.04
m2	R	5546	276	58	59.25-261.72	155.02	56.08	2.94-6.08	4.35	0.59	3.66-6.46	4.86	0.90	3.43-7.25	4.77	1.00
M2	L	265	183	61	55.92-332.94	158.71	33.99	3.34-5.69	3.53	0.61	3.66-6.25	3.99	0.68	2.90-7.82	3.72	0.68
M2	R	1609	191	67	31.19-270.16	205.12	27.88	3.34-5.69	5.10	0.83	3.88-6.25	4.48	0.30	3.46-6.47	4.87	1.20
M2	L	1609	197	53	59.05-276.83	258.78	25.53	3.53-6.59	4.81	1.25	3.79-6.25	4.78	0.14	3.42-5.99	4.04	0.10
m2	R	5547	194	79	58.07-283.50	118.80	41.76	3.34-5.69	4.32	0.28	3.88-6.25	4.07	0.06	3.20-5.99	3.44	0.34
m2	L	5547	148	62	59.05-280.16	121.15	47.58	3.34-5.89	4.22	0.42	3.95-6.09	4.73	0.99	3.24-5.75	3.90	0.31
m1	R	98	93	29	32.72-271.34	125.76	45.78	3.34-6.67	5.30	1.94	3.66-6.89	4.98	1.47	3.02-6.33	4.15	0.66
m1	L	98	76	26	44.54-289.58	103.59	69.36	3.34-5.30	4.41	0.42	3.69-6.25	3.86	0.24	3.02-6.51	3.67	0.50
d3	R	219	27	15	44.54-205.41	142.14	56.19	3.92-5.69	5.10	0.28	3.86-5.82	4.70	0.64	3.77-5.08	4.18	0.39
d3	L	219	33	17	45.32-252.11	141.65	21.09	3.53-5.49	4.61	0.97	3.98-5.85	4.77	0.64	3.02-5.95	4.45	0.68
d4	R	219	38	10	59.05-257.78	112.12	20.67	3.53-5.10	4.51	0.55	3.93-5.85	4.85	0.73	3.42-5.18	4.40	0.55
d4	L	219	36	17	39.43-248.58	224.54	14.01	3.53-5.30	4.22	0.42	3.68-5.85	4.36	0.57	3.40-5.75	4.23	0.59
D4	R	5298	65	23	65.53-260.55	186.38	52.55	3.34-5.30	4.27	0.49	3.96-5.86	4.76	0.69	3.02-5.75	4.30	0.63
D4	L	5298	78	29	44.54-264.47	121.35	38.98	3.34-6.08	4.40	0.83	3.66-5.62	4.85	0.87	2.90-5.20	4.57	0.43

Table 4 Microwear measurements expressed in microns (Sc.= number of scratches; Pt. = number of pits; Sc. L. Range = scratches length range; M. Sc. L. = mean scratches length; D.S. = standard deviation; Sc. W. Range = scratches width range; M. Sc. W. = mean scratches width; Pt. L. Range = pits length range; M. Pt. L. = mean pits length; Pt. W. Range = pits width range; M. Pt. W. = mean pits width).

Tooth	Side	Specimens	Sc.	CS	FS	Mixed	CS%	FS%	MS%	Pt.	LP	SP	Mixed	LP%	SP%	MP%
m3	R	5500	311	5	230	76	2	74	24	53	12	17	24	23	32	45
m2	R	5546	276	16	198	62	6	72	22	58	11	21	26	19	36	45
M2	L	265	183	10	134	39	5	73	21	61	13	13	35	21	21	57
M2	R	1609	191	17	138	36	9	72	19	67	13	15	39	19	22	58
M2	L	1609	197	22	125	50	11	63	25	53	5	18	30	9	34	57
m2	R	5547	194	18	93	37	9	48	19	79	10	23	46	13	29	58
m2	L	5547	148	28	67	53	19	45	36	62	15	17	30	24	27	48
m1	R	98	93	13	59	21	14	63	23	29	10	14	5	34	48	17
m1	L	98	76	11	34	31	14	45	41	26	7	11	8	27	42	31
d3	R	219	27	6	10	11	22	37	41	15	2	6	7	13	40	47
d3	L	219	33	6	21	9	18	64	27	17	5	5	7	29	29	41
d4	R	219	38	6	21	11	16	55	29	10	3	4	3	30	40	30
d4	L	219	36	5	22	9	14	61	25	17	2	8	7	12	47	41
D4	R	5298	65	8	30	27	12	46	42	23	3	9	11	13	39	48
D4	L	5298	78	10	35	33	13	45	42	29	3	11	15	10	38	52

Table 5 Microwear calculations (Sc.= number of scratches; Pt. = number of pits; CS = coarse scratches; FS = fine scratches; Mixed = mixed scratches; LP = large pits; SP = small pits; Mixed = mixed pits) and corresponding frequencies assessment.

5.2.5 Discussion

Modern elephants are regarded as a particular kind of mixed-feeders with complex behavior. Depending on the availability of different kinds of plants as well as on climatic conditions, they show most variable feeding habits. Microwear patterns can therefore change considerably and rapidly both seasonally and geographically (Grube et al., 2010).

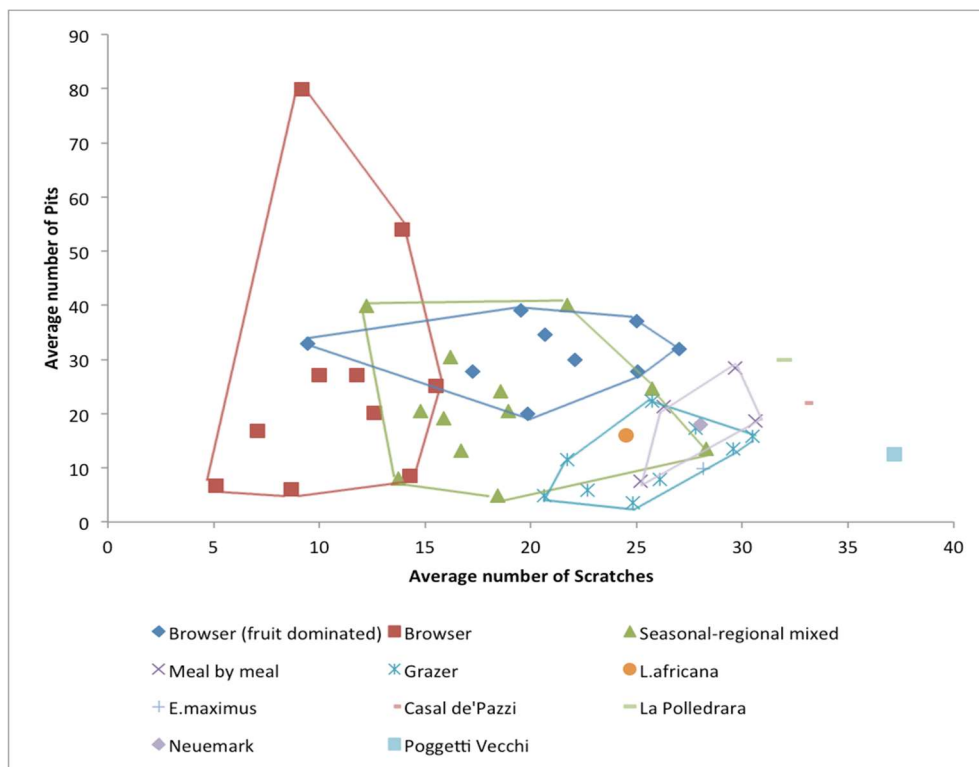


Figure 26 Bivariate plot of the average number of scratches versus the average number of pits and corresponding feeding morphospace envelopes (leaf browsing, fruit browsing, grazing, seasonal and meal by meal mixed-feeders taxa). Data for extant ungulates and elephants were drawn from Solounias and Semperebon (2002) and those of palaeoloxodonts specimens from Neumark-Nord, La Polledrara di Cecanibbio and Casal de'Pazzi were sourced from Grube et al. (2010).

Peculiar microwear patterns are revealed comparing morphospace boundaries obtained by plotting the average numbers of scratches of each dietary category against the average numbers of pits (**Figure 26**). The plots show that the grazers cluster in the high-scratch morphospace and are separated from the low-scratch morphospace of browsers. Mixed-feeders species mostly cluster in the gap between browsers and grazers; they are also spaced from most of fruit-dominated browsers. Modern elephants plot in the grazing morphospace. Based on specific dietary adaptations (African elephants usually consume a wider variety of plants, including herbs, grass, leaves, fruit and bark, as well as aquatic vegetation, than Indian elephants, which eat prevalently grass); *Loxodonta africana* is closer to mixed feeders,

whereas *Elephas maximus* plots in the grazing morphospace. The *Palaeoloxodon antiquus* populations from Casal de'Pazzi, La Polledrara, and Neumark-Nord plot in the so-called meal-by-meal mixed feeders, which are opportunists capable of changing the dietary behavior depending on the abundance or the palatability of the food (Grube et al., 2010). In particular, the Neumark-Nord elephants fall in the gap between typical browsers and grazers (**Figure 26**) and rather close to *L. africana* (Grube et al., 2010); on the other hand, Italian palaeoloxodonts have molars showing a higher number of scratches (Palombo et al., 2005). The Poggetti Vecchi elephants cluster within grazers. The number of pits is not only lower than in extant elephants, but also than in the other palaeoloxodonts; in general, the microwear pattern shows lower amount of coarse, hypercoarse scratches and gouges, which are usually suggestive of hard fruit, seed or root feeding (Solounias and Semprebon, 2002). In contrast, the high percentage of mixed and fine scratches associated with abraded micro-areas observed on the teeth from Poggetti Vecchi indicates feeding on abrasive food, containing high amounts of opal phytoliths, but also of soil particles ingested together with grasses. Hence, the differences between the various Italian palaeoloxodonts may indicate different preferential diets and a high plasticity to adapt to local environmental and microclimatic conditions. Elephants increase grass intake during more humid periods (Sukumar and Ramesh, 1995). The microwear pattern of the Poggetti Vecchi straight-tusked population is indicative of grass consumption under rather cold and wet climatic conditions.

5.3 Isotopic analyses

5.3.1 Materials and methods

A tooth slice including the entire central plate was completely detached from the center of the second molar (n. 1365) using a drill with a circular rotary disc (**Figure 27**). A section of the enamel was manually separated from the basal portion of the slice, mechanically cleared of dentine and cement using tungsten-carbide rotary tools and finally ground with an agate mortar.

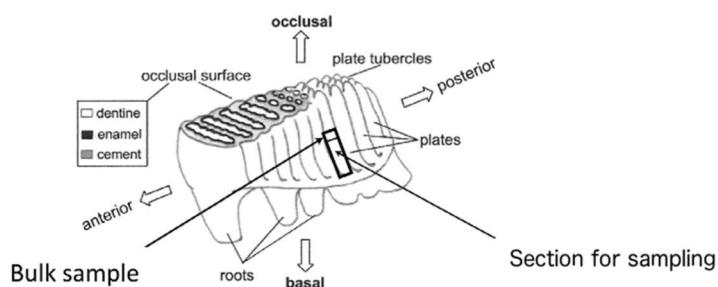


Figure 27 Idealized elephant tooth with bulk and sample area (adapted from Metcalfe, 2016).

The purity and crystallinity of the fine enamel powder was monitored by X-ray diffraction analysis. A randomly-oriented powdered sample was mounted on glass slides and scanned. The diffraction pattern was collected on a Philips PW 1050/37 diffractometer using graphite-monochromatised CuK α radiation, obtained at 40 kV and 20 mA. The sample was scanned from 5° to 60° with a step size of 0.02° 2 θ and a counting time of 2s.

Some scholars (i.e., Koch et al., 1997; Garvie-Lok et al., 2004) recommend, prior to performing the isotopic analyses, a pretreatment on structural carbonate, to remove organic material and exogenous carbonates. Several contaminants may have been incorporated or have adhered to the teeth over time during life or during fossilization, forming secondary carbonate deposits. Following the pretreatment schedule, the sample should first be reacted with 2.5% sodium hypochlorite (NaOCl) for 24 h at 20° C to oxidize organic residues and then rinsed with distilled water. This step is repeated twice; then, the compound should be reacted with 0.1 M acetic acid-calcium acetate buffer (pH 4.75) for 24h at 20 °C to remove exogenous carbonate (Bocherens et al., 1996; Koch et al., 1997; Ecker et al., 2013). It is washed again with distilled water and dried at 45° C.

Nonetheless, Chenery et al. (2012) advised that leaching causes slight modifications. For this reason, the sample was not subjected to pre-treatment. It was decided to subject the sample to acid hydrolysis: about 150-200 mg of enamel powder was reacted with 100% orthophosphoric acid (H₃PO₄) at 25°C for three days to produce CO₂, which was collected by cryogenic separation. Finally, the sample was measured by Finnigan Mat 252 mass spectrometer. The phases of CO₂ release and separation were carried out in the geochemistry laboratory of the Department of Earth Sciences at the University of Florence; the determination of isotopic ratios was performed at the CNR Institute of Geosciences and Earth Resources, in Pisa. The concentrations of carbon and oxygen isotopes in the CO₂ were measured and the corresponding ratios (¹³C/¹²C and ¹⁸O/¹⁶O) were reported

in delta (δ) notation relative to the Pee Dee Belemnite (PDB) international standard following the equation (drawn from Cerling et al., 1999):

$$\delta = (R \text{ sample} - R \text{ standard}) - 1 \times 1000$$

in which $R = {}^{13}\text{C}/{}^{12}\text{C}$ or ${}^{18}\text{O}/{}^{16}\text{O}$. The amount of ${}^{13}\text{C}$ in the enamel was enriched compared to amount deriving from the diet intake and expressed using the conventional enrichment factors ε (Cerling et al., 1999), where:

$$\varepsilon \text{ enamel} - \text{diet} = R \text{ enamel} / R \text{ diet} - 1 \times 1000$$

Cerling et al. (1997) and Cerling and Harris (1999) calculated that, in an enamel sample, the enrichment factor for large mammals including elephants is 14.1.

The $\delta^{18}\text{O}_\text{C}$ value was converted from PDB into SMOW (Standard Mean Ocean Water) using the conversion equation introduced by Coplen (1988):

$$\text{SMOW} = 1.03091 \times R \text{ PDB} + 30.91$$

The orthophosphate ion PO_4^{3-} and structural CO_3^{2-} ion are assumed to be co-genetic, oxygen-bearing phases, in isotopic equilibrium with the same oxygen reservoir at the same temperature (e.g., in mammals the reservoir is considered body water at about 37°C: Iacumin et al., 1996). If so, a linear correlation should exist between oxygen isotopic composition of phosphate ($\delta^{18}\text{O}_\text{P}$) and structural carbonate ($\delta^{18}\text{O}_\text{C}$) values, which can be determined by regressing the data using “Functional Relationship Estimation by Maximum Likelihood” (FREML: Chenery et al., 2012). This correlation is species-specific and was established for several modern and extinct animal species (Iacumin et al., 1996). In addition, deviations of linear relationship between the two ions could be used as a tool to assess whether post-depositional interaction with meteoric water had affected the apatite CO_3^{2-} ion and its pristine $\delta^{18}\text{O}$ value. If a set of data lie along the line or straight close to the best fit for modern mammals ($\delta^{18}\text{O}_\text{P} = 0.98 \times \delta^{18}\text{O}_\text{C} - 8.5$) it is assumed that the ratios are pristine (Iacumin et al. 1996; Chenery et al., 2012). The $\delta^{18}\text{O}_\text{C}$ into $\delta^{18}\text{O}_\text{P}$ conversion allows to directly convert enamel $\delta^{18}\text{O}_\text{C}$ values to drinking water $\delta^{18}\text{O}$ values and thus to derive fundamental paleoenvironmental and paleoclimatic information. The $\delta^{18}\text{O}_\text{C}$ into $\delta^{18}\text{O}_\text{P}$ conversion equation: $\delta^{18}\text{O}_\text{P} = \delta^{18}\text{O}_\text{C} \times 1.035 - 9.75$ is recommended dealing with data from warm humid, temperate and cold climates (Chenery et al., 2012). In more hot-arid climate contexts more accurate results can be obtained using Iacumin et al.’s

(1996) and Metcalfe et al.'s (2009) equation $\delta^{18}O_p = 1.122 \times \delta^{18}O_c - 13.73$. Nonetheless, the question is raised as to which equations are most reliable and to how to apply them. Primary aspects to be considered is which is the most appropriate equation to assess the environmental and climatic conditions that existed in the investigated area (Chenery et al., 2012). Additional uncertainties are associated with the fact that errors associated with the $\delta^{18}O_w$ values obtained from the conversion of $\delta^{18}O_p$ values measured in animal dental enamel are very much dependent on the correlation between the comparative data used to perform the regression (Pollard et al., 2011). These errors are usually greater than ± 1.0 and can reach $\pm 3.5\%$. Nonetheless, Chenery et al. (2012) determined that using Daux et al.'s (2008) equation:

$$\delta^{18}O_w = 1.590 \times \delta^{18}O_c (SMOW) - 48.634$$

to calculate drinking water values directly from the carbonate analyses generates an overall uncertainty of $\pm 1.0\%$ (2σ), which is close to the $\pm 1\%$ (95% CI) error indicated by Pollard et al. (2011) as the minimum uncertainty associated with converting phosphate oxygen into drinking water oxygen.

5.3.2 Results

$\delta^{13}C_{sc} \text{‰}$ (PBB)	$\delta^{13}C_{diet} \text{‰}$ (PBB)	$\delta^{18}O_{sc} \text{‰}$ (PDB)	$\delta^{18}O_{sc} \text{‰}$ (SMOW)	$\delta^{18}O_p \text{‰}$ (SMOW)	$\delta^{18}O_w \text{‰}$ (SMOW)
-11.05	-25.14	-4.08	26.70	17.89	-6.32

Table 6 Carbon and oxygen isotope enamel determination and paleodiet calculation.

No phase impurity was detected; all the peaks were characteristic of apatite (**Figure 28**). The values differ from hydroxyl apatite but are close to those of mammal enamel (Elliott, 2002; Wilson et al., 1999; Michel et al., 1995) and rather similar to enamel phase in both modern and fossil elephants (Ayliffe et al., 1994). The paleodiet of the Poggetti Vecchi population of *Palaeoloxodon antiquus* was inferred based on these results and using the carbon isotope fractionation method proposed by Cerling and Harris (1999), which calculates the isotope enrichment between diet and bioapatite.

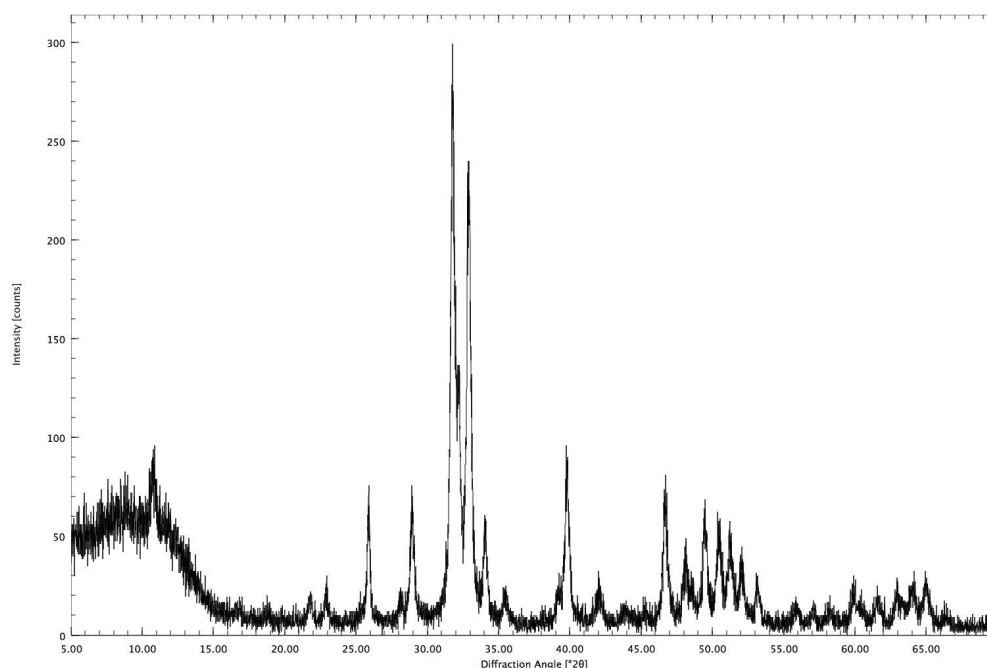


Figure 28 XRD pattern of dental enamel sample.

Carbon and oxygen values and corresponding calculations are reported in **Table 6** and **Figure 29**. The carbon isotopic value of the enamel structural carbonate (-11.05‰ $\delta^{13}\text{C}_{\text{sc}}$ versus PDB-1) as well as, the corresponding calculated paleodiet (-25.14‰ $\delta^{13}\text{C}_{\text{diet}}$ versus PDB-1) suggests that the straight-tusked elephant population of Poggetti Vecchi falls in the “C3-dominated diet” field. The oxygen isotope value (-4.08‰ $\delta^{18}\text{O}_{\text{sc}}$ versus PDB-1) was obtained from the structural carbonate and was then converted into SMOW (26.70‰ $\delta^{18}\text{O}_{\text{sc}}$ versus SMOW) using Coplen’s (1988) conversion equation. Linear regression (FREML) allowed the subsequent conversion into $\delta^{18}\text{O}_{\text{p}}$ (17.89‰ SMOW). Using Daux et al.’s (2008) equation, the oxygen isotope composition of the structural carbonate was directly translated into the isotope composition of the environmental water (-6.18‰ $\delta^{18}\text{O}_{\text{w}}$ versus SMOW). The carbonate and the calculated phosphate oxygen isotope values lie very close to the equilibrium line reported by Iacumin et al. (1996), supporting the hypothesis that the sample is likely preserved the pristine $\delta^{18}\text{O}_{\text{c}}$ value (**Figure 30**).

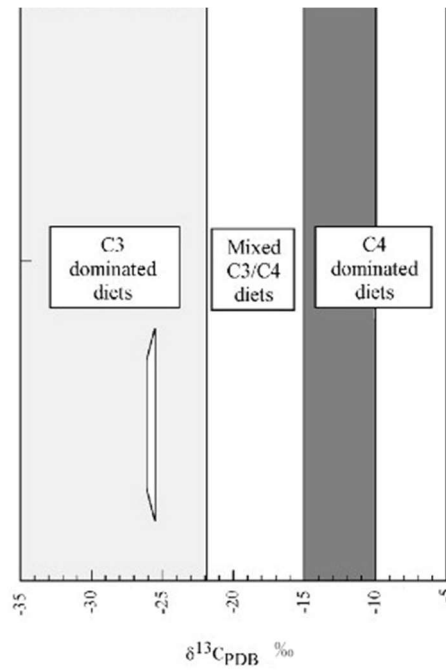


Figure 29 Calculated paleodietary adaptations of elephant population.

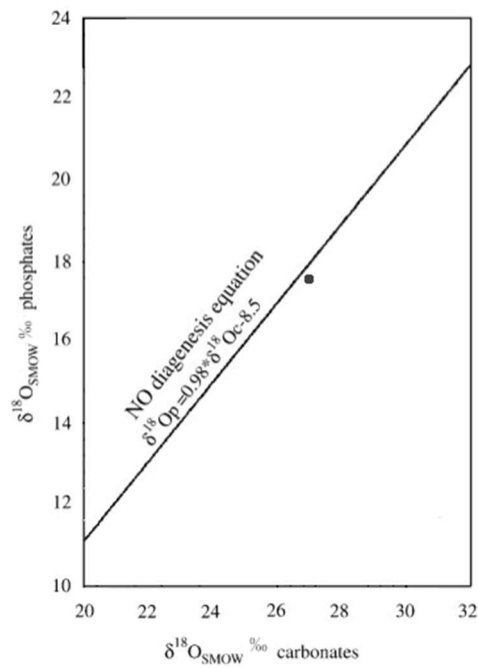


Figure 30 Scatter plot of $\delta^{18}\text{O}_\text{P}$ and $\delta^{18}\text{O}_\text{C}$ in enamel bioapatite. The straight line refers to the line of non-diagenetic equation drawn from Iacumin et al. (1996).

5.3.3 Discussion

The isotopic concentration was determined on a single sample, and the range of variability is not known. Consequently, the results on the paleodietary habits and on the paleoenvironmental conditions are essentially compared with published data.

The close agreement of the carbon and oxygen isotopic values with those obtained from three samples collected from Italian (La Polledrara and Casal de'Pazzi) and German (Neumark-Nord) Middle Pleistocene straight tusked elephant remains indicates that the average climatic and environmental conditions inferred for the latter localities (Grube et al., 2010) were similar to those that existed at Poggetti Vecchi.

The carbon isotope measurement of the structural carbonate in the bioapatite of the elephant molars from Poggetti Vecchi is -11.05 ‰. The offset between diet and enamel carbonate is -14‰. Therefore, the corresponding calculated $\delta^{13}\text{C}$ value of the diet is -25.14‰ and falls into the field of C3 plants. At Neumark-Nord, $\delta^{13}\text{C}_{\text{sc}}$ values range between -14.1 and -11.2‰ with mean value of -12.4‰; the "Campagna Romana" samples range from -9.9 and -13.7‰ (Casal de'Pazzi) and -9.0 and -10.9‰ (La Polledrara). Hence, the overall $\delta^{13}\text{C}$ values of the diet vary from -23.1‰ to -28.1 (Grube et al., 2010). Variations of about 1‰ are not uncommon in plants and in natural systems and reflect seasonal climatic and environment fluctuations, as well as possible changes in plant physiology (Heaton 1999). Over time, possible changes in temperature and humidity could affect in different ways the isotopic composition of the enamel specimens; in addition, there can be seasonal variation on the types of plants growing in a specific area, e.g., evergreen trees are about +3‰ relative to deciduous trees (Brooks et al. 1997). In arid environments, $\delta^{13}\text{C}$ values are related to plant longevity [e.g., they are more negative annual plants than in short-lived ones, and these have more negative values than long-lived plants; on the other hand, $\delta^{13}\text{C}$ values are higher in woody plants than in herbaceous ones (Tieszen, 1991)]. In addition, in xeric climate C3 plants tend to have higher carbon isotope composition, whereas a closed canopy forest is normally associated with lower $\delta^{13}\text{C}$ values. Modern elephants show seasonal fluctuations in their diets; assuming that the same occurred in extinct species (Cerling et al., 1999), the dietary shift towards more grazing habits in the Poggetti Vecchi population of *Palaeoloxodon antiquus* can be a response to more humid conditions; in other words, the Poggetti Vecchi elephants had to turn to grass-eating, as living elephants do today in special seasonal circumstances.

The $\delta^{18}\text{O}$ values vary considerably in the teeth of *P. antiquus* from other localities that are used here for comparison. In particular, the La Polledrara (MIS9) and Casal de'Pazzi (MIS7) specimens gave water $\delta^{18}\text{O}$ values ranging from -6.7 to -8.3‰ (mean value -7.6‰) and from -6.2 to -8.5‰ (mean value -7.1‰) respectively (Palombo et al. 2005); in the Neumark-Nord specimens $\delta^{18}\text{O}$ ranges from -6.1 to -8.8‰ (mean -7.2‰; Grube et al., 2010). There is a small but not negligible offset between the mean values in past and present precipitations in these different localities. The Italian samples are somewhat more negative, which indicates that the mean rainfall over the same area was about 1‰ lower than it is today

(modern mean $\delta^{18}\text{O}_w$ is -6.4); the German elephants are enriched in ^{18}O by about 2‰ in comparison to modern precipitation (mean annual value -9.5‰) in the Leipzig area (Grube et al., 2010). In contrast to the Italian elephants, which likely relied on two sources of drinking water, i.e., ponds/lakes (filled with local rainwater) and rivers, the German population watered mainly from local lake. River water is not subject to intense evaporation; it can give more negative $\delta^{18}\text{O}_w$ values than local rain, mainly because rivers carry water long distances from the catchment basin, and, perhaps, from higher elevation. In contrast, lakes and ponds undergo evaporation and become enriched in heavy isotope molecules. In particular, variations of about 0.8–1.3 ‰ in $\delta^{18}\text{O}_w$ values may reflect mean temperature variations from 1°C to 2°C and values about 0.5 ‰ may indicate temperature shifts in the same area over time (e.g., MIS9 was slightly warmer than MIS7); alternatively, they could be related to humidity fluctuations. According to these results, average environmental conditions during MIS9 and MIS7 were probably not far from modern ones (Grube et al., 2010). The water $\delta^{18}\text{O}_w$ at Poggetti Vecchi (-6.18 ‰) is slightly more positive than those calculated from the “Campagna Romana” and Neumark-Nord remains; furthermore, it seems in equilibrium with the isotopic values of modern local precipitations (which range from -6‰ to -7‰; Giustini et al., 2016). Our results seem therefore in line with those from Casal de’Pazzi (MIS7) and confirm the general environmental scenario for the Middle Pleistocene of central Italy. Hence, both $\delta^{18}\text{O}_w$ and the calculated diet isotopic composition of the Poggetti Vecchi elephant molars are consistent with a landscape dominated by wooded grasslands, under colder and/or wetter conditions than the present ones (**Figure 31**).

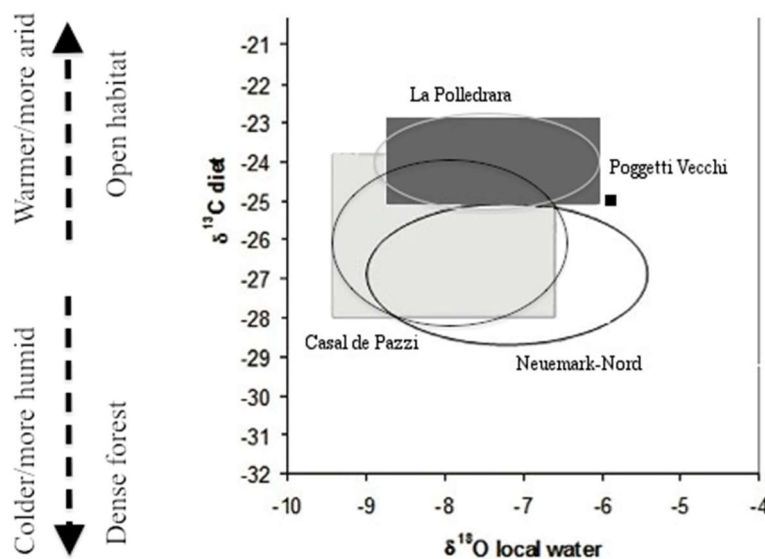


Figure 31 Variations of carbon and oxygen isotope values of calculated diet and local meteoric water. Comparative data for palaeoloxodonts specimens from Neumark-Nord, la Polledrara di Ceganibbio and Casal de’Pazzi were drawn from Grube et al. (2010).

5.4 Mesowear

5.4.1 Introduction

Mesowear analysis was originally meant to be applied only to selenodont and ectolophodont molars, with buccal ridges bearing well-marked wear facets (e.g. Kaiser, 2004; Kahlke and Kaiser, 2011). It has thus been extensively used to investigate the feeding habits of ungulate faunas and considered a main proxy for paleoenvironmental reconstructions (Kaiser and Schulz, 2006). Its application was recently extended to herbivorous mammals with other kinds of tooth morphology. In particular, Saarinen et al. (2015) partially modified the traditional method to apply it to proboscideans, because the original protocol was not suitable for elephants which chew with fore-aft movements of the mandible and with oblique shearing of the enamel lamellae against each other. This specialized chewing mechanism does not allow the development of easily measurable facets on the occlusal surface; nonetheless, the theoretical principles of tooth wear are expected to be similar to those of other herbivores. Mesowear is therefore considered as a proxy for grazing habits; higher tooth relief is maintained if non-abrasive plants are the dominant food items. In this case the occlusal surfaces show high wear-resistant enamel ridges and deeper valleys carved into the softer dentin (Saarinen et al., 2015). Conversely, abrasive plants produce the blunter occlusal surfaces.

According to the biomechanics of the chewing apparatuses of elephants, mesowear angles are taken from the bottom of worn dentin valleys, where the most reliable dietary signals can be recorded (Saarinen et al., 2015). Furthermore, from a functional morphological perspective, the central portion of each molar represents the focus area for mesowear analysis, and not the front plates, which suffer the most severe wear, nor the rear ones. Saarinen et al. (2015) used a digital goniometer to evaluate mesowear angles: the vertex of the instrument was easily put at the bottom of the worn dentine valleys and the arms placed tangent to the top of the adjacent enamel ridge. The average values were estimated based on angle measures of the three central lamellae of each molar analyzed; when the number of plate is even, the three central lamellae must be selected so that one is anterior and two posterior to the geometric center of the tooth. Then, Saarinen et al. (2015) used the linear regression between mean mesowear angles and enamel $\delta^{13}\text{C}$ values in modern and fossil elephants to calculate boundary values of mean mesowear angles corresponding to the average thresholds between dominance of C3 or C4 plants (>70%) and essentially pure C3 or C4 (>90%) diets. Positive correlation between mesowear angles and enamel $\delta^{13}\text{C}$ values supports the hypothesis that mesowear angles reflect specifically the abundance of grasses in the living environments and not just general landscape openness. The mesowear angles/enamel $\delta^{13}\text{C}$

values relationship can be roughly used to assign proboscideans to grass- or browse-dominated feeders also outside tropical areas, because it compares the amounts of abrasive and non-abrasive plant material that is consumed independently of the metabolic pathway involved. The late Pleistocene Columbian mammoth specimens (*Mammuthus columbi*) from Rancho la Brea were specialized grazers and thus likely grass- and sedge-dominated feeders, because mesowear angles exceed the “pure grazer” threshold value of 130° (Saarinen et al., 2015).

As already mentioned previously, several isotopic studies indicated that both modern African and Asian elephant are mixed-feeders with C3-dominated diet (Sukumar and Ramesh, 1995; Cerling et al., 1999). Nonetheless, some individuals may have a considerable C4 component in their diet, especially elephants that live in open grass-dominated environments (Cerling et al., 1999, 2004); although their physiology and dental morphology have adapted to the grassy or open-ground surroundings, these animals may still include a substantial browsing component in their diet. Mesowear supports this hypothesis: angles up to about 120° indicate a C4-dominated diet and average mesowear angles of about 110° are usually associated with the consumption of C3 plants (Saarinen et al., 2015). Saarinen et al. (2015) stated that all the East African extinct elephant species with supposed average grass-dominated diets show almost similar mesowear values, indicating more blunt enamel structures than in modern taxa. In proboscideans mesowear-based dietary analysis should only be used at the level of species or populations because individual correlation between angles and isotopic values, which still is significant, appears weaker than in the former case, mainly due to the size biases of each specimen (Saarinen et al., 2015). Mesowear and isotope composition do not provide the same dietary indications because tooth wear refers to the latest stage of an individual's life, whereas the isotopic composition reflects earlier phases. Quite remarkable differences in mesowear angles can be observed in left and right molars of each individual, probably due to one-side chewing habits. Several studies on modern taxa show that changes in the feeding habits occur throughout the life of each individual and can also be affected by seasonal shifts in the dietary preferences (Sukumar and Ramesh, 1995; Cerling et al., 2006, 2009; Rivals et al., 2012).

5.4.2 Materials and methods

The specimens are the same used for the microwear analysis. The sample included upper and lower premolars and molars. All the specimens are at a middle stage of wear. Empirical observations exclude significant differences in angular measurements, which can therefore be obtained arbitrarily on either lower or upper molars (Kaiser and Fortelius, 2003).

The method used here is similar to that proposed by Saarinen et al.

(2015), with minor changes aimed at simplifying the selection of the widest portion of each enamel loop and the subsequent acquisition of the measures. The mesowear angles were measured on detailed profiles rather than using the goniometer directly on the specimens. A Burton's steel professional comb was employed to evaluate the profile of the occlusal surface of each specimen. Then, contour gauges were used to identify the dentine valleys (Figure 32). Following Saarinen et al.'s (2015) indication, the mesowear angle measurements were taken using a digital goniometer with 0.1 precision. In addition, given that the sample includes also complete upper and lower mandibles, whenever possible, to detect any possible variation within each individual, comparative measurements were taken on right and left sides. According to Saarinen et al. (2015), the average mesowear angles were calculated based on the measurements obtained from the three central lamellae. The results were then compared with those reported by Saarinen et al. (2015). Finally, following the indications given by Saarinen and Lister (2016), the average mesowear angles were correlated with the percentages of the local pollen of non-arboreal species (NAP) and, in particular, of Graminae, to evaluate how much local vegetation is reflected by the inferred dietary habits.

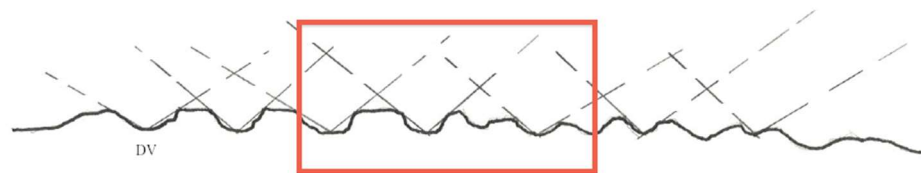


Figure 32 An example of the occlusal profile obtained with the Burton's comb with mesowear angles. DV = dentine valley. The three central dentin valleys are shown in the red box.

5.4.3 Results

The mean mesowear angles and the corresponding ranges of values including the standard errors (for each sample and for the whole population) are reported in **Table 7** and **8**. Each specimen yielded wide ranges of mean acute mesowear angles. In each specimen, the mean mesowear angles range from 90.95° to 119.82°, and in the population as whole, the angle measurements vary from 102.63° to 119.82°.

Tooth	Side	Specimen	Mesowear angle range (°)	Mean mesowear angle (°)	St. Err.
m3	Right	5500	100.95-110.00	106.73	2.90
M2	Left	265	91.30-107.95	102.63	5.67
m2	Right	5546	95.45-115.50	108.73	6.64
M2	Right	1609	99.90-107.95	105.20	2.65
M2	Left	1609	93.80-111.65	101.73	5.25
m2	Right	5547	111.90-129.45	119.82	5.14
m2	Left	5547	96.70-107.30	103.15	3.27
m1	Right	98	86.15-96.10	90.95	2.88
m1	Left	98	98.40-113.25	112.60	8.02
d3	Right	219	103.55-114.25	110.22	3.36
d3	Left	219	84.50-118.70	101.32	9.88
d4	Right	219	102.85-118.70	111.02	4.58
d4	Left	219	104.30-117.45	111.13	3.80
D4	Right	5298	99.85-116.65	107.93	4.86
D4	Left	5298	99.15-105.90	102.53	1.95

Table 7 Mesowear angle calculations for each specimen with standard errors.

Genus	Species	Mesowear angle range (°)	Mean mesowear angle (°)	St. Err.	N
Palaeoloxodon	<i>P. antiquus</i>	102.63-119.82	108.67	1.91	8

Table 8 Mean mesowear angle calculations for population with standard errors.

The regression analysis is shown in **Figure 33**; the comparison of the mean mesowear angles with the relative Graminae pollen frequencies calculated at Poggetti Vecchi (M. Mariotti Lippi personal communication) are shown in **Figure 34**.

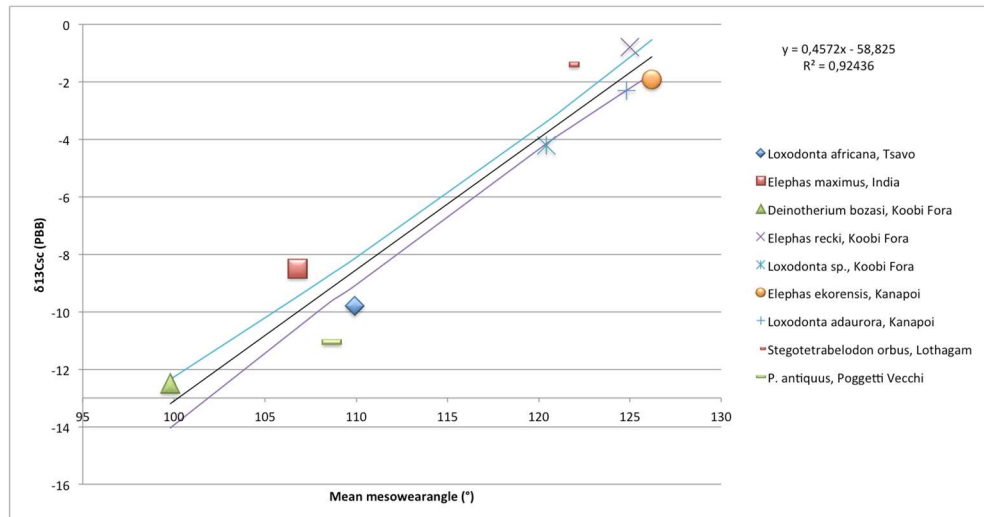


Figure 33 Linear regressions of $\delta^{13}\text{C}$ values from tooth enamel and mean mesowear angles. Value obtained from molar sampled at Poggetti Vecchi was compared with data drawn from Saarinen et al. (2015). The 95% confidence limits are shown as dashed lines. (Coefficient $R^2 = 0.92$, Student's t-tests $P < 0.001$).

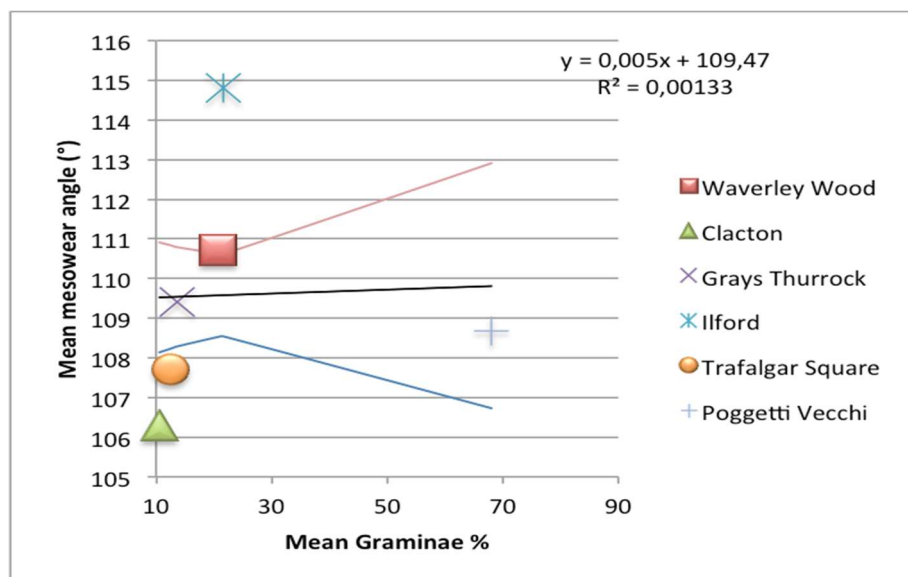


Figure 34 Regressions between mean mesowear angles and mean Graminae (grass) %. Values obtained from molars sampled at Poggetti Vecchi were compared with data drawn from Saarinen and Lister (2016). (Coefficient $R^2 = 0,00133$. Student's t-tests $P = 0.001$).

5.4.4 Discussion

Compared to other methods (i.e., isotope and microwear analyses), mesowear is faster, not exposed to the risks of contamination, non-destructive, easy-to-do and generally applicable. It provides a direct indication of the amount of abrasive and nonabrasive plants regardless of the photosynthetic pathways employed by the terrestrial plants, and allows

the detection of C3-grazing, which is not indicated as directly as it is by the $\delta^{13}\text{C}$ values. Consequently, mesowear can also be employed outside the tropical area. Based on the mesowear results, the Poggetti Vecchi straight-tusked elephants had a browse-dominated mixed diet with relatively flexible feeding behaviors. The weak positive correlation between the mean angle measure and the percentage of Graminae pollen confirms this suggestion.

5.5 Surface topography assessment

5.5.1 Introduction

Conventional 2D-microwear analysis is a useful tool in assessing basic physical properties of the diet and dental function; however, it is unable to explain how scars are physically and chemically related to specific food items, and in which extent they are the result of tooth morphology and function, foraging and chewing behavior, and digestive physiology (Every et al., 1998). Rensberger (1978) suggested to analyze surface texture to address paleodietary issues. Any surfaces can be described as a complex landscape with peculiar geometric form and textural alterations; these include the more widely spaced modifications from the nominal shape (waviness); as well as roughness, which consists of the finest ones (Kaiser and Brinkmann, 2006). Surface textures that appear smooth at coarse scales can be demonstrably rough at sufficiently fine scales. Roughness parameters, which describe vertical surface features (height parameters), horizontal features (spacing parameters) and integrated parameters, are a highly indicative statistical tool to characterize surface micro texture (ISO 4287, 1997). Worn enamel finds correspondence with industrially manufactured surfaces; therefore, 2D-surface roughness parameters can be used to characterize the physical topography of enamel facets, quantifying the universal attrition–abrasion equilibrium controlling dental wear. Hence, roughness permits to discriminate individuals of the major feeding categories based on their paleodietary habits (Kaiser and Brinkmann, 2006). Dental wear analysis allows not only to describe irregularities of the tooth surfaces but also to detect alterations that represent areas of differential wear resistance, which are revealed by their uniform frequency and amplitude. The tooling process (e.g. sawing, planing, milling, grinding) may produce unidirectionally aligned striations on technical surfaces; these mimic the micro-texture alignments observed also in herbivorous cheek teeth, which indicate the chewing power stroke direction.

Describing complex geometry patterns using the jargon of fractal analysis can convey some of the complexity inherent in their design; it applies non-traditional mathematics to patterns that defy understanding with Euclidean concepts. Whatever type of fractal analysis is used, it rests on

some kind of fractal dimension that represents a measure of complexity. The latter is a change in detail with change in scale. Anisotropy is the opposite of complexity and is a measure of directionality of surface roughness (**Figure 35**). This description of directionality may be used to test hypotheses relating to the directionality of jaw movements during mastication (Scott et al., 2006).

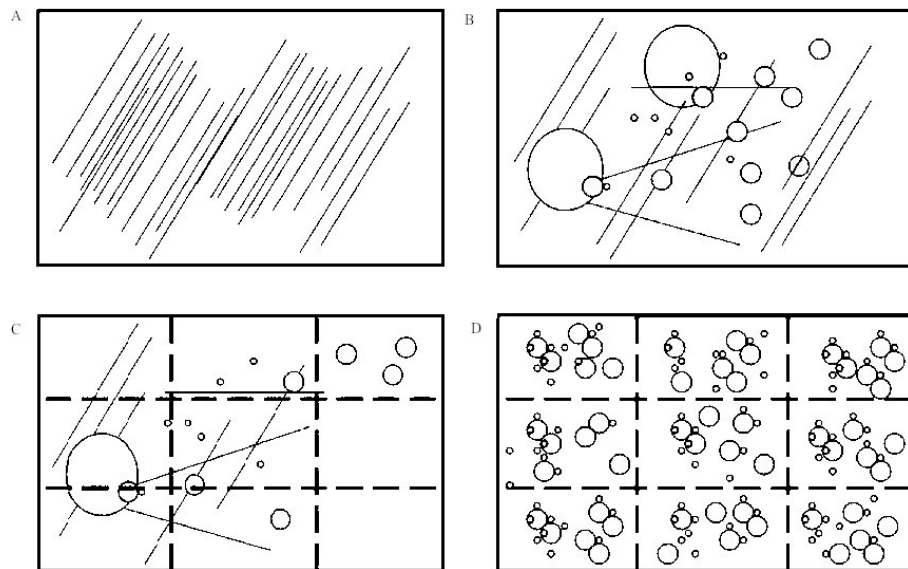


Figure 35 Hypothetical microwear surface texture schemes. A) Anisotropic; B) complex; C) heterogeneous and D) homogeneous texture. (Drawn from Scott et al., 2006).

Contact and non-contact methods are used to record the surface patterns. Surface measuring systems reconstruct 3D-surface models by assembling line profiles. However, especially in finely striated surface, much of the topographic information is encapsulated in a single line profile that can much easier be measured than 3D-surface models (Kaiser and Brinkmann, 2006). In this study, epoxy casts of enamel surfaces were scanned using a high resolution digital 3D KH 7700 Hirox microscope, which produces high-resolution 3D images rendered in a color scale. The microscope also allows linear, angular and profile (x, y and z) measurements of the topographic roughness of a tooth surface. The method differs from the traditional Dental microwear texture analysis (DMTA), which typically uses an optical profiler to examine three-dimensional tooth surfaces via scale-sensitive fractal properties (SSFA) or standardized surface parameters (e.g., Ungar et al., 2003; Scott et al., 2005; 2006, Schulz et al., 2010; Purnell et al 2012). However, the 3D digital microscopy method maintains the conceptual framework and important parameters (2D roughness criterion, isotropy and fractal dimensions) needed to characterize enamel texture patterns extracted from digital images.

Amplitude parameters	Description	Unit
Rt	Total height of the profile: height between the deepest valley and the highest peak on the evaluation length. Rt is very sensitive to abnormal points (deep holes or extreme peaks).	μm
Rp	Maximum profile peak height: height of the highest peak from the mean line, defined on the sampling length.	μm
Rv	Maximum profile valley depth: depth of the deepest valley from the mean line, defined on the sampling length.	μm
Rz	Maximum height of the profile defined on the sampling length. This parameter is frequently used to check whether the profile has protruding peaks that might affect static or sliding contact function.	μm
Ra	Arithmetic mean deviation of the assessed profile. Result is expressed in the length unit of the Z-axis.	μm
Rq	Root mean square deviation of the assessed profile corresponds to the standard deviation of the height distribution, defined on the sampling length. Rq provides the same information as Ra.	μm
Rc	Mean height of profile elements defined on the evaluation length.	μm
Rsk	The skewness of the assessed profile: asymmetry of the height distribution, defined on the sampling length. This parameter is important as it gives information on the morphology of the surface texture. Positive values correspond to high peaks spread on a regular surface (distribution skewed towards bottom) while negative values are found on surfaces with pores and scratches (distribution skewed towards top. However, this parameter does not give any information on the absolute height of the profile, contrary to Ra.	No unit
Rku	Kurtosis of the assessed profile: sharpness of the height distribution, defined on the sampling length.	No unit
Spacing parameter	Description	Unit
RSm	Mean width of profile elements, within a sampling length given in length unit of the X-axis. In case of a periodical or pseudo-periodical profile, RSm will give the length of the period.	μm
Hybrid parameters	Description	Unit
Rdq	Root mean square slope of the assessed profile defined on the sampling length. Rdq is a first approach to	°

	surface complexity. A low value is found on smooth surfaces while higher values can be found on rough surfaces having microroughness.	
Rda	The average absolute slope of the profile within the sampling length.	°
Bearing ratio curve parameters		
RTp	Bearing ratio of the complete profile at a given level (expressed in percent). The level can be specified in height or depth from the average, in depth from the highest point, in height from the lowest point, or in height or depth from a reference given by its bearing ratio (which is defined in depth from the highest point). The level (p) is specified as 2.5 ym (yoctometer) depth from the highest point that is the default reference most commonly used in technical applications.	%
RHTp	Bearing height. Height of the bearing ratio of the complete profile. It gives the vertical distance between two cut levels given their bearing ratio. The result is expressed in the Z-axis length unit.	µm
Other		
Rdf	Gives the value of the fractal dimension computed using the boxes method. The fractal dimension of a profile is between 1 and 2.	No unit
RS	Mean spacing of local swells of the profile. This parameter computes the mean distance between 2 local swells (peaks) of the profile.	µm
RD	Swell density. Equal to the inverse of the mean spacing between two swells. It is expressed in swells (peaks) by length unit.	1/µm
Rlq	Calculated on basis of RDq and Rq. Quadratic mean wavelength of the profile. The result is expressed in length unit of the X-axis.	µm
R3z	Third points height. R3z is defined on a sampling length as the height between the highest peak, to the third deepest hole. Result is expressed in length unit of the Z-axis.	µm
RzJIS	Ten points height. The RzJIS is defined on each sampling length as being the sum of the 5 highest peaks and the 5 deepest holes, divided by 5. The result is expressed in length unit of the Z-axis.	µm
RH	Swedish height. Equal to the height of the bearing ratio (XHTp) between 5% and 95%.	µm
RHSC	Spot count. Counts the number of local peaks above a given threshold.	No unit
Rlo	Developed length of the profile. It is the ratio between	%

	the length measured following the profile curve, and the profile length, expressed in excess of 100%; values are usually between 0% and 10%.	
RVo	Volume of retention of fluid.	$\mu\text{m}^3/\mu\text{m}^2$
Rmax	Largest single roughness depth within the evaluation length.	μm
Rtm	Average maximum peak to valley height of five consecutive sampling lengths within the measurement length.	μm
Ry	Maximum height of the profile.	μm
Rla	Average wavelength of the profile.	μm
Rpm	Average maximum profile peak height.	μm
Rp1max	Larger single peak from the mean line.	μm
Rv1max	Larger single valley from the mean line.	μm
Rz1max	Larger Rz value from the mean line.	μm

Table 9 Detailed description of the 2D-roughness texture parameters calculated by the software MountainsMap7® Image (DigitalSurf, France).

5.5.2 Materials and methods

The two specimens that have been selected for this investigation are the molar 5500, which belong to a full adult individual, and 98, which instead is of an about 8-year-old elephant cub. Digital images were acquired at the Department of Physical, Earth and Environmental Sciences of the University of Siena using a Hirox KH-7700 digital microscope with an MXG-10C body, an OL-140II lens and an AD-10S Directional Lighting Adapter. The Auto Multi Focus tool enabled the creation of 3D images obtained by composing a set of planes taken at different focuses. On the samples surface, a rectangular area of about $450 \times 600 \mu\text{m}$ was scanned using a 500x objective; almost three ROIs (regions of interest) were selected at the center of the two central enamel loops of the teeth and scanned to inspect if and how the surface texture varies on each sample. The ROIs were selected based on a preliminary survey and acquisition performed using a 100X objective to document the imaging process; then the same areas were scanned at 500x. The scans were performed at $1.909 \mu\text{m}$ and at $0.381 \mu\text{m}$ resolution with the 100x and 500x lens, respectively. An average of fifteen planes were taken with a vertical step ranging from 4 to $8 \mu\text{m}$ (depending on the topographic features of the sample), covering a depth from 100 (in sample 98, area 2) to 55 (in sample 5500, area 4) μm .

The software MountainsMap7® Image (DigitalSurf, France) was used to obtain 2D images of the topography of the acquired areas. In addition, almost 10 roughness profiles along with ISO 4287 (1997) standard parameters were extracted from each image by applying a Gaussian filter (to clean the raw data) of 0.08 mm and 0.25 mm for samples 98 and 5500, respectively (an example is shown in **Figure 36**).

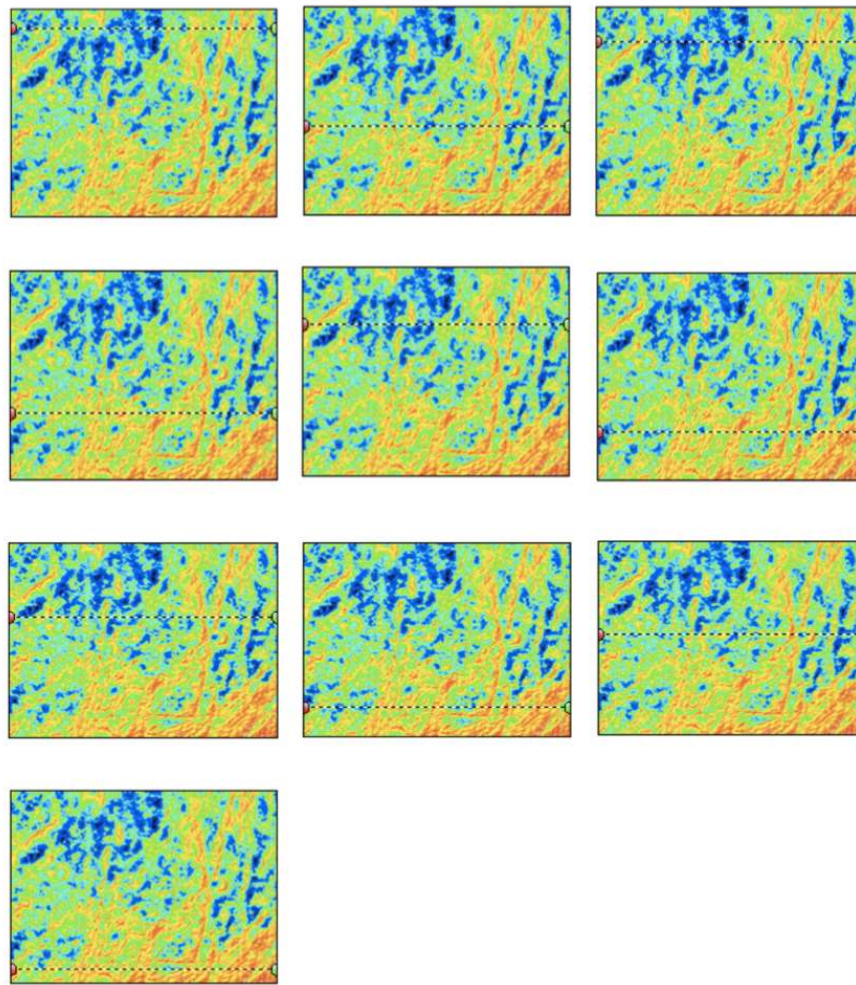


Figure 36 The location of the 10 2D-roughness profiles extracted from one of the selected ROIs of the specimen number 5500.

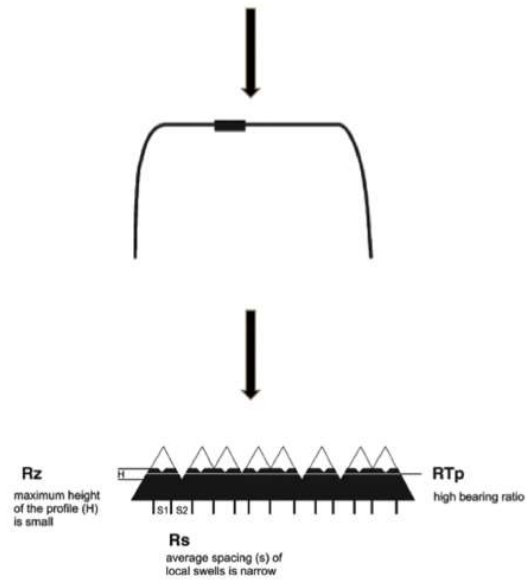
The 2D-roughness standard parameters that have been calculated are listed and briefly described in **Table 9**. However, only a few parameters are informative in paleodietary analysis (Kaiser and Brinkmann 2006). In particular, R_a is the roughness average computed as arithmetic mean deviation of the assessed profile. It is the most commonly applied industrial surface roughness parameter; its results are expressed in the length unit of the Z-axis. Kaiser and Brinkmann (2006) found that grazers show the highest R_a -values and browsers the lowest. R_a increases when more coarse surface elements are introduced. Similarly to R_a , R_z computes the maximum height of the profile within a sampling length. The maximum height of a profile (R_z) of a local swell or valley needs to exceed all the other topographic features of the surface (swells and valleys) in its vertical dimensions; only coarse scratches can produce these kinds of alterations; R_z is therefore a measure for coarse scratches. R_p is the maximum profile peak height within a sampling length. R_p is highest in grazers and lowest in

browsers, whereas in mixed feeders R_p values are roughly intermediate between those of pure grazers and browsers. RS computes the mean distance between 2 local swells (peaks) of the profile. The spacing RS_m and the hybrid R_{lq} parameters give the mean width of profile elements and the quadratic mean wavelength of the profile, respectively; both are expressed in length units of the X-axis. The bearing ratio parameters (R_{Tp} and R_{HTp}) have the highest potential in discriminating browser, grazer and mixed feeders and, consequently, may characterize the enamel surfaces (facets), and thus help placing animals into different feeding categories (Kaiser and Brinkmann 2006). R_{Tp} gives the bearing ratio of the complete profile at 2.5 μm below the highest point of the profile; this is the default reference most commonly used in technical applications (Kaiser and Brinkmann, 2006). Theoretically, this parameter gives information on the amount of surface area (i.e., technical surfaces exposed to friction) that is available for load after a certain amount of initial wear has taken place. The bearing ratio was found to be the highest in browsers and the lowest in grazers; we must therefore expect a much flatter wear profile in the former (**Figure 37A** and **B**). In contrast to R_{Tp} , R_{HTp} indicates the height difference of the bearing ratio curve between two points of the profile (expressed in the Z-axis length unit) independently of the highest point of the profile section. High R_{HTp} -values characterize pure grazers and indicate a steep bearing ratio curve, low values a flatter one. Abrasion and attrition are the two major factors controlling tooth wear; mesowear indicates that the two factors result in an equilibrium that remains stable over long periods of time. However, attrition prevails in browsers, whereas abrasion is the most effective agent of tooth wear in grazers. The physical properties (hardness and softness) of foods eaten by grazers and browsers are very different. For instance, dicotyledonous plants are physically heterogeneous, i.e., softer or tougher, but anyhow less abrasive than grasses. Furthermore, thickness of plants and the level of resistance to breakage can vary widely (Sanson, 1989). Attritional tooth wear prevails in browsers than in grazers, in which wear is dominated by abrasion; in general, it only takes place at the facet in the center of the enamel ridge, creating a platform and re-sharpening the edges (**Figure 37A**). Larger vascular bundles require shearing blades with sufficient relief (Archer and Sanson, 2002) and a highly efficient cutting-edge alignment to achieve fracture. In contrast, thickness is generally more uniform in grass than in dicotyledonous; grass diet is much harder, more brittle and much more abrasive, causing increased tooth wear. Grazers are on the other extreme of the dietary spectrum (**Figure 37B**). In grazers the lower bearing ratio seems to reflect the heavily striated and usually deeply incised surface of abrasion produced by more abrasive foods, which increase the cutting-edge radius. The higher degree of abrasion in grazers is reflected by low values R_{Tp} , and the rounded bearing ratio profile, as indicated by high R_{HTp} dimensions, are compatible with more grazer-

dominated mixed feeding habits. As reported in **Table 9** the hybrid parameter Rd_q (root mean square slope of the assessed profile defined on the sampling length) provides a preliminary assessment of 2D-profile complexity and low Rd_q values are usually associated with smooth surfaces (ISO 4287 1997).

A

Wear dominated by attrition: enamel facet flattened



B

Wear dominated by abrasion: enamel facet rounded

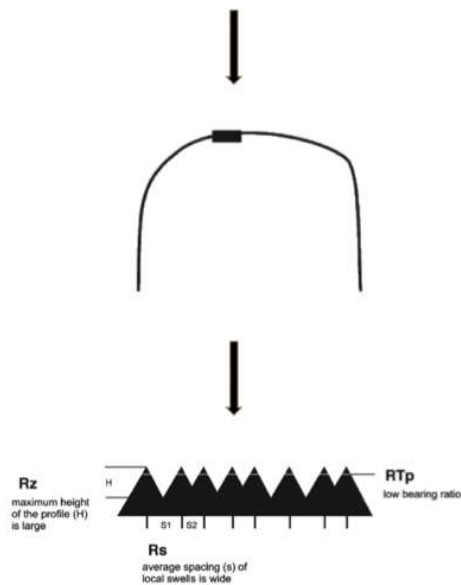


Figure 37 Hypothetical cross section of the apex of an enamel ridge in extreme of the dietary spectrum: browser (A) and a grazer (B). (Modified from Kaiser and Brinkmann, 2006).

In addition, the software MountainsMap7® also includes tools specifically designed to assess fractal dimension and isotropy by processing digital maps. In fractal geometry the fractal dimension (Df) is a ratio providing a statistical index of complexity comparing how detail in a fractal

pattern change with the scale at which it is measured (Falconer, 2003). The fractal dimension (Df) of a surface is a value within the range $2 \leq Df \leq 3$; values close to 2 indicate smooth surfaces and those tending towards 3 indicate more complex, irregular, rough surfaces). In this study, Df was calculated by processing microphotographs using a specific software tool of MountainsMap7®, i.e., the “enclosing boxes” method with a linear interpolation type. Hence the fractal dimension was calculated from the slope of the best fits of regression lines. The number of enclosed boxes or area depends on the scale (i.e., the size of the boxes or structuring elements) of the analyzed surfaces. In addition, a MountainsMap7® specific tool, which integrates the Fourier transform with the autocorrelation function, was used to determine the direction of the texture. It estimates the degree of isotropy (the higher the percentage value the more the surface resembles itself in every direction) and the three most dominant lay directions of a surface (in degree units). The results are displayed as dominant directions of roughness surface on a polar (or Cartesian).

Finally, 3D reconstructions were here obtained by the use of Interactive 3D-Surface Plot plugin of ImageJ software, which creates interactive surface plots (i.e., dots, lines, mesh, filled, display colors. etc.) from all kinds of images. 3D- images can be created in various ways, e.g., the 3D-projection and the dimension of the surface plot can be changed by adjusting the size of the data grid, and of the “perspective” and “scale” sliders. In addition, the plot height may be scaled with the Z-Ratio slider; noisy images can be smoothed with the “smoothing” slider; the “lighting” slider gives the impression that the plot was illuminated and so improves the visibility of small differences.

5.5.3 Results

The average roughness parameter values are listed in **Tables 10** and **11**. Despite some of them do not identify the specimens specifically enough to assign to a dietary category, especially in the case of mixed feeders, which can show variable values (Kaiser and Brinkmann 2006), they were anyhow included in our analysis. A small subset of parameters seems to characterize more efficiently the texture profiles of the Poggetti Vecchi elephants. Corresponding roughness parameters and geometry calculations are listed in **Table 12** and bar chart comparisons are summarized in **Figure 38**. Within the various ROIs, the average Ra values range from 2.93 to 6.10 μm and 18.53 to 42.27 in the specimen 5500, and Rz values from 3.34 to 9.16 μm and from 24.09 to 62.70 in the specimen 98. The average RS data range from 5.54 to 7.93 μm in 5500 and from 4.09 to 4.51 μm in 98, which indicates that the texture elements are somewhat more densely packed in the specimen 98. The average RSm and Rlq profiles obtained for the Poggetti Vecchi specimens are wider for the adult specimen 5500 (12.32 μm) and

narrower for the cub 98 (7.00 μm). The average R_{TP} value is 0.21% in the specimen 98 and 0.31% in 5500.

ISO 4287	98-1	98-2	98-3	Average	Dev.st	Unit
Rp	19.13	41.20	14.60	24.98	14.23	μm
Rv	11.73	21.50	9.50	14.24	6.38	μm
Rz	30.87	62.70	24.09	39.22	20.61	μm
Rc	12.84	27.21	9.32	16.46	9.48	μm
Rt	32.88	73.03	24.74	43.55	25.85	μm
Ra	4.22	9.16	3.34	5.57	3.14	μm
Rq	5.25	11.69	4.13	7.02	4.08	μm
Rsk	0.50	0.82	0.34	0.56	0.25	no unit
Rku	3.27	3.97	3.08	3.44	0.47	no unit
Rp1max	19.13	48.60	14.60	27.44	18.46	μm
Rv1max	11.73	24.40	9.50	15.21	8.04	μm
Rz1max	30.87	70.27	24.09	41.74	24.93	μm
RSm	7.62	5.30	8.08	7.00	1.49	μm
Rdq	81.93	87.09	80.18	83.07	3.59	°
RLq	23.04	48.33	18.54	29.97	16.06	μm
Rda	79.15	85.95	76.95	80.69	4.69	°
RLa	19.16	38.35	15.64	24.38	12.22	μm
RLo	455.75	1363.20	350.89	723.28	556.66	%
RzJIS	25.28	47.87	19.16	30.77	15.12	μm
R3z	24.74	46.07	18.17	29.66	14.59	μm
Rmax	30.87	70.27	24.09	41.74	24.93	μm
Rtm	30.87	62.70	24.09	39.22	20.61	μm
Ry	30.87	70.27	24.09	41.74	24.93	μm
RH	17.32	38.12	13.48	22.97	13.25	μm
RHSC	1.20	1.10	1.60	1.30	0.26	no unit
RD	0.13	0.20	0.13	0.15	0.04	1/ μm
RS	4.51	3.67	4.09	4.09	0.42	μm
RVo	0.00	0.00	0.00	0.00	0.00	$\mu\text{m}^3/\mu\text{m}^2$
Rrms	5.25	11.69	4.13	7.02	4.08	μm
RTp	0.16	0.25	0.22	0.21	0.04	%
RHTp	8.82	18.57	6.99	11.46	6.23	μm
Rfd	1.69	1.71	1.69	1.70	0.01	no unit
Rpm	19.13	41.20	14.60	24.98	14.23	μm
Isotropy	28.5	38.5	27.5	31.50	6.08	%
Fractal Dimension	2.72	2.77	2.74	2.74	0.03	no unit

Table 10 2D-Roughness and geometric calculations obtained from the three selected enamel ROIs studied for the molar n. 98.

ISO 4287	5500-2	5500-3	5500-4	Average	Dev.st	Unit
Rp	25.99	14.20	10.43	16.87	8.11	μm
Rv	16.28	16.06	8.10	13.48	4.66	μm
Rz	42.27	30.26	18.54	30.36	11.87	μm
Rc	17.55	10.80	6.36	11.57	5.63	μm
Rt	45.63	31.20	18.91	31.92	13.38	μm
Ra	6.10	4.50	2.94	4.51	1.58	μm
Rq	7.54	5.70	3.59	5.61	1.98	μm
Rsk	0.25	-0.20	0.27	0.11	0.27	no unit
Rku	2.90	3.04	2.73	2.89	0.15	no unit
Rp1max	25.99	14.20	10.43	16.87	8.11	μm
Rv1max	16.28	16.06	8.10	13.48	4.66	μm
Rz1max	42.27	30.26	18.54	30.36	11.87	μm
RSm	10.92	12.70	13.34	12.32	1.26	μm
Rdq	83.20	75.30	67.68	75.40	7.76	°
RLq	32.62	27.21	19.05	26.29	6.83	μm
Rda	81.01	71.03	61.74	71.26	9.64	°
RLa	27.12	22.79	17.08	22.33	5.03	μm
RLo	565.16	244.58	132.51	314.08	224.54	%
RzJIS	34.07	21.48	12.79	22.78	10.70	μm
R3z	33.71	20.60	12.05	22.12	10.91	μm
Rmax	42.27	30.26	18.54	30.36	11.87	μm
Rtm	42.27	30.26	18.54	30.36	11.87	μm
Ry	42.27	30.26	18.54	30.36	11.87	μm
RH	25.70	19.22	11.51	18.81	7.11	μm
RHSC	1.20	1.70	1.90	1.60	0.36	no unit
RD	0.09	0.09	0.08	0.09	0.01	1/μm
RS	5.54	7.93	6.82	6.77	1.20	μm
RVo	0.00	0.00	0.00	0.00	0.00	μm ³ /μm ²
Rrms	7.54	5.70	3.59	5.61	1.98	μm
RTp	0.15	0.39	0.39	0.31	0.14	%
RHTp	13.82	9.57	6.17	9.85	3.83	μm
Rfd	1.64	1.58	1.57	1.60	0.04	no unit
Rpm	25.99	14.20	10.43	16.87	8.11	μm
Isotropy	40.90	18.60	21.00	26.83	12.24	%
Fractal Dimension	2.74	2.64	2.59	2.66	0.08	no unit

Table 11 2D-Roughness and geometric calculation obtained from the main three-selected enamel ROIs studied for the molar n. 5500.

Parameters	98	5500	Unit
RTp	0.21	0.31	%
RHTp	11.46	9.85	μm
RS	4.09	6.77	μm
Rz	39.22	30.36	μm
RSm	7.00	12.32	μm
RLq	29.97	26.29	μm
Rp	24.98	16.87	μm
Ra	5.57	4.51	μm
Isotropy	31.50	26.83	%
Fractal Dimension	2.74	2.66	No unit

Table 12 A selection of 2D-roughness texture parameters and geometric patterns employed in this study and corresponding average values.

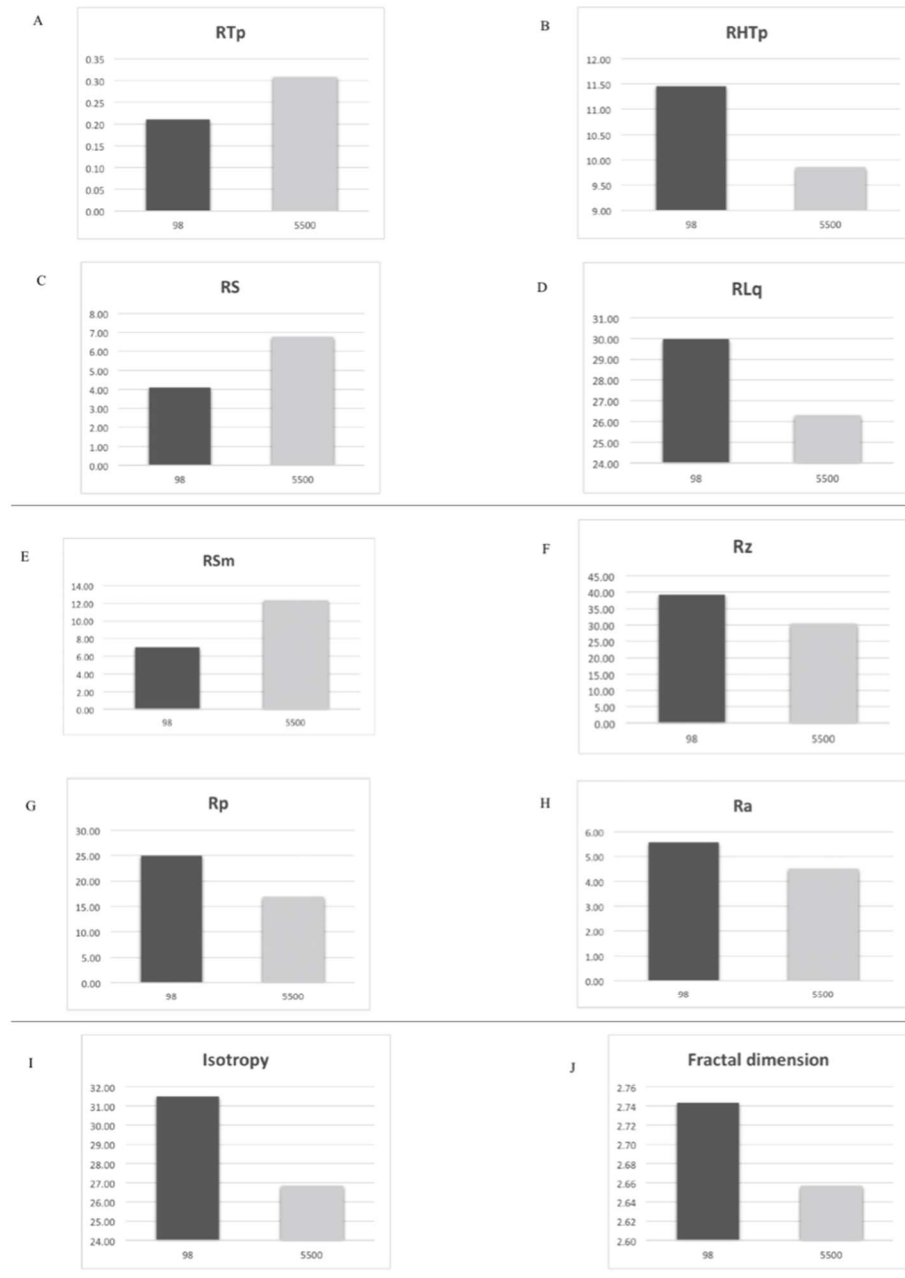
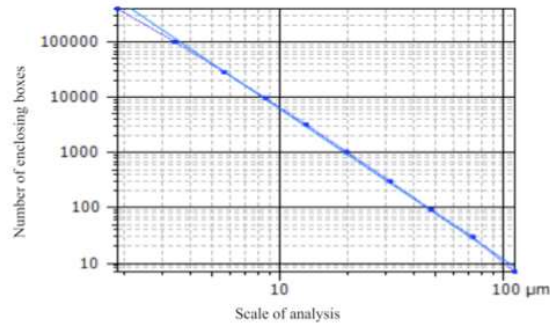


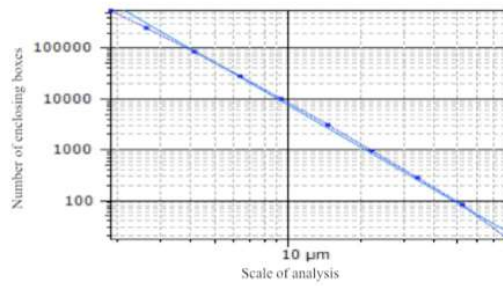
Figure 38 A-J Comparative bar charts of 2D-roughness parameters and geometric pattern calculations.

A



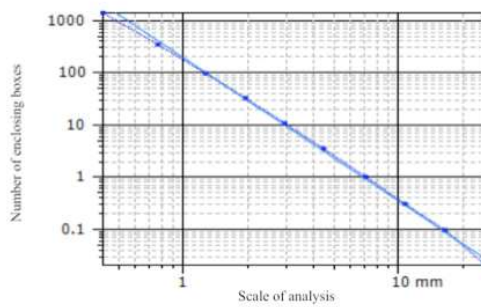
Information	
Method	Enclosing boxes
Parameters	
Fractal dimension	2.72
R ² (1)	0.999

B



Information	
Method	Enclosing boxes
Parameters	
Fractal dimension	2.77

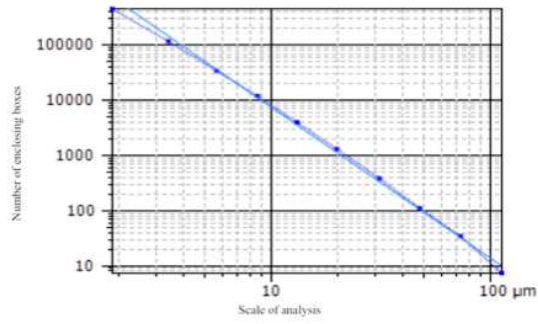
C



Information	
Method	Enclosing boxes
Parameters	
Fractal dimension	2.74
R ² (1)	0.998

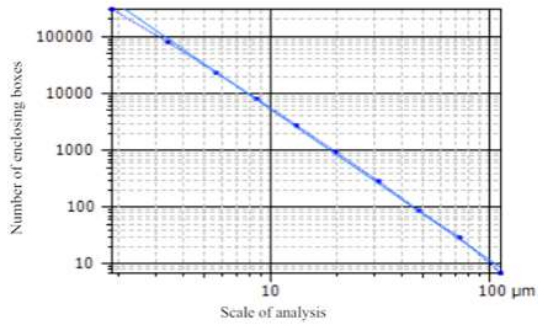
Figure 39 Example of fractal dimension analysis calculation for one the selected enamel ROIs studied for the molar n. 5500 following the enclosing boxes method [with the slope and correlation coefficient (R^2) of regression line].

A



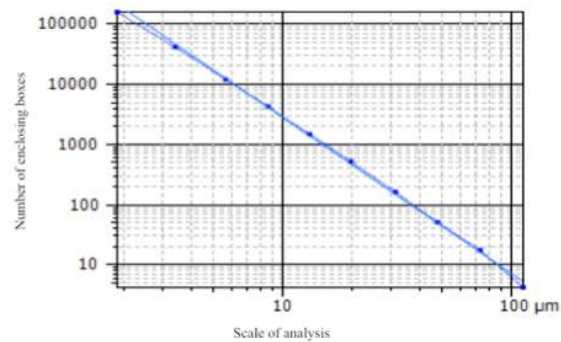
Information	
Method	Enclosing boxes
Parameters	
Fractal dimension	2.74
R ² (1)	0.998

B



Information	
Method	Enclosing boxes
Parameters	
Fractal dimension	2.64
R ² (1)	0.999

C

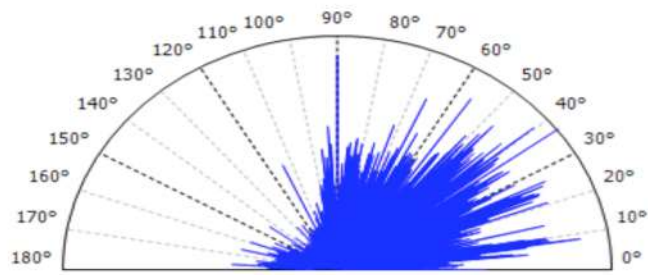


Information	
Method	Enclosing boxes
Parameters	
Fractal dimension	2.59
R ² (1)	0.999

Figure 40 A-B-C Fractal dimension analysis calculations of the main three selected enamel ROIs studied for the molar n. 5500 following the enclosing boxes method [with the slope and correlation coefficient (R²) of regression line].

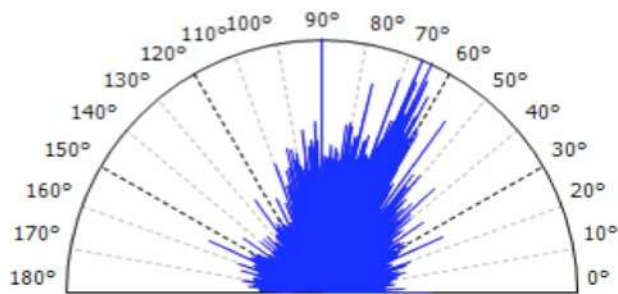
The fractal dimension was found to be rather similar in both the Poggetti Vecchi specimens; the average values are 2.66 in 5500 and 2.74 in 98, as shown by the **Figure 39** and **40**. The **Figures 41** and **42** summarizes the orientation of the roughness features (isotropy/anisotropy texture), which are expressed as angular values and isotropy percentage; the latter are more heterogeneous in the specimen 5500, varying from 18.6 to 40.9%, whereas the average value in the specimen 98 is 31.50%.

A



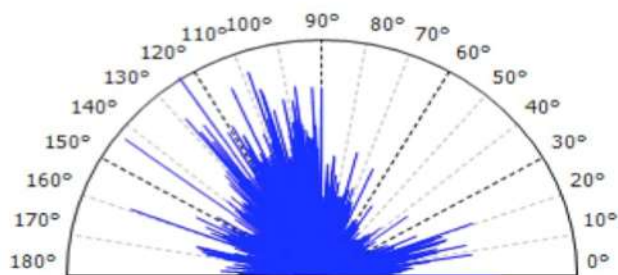
Parameters	Value	Unit
Isotropy	28.5	%
First direction	36.7	°
Second direction	90.0	°
Third direction	8.52	°

B



Parameters	Value	Unit
Isotropy	38.5	%
First direction	64.5	°
Second direction	90.0	°
Third direction	70.2	°

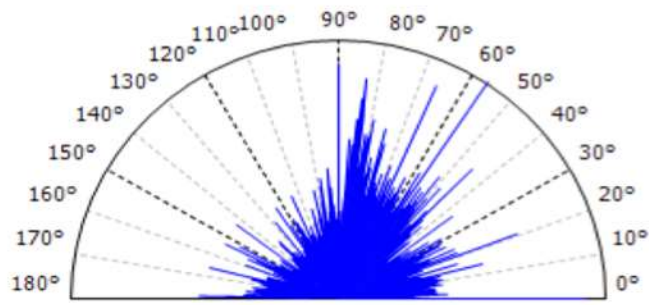
C



Parameters	Value	Unit
Isotropy	27.5	%
First direction	124	°
Second direction	143	°
Third direction	109	°

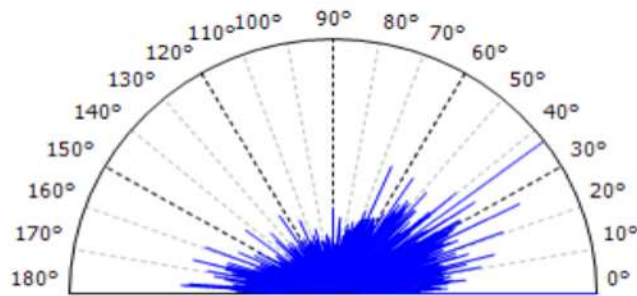
Figure 41 A-B-C Polar diagrams showing texture direction and related parameters of the three selected enamel ROIs studied for the molar n. 98.

A



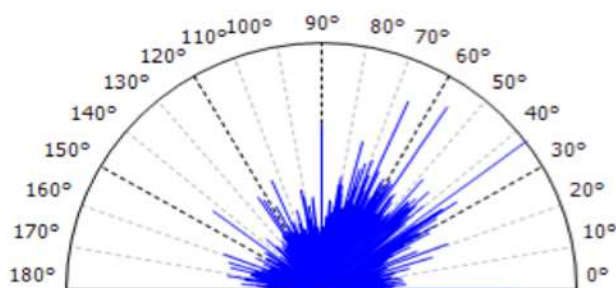
Parameters	Value	Unit
Isotropy	40.9	%
First direction	56.2	°
Second direction	0.208	°
Third direction	90.0	°

B



Parameters	Value	Unit
Isotropy	18.6	%
First direction	0.206	°
Second direction	36.7	°
Third direction	26.5	°

C

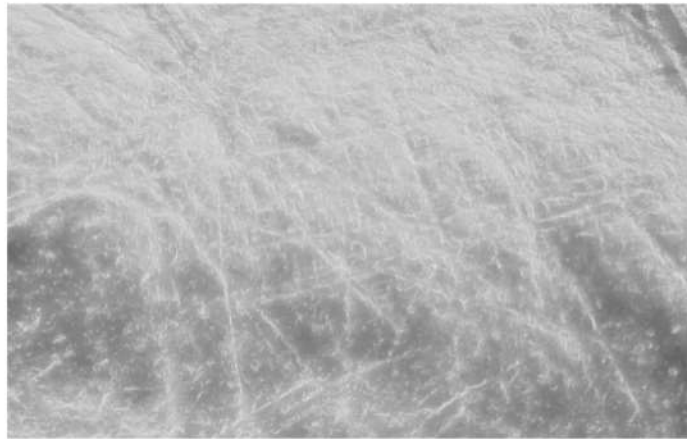


Parameters	Value	Unit
Isotropy	21.0	%
First direction	36.7	°
Second direction	56.3	°
Third direction	66.0	°

Figure 42 Polar diagrams showing texture direction and related parameters of the main three selected enamel ROIs studied for the molar n. 5500.

Figure 43 and **44** show the texture surface in its original aspect (**A**) and in false colors (**B**). 3D-reconstructions of the enamel samples are shown in **Figure 45 A** and **B**.

A



B

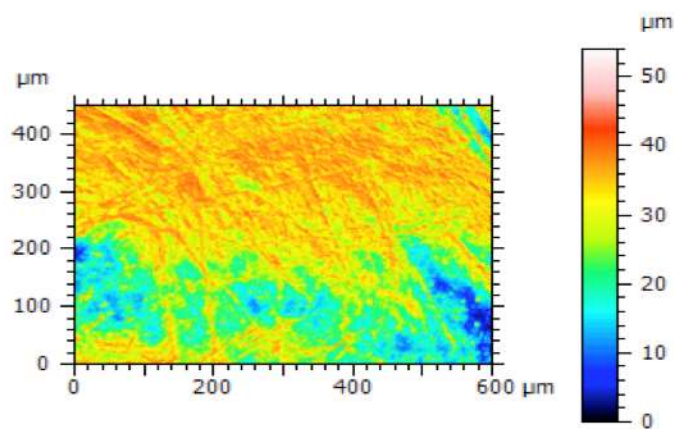
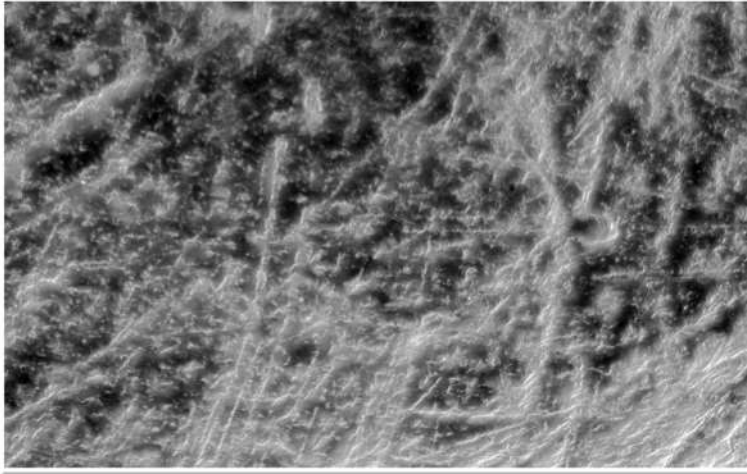


Figure 43 A) An example of enamel surface texture scan of the specimen 98 obtained using the digital microscope at 500x magnification; B) False color appearance.

A



B

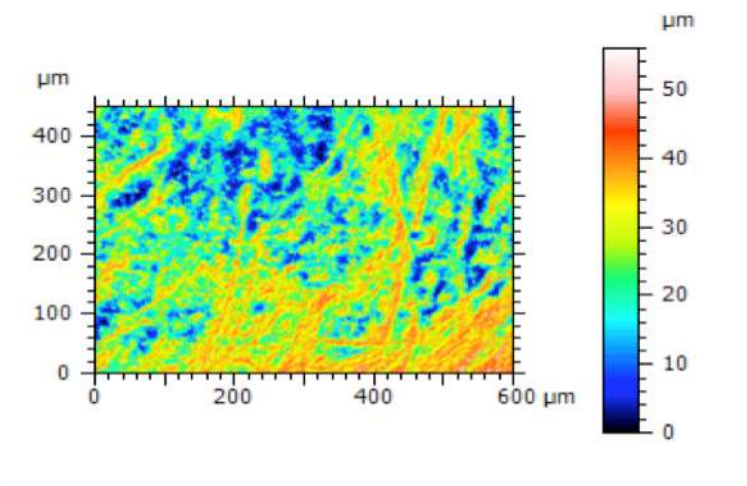
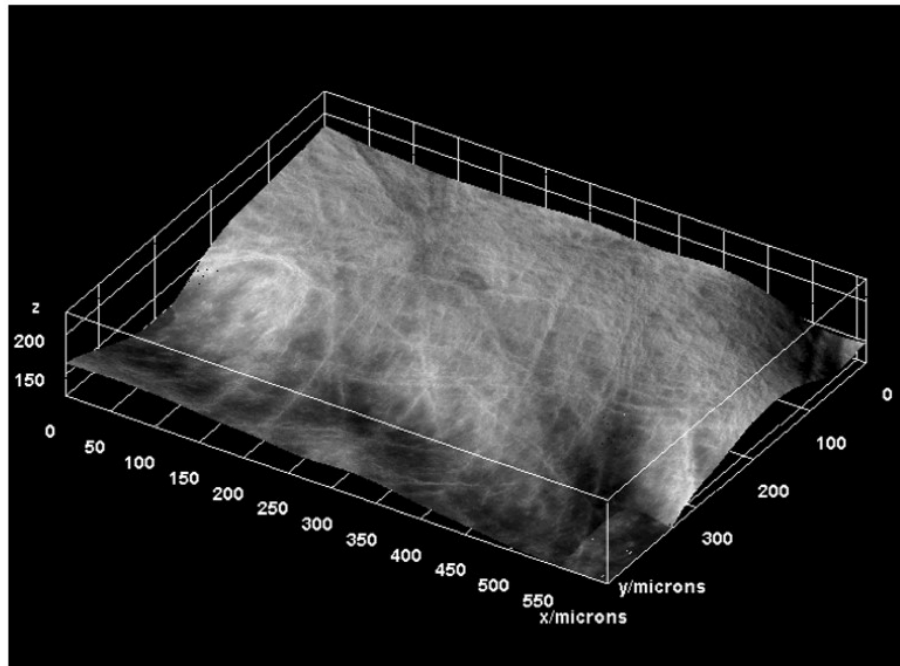


Figure 44 A) An example of enamel surface texture scan of the specimen 5500 obtained using the digital microscope at 500x magnification; B) False color appearance.

A



B

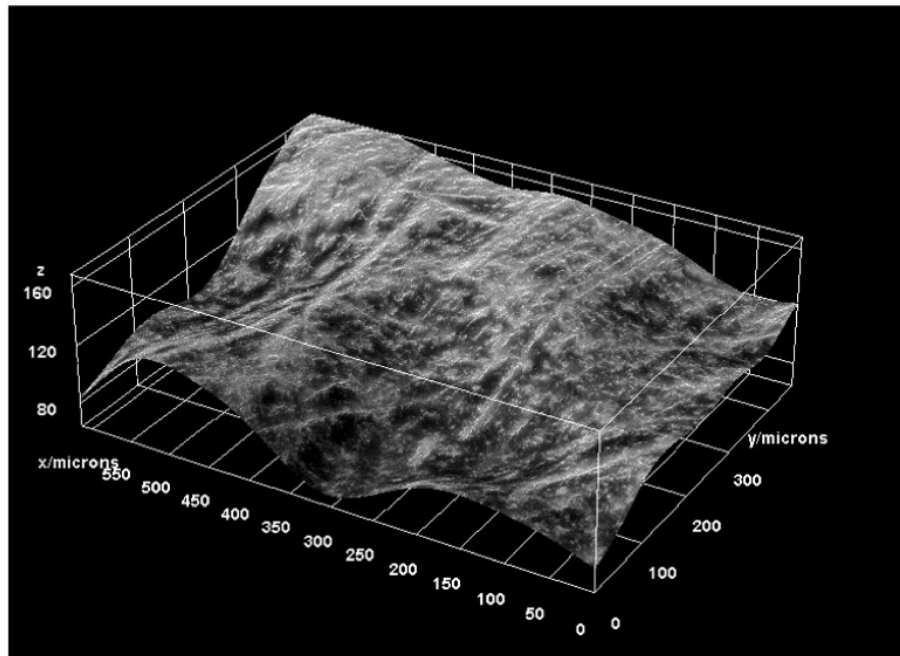


Figure 45 Examples of 3D-surface models by assembling roughness line profiles: A) specimen 98; B) specimen 5500.

5.5.4 Discussion

The results here presented confirm that micro-roughness features can be effectively described by 2D-roughness and geometry calculations. The Ra and Rz values of the Poggetti Vecchi specimens are typical of mixed-feeders and this result is consistent with the presence of coarse scratches at the center of the enamel loops. The average RSm and Rlq results are wider for the adult specimen 5500 and narrower for the cub 98; however, the results fall within the fields of variation of mixed-feeders and grazers. Differences in RS and Rlq, as well as in the spacing parameter RSm calculations, suggest that these parameters are capable to measure the scale of surface alterations recorded by the system and, consequently, capture conventional microwear signals. The bearing ratio parameter calculations (RTp and RHTp) confirm that the Poggetti Vecchi elephants fall within the thresholds of grazer-dominated animals with mixed-feeding habits. The polar spectrum shows that the angular data vary widely, which indicates the lack of mainly unidirectional structures and, therefore, the absence of strong anisotropy signals. This is corroborated by both average Rdq results, which roughly represent the complexity of 2D profiles as shown by the data reported in **Tables 10** and **11**, as well as by the relatively higher average values of the fractal dimension calculations; the latter clearly indicate that both the specimens here studied have a quite complex surface texture. However, even if these results contribute to paleodiet reconstruction, the real significance of the calculations obtained could be evaluated by increasing the number of specimens analyzed and expanding the database, for example, by including other taxa and by making cross comparison observations.

5.6 Conclusion

The results of this pooled analysis of the Poggetti Vecchi elephants show that the use of different methods is a potentially more effective way to constructively address the many issues on the feeding adaptations of extinct elephants than is relying on only one method. The methodology used in this study reveals the wealth of information that a multiproxy approach can contribute in studies aimed at paleodietary and paleoenvironmental reconstructions.

Todd et al., (2007) showed how effectively the many issues related to the microwear patterns of elephants, to their dietary preferences and to their grouping in feeding categories can be tackled through the lens of the low-magnification technique. The results of the present study confirm that conclusion. Using low-magnification, the male and female elephants of Poggetti Vecchi, regardless their ontogenetic age, were found to have upper and lower molars with quite homogeneous microwear patterns. In contrast,

and quite expectedly, the scar patterns observed on the lateral and buccal sides of the molars are quite variable. The collected evidence verified that the middle portion of the central plates is the best from which to derive dietary signals. Microwear decreases from the anterior to posterior ends of the molars. The most intensely worn plates show the highest wear damages, thereby confirming the strong correlation that exists between attritional wear and the density/proportion of microwear. The distributions of the scars, therefore, are perfectly in line with Palombo et al.'s (2005) and Todd and al.'s (2007) conclusions.

Scratches were found to greatly outnumber pits; they concentrate especially on the enamel loops of the central plates. In contrast, cross scratches and considerably large pits are sometimes more frequent on anterior (more worn) and posterior (less worn) enamel loops, respectively. The carbon and oxygen isotope measurements on the structural carbonate of the biogenic apatite suggest that a wooded grassland dominated the landscape, subject to wet and cold conditions, existed at the time when the fossiliferous levels deposited in the Poggetti Vecchi valley. Modern savannah elephants are known to adapt to grazing habits, increasing their grass intake, during more humid periods, and to opportunistically switch to browsing when grass declines, as reported for the most of elephants. The same occurred also with extinct species, as indicated by the information disclosed by the microwear scar patterns and the concordant isotopic data. The microwear pattern was also confirmed by 2D-roughness parameter calculations, as well as by the surface textures, which resulted being complex with the absence of clear anisotropy signals. These clues add weight to the hypothesis that *Palaeoloxodon* elephants were prevalently adapted to a generalistic, intermediate dietary behavior, involving the consumption of a great amount of graminaceae or other plants quite rich in phytoliths. Mesowear angles instead indicate more browse-dominated, mixed diet. This mismatch could be essentially due to differences in the temporal resolution of the two methods. In contrast to microwear, which reveals the feeding behavior in the last days of the animal's life, mesowear records the dietary signals over a longer time span, from the last months of life up to a year before death. Considering that palaeoloxodonts shifted from more browsing or mixed-feeding to more grazing in accordance with local context, mesowear is probably more effective than microwear in capturing the minimum seasonal variations in diet. Nonetheless, similarly to other proboscideans, palaeoloxodonts likely had a comparatively higher grass intake in open, grass-dominated environments.

Chapter 6 Conclusion and remarks

The radiometric dating of about 171ka indicates that the Poggetti Vecchi archeo-paleontological site developed during the Middle-Late Pleistocene and, hence, that the stone and wooden implements from the site were produced by early Neanderthals. Multiproxy analysis shows that at the time when the bone accumulation was formed the area was characterized by widespread, open, wet grassland with scattered water bodies and woods. The hot thermal springs in one of these water bodies located in a small embayment, probably created an attractive recess for the resident fauna, especially in a time period when the climate was globally deteriorating.

The combined paleobiological and taphonomical evidence reveals distinct phases of formation of the bone assemblage. After a few components of a family of elephants were probably killed by a cold snap, the corpses lied partially submerged in the water body. The rotting carcasses could be accessed only very limitedly by scavengers, including humans. Meat-stripping by both humans and carnivores led to a first defleshing of the corpses. Decomposition then progressed to the complete skeletonization and disarticulation of the carcasses. Notable is that once the corpses had been skeletonized, the bones were unexpectedly exposed to minimum gnawing, thereby suggesting that for some reason scavengers had limited access to the carcasses. We cannot exclude that scavengers may have removed some of the bones; nonetheless, the very low incidence of carnivore ravaging at the site seems ruling out this possibility. The taphonomic evidence indicates that after the disarticulation of the skeletons, the loose bones were trampled on, and thus variously scratched and broken, by bypassing animals, which were possibly responsible also of the scattering of the skeletal parts.

The isotopic signature coupled with low magnification microwear analysis and surface texture assessment of the enamel molars suggest that the local straight-tusked elephant population had prevalently developed a graze-dominated C3-mixed feeding habit. During the last days of life they consumed a great amount of graminaceae or of other plants relatively rich in phytoliths. The $\delta^{18}\text{O}_w$ and diet values are also consistent with a landscape dominated by wooded grasslands, probably under colder and/or wetter conditions than the present ones. The dietary signal of the last meals typically describes grazing-mixed feeding behavior and hence microwear pattern and texture results seem to agree with preliminary environment reconstruction based on both paleobiological and taphonomic investigation, as well as with preliminary geoarcheological insight. These considerations reinforce the idea that the elephants were forced to stay in a very limited area near the only heat source, probably due to climate deterioration that has prevented to leave the valley. Thereafter they consumed all the vegetation,

in particular grasses and graminaceae that dominated the landscape in the surrounding area and finally died of starvation.

Likewise classical microwear, surface texture signals in proboscideans can be affected by some confounding factors that are potentially related to non-dietary noise, to their large size and morphological variability as well as to small fields of view and high resolution used for collecting texture data. Consequently, the multiproxy approach here reported can be an attempt to obtain cross-data that that is as objective as possible. All surface measuring systems reconstruct 3D surface models by assembling line profiles. However much more detailed information about enamel wear is encapsulated in 2D-roughness parameters rather than 3D-models. Hence roughness data and geometric pattern employed in this study confirm that the bearing ratio parameters (RTp and RHTp) measures the universal attrition–abrasion equilibrium controlling dental wear and results previously obtained with the traditional microwear diagnosis methods (at low and high magnifications). Since the mesowear patterns are the result of additive wear actions over several months/years of feeding, sometimes microwear and mesowear proxies may not give similar results that probably reflect the variations of temporal resolution of the two methods. At Poggetti Vecchi mesowear signal is concordant with a more browse-dominated mixed dietary behavior. So, in this case, mesowear measures probably record the seasonal dietary variations, as well as the possible movement of the elephants from other areas, in which the landscape was otherwise dominated by woods, towards the grassland valley of Poggetti Vecchi during the final stage of their life.

References

1. Aaris-Sørensen, K., 2009. Diversity and dynamics of the mammalian fauna in Denmark throughout the last glacial-interglacial cycle, 115-0 kyr BP. *Fossils and Strata* 57, 1e59.
2. Adelson, L., 1966. Fatal hydrogen sulfide intoxication. *Arch Pathol* 81:375–80.
3. Aguirre, E., 1969. Evolutionary history of the elephant. *Science* 164 (3886), 1366–1376.
4. Aguirre, E., 1968–1969. Revision Sistemática de los Elephantidae, por su morfología y morfometría dentaria. *Estudios Geológicos* 24, 109–167, 25, 123–177, 317–367.
5. Albayrak, E., and Lister, A. M. (2012). Dental remains of fossil elephants from Turkey. *Quaternary International*, 276, 198-211.
6. Ambrosetti, P., 1968. The Pleistocene dwarf elephant of Spinagallo. *Geologica Romana* 7, 277–398.
7. Anthony, C. and Fraiant, M., 1941. Introduction à la connaissance de la dentition des Proboscidiens: Mem. Soc. Geol. Helv. Vol.59 (1): 541-564.
8. Anzidei, A.P., Bulgarelli, G.M., Cerilli, C., Gallotti, R., Lemorini, C., Manzi, G., Milli, S., Palombo, M.R., Santucci, E., 2010. The Middle Pleistocene Paleolithic site with large mammal fauna of La Polledrara di Cecanibbio (Rome, Italy): recent data and prospects. *Quaternaire Hors-série* 3, 119e121.
9. Anzidei A.P., Arnoldus Huyzendveld A., Caloi I., Lemorini C. and Palombo M.R. (1999) - Two Middle Pleistocene Sites near Rome (Italy): La Polledrara di Cecanibbio and Rebibbia – Casal de' Pazzi. The Role of Early Humans in the accumulation of European Lower and Middle Palaeolithic bone assemblages, Mainz, 173-183.
10. Anzidei A.P., Bulgarelli G.M., Catalano P., Cerilli E., Gallotti R., Lemorini C., Milli S., Palombo M.R., Pantano W. and Santucci E., 2012 - Ongoing research at the late Middle Pleistocene site of La Polledrara di Cecanibbio (central Italy), with the emphasis on human-elephant relationships. *Quaternary International*, 255, 171-187.
11. Archer, D., Sanson, G., 2002. Form and function of the selenodont molar in southern African ruminants in relation to their feeding habits. *Journal of Zoology* 257, 13–26.
12. Auguste, P., 1992. Etude Archeozoologique des grands mammifères du site Pleistocène Moyen de Biache-Saint-Vaast (Pas-de-Calais, France): apports Biostratigraphiques et Palethnographiques. *L'Anthropologie* 96, 49–70.
13. Aureli, D., Contardi, A., Giaccio, B., Jich, B., Lemorini, C., Madonna, S., Magri, D., et al., 2015. Palaeoloxodon and human interaction: depositional setting, chronology and archaeology at the Middle Pleistocene Ficoncella Site (Tarquinia, Italy). *PLOS ONE* 10: e0124498. <http://dx.doi.org/10.1371/journal.pone.0124498>.
14. Ayalon, A., Bar-Matthews, M., Kaufman, A., 2002. Climatic conditions during marine oxygen isotope stage 6 in the eastern

- Mediterranean region from the isotopic composition of speleothems of Soreq Cave, Israel. *Geology* 30, 303–306.
15. Ayliffe, L.K., Chivas, A.R., Leakey, M.G., 1994. The retention of primary oxygen isotope compositions of fossil elephant skeletal phosphate. *Geochimica et Cosmochimica Acta* 54, 5291–5298.
 16. Azzaroli, A., De Giuli, C., Ficarelli, G., & Torre, D. (1988). Late Pliocene to early mid-Pleistocene mammals in Eurasia: faunal succession and dispersal events. *Palaeogeography, Palaeoclimatology, Palaeoecology*, 66(1-2), 77-100.
 17. Baker, G., Jones, L.H.P., Wardrop, I.D., Cause of wear in sheeps teeth, *Nature* 184 (1959) 1583–1584.
 18. Baldi, P., Bellani, S., Ceccarelli, A., Fiordelisi, A., Squarci, P., Taffi, L., 1995. Geothermal anomalies and structural features of southern Tuscany. *World Geothermal Congress Proceedings, Florence*, 1287–1291.
 19. Baryshnikov, G.F., 1987. Mammals of the Caucasus of the early Paleolithic. *Trudy Zool. Inst. AN. SSSR* 68, 3e20 (in Russian).
 20. Behrensmeyer, A.K., 1975. The taphonomy and paleoecology of Plio-Pleistocene vertebrate assemblages east of Lake Rudolf, Kenya. *Bulletin of the Museum of Comparative Zoology* 146, 473–578.
 21. Behrensmeyer, A.K., 1978. Taphonomic and ecological information from bone weathering. *Paleobiology* 4, 150–162.
 22. Biddittu, I., Cassoli, P.F., Radicati di Brozolo, F., Segre, A.G., Segre Naldini, E., Villa, I., 1979. Anagni a K–Ar dated Lower and Middle Pleistocene site, Central Italy, Preliminary Report. *Quaternaria* 21, 53–71.
 23. Bigga, G., Schoch, W.H., Urban, B., 2015. Paleoenvironment and possibilities of plant exploitation in the Middle Pleistocene of Shöningen (Germany). Insights from botanical macro-remains and pollen. *J Hum Evol.*, 89: 92-104.
 24. Binford, L.R., 1987. Data, relativism and archaeological science. *Man* 22, 391–404.
 25. Blainville, H.M.D., 1836. Classification presented in 1834. In *Dictionnaire Pittoresque d'Historire Naturelle, Vo. 4.*, F.E. Guérin ed. Paris: Bureau de Souscription, p. 619.
 26. Bocherens, H., Koch, P.L., Mariotti, A., Geraads, D., Jaeger, J.-J., 1996. Isotopic biogeochemistry (^{13}C , ^{18}O) of mammal enamel from African Pleistocene hom- inid sites: implications for the preservation of paleoclimatic isotopic signals. *Palaios* 11, 306e318.
 27. Bocherens, H., 2011. Diet and ecology of Neanderthals: insights from bone and tooth biogeochemistry. In: Conard, N.J., Richter, J. (Eds.), *Neanderthal Life- ways, Subsistence and Technology*. In: Delson, E., MacPhee, R. (Eds.), *Vertebrate Paleobiology and Paleoanthropology*. Springer, Heidelberg, New York, pp. 73e85.
 28. Bonfiglio, L., Berdar, A., 1983. Gli elefanti del Pleistocene superiore di Archi (Reggio Calabria). Nuove evidenze di insularita" della Calabria meridionale durante il ciclo Tirreniano. *Bollettino della Societa" Paleontologica Italiana* 25 (1), 9–34.

29. Boschian, G., Sacca, D., 2014. In the elephant, everything is good: carcass use and reuse at Castel di Guido (Italy). *Quaternary International* 361, 288–296.
30. Bravetti, L., Pranzini, G., 1987. L'evoluzione quaternaria della pianura di Grosseto (Toscana): prima interpretazione dei dati del sottosuolo. *Geografia Fisica e Dinamica Quaternaria* 10, 85–92.
31. Brewer, D., 1992. Zooarchaeology: method, theory, and goals. *Archaeological Method and Theory* 4, 195–244.
32. Brown, W. A. B. & Chapman, N. G., 1990. The dentition of red deer (*Cervus elaphus*): a scoring scheme to assess age from wear of the permanent molariform teeth. *Journal of Zoology*, 224, 519–36.
33. Brooks, J.R., Flanagan, L.B., Buchmann, N., Ehleringer, J.R., 1997. Carbon isotope composition of boreal plants: functional grouping of life forms. *Oecologia* 110, 301–311.
34. Burk, R.L. and Stuiver, M., Oxygen isotope ratios in trees reflect mean annual temperature and humidity. *Science* 211, 1981, 1417–1419.
35. Burgio, E., Cani, M., 1988. Sul ritrovamento di elefanti fossili ad Alcamo (Trapani, Sicilia). *Naturalista Siciliano* 12, 87–97.
36. Bunn, J. M., Ungar, P. S., 2009, Dental topography and diets of four old world monkey species. *Am. J. Primatol.*, 71: 466–477. doi:10.1002/ajp.20676.
37. Butler, P.M., The milk molars of Perissodactyla, with remarks on molar occlusion, *Proc. Zool. Soc. Lond.* 121 (1952) 777–817.
38. Butzer, K.W., 1982. *Archaeology as Human Ecology*. Cambridge University Press, Cambridge, UK.
39. Cahill, J.A., Green, R.E., Fulton, T.L., Stiller, M., Jay, F., Ovsyanikov, N., Salamzade, R., St John, J., Stirling, I., Slatkin, M., Shapiro, B. 2013. Genomic evidence for island population conversion resolves conflicting theories of polar bear evolution. *PLoS Genetics* 9:e1003345. doi: 10.1371/journal.pgen.1003345, PMID: 23516372.
40. Calandra, I., Göhlich, U. B., & Merceron, G. (2008). How could sympatric megaherbivores coexist? Example of niche partitioning within a proboscidean community from the Miocene of Europe. *Naturwissenschaften*, 95(9), 831-838.
41. Calandra I., Göhlich U.B., Merceron G., 2010. Feeding preferences of *Gomphotherium subtapiroideum* (Proboscidea, Mammalia) from the Miocene of Sandelzhausen (Northern Alpine Foreland Basin, southern Germany) through life and geological time: evidence from dental microwear analysis. *Paläontologische Zeitschrift* 84: 205–215.
42. Caloi, L., Kotsakis, T., Palombo, M.R., Petronio, C., 1996. The Pleistocene dwarf elephants of Mediterranean islands. In: Shoshani, J., Tassy, P. (Eds.), *The Proboscidea: Evolution and Palaeoecology of Elephants and their Relatives*. Oxford University Press, Oxford, pp. 234–239.
43. Capozza, M., 2001. Microwear analysis of *Mammuthus meridionalis* (Nesti, 1825) molar from Campo del Conte, Frosinone, Italy. In:

- Proceedings of the First International Congress, The World of Elephants, Rome, Italy, October 2001, pp. 520–533.
44. Cerling, T.E. 1999. Paleorecords of C4 plants and ecosystems. In C4 plant biology, ed. R.F. Sage and R.K. Monson, 445–69. San Diego: Academic Press.
 45. Cerling, T.E., Harris, J.M., McFadden, B.J., Leakey, M.G., Quade, J., Eisenmann, V., and Ehleringer, J.R., 1997. Global vegetation change through the Miocene/Pliocene boundary. *Nature* 389:153–158.
 46. Cerling, T.E., Harris, J.M., 1999. Carbon isotope fractionation between diet and bioapatite in ungulate mammals and implications for ecological and paleoecological studies. *Oecologia* 120, 347–363.
 47. Cerling, T.E., Harris, J.M., Leakey, M.G., 1999. Browsing and grazing in elephants: the isotope record of modern and fossil proboscideans. *Oecologia* 120, 364e374.
 48. Cerling, T.E. et al. Woody cover and hominin environments in the past 6 million years. *Nature* 476, 51–56 (2011).
 49. Cerling, T.E., Passey, B.H., Ayliffe, L.K., Cook, C.S., Ehleringer, J.R., Harris, J.M., Dhidha, M. B. and Kasiki S. M., 2004. Orphans' tales: seasonal dietary changes in elephants from Tsavo National Park, Kenya. *Palaeogeography, Palaeoclimatology, Palaeoecology* 206:367–376.
 50. Cerling, T.E., Wittemyer, G., Rasmussen, H. B., Vollrath, F., Cerling, C. E., Robinson, T. J. and Douglas-Hamilton, I., 2006. Stable isotopes in elephant hair document migration patterns and diet changes. *Proceedings of the National Academy of Sciences of the United States of America* 103:371–373.
 51. Cerling, T. E., Wittemyer, G., Ehleringer, J. R., Remien, C. H. and Douglas-Hamilton, I., 2009. History of animals using isotope records (HAIR): a 6-year dietary history of one family of African elephants. *Proceedings of the National Academy of Sciences of the United States of America* 106:8093–8100.
 52. Censini, G., Costantini, A. 2002. Il sottosuolo della pianura tra Grosseto e Ribolla: ipotesi sul suo assetto strutturale. Le voragini catastrofiche: un nuovo problema per la Toscana. Atti del Convegno di Grosseto del 31 Marzo 2000, Edizioni Regione Toscana, Firenze.
 53. Cianfanelli, S., 2010. *Melanopsis etrusca*. The IUCN Red List of Threatened Species. Version 2014.3 (accessed May 18, 2015). <http://www.iucnredlist.org>.
 54. Cianfanelli, S., Bodon, M., Giusti, F., Manganelli, G., 2010. *Belgrandia thermalis*. The IUCN Red List of Threatened Species. Version 2014.3 (accessed May 18, 2015). <http://www.iucnredlist.org>.
 55. Chenery, C.A., Pashley, V., Lamb, A.L., Sloane, H.J., Evans, J.A., 2012. The oxygen isotope relationship between the phosphate and structural carbonate fractions of human bioapatite. *Rapid Communications in Mass Spectrometry* 26, 309e319.
 56. Chilardi, S., 1996. I macromammiferi. In: Basile, B., Chilardi, S. (Eds.), *Le ossa dei Giganti. Lo scavo paleontologico di Contrada Fusco*. Arnaldo Lombardi, Siracusa, pp. 27–34.

57. Crader, D. C., 1983. Recent single-carcass bone scatters and the problem of “butchery” sites in the archaeological record. In: Clutton-Brock, J., Grigson, C. (Eds.), *Animals and Archaeology, Hunters and Their Prey*. BAR International Series 163, vol. 1, Oxford.
58. Codron, J., Lee-Thorp, J. A., Sponheimer, M., Codron, D., Grant, R. C., & de Ruiter, D. J., 2006. Elephant (*Loxodonta africana*) diets in Kruger National Park, South Africa: spatial and landscape differences. *Journal of Mammalogy*, 87(1), 27-34.
59. Coles, J., Heal, S., & Orme, B., 1978. The Use and Character of Wood in Prehistoric Britain and Ireland. *Proceedings of the Prehistoric Society*, 44, 1-45. doi:10.1017/S0079497X00009968.
60. Coplen, T.B. Normalization of oxygen and hydrogen isotope data. *Chem. Geol.: Isotope Geoscience Section* 1988, 72, 293.
61. Corrado, P., Magri, D., 2011. A late Early Pleistocene pollen record from Fontana Ranuccio (central Italy). *Journal of Quaternary Science* 26, 335–344.
62. Dabney, J., Knapp, M., Glocke, I., Gansauge, M, T., Weihmann, A., Nickel, B., Valdiosera, C., Garcia, N., Paabo, S., Arsuaga, J. L., Meyer, M. 2013. Complete mitochondrial genome sequence of a Middle Pleistocene cave bear reconstructed from ultrashort DNA fragments. *PNAS* 110:15758–15763. doi: 10.1073/pnas.1314445110, PMID: 24019490.
63. D’Amico, C., Esu, D., Magnatti, M., 2014. Land mollusc palaeocommunity dynamics related to palaeoclimatic changes in the Upper Pleistocene alluvial deposits of Marche Apennines (central Italy). *Italian Journal of Geoscience* 133, 235–248.
64. De Lorenzo, G., D’Erasmus, G., 1927. L’*Elephas antiquus* nell’Italia meridionale. *Atti della Regia Accademia di Scienze Fisiche e Matematiche di Napoli* 17 (11), 1–105. De Lorenzo, G., D’Erasmus, G., 1927. L’*Elephas antiquus* nell’Italia meridionale. *Atti della Regia Accademia di Scienze Fisiche e Matematiche di Napoli* 17 (11), 1–105.
65. Debruyne, R, Barriel, V., Tassy, P. Mitochondrial cytochrome b of the Lyakhov mammoth (Proboscidea, Mammalia): new data and phylogenetic analyses of Elephantidae, *Mol. Phyl. Evol.* 26 (2003) 421–434.
66. DeNiro, M.J., Stable isotopes and archaeology. *American Scientist* 75, 1987, 182–191.
67. D’Erasmus, G. and Montcharmon Zei, M., 1955. Il cranio giovanile di *Elephas antiquus italicus* di Pignataro Interamna. *Rendiconti della Regia Accademia di Scienze Fisiche e Matematiche di Napoli, Series 4* 17, 259–326.
68. D’Errico, F., Backwell, L., Villa, P., Degano, I., Lucejko, J.J., Bamford, M.K., ... and Beaumont, P.B., 2012. Early evidence of San material culture represented by organic artifacts from Border Cave, South Africa. *Proceedings of the National Academy of Sciences*, 109(33), 13214-13219.
69. Daux, V., Lécuyer, C., Héran, M. A, Amiot, R., Simon, L., Fourel, F., Martineau, F., Lynnerup, N., Reyhler, H., Escarguel, G. Oxygen

- isotope fractionation between human phosphate and water revisited. *J. Hum. Evol.* 2008, 55, 1138.
70. Dongman, G., Nürnberg, H.W., Förstel, H.W., Wagner, K., On the enrichment of H₂¹⁸O in the leaves of transpiring plants. *Radiation and Environmental Biophysics* 11, 1974, 41–52.
 71. Eggert, L.S., Rasner, C.A., Woodruff, D.S., 2002. The evolution and phylogeography of the African elephant inferred from mitochondrial DNA sequence and nuclear microsatellite markers. *Proceeding of the Royal Society of London B* 269, 1993–2006.
 72. Ecker, M., Bocherens, H., Julien, M.A., Rivals, F., Raynal, J.P., Moncel, M.H., 2013. Middle Pleistocene ecology and Neanderthal subsistence: insights from stable isotope analyses in Payre (Ardèche, France). *Journal of Human Evolution* 65, 363e373.
 73. Eizirik, E., Murphy, W.J., O'Brian, S.J., 2001. Molecular dating and biogeography of the early placental mammal radiation. *The American Genetic Association* 92, 212–219.
 74. Elliott, J.C., 2002. Calcium phosphate biominerals. *Reviews in Geochemistry and Mineralogy* 48, 427–453.
 75. Evans, A.R., Harper, I.S., Sanson, G.D., 2001. Confocal imaging, visualization and 3-D surface measurement of small mammalian teeth. *Journal of Microscopy* 204 (2), 108–119.
 76. Every, D., Tunnicliffe, G.A., Every, R.G., 1998. Tooth-sharpening behaviour (thegosis) and other causes of wear on sheep teeth in relation to mastication and grazing mechanisms. *Journal of the Royal Society of New Zealand* 28 (1), 169–184.
 77. Falconer, H. and Cautley, P.T., 1847. *Fauna Antiqua sivalensis, Being the Fossil Zoology of the Sewalik Hills in the North of India.* Smith Elder and Co., London.
 78. Falconer, K., 2003. *Fractal Geometry.* New York: Wiley. p. 308.
 79. Farquhar, G.D., Ehleringer, J.R., Hubick, K.T., 1989. Carbon isotope discrimination and photosynthesis. *Annual Reviews of Plant Physiology and Plant Molecular Biology* 40, 503–537.
 80. Ferretti, M.P., 2008. The dwarf elephant *Palaeoloxodon mnaidriensis* from Puntali Cave, Carini (Sicily, late Middle Pleistocene): anatomy, systematics and phylogenetic relationships. *Quaternary International*, 182(1), 90-108.
 81. Ferrio, J. P., Resco, V., Williams, D. G., Serrano, L., & Voltas, J. (2005). Stable isotopes in arid and semi-arid forest systems. *Forest Systems*, 14(3), 371-382.
 82. Filippi, M.L., Palombo, M.R., Barbieri, M., Capozza, M., Iacumin, P., Longinelli, A., 2001. Isotopic and microwear analyses on teeth of late–Middle Pleistocene *Elephas antiquus* from the Rome area (La Polledrara, Casal de'Pazzi). In: Cavaretta, G., Gioia, P., Mussi, M., Palombo, M.R. (Eds.), *The World of Elephants. Proceedings of the First International Congress, Rome, 16–20 October.* Consiglio Nazionale delle Ricerche, Roma, pp. 534–539.
 83. Fisher Jr., J.W., 1992. Observations on the late Pleistocene bone assemblage from the Lamb Spring site, Colorado. In: Stanford, D.J., Day, J.S. (Eds.), *Ice Age Hunters of the Rockies.* Denver Museum of

- Natural History and University Press of Colorado, Niwot (CO), pp. 51e81.
84. Fischer, M.S. Un trait unique de l'oreille des éléphants et des siréniens (Mammalia): un paradoxe phylogénétique, C. R. Acad. Sci. Paris, Ser. III 311 (1990) 157–162.
 85. García, N., Arsuaga, J.L., Torres, T., 1997. The carnivore remains from the Sima de los Huesos Middle Pleistocene site (Sierra de Atapuerca, Spain). *Journal of Human Evolution* 33, 155–174.
 86. Gaudzinski, S., 1996. Karlich-Seeufer: Untersuchungen zu einer Altpaläolithischen Fundstelle in neuwieder Becken (Rheinland-Platz). *Jahrbuch des Römisch-Germanischen Zentralmuseums Mainz* 43, 1–242.
 87. Grube R., Palombo M.R., Iacumin P., Di Matteo A., 2010. What did the fossil elephants from Neumark-Nord eat? In: H. Meller (Ed.), *Elefantenreich – Eine fossilwelt in Europa*. Landsmuseum für Vorgeschichte, Halle, pp. 253-272. ISBN 978-3-939414-48-3.
 88. Follieri, M., Magri, D., Sadori, L., 1986. Late Pleistocene *Zelkova* extinction in Central Italy. *New Phytologist* 103, 269–273.
 89. Fortelius, M., Solounias, N., 2000. Functional characterization of ungulate molars using the Abrasion–Attrition wear gradient: a new method for reconstructing paleodiets. *American Museum of Natural History Novitates* (3301), 1–36.
 90. Foster, B., 1997. *Optimizing Light Microscopy for Biological and Clinical Laboratories*. Kendall/Hunt Publishing Co, Dubuque, IA.
 91. Fritz, H., Duncan, P., Gordon, I.J., Illius, A.W., 2002. Megaherbivores influence trophic guilds structure in African ungulate communities. *Oecologia* 131, 620e625.
 92. Garutt, V.E., 1986. Proishozhdenie slonov i puty ih philogenii. *Trudy Zoologicheskogo Instituta AN SSSR* 149, 15e32 (in Russian).
 93. Garvie-Lok, S.J., Varney, T.L., Katzenberg M.A. Preparation of bone carbonate for stable isotope analysis: the effects of treatment time and acid concentration. *J. Arch. Sci.* 2004, 31, 763.
 94. Gaudzinski S., 1995a. Wisentjünger in Wallertheim. Zur Taphonomie einer mittelpaläolithischen Freilandfundstelle in Rheinhessen. *Jahrbuch des RGZM*, 39: 245-423.
 95. Gaudzinski S., 1995b. Wallertheim revisited: a reanalysis of the fauna from the middle Palaeolithic site of Wallertheim (Rheinhessen / Germany). *Journal of Archaeological Science*, 22: 51-66.
 96. Gheerbrant, E. Paleocene emergence of elephant relatives and the rapid radiation of African ungulates. *Proceedings of the National Academy of Sciences*, 2009, 106.26: 10717-10721.
 97. Gheerbrant, E., Tassy, P. (2009). L'origine et l'évolution des éléphants. *Comptes Rendus Palevol*, 8(2), 281-294.
 98. Ghilardi, M., Desruelles, S., 2009. Geoarchaeology: where human, social and earth sciences meet with technology. *Surveys and Perspectives Integrating Environment and Society (S.A.P.I.E.N.S.)* 2.2., 1–9.
 99. Giustini, F., Brilli, M., Patera, A., 2016. Mapping oxygen stable isotopes of precipitation in Italy. *Journal of Hydrology: Regional Studies*, 8, 162-181.

100. Global chronostratigraphical correlation table for the last 2.7 million years (v. 2016a).
101. Godfrey, L.R., Semprebon, G.M., Jungers, W.L., Sutherland, M.R., Simons, E.L., Solounias, N., 2004. Dental use wear in extinct lemurs: evidence of diet and niche differentiation. *Journal of Human Evolution* 47, 145–170.
102. Gordon, K.D., 1982. A study of microwear on chimpanzee molars: implications for dental microwear analysis. *Am. J. Phys. Anthropol.* 59, 195–215.
103. Gordon, K.D., 1988. A review of methodology and quantification in dental microwear analysis. *Scanning Microscopy* 2, 1139–1147.
104. Gray, J.E. On the natural arrangements of vertebrate animals. *London Medical Repository* 1821, 15(88): 296-310.
105. Grayson, D.K., 1978. Minimum numbers and sample size in vertebrate faunal analysis. *American Antiquity* 43, 53–65.
106. Grayson, D.K., 1984. *Quantitative Zooarchaeology: Topics in the Analysis of Archaeological Faunas*. Academic Press, Orlando.
107. Green, J.L., Semprebon, G.M., Solounias, N., 2005. Reconstructing the palaeodiet of Florida *Mammot americanum* via low-magnification stereomicroscopy. *Palaeogeography, Palaeoclimatology, Palaeoecology* 223, 34–48.
108. Grine, F.E., Analysis of early hominid deciduous molar wear by scanning electron microscopy: a preliminary report, *Proc. Electron Microsc. Soc. S. Afr.* 7 (1977) 157–158.
109. Grine, F.E., Dental evidence for dietary differences in *Australopithecus* and *Paranthropus*: A quantitative analysis of permanent molar microwear, *J. Hum. Evol.* 15 (1986) 783–822.
110. Grine, F.E., Ungar, P.S., Teaford, M.F., Error rates in dental microwear quantification using scanning electron microscopy, *Scanning* 24 (2002) 144–153.
111. Grubb, P., Groves, C.P., Dudley, J.P., Shoshani, J., 2000. Living African elephants belong to two species: *Loxodonta africana* (Blumenbach, 1797) and *Loxodonta cyclotis* (Matschie, 1900). *Elephant* 2 (4), 1–4.
112. Guthrie, R.D., 1984. Mosaics, allelochemicals and nutrients: an ecological theory of Late Pleistocene megafaunal extinctions. In: Martin, P.S., Klein, R.G. (Eds.), *Quaternary Extinctions: A Prehistoric Revolution*. University of Arizona Press, Tucson, AZ, pp. 259e298.
113. Haynes, G., 1983. Frequencies of spiral and green bone fractures on ungulate limb bones in modern surface assemblages. *American Antiquity* 48, 102–114.
114. Haynes, G., 1991. *Mammoths, Mastodons, and Elephants: Biology, Behavior, and the Fossil Record*. Cambridge University Press, Cambridge.
115. Haynes, G., 2005. Las acumulaciones modernas de huesos de elefante como modelo para interpretar Ambrona y otras áreas con fauna fosil a orillas del agua. In: Santonja, M., Pérez Gonzalez, A. (Eds.), *Los yacimientos paleolíticos de Ambrona y Torralba (Soria)*.

- Un siglo de investigaciones arqueológicas, Zona Arqueológicas, vol. 5. Museo Arqueológico Regional, Madrid, pp. 154e174 .
116. Haynes, G., Klimowicz, J. (2015). Recent elephant-carcass utilization as a basis for interpreting mammoth exploitation. *Quaternary International*, 359, 19-37.
 117. Heaton, T.H.E. Spatial, species, and temporal variation in the $^{13}\text{C}/^{12}\text{C}$ ratios of C3 plants: Implications for palaeodiet studies. *Journal of Archaeological Science* 26, 1999, 637–649.
 118. Heinrich, W.D., 1978. Zur biometrischen Erfassung eines Evolutionstrends bei *Arvicola* (Rodentia, Mammalia) aus dem Pleistozän Thüringens. *Säugetierkundliche Informationen* 2, 3–21.
 119. Herridge V.L., 2010. Dwarf elephants on Mediterranean islands: a natural experiment in parallel evolution. PhD thesis, University College London. Available from <http://discovery.ucl.ac.uk/133456/>.
 120. Hillson, S. (2005). *Teeth*. Cambridge University Press.
 121. Iacumin, P., Bicherens, H., Mariotti, A., Longinelli, A., 1996. Oxygen isotope analyses of co-existing carbonate and phosphate in biogenic apatite: a way to monitor diagenetic alteration of bone phosphate? *Earth and Planetary Sciences Letters* 142, 1–6.
 122. Ikeda N, Takahashi H, Umetsu K, Suzuki T. 1989. The course of respiration and circulation in death by carbon dioxide poisoning. *Forensic Sci Int* 41:93–99.
 123. Imbesi, M., 1956. Sugli elefanti nani della grotta di Luparello (Palermo). Proceedings of the INQUA Congress, Rome–Pisa.
 124. Inuzuka, N., 1977a. On a fossil skull of *Palaeoloxodon naumanni* from Saruyama, Shimosa-machi, Chiba Prefecture, Central Japan. *Journal of the Geological Society of Japan* 83, 523–536.
 125. Inuzuka, N., 1977b. On the origin of *Palaeoloxodon naumanni* - a comparative osteology of the cranium. *Journal of the Geological Society of Japan* 83, 639–655.
 126. ISO 4287:1997. Geometrical Product Specifications (GPS) - Surface texture: Profile method - terms, definitions and surface texture parameters. Replaces ISO 4287-1:1984.
 127. Janis, C. M. in *The Ecology of Browsing and Grazing* (eds Gordon, I. J. & Prins, H.H.T.) 21–45 (Springer, 2008).
 128. Janis, C.M., Fortelius, M., On the means whereby mammals achieve increased functional durability of their dentitions, with special reference to limiting factors, *Biol. Rev.* 63 (1988) 197–230.
 129. Johnson, D. L. (1980). Problems in the land vertebrate zoogeography of certain islands and the swimming powers of elephants. *Journal of Biogeography*, 383-398.
 130. Kahlke, H. D. (1986). Biostratigraphical correlations (mammals) of the Quaternary continental deposits of Europe and the Far East. *Quartärpaläont*, 6, 83-86.
 131. Kaiser, T. M. 2004. The dietary regimes of two contemporaneous populations of *Hippotherium primigenium* (Perissodactyla, Equidae) from the Vallesian (Upper Miocene) of Southern Germany. *Palaeogeography, Palaeoclimatology, Palaeoecology* 198:381–402
 132. Kaiser, T.M., Katterwe, H., 2001. The application of 3D-Microprofilometry as a tool in surface diagnosis of fossil and subfossil

- vertebrate hard tissue. An example from the Pliocene Upper Laetolil Beds, Tanzania. *International Journal of Osteoarchaeology* 11, 350–356.
133. Kahlke, R.D., Kaiser, T.M., 2011. Generalism as a subsistence strategy: advantages and limitations of the highly flexible feeding traits of Pleistocene *Stephanorhinus hundsheimensis* (Rhinocerotidae, Mammalia). *Quaternary Science Reviews* 30:2250–2261.
 134. Kaiser, T.M., Fortelius, M., 2003. Differential mesowear in occluding upper and lower molars: opening mesowear analysis for lower molars and premolars in hypsodont horses. *Journal of Morphology* 258:67–83.
 135. Kaiser, T.M., Brinkmann, G. 2006. Measuring dental wear equilibriums – the use of industrial surface texture parameters to infer the diets of fossil mammals. – *Palaeogeography, Palaeoclimatology, Palaeoecology* 239: 221-240.
 136. Kaiser, T.M., Schulz, E., 2006. Tooth wear gradients in zebras as an environmental proxy - a pilot study. *Mitteilungen aus dem Hamburgischen Zoologischen Museum und Institut* 103:187-210.
 137. Kalb, E.J., Mebrate, A., 1993. Fossil elephantoids from the hominid-bearing Awash Group, Middle Awash Valley, Afar Depression, Ethiopia. *Transactions of the American Philosophical Society* 83(1), 1–114.
 138. Kalb, J.E., Froehlich, D.J., Bell, G.L., 1996. Phylogeny of African and Eurasian Elephantoida of the late Neogene. In: Shoshani, J., Tassy, P. (Eds.), *The Proboscidea: Evolution and Palaeoecology of Elephants and their relatives*. Oxford University Press, Oxford, pp. 101–116
 139. Kangwana, K., 1996. Studying Elephants. In: AWF Technical Handbook Series, vol. 7. African Wildlife Foundation, Nairobi, Kenya, 178 pp.
 140. Koch, P.L., Tuross, N., Fogel, M.L., 1997. The effects of sample treatment and diagenesis on the isotopic integrity of carbonate in biogenic hydroxylapatite. *Journal of Archaeological Science* 24, 417–429.
 141. Kohn, M.J., Cerling, T.E., 2002. Stable isotope compositions of biological apatite. *Reviews in Mineralogy and Geochemistry* 48, 455–488.
 142. Konidaris, G. E., Athanassiou, A., Turloukis, V., Thompson, N., Giusti, D., Tsartsidou, G., ... & Harvati, K. The *Elephas antiquus* skeleton and other large mammals from Marathousa 1 site (Megalopolis Basin, Greece): preliminary results on taxonomy, biochronology, palaeo-ecology and taphonomy.
 143. Konidaris, G. E., Athanassiou, A., Turloukis, V., Thompson, N., Giusti, D., Panagopoulou, E., & Harvati, K. (2017). The skeleton of a straight-tusked elephant (*Palaeoloxodon antiquus*) and other large mammals from the Middle Pleistocene butchering locality Marathousa 1 (Megalopolis Basin, Greece): preliminary results. *Quaternary International*.
 144. Krause, J., Dear, P.H., Pollack, J.L., Slatkin, M., Spriggs, H., Barnes, I., Lister, A.M., Ebersberger, I., Paabo, S., Hofreiter, M., 2006.

- Multiplex amplification of the mammoth mitochondrial genome and the evolution of Elephantidae. *Nature* 439 (7077), 724–727.
145. Krumrey, W.A., and Buss, I.O., 1968. Age estimation, growth, and relationships between body dimensions of the female African elephant. *Journal of mammalogy*, 49(1), 22-31.
 146. Lari, M., Di Vincenzo, F., Borsato, A., Ghirotto, S., Micheli, M., Balsamo, C., Collina, C, et al. 2015. The Neanderthal in the karst: first dating, morphometric, and paleogenetic data on the fossil skeleton from Altamura (Italy). *Journal of Human Evolution* 82, 88–94.
 147. Larramendi, A. (2015). Shoulder height, body mass, and shape of proboscideans. *Acta Palaeontologica Polonica*, 61(3), 537-574.
 148. Laws, R.M. Age criteria for the African elephant, *Loxodonta a. africana*. *East African Wildlife Journal* 4, 1–37 (1966).
 149. Laws, R.M., Parker. I.S.C. & Johnstone, R.C.B., 1970. Elephants and habitats In North Bunyoro, Uganda. *East African Wildlife Journal* 8, 163-18.
 150. Lelièvre, H., Blouin-Demers, G., Bonnet, X., Lourdais, O., 2010a. Thermal benefits of artificial shelters in snakes: A radiotelemetric study of two sympatric colubrids. *Journal of Thermal Biology* 35, 324–331.
 151. Lelièvre, H., Le Hénanff, M., Blouin-Demers, G., Naulleau, G., Lourdais, O., 2010b. Thermal strategies and energetics in two sympatric colubrid snakes with contrasted exposure. *Journal of Comparative Physiology B* 180, 415–425.
 152. Lefevre, D., Piperno, M., Raynal, J.P., Tagliacozzo, A., 1998. Notarchirico: an early Middle Pleistocene site in the Venosa basin. *Anthropologie* XXXVI, 85–90.
 153. Levin, N.E., Brown, F.H., Behrensmeier, A.K., Bobe, R. and Cerling, T.E. Paleosol carbonates from the Omo Group: isotopic records of local and regional environmental change in East Africa. *Palaeogeogr. Palaeoclimatol. Palaeoecol.* 307, 75–89 (2011).
 154. Li G., Davis B.W., Eizirik E., Murphy W.J., 2016. Phylogenomic evidence for ancient hybridization in the genomes of living cats (Felidae). *Genome Research* 26:1–11. doi: 10.1101/gr.186668.114, PMID: 26518481.
 155. Lisiecki, L. E., and Raymo, M. E. (2005). A Pliocene-Pleistocene stack of 57 globally distributed benthic $\delta^{18}\text{O}$ records. *Paleoceanography*, 20(1).
 156. Lister, A.M. 1996 - Sexual dimorphism in the mammoth pelvis: an aid to gender determination - in: Shoshani, J. & Tassy, P. (eds.) - *The Proboscidea* - Oxford University Press, Oxford, pp. 254-259.
 157. Lister, A.M., 1999. Epiphyseal fusion and postcranial age determination in the woolly mammoth, *Mammuthus primigenius* (Blum.). *Deinsea* 6: 79-88. [25]. *Deinsea: Annual of the Natural History Museum Rotterdam*, 6: 79 – 88.
 158. Lister, A.M., 2004. Ecological Interactions of elephantids in Pleistocene Eurasia: *Palaeoloxodon* and *Mammuthus*, In: *Human Paleoeology in the Levantine Corridor*, Goren-Inbar N, Speth JD (Eds). Oxbow : Oxford. 53 – 60.

159. Lister, A.M., 2013. The role of behaviour in adaptive morphological evolution of African proboscideans. *Nature*, 500 (7462): 331 - 334. doi: [10.1038/nature12275](https://doi.org/10.1038/nature12275).
160. Lister A.M., 2017. On the type material and evolution of North American mammoths. *Quaternary International*, 443: 14 - 31. doi: [10.1016/j.quaint.2017.02.027](https://doi.org/10.1016/j.quaint.2017.02.027)
161. Lister, A. M., Keen, D. H., Crossling, J., 1990. Elephant and molluscan remains from the basal levels of the Baginton-Lillington Gravels at Snitterfield, Warwickshire. Proceedings of the Geologists' Association, 101 (3) : 203 - 212. doi: [10.1016/S0016-7878\(08\)80005-3](https://doi.org/10.1016/S0016-7878(08)80005-3).
162. Lister, A.M. and Sher, A.V. Gradual evolution and speciation in the origin of the woolly mammoth. *Science* 294, 1094–1097 (2001).
163. Lister, A.M., Sher, A.V., 2015. Evolution and dispersal of mammoths across the Northern Hemisphere. *Science* 350 (6262), 805e809.
164. Longinelli, A., Oxygen isotopes in mammal bone phosphate: a new tool for paleohydrological and paleoclimatological research? *Geochimica et Cosmochimica Acta* 48, 1984, 385–390.
165. Lucas, P.W., Omar, R., 2012. New perspectives on tooth wear. *International Journal of Dentistry* 2012: 287573.
166. Maccagno, A.M., 1962a. L'*Elephas meridionalis* Nesti di Contrada Madonna della strada, Scoppito (AQ). *Atti dell'Accademia di Scienze Fisiche e Matematiche di Napoli, Series 3 4* (1), 38–12.
167. Maccagno, A.M., 1962b. L'*Elephas antiquus* di Riano, Roma. *Geologica Romana* 1, 77–131.
168. Mackaye, H.T, Brunet, M, Tassy, P. *Selenotherium kolleeensis* nov. gen. nov. sp.: un nouveau Proboscidea (Mammalia) dans le Pliocène tchadien. *Geobios* 38, 2005, 765–777.
169. Maglio V.J., 1973. Origin and evolution of the Elephantidae. *Trans Am Philos Soc* 633:1–149.
170. Mallick, R., Frank, N. 2002. A new technique for precise uranium-series dating of travertine micro-samples. *Geochimica Et Cosmochimica Acta* 66:4261–4272. doi: [10.1016/S0016-7037\(02\)00999-7](https://doi.org/10.1016/S0016-7037(02)00999-7).
171. Mania, D., Mania, U., 1998. Gerate aus Holz von der altpalaolithischen Fundstelle bei Bilzingsleben. *Praehistoria Thuringica* 2, 32e72.
172. Manolagas, S.C., 2000. Birth and death of bone cells: Basic regulatory mechanisms and implications for the pathogenesis and treatment of osteoporosis. *Endocrine Reviews*, 21(2): 115-137.
173. Markov, G.N., 2012. *Mammuthus rumanus*, early mammoths, and migration out of Africa: some interrelated problems. *Quaternary International* 276e277, 23e26.
174. Masini, F, Petruso, D, Bonfiglio, L, and Mangano, G., 2008. Origination and extinction patterns of mammals in three Central Western Mediterranean islands from the Late Miocene to Quaternary. *QUATERNARY INTERNATIONAL*, 182, 63-79.
175. Matsumoto, H., 1924. Preliminary note on fossil elephants in Japan. *The Journal of the Geological Society of Tokyo* 31 (371), 255–272.

176. Mazza, P.P.A., Martini, F., Sala, B., Magi, M., Colombini, M.P., Giachi, G., Landucci, F., Lemorini, C., Modugno, F., Ribechini, E., 2006. A new Palaeolithic discovery: tar-hafted stone tools in a European mid-Pleistocene bone-bearing bed. *Journal of Archaeological Science* 33, 1310–1318.
177. Meyer M., Arsuaga, J.L., de Filippo, C., Nagel, S., Aximu-Petri, A., Nickel, B., Martinez, I., Gracia, A., Bermudez de Castro, J. M., Carbonell, E., Viola, B., Kelso J., Prufer, K., Pääbo, S., 2016. Nuclear DNA sequences from the Middle Pleistocene Sima de los Huesos hominins. *Nature* 531:504–507. doi: 10.1038/nature17405, PMID: 26976447
178. Meyer, M., Palkopoulou, E., Baleka, S., Stiller, M., Penkman, K. E., Alt, K. W., ... & Meller, H. (2017). Palaeogenomes of Eurasian straight-tusked elephants challenge the current view of elephant evolution. *eLife*, 6.
179. Merceron, G., Viriot, L., Blondel, C., 2004a. Tooth microwear pattern in roe deer (*Capreolus capreolus*, L.) from Chizé (Western France) and relation to food composition. *Small Ruminant Research* 53, 125–138.
180. Merceron, G., Blondel, C., Brunet, M., Sen, S., Solounias, N., Viriot, L., Heintz, E., 2004b. The late Miocene paleoenvironment of Afghanistan as inferred from dental microwear in artiodactyls. *Palaeogeography, Palaeoclimatology, Palaeoecology* 207, 143–163.
181. Merceron, G., Bonis, L., de Viriot, L., Blondel, C., 2005a. Dental microwear of fossil bovids from Northern Greece: paleoenvironmental conditions in the Eastern Mediterranean during the Messinian. *Palaeogeography, Palaeoclimatology, Palaeoecology* 217, 173–185.
182. Merceron, G., Bonis, L., de Viriot, L., Blondel, C., 2005b. Dental microwear of the late Miocene bovids of Northern Greece: the Vallesian/Turolian environmental changes as explanation of the disappearance of *Ouranopithecus macedoniensis*? *Bulletin de la Société Géologique de France* 5, 491–500.
183. Metcalfe, Z.J., Longstaffe, F.J., White, C. D. Method-dependent variations in stable isotope results for structural carbonate in bone bioapatite. *J. Arch. Sci.* 2009, 36, 110.
184. Michel, V., Ildefonse, P., Morin, G., 1995. Chemical and structural changes in *Cervus elaphus* tooth enamels during fossilization (Lazaret cave): a combined IR and XRD Rietveld analysis. *Applied Geochemistry* 10, 145–159.
185. Muhlbachler, M. C., Rivals, F., Solounias, N. & Semprebon, G. M. Dietary change and evolution of horses in North America. *Science* 331, 1178–1181 (2011).
186. Muhlbachler, M. C., B. L. Beatty, A. Caldera-Siu, D. Chan, and R. Lee. 2012. Error rates and observer bias in dental microwear analysis using light microscopy. *Palaeontologia Electronica* 15:1–22.
187. Mills, J.R.E., Ideal dental occlusion in primates, *Dent. Pract.* 6 (1955) 47–51.
188. Mirceta, S., Signore, A.V., Burns, J.M., Cossins, A.R., Campbell, K.L., and Berenbrink, M. (2013). Evolution of mammalian diving

- capacity traced by myoglobin net surface charge. *Science*, 340(6138), 1234-1236.
189. Mol, D. The Langebaanweg locality: an important site for a better view of the evolutionary history of the mammoths, *African Nat. Hist.* 2 (2006) 190–191.
 190. Murphy, J.W., Eizirik, E., Johnson, W.E., Zhang, Y.P., Ryder, O.A., O’Brian, S.J., 2001. Molecular phylogenetics and the origin of placental mammals. *Nature* 409, 614–618.
 191. Nanci, A., 2003a. Dentin-pulp complex. In: A. Nanci (Editor), *Ten Cate's Oral Histology: Development, Structure, and Function*. Mosby, St. Louis, pp. 192-239.
 192. Nanci, A., 2003b. Enamel: composition, formation, and structure. In: A. Nanci (Editor), *Ten Cate's Oral Histology: Development, Structure, and Function*. Mosby, St. Louis, pp. 145-191. Kohn et al., 2002.
 193. Nanda, A.C., 2002. Upper Siwalik mammalian faunas of India and associated events. *Journal of Asian Earth Sciences* 21, 47–58.
 194. Nanda, A.C., 2008. Comments on the Pinjor mammalian fauna of the Siwalik Group in relation to the post-Siwalik faunas of peninsular India and Indo-Gangetic Plain. *Quaternary International* 192, 6–13.
 195. Nelson, S., Badgley, C., Zakem, E., 2005. Microwear in modern squirrels in relation to diet. *Paleontologica Electronica* (PE Article Number: 8.1.2).
 196. Noro, M., Masuda, R., Dubrovo, I. A., Yoshida, M.C., Kato, M., 1998. Molecular phylogenetic inference of the woolly mammoth, *Mammuthus primigenius*, based on complete sequences of mitochondrial cytochrome b and 12S ribosomal RNA genes. *J Mol Evol* 46:314-326.
 197. Novotný, M., Danko, S., Havaš, P., 2004. Activity cycle and reproductive characteristics of the European pond turtle (*Emys orbicularis*) in the Tajba National Nature Reserve, Slovakia. In: Fritz, U., Havaš, P. (Eds.), *Proceedings of the 3rd International Symposium on Emys orbicularis, Košice 2002*. *Biologia* 59 (Suppl. 14). Slovak Academic Press, Bratislava, pp. 113–121.
 198. Nugent, S., 2006 Applying use-wear and residue analyses to digging sticks. *Memoirs of the Queensland Museum: Cultural Heritage Series* 4:89-105.
 199. Oakley K., Andrews P., Keeley L., Clark J., 1977. A Reappraisal of the Clacton Spearpoint. *Proc Prehist Soc* 43:13-30.
 200. O’Leary, M.H., 1988. Carbon isotopes in photosynthesis. *Bioscience* 38, 328–336.
 201. Orain, R., Lebreton, V., Ermolli, E.R., Combourieu-Nebout, N., Sémah, A.M., 2013. *Carya* as marker for tree refuges in southern Italy (Boiano basin) at the Middle Pleistocene. *Palaeogeography, Palaeoclimatology, Palaeoecology* 369, 295–302.
 202. Orlando, L., Pages, M., Calvignac, S., Hughes, S., Hanni, C., 2007. Does the 43 bp sequence from an 800 000 year old Cretan dwarf elephantid really rewrite the textbook on mammoths? *Biology Letters* 3 (1), 57–59.
 203. Orlando L., Ginolhac A., Zhang G., Froese D., Albrechtsen A., Stiller M., Schubert M., Cappellini E., Petersen B., Moltke I., Johnson

- P.L., Fumagalli M., Vilstrup J.T., Raghavan M., Korneliussen T., Malaspinas A.S., Vogt J., Szklarczyk D., Kelstrup C.D., Vinther J., et al. 2013. Recalibrating Equus evolution using the genome sequence of an early Middle Pleistocene horse. *Nature* 499:74–78. doi: 10.1038/nature12323, PMID: 23803765.
204. Osborn, H.F., 1942. Proboscidea: a monograph of the discovery, evolution, migration and extinction of the mastodonts and elephants of the world. Stegodontoidea, Elephantoidea, Vol. II. The American Museum Press, New York.
205. Osborn, H.F., 1942. Proboscidea 2: Stegodontoidea, Elephantoidea. The American Museum of Natural History, New York.
206. Osborn, J. W. (1970). The mechanism of ameloblast movement: a hypothesis. *Calcified Tissue International*, 5(1), 344-359.
207. Owen-Smith N. 2013. Contrasts in the large herbivore faunas of the southern continents in the late Pleistocene and the ecological implications for human origins. *Journal of Biogeography* 40:1215–1224. doi: 10.1111/jbi. 12100.
208. Pacher, M, Stuart, A.J., 2008. Extinction chronology and palaeobiology of the cave bear (*Ursus spelaeus*). *Boreas* 38, 189–206.
209. Palombo, M.R., 1986. Observations sur *Elephas antiquus* Falconer and Cautley du Pleistocene moyen d’italie, essai d’évaluation des caracteres dentaires. *Geologica Romana* 23 (1984), 99–109.
210. Palombo, M.R., 1994. Gli elefanti del Pliocene superiore e del Pleistocene dell’Italia centrale peninsulare, alcune considerazioni, Vol. speciale. *Studi Geologici Camerti*, ‘‘Biostratigrafia dell’Italia centrale’’ 1994, 447–457.
211. Palombo, M.R., 2017. Discrete dispersal bioevents of large mammals in Southern Europe in the post-Olduvai Early Pleistocene: A critical overview. *Quaternary International*, 431, 3-19.
212. Palombo, M.R., Albayrak, E., Marano, F., 2010. The straight-tusked Elephants from Neumark-Nord, a glance to a lost world. In: Meller, H. (Ed.), *Elefantenreich-Eine Fossilwelt in Europa*. Katalog zur Sonderausstellung im Landesmuseum für Vorgeschichte Halle, pp. 219e247.
213. Palombo, M.R., Anzidei, A.P., Arnoldus-Huyzendveld, A., 2003. La Polledrara di Cecanibbio: one of the richest *Elephas (Palaeoloxodon) antiquus* sites of the late Middle Pleistocene in Italy. In: Reumer, J.W.F., De Vos, J., Mol, D. (Eds.), *Advances in Mammoth Research*. Proceedings of the Second International Mammoths Conference, Rotterdam, May 16–20, 1999. *Deinsea* 9, 317–330.
214. Palombo, M. R., Filippi, M., Iacumin, P., Longinelli, A., Barbieri, M., Maras A., Coupling tooth microwear and stable isotope analyses for palaeodiet reconstruction: the case study of Late Middle Pleistocene *Elephas (Palaeoloxodon) antiquus* teeth from Central Italy (Rome area). *Quaternary International* 126–128, 2005, 153–17.
215. Palombo, M.R., Villa, P., 2001. Schreger lines as support in the Elephantinae identification. In: Cavaretta, G., Gioia, P., Mussi, M., Palombo, M.R. (Eds.), *The World of Elephants*. Consiglio Nazionale delle Ricerche, Roma, pp. 656e660.

216. Palombo, M.R., Villa, P., 2003. Sexually dimorphic characters of *Elephas (Palaeoloxodon) antiquus* from Grotte Santo Stefano (Viterbo, Central Italy). In: Reumer, J.W.F., DeVos, J., Mol, D. (Eds.), *Advances in Mammoth Research. Proceedings of the Second International Mammoths Conference, Rotterdam, May 16–20, 1999*. *Deinsea* 9, 293, 315.
217. Palombo, M.R., and Ferretti, M.P. (2005). Elephant fossil record from Italy: knowledge, problems, and perspectives. *Quaternary International*, 126, 107-136.
218. Panagopoulou E, et al. (2015) Marathousa 1: a new Middle Pleistocene archaeological site from Greece. *Antiquity Project Gallery* 83:1-8.
219. Pastor, R.F., 1993. Dental microwear among inhabitants of the Indian subcontinent: a quantitative and comparative analysis. Ph.D. Dissertation, University of Oregon.
220. Penkman K.E., Preece R.C., Bridgland D.R., Keen DH, Meijer T, Parfitt SA, White TS, Collins MJ. 2011. A chronological framework for the British Quaternary based on Bithynia opercula. *Nature* 476:446–449. doi: 10.1038/nature10305, PMID: 21804567.
221. Petit, J.R., Jouzel, J., Raynaud, D., Barkov, N.I., Barnola, J.M., Basile, I., Bender, M., et al. 1999. Climate and atmospheric history of the past 420,000 years from the Vostok ice core, Antarctica. *Nature* 399, 429–436.
222. Petit R.J., Excoffier L., 2009. Gene flow and species delimitation. *Trends in Ecology and Evolution* 24:386–393. doi: 10.1016/j.tree.2009.02.011, PMID: 19409650.
223. Peuke, A.D., Windt, C.W., Van As, H., 2006. Effects of cold girdling on flows in the transport phloem in *Ricinus communis*: is mass flow inhibited? *Plant Cell Environ* 29:15–25.
224. Piperno, M., 1999. Notarchirico. Un sito del Pleistocene medio iniziale nel bacino di Venosa. Osanna, Venosa.
225. Piperno, M., Tagliacozzo, A., 2001. The elephant butchery area at the Middle Pleistocene site of Notarchirico (Venosa, Basilicata, Italy). In: Cavaretta, G., Gioia, P., Mussi, M., Palombo, M.R. (Eds.). *The World of Elephants. Proceedings of the First International Congress, Rome, 16–20 October. Consiglio Nazionale delle Ricerche, Roma*, pp. 230–236.
226. Piperno, M., Tagliacozzo, A., 2001. The elephant butchery area at the middle Pleistocene site of Notarchirico (Venosa, Basilicata, Italy). In: Cavaretta, G., Gioia, P., Mussi, M., Palombo, M.R. (Eds.), *The World of Elephants. Consiglio Nazionale delle Ricerche, Rome*, pp. 230–236.
227. Poinar, H. N., Schwarz, C., Ji, Qi, Shapiro, B., MacPhee, R.D.E., Buigues, B., Tikhonov, A., Huson, D.H., Tomsho, L.P., Auch, A., Rapp, M., Miller, W., Schuster, S.C., 2006. Metagenomics to paleogenomics: large-scale sequencing of mammoth DNA. *Science* 311, 392–394.
228. Pollard, A. M., Pellegrini, M., Lee-Thorp, J. A. Technical note: Some observations on the conversion of dental enamel $\delta^{18}\text{O}_\text{P}$ values to

- $\delta^{18}\text{O}_w$ to determine human mobility. *Am. J. Phys. Anthropol.* Supplement 2011, 145, 499.
229. Poulakakis, N., Mylonas, M., Lymberakis, P., Fassoulas, C., 2002. Origin and taxonomy of the fossil elephants of the island of Crete (Greece): problems and perspectives. *Palaeogeography Palaeoclimatology Palaeoecology* 186, 163–183.
230. Poulakakis, N., Parmakelis, A., Lymberakis, P., Mylonas, M., Zouros, E., Reese, D.S., Glaberman, S., Caccone, A., 2006. Ancient DNA forces reconsideration of evolutionary history of Mediterranean pygmy elephantids. *Biology Letters* 2 (3), 451–454.
231. Purnell, M. A., Seehausen, O. and Galis, F. (2012). Quantitative three-dimensional microtextural analyses of tooth wear as a tool for dietary discrimination in fishes. *J.R. Soc. Interface* 9, 2225–2233.
232. Pushkina, D., 2007. The Pleistocene easternmost Eurasian distribution of the species associated with the Eemian *Palaeoloxodon antiquus* assemblage. *Mammal Review* 37, 224e245.
233. Pushkina, D., Bocherens, H., Chaimanee, Y., Jaeger, J.J., 2010. Stable carbon isotope reconstructions of diet and paleoenvironment from the late Middle Pleistocene Snake Cave in Northeastern Thailand. *Naturwissenschaften* 97 (3), 299e309.
234. Rabinovich, R., Ackermann, O., Aladjem, E., Barkai, R., Biton, R., Milevski, I., Solodenko, N., Marder, O., 2012. Elephants at the Middle Pleistocene Acheulian open-air site of Revadim Quarry, Israel. *Quaternary International* 276–277, 183–197.
235. Rabinovich, R., and Lister, A. M. (2017). The earliest elephants out of Africa: Taxonomy and taphonomy of proboscidean remains from Bethlehem. *Quaternary International*, 445, 23-42.
236. Radmilli A. M. & Boschian, G. Gli scavi di Castel di Guido. Il più antico giacimento di cacciatori del Paleolitico inferiore nell'Agro Romano. Istituto Italiano di Preistoria e Protostoria. Firenze, 1996.
237. Rapp, Jr. G.R., Hill, C.L., 1998. *Geoarchaeology: The Earth-science approach to archaeological interpretation*. Yale University Press, New Haven.
238. Rasmussen, H. B., Wittemyer, G., & Douglas-Hamilton, I. (2005). Estimating age of immobilized elephants from teeth impressions using dental silicon. *African Journal of Ecology*, 43(3), 215-219.
239. Rivals, F., Semprebon, G. and Lister A., 2012. An examination of dietary diversity patterns in Pleistocene proboscideans (*Mammuthus*, *Palaeoloxodon* and *Mammut*) from Europe and North America as revealed by dental microwear. *Quaternary International* 255:188–195.
240. Reitz, E. & Wing, E. 2010. *Zooarchaeology* (Third edition), Cambridge, Cambridge University Press.
241. Rensberger, J.M., 1978. Scanning electron microscopy of wear and occlusal events in some small herbivores. In: Butler, P., Percy, M., Joysey, K.A. (Eds.), *Development, function and evolution of teeth*. Academic Press, London, pp. 415–438.
242. Rivals, F., Schulz, E., Kaiser, T.M., 2008. Climate-related dietary diversity of the ungulate faunas from the middle Pleistocene succession (OIS 14-12) at the Caune de l'Arago (France). *Paleobiology* 34, 117e127.

243. Rivals F., Semprebon G., Lister A., 2012. An examination of dietary diversity patterns in Pleistocene proboscideans (*Mammuthus*, *Palaeoloxodon*, and *Mammot*) from Europe and North America as revealed by dental microwear. *Quaternary International* 255: 188–195.
244. Rivals F., Mol D., Lacombat F. et al., 2015. Resource partitioning and niche separation between mammoths (*Mammuthus rumanus* and *Mammuthus meridionalis*) and gomphotheres (*Anancus arvernensis*) in the Early Pleistocene of Europe. *Quaternary International* 379: 164–170.
245. Roth, V.L., 1989. Fabricational noise in elephant dentitions. *Paleobiology* 15 (2), 165–179. LeGeros, R. Z. (ed.). 1991. Calcium Phosphates in Oral Biology and Medicine. *Monographs in Oral Science* 15.
246. Rousseau, D. D., 1989. Réponses des malacofaunes terrestres quaternaires aux contraintes climatiques en Europe septentrionale. *Palaeogeography, Palaeoclimatology, Palaeoecology* 69, 113–124.
247. Ruggiero, R. G., 1992. Seasonal forage utilisation by elephants in central Africa. *African Journal of Ecology* 30, 137–148.
248. Roca, A. L., Georgiadis, N., Pecon-Slattery, J., O'Brien, S.J., 2001. Genetic evidence for two species of elephant in Africa. *Science* 293, 1473–1477.
249. Roca A. L., Georgiadis N., O'Brien S. J., 2005. Cytonuclear genomic dissociation in African elephant species. *Nature Genetics* 37:96–100. doi: 10.1038/ng1485.
250. Rogaev, E.I., Moliaka, Y.K., Malyarchuk, B.A., Kondrashov, F. A., Derenko, M.V., Chumakov, I. and Grigorenko, A.P. (2006). Complete mitochondrial genome and phylogeny of Pleistocene mammoth *Mammuthus primigenius*. *PLoS Biology*, 4, 403–410.
251. Rohland N, Malaspinas AS, Pollack JL, Slatkin M, Matheus P, Hofreiter M. 2007. Proboscidean mitogenomics: chronology and mode of elephant evolution using mastodon as outgroup. *PLoS Biology* 5:e207. doi: 10.1371/ journal.pbio.0050207, PMID: 17676977.
252. Rohland N, Reich D, Mallick S, Meyer M, Green RE, Georgiadis NJ, Roca AL, Hofreiter M. 2010. Genomic DNA Sequences from mastodon and woolly mammoth reveal deep speciation of forest and savanna elephants. *PLoS Biology* 8:e1000564. doi: 10.1371/journal.pbio.1000564.
253. Ron, H., Porat, N., Ronen, A., Tchernov, E., Horwitz, L.K., 2003. Magnetostratigraphy of the Evron Member—implications for the age of the Middle Acheulian site of Evron Quarry. *Journal of Human Evolution* 44, 633–639.
254. Roth, V. L. (1984). How elephants grow: heterochrony and the calibration of developmental stages in some living and fossil species. *Journal of Vertebrate Paleontology*, 4 (1), 126–145.
255. Saarinen J., Karme A., Cerling T. et al., 2015. A new tooth wear-based dietary analysis method for Proboscidea (Mammalia). *Journal of Vertebrate Paleontology* 35.

256. Saarinen, J., and Lister, A. M., 2016. Dental mesowear reflects local vegetation and niche separation in Pleistocene proboscideans from Britain. *Journal of Quaternary Science*, 31(7), 799-808.
257. Saegusa, H., and Gilbert, W.H., in *Homo erectus* in Africa, Pleistocene Evidence from the Middle Awash (eds Henry, W., Gilbert, W. H. & Asfaw, B.) 193–226 (Univ. of California Press, 2008).
258. Sala, B., 1983. La fauna del giacimento di Isernia La Pineta (nota preliminare). In: Isernia La Pineta un accampamento più antico di 700.000 anni. Calderini Edizioni Bologna, pp. 71–79.
259. Sala, B., Barbi, G. L., 1996. Capitolo 3: Descrizione della fauna In: Radmilli, A. M., Boschian G. (Eds.). Il più antico giacimento di cacciatori del Paleolitico inferiore dell'Agro Romano. Edizioni Istituto Italiano di Preistoria e Protostoria di Firenze, pp. 55–90.
260. Sala B., 1996. Gli animali del giacimento di Isernia La Pineta. In: Peretto C, editor. I reperti paleontologici del giacimento paleolitico di Isernia La Pineta, l'Uomo e l'ambiente. Istituto Regionale per gli Studi Storici del Molise "Cuoco V." Cosmo Iannone Editore, Isernia, 25–49.
261. Sanchez Yustos, P., and Diez Martin, F., 2015. Dancing to the rhythms of the Pleistocene? Early Middle Paleolithic population dynamics in NW Iberia (Duero Basin and Cantabrian Region). *Quaternary Science Reviews* 121, 75–88.
262. Sanders, W.J., Comparative description and taxonomy of proboscidean fossils from Langebaanweg, South Africa, *African Nat. Hist.* 2 (2006) 196–197.
263. Sanders, W. J., in *Paleontology and Geology of Laetoli: Human Evolution in Context. Volume 2: Fossil Hominins and the Associated Fauna* (ed. Harrison, T.) 233–262 (Springer, 2011).
264. Sanders, W. J. and Haile-Selassie, Y. A new assemblage of Mid-Pliocene proboscideans from the Woranso-Mille Area, Afar Region, Ethiopia: taxonomic, evolutionary, and paleoecological considerations. *J. Mamm. Evol.* 19, 105–128 (2012).
265. Sanson, G.D., 1989. Morphological adaptations of teeth to diets and feeding in Macropodidae. In: Grigg, G., Jarman, P., Hume, I. (Eds.), *Kangaroos, wallabies and ratkangaroos*. Surrey Beatty, Sydney, pp. 151–168.
266. Santucci, E., Marano, F., Cerilli, E., Fiore, I., Lemorini, C., Palombo, M.R., Anzidei, A.P., Bulgarelli, G.M., 2015. Palaeoloxodon exploitation at the middle Pleistocene site of La Polledrara di Cecanibbio (Rome, Italy). *Quaternary International* 406, 169–182.
267. Schoch W., Bigga G., Böhner U., Richter P., Terberger T., 2015. New insights on the wooden weapons from the Paleolithic site of Schöningen. *J Hum Evol* 89:214-225.
268. Schüler T., 2003. ESR dating of a new Palaeolithic find layer of the travertine site of Weimar-Ehringsdorf (Central Germany). *Terra Nostra* 2:233–235.
269. Schulz, E., Calandra, I., Kaiser, T.M., 2010. Applying tribology to teeth of hoofed mammals. *Scanning* 32, 162–182.
270. Scott, R.S., Ungar, P.S., Bergstrom, T.S., Brown, C.A., Grine, F.E., Teaford, M.F. and Walker, A. (2005). Dental microwear texture

- analysis shows within-species diet variability in fossil hominins. *Nature* 436, 693–695.
271. Scott, R. S., Ungar, P.S., Bergstrom, T.S., Brown, C.A., Childs, B.E., Teaford, M.F. & Walker, A. (2006). Dental microwear texture analysis: technical considerations. *J. Hum. Evol.* 51, 339–349.
272. Scott, B., Bates, M., Bates, R., Conneller, C.H., Pope, M., Shaw, A., Smith, G., 2014. A new view from La Cotte de St. Brelade, Jersey. *Antiquity* 88, 13–29.
273. Semprebon, G., Janis, C., Solounias, N., 2004. The diets of the Dromomerycidae (Mammalia: Artiodactyla) and their response to Miocene vegetational change. *J. Vertebr. Paleontol.* 24, 430e447.
274. Semprebon, G., Janis, C., Solounias, N., 2004b. The diets of the Dromomerycidae (Mammalia: Artiodactyla) and their response to Miocene vegetational change. *Journal of Vertebrate Paleontology* 24, 427–444.
275. Semprebon, G.M., Godfrey, L.R., Solounias, N., Sutherland, M.R., Jungers, W.L., 2004. Can low-magnification stereomicroscopy reveal diet? *Journal of Human Evolution* 47, 115e144.
276. Semprebon, G. M., Rivals, F., Solounias, N., & Hulbert, R. C., 2016. Paleodietary reconstruction of fossil horses from the Eocene through Pleistocene of North America. *Palaeogeography, Palaeoclimatology, Palaeoecology*, 442, 110-127.
277. Shikama, T., 1975. *Paleontology*, new ed., 3 volumes. Asakura, Tokyo.
278. Shoshani, J., 1998. Understanding proboscidean evolution: a formidable task. *Trends in Ecology & Evolution*, 13(12), 480-487.
279. Shoshani, J., Ferretti, M. P., Lister, A. M., Agenbroad, L. D., Saegusa, H., Mol, D., Takahashi, K. 2007. Relationships within the Elephantinae using hyoid characters. *Quaternary International* 169-170:174–185. doi: 10.1016/j.quaint.2007.02.003.
280. Shoshani, J., McKenna, M.C., 1998. Higher taxonomic relationships among extant mammals based on morphology, with selected comparison of results from molecular data. *Molecular Phylogenetics and Evolution* (Special Issue) 9(3), 572–584, plus seven appendices on the website, <http://www.idealibrary.com>.
281. Shoshani, J., Tassy, P. (Eds.), 1996. *The Proboscidea: Evolution and Palaeoecology of Elephants and their Relatives*. Oxford University Press, Oxford.
282. Shoshani, J and Tassy, P. Advances in proboscidean taxonomy & classification, anatomy & physiology, and ecology & behavior, *Quat. Int.* 126–128 (2005) 5–20.
283. Sier M.J., Roebroeks W., Bakels C.C., Dekkers M.J., Brühl E., De Loecker D., Gaudzinski-Windheuser S., Hesse N., Jagich A., Kindler L., Kuijper W.J., Laurat T., Mùcher H.J., Penkman K.E., Richter D., van Hinsbergen D.J., 2011. Direct terrestrial-marine correlation demonstrates surprisingly late onset of the last interglacial in central Europe. *Quaternary Research* 75:213–218. doi: 10.1016/j.yqres.2010.11.003, PMID: 2652307.

284. Sikes, S. K. (1966), The African elephant, *Loxodonta africana*: a field method for the estimation of age. *Journal of Zoology*, 150: 279–295. doi:10.1111/j.1469-7998.1966.tb03009.x.
285. Simpson, G.G., Mesozoic Mammalia, IV, the Multituberculates as living animals, *Am. J. Sci.* 11 (1926) 228–250.
286. Simpson, G.G., Paleobiology of Jurassic mammals, *Paleobiologica* 5 (1933) 127–158.
287. Smith, Geoff., 2003. Damage inflicted upon animal bone by wooden projectiles: Experimental results and archaeological applications. *Journal of Taphonomy*. 1. 3-12.
288. Solounias, N., Fortelius, M., Freeman, P., 1994. Molar wear rates in ruminants: a new approach. *Annales Zoologici Fennici* 31, 219–227.
289. Solounias, N., Moelleken, S. M. C., 1992a. Tooth microwear analysis of *Eotragus sansaniensis* (Mammalia: Ruminantia), one of the oldest known bovids. *Journal of Vertebrate Paleontology* 12 (1), 113–121.
290. Solounias, N., Moelleken, S. M. C., 1992b. Dietary adaptations of two goat ancestors and evolutionary considerations. *Geobios* 25, 797–809.
291. Solounias, N., Moelleken, S. M. C., 1993a. Tooth microwear and premaxillary shape of the archaic antelope. *Lethaia* 26, 261–268.
292. Solounias, N., Moelleken, S. M. C., 1993b. Dietary adaptation of some extinct ruminants determined by premaxillary shape. *Journal of Mammalogy* 74, 1059–1071.
293. Solounias, N., Semprebon, G., 2002. Advances in the reconstruction of ungulate ecomorphology with application to early fossil equids. *American Museum Novitates* 3366, 1–49.
294. Solounias, N., Teaford, M.F., and Walker, A., Interpreting the diet of extinct ruminants: the case of a non-browsing giraffid. *Paleobiology* 14, 1988, 287–300.
295. Speth, J.D., 2000. Boiling vs baking and roasting: a taphonomic approach to the recognition of cooking techniques in small mammals. In: Rowley-Conwy, P. (Ed.), *Animal Bones, Human Societies*. Oxbow Books, Oxford, pp. 89–105.
296. Springer, M.S., and de Jong, W.W., 2001. Which mammalian supertree to back up? *Science* 291, 1709–1711.
297. Stea, B., Tenerini, I., 1996. L'ambiente naturale della pianura grossetana e la sua evoluzione dalla preistoria alla cartografia rinascimentale. In: Ed. Citter, C. (Ed.), *Grosseto, Roselle e il Prile*. Florence, pp. 12–24.
298. Stewart, J.R., 2008. The progressive effect of the individualistic response of species to Quaternary climate change: an analysis of British mammalian faunas. *Quaternary Science Reviews* 27, 2499e2508.
299. Stuart, A.J. (1982). *Pleistocene vertebrates in the British Isles*. Longman Financial Service.
300. Stuart, A.J., 1991. Mammalian extinctions in the late Pleistocene of Northern Eurasia and North America. *Biological Reviews* 66, 453e562.
301. Stuart A.J. 2005. The extinction of woolly mammoth (*Mammuthus primigenius*) and straight-tusked elephant (*Palaeoloxodon antiquus*) in

- Europe. *Quaternary International* 126-128:171–177. doi: 10.1016/j.quaint.2004.04.021.
302. Stuart, A. J., Lister, A. M., 2007. Patterns of Late Quaternary megafaunal extinctions in Europe and northern Asia. *Courier Forschungsinstitut Senckenberg* 259, 287e297.
303. Suga, S., 1982. Progressive mineralization pattern of developing enamel during the maturation stage. *Journal of Dental Research*: 1532-1542.
304. Sukumar, R., 1989. *The Asian Elephant: Ecology and Management*. Cambridge University Press, Cambridge.
305. Sukumar, R., 2003. *The living elephant: evolutionary ecology, behavior, and conservation*. Oxford University Press, Oxford, 478 pp.
306. Sukumar, R. & R. Ramesh. 1995. Elephant foraging: is browse or grass more important?, pp. 368–374 in J. C. Daniel and H. Datye (eds.), *A Week With Elephants*. Bombay Natural History Society, Bombay, India.
307. Surovell, T.A., Waguespack, N.M., 2008. How many elephant kills are 14? Clovis mammoth and mastodon kills in context. *Quaternary International* 191, 82–97.
308. Takahashi, K., Inuzuka, N., Kawamura, Y., Nasu, T., 1991. Paleontology of *Palaeoloxodon naumanni*. In: Kamei, T. (Ed.), *Japanese Proboscidean Fossils*. Tsukiji-Shokan, Tokyo, pp. 11–179.
309. Tassy, P., 2003. Elephantoida from Lothagam. In: Leakey, M.G., Harris, J.M. (Eds.), *Lothagam: The Dawn of Humanity in Eastern Africa*. Columbia University Press, New York, pp. 331–358.
310. Tassy, P. and Shoshani, J., 1988. The Tethytheria: elephants and their relatives. *The phylogeny and classification of the tetrapods*, 2, 283-315.
311. Tchernov, E., Horwitz, L.K., Ronen, A., Lister, A., 1994. The faunal remains from Evron Quarry in relation to other Lower Paleolithic hominid sites in the southern Levant. *Quaternary Research* 42, 328–339.
312. Teaford, M. F. 1988 A review of dental microwear and diet in modern mammals *Scanning Microsc.* 2 1149–66
313. Thieme H., Veil S., 1985. Neue Untersuchungen zum eemzeitlichen Elefanten-Jagdplatz Lehringen. *Ldkr Verden Die Kunde* 36:11-58.
314. Thomas, M.G., Hegelberg, E., Jones, H.B., Yang, Z., Lister, A.M., 2000. A molecular and morphological evidence on the phylogeny of the Elephantidae. *Proceeding of the Royal Society London B* 267, 2493–2525.
315. Tieszen, L. L. Natural variation in the carbon isotope values of plants: Implications for archaeology, ecology, and paleoecology. *Journal of Archaeological Science* 18, 1991, 227–24.
316. Todd NE. 2010. New phylogenetic analysis of the family Elephantidae based on cranial-dental morphology. *The Anatomical Record: Advances in Integrative Anatomy and Evolutionary Biology* 293:74–90. doi: 10.1002/ar. 21010.
317. Todd, N. E, Falco, N., Silva, N., Sanchez, C., Dental microwear variation in complete molars of *Loxodonta africana* and *Elephas maximus*. *Quaternary International* 169–170, 2007, 192–202.

318. Trevisan, L., 1948. Lo scheletro di *Elephas antiquus italicus* di Fonte Campanile (Viterbo). *Paleontographia Italica* 44, 2–78.
319. Tykot R.H., 2004. Stable isotopes and diet: you are what you eat. In: M. Martini, M. Milazzo and M. Piacentini (eds), *Proceedings of the International School of Physics “Enrico Fermi”, Course CLIV*, IOS Press, Amsterdam.
320. Ungar, P.S., Incisor microwear and feeding behavior in *Alouatta seniculus* and *Cebus olivaceus*, *Am. J. Primatol.* 20 (1990) 43–50.
321. Ungar, P.S., 2015. Mammalian dental function and wear: A review. *Biosurface Biotribol.* 1, 25e41.
322. Ungar, P.S., Brown, C.A., Bergstrom, T.S., Walker, A. 2003. A quantification of dental microwear by tandem scanning confocal microscopy and scale-sensitive fractal analyses. *Scanning* 25:189–193.
323. Uno, K.T. et al. Late Miocene to Pliocene carbon isotope record of differential diet change among East African herbivores. *Proc. Natl Acad. Sci. USA* 108, 6509–6514 (2011).
324. Van Valen, L., 1973. Body size and numbers of plants and animals. *Evolution*, 27(1), 27-35.
325. Vaufrey, R., 1929. Les éléphants nains des îles méditerranéennes et la question des isthmes pléistocènes. *Archives de Institut de Paléontologie Humaine*, Paris 6, 1–220.
326. Villa, P. and Mahieu, E., 1991. Breakage patterns of human long bones. *Journal of Human Evolution* 21, 27–48.
327. Villa, P., Soto, E., Santonja, M., Perez-Gonzalez, A., Mora, R., Parcerisas, J., Sesé, C., 2005. New data from Ambrona: closing the hunting versus scavenging debate. *Quaternary International* 126–128, 223–250.
328. Von Koenigswald, W., 2003. Mode and causes for the Pleistocene turnovers in the mammalian fauna of Central Europe. *Deinsea* 10, 305e312.
329. Voorhies, M., 1969. Taphonomy and population dynamics of an Early Pliocene vertebrate fauna, Knox Country, Nebraska. University of Wyoming Contributions to Geology Special Paper No. 1, Larmie.
330. Waguespack, N., Surovell, T., Denoyer, A., Dallow, A., Savage, A., Hyneman, J., & Tapster, D., 2009. Making a point: Wood- versus stone-tipped projectiles. *Antiquity*, 83 (321), 786-800. doi:10.1017/S0003598X00098999.
331. Weber, T., 2000. The Eemian *Elephas antiquus* finds with artifacts from Lehringen and Grobern: are they really killing sites? *Anthropologie et Préhistoire* 111, 177–185.
332. Wenban-Smith, F.F., Allen, P., Bates, M.R., Parfitt, S.A., Preece, R.C., Stewart, J.R., Turner, C., Whittaker, J.E., 2006. The Clactonian elephant butchery site at Southfleet Road, Ebbsfleet, UK. *Journal of Quaternary Science* 21, 471–483.
333. West, J. B., 2001. Snorkel breathing in the elephant explains the unique anatomy of its pleura. *Respiration physiology*, 126(1), 1-8.
334. White, L.J.T., Tutin, C.E.G. and Fernandez, M., 1993. Group composition and diet of forest elephants, *Loxodonta africana cyclotis*

- Matschie 1900, in the Lope Reserve. Gabon. *African Journal of Ecology* 31, 181-199.
335. Wilson, R.M., Elliott, J.C., Dowker, S.E.P. Rietveld refinement of the crystallographic structure of human dental enamel apatites. *Am. Mineral.* 1999, 84, 1406.
336. Wopenka, B. and Pasteris, J.D.: A mineralogical perspective on the apatite in bone, *Mater. Sci. Eng.: C*, 25, 131–143, 2005.
337. Yravedra, J., Domínguez-Rodrigo, M., Santonja, M., Pérez-González, A., Panera, J., Rubio-Jara, S., Baquedano, E., 2010. Cut marks on the Middle Pleistocene elephant carcass of Áridos 2 (Madrid, Spain). *Journal of Archaeological Science* 37, 2469–2476.
338. Yravedra, J., Panera, J., Rubio-Jara, S., Manzano, I., Expósito, A., Pérez-González, A., Soto, E., López-Recio, M., 2014. Neanderthal and *Mammuthus* interactions at EDAR Culebro 1 (Madrid, Spain). *Journal of Archaeological Science* 42, 500–508
339. Zagwijn, W.H. (1996): The Cromerian Complex Stage of the Netherlands and correlation with other areas in Europe. – In: Turner, C. (ed.): *The Middle Pleistocene in Europe: 145–172*, Rotterdam (Balkema).
340. Zhang, Y., Zong, G., 1983. Genus *Palaeoloxodon* of China (in Chinese with English abstract). *Vertebrata Palasiatica* 21, 301e314.
341. Zazzo, A. et al. Herbivore paleodiet and paleoenvironmental changes in Chad during the Pliocene using stable isotope ratios of tooth enamel carbonate. *Paleobiology* 26, 294–309 (2000).
342. Zazzo, A., Balasse, M., Patterson, W. P. and Patterson, P., 2005. High-resolution $\delta^{13}\text{C}$ intratooth profiles in bovine enamel: Implications for mineralization pattern and isotopic attenuation. *Geochimica et Cosmochimica Acta*, 69(14): 3631-3642.

Paleoenvironmental context of the early Neanderthals of Poggetti Vecchi for the late middle Pleistocene of Central Italy

Marco Benvenuti^{a*}, Jean-Jacques Bahain^b, Chiara Capalbo^{a,c}, Chiara Capretti^d, Francesco Ciani^e, Carmine D'Amico^f, Daniela Esu^g, Gianna Giachi^h, Claudia Giuliani^e, Elsa Gliozziⁱ, Simona Lazzeri^f, Nicola Macchioni^f, Marta Mariotti Lippi^e, Federico Masini^c, Paul Peter A. Mazza^a, Pasquino Pallecchiⁱ, Anna Revedin^k, Andrea Savorelli^l, Marco Spadi^j, Lorena Sozzi^f, Amina Vietti^{b,k}, Mario Voltaggio^l, Biancamaria Aranguren^h

^aDipartimento di Scienze della Terra, Università di Firenze, 50121 Florence, Italy

^bDépartement de Préhistoire du Muséum National d'Histoire Naturelle, UMR 7194 du CNRS, 75013 Paris, France

^cDipartimento di Scienze della Terra e del Mare (DISTEM), Università di Palermo, 90123 Palermo, Italy

^dCNR - IVALSA, 50019 Florence, Italy

^eDipartimento di Biologia, Università degli Studi di Firenze, 50019 Florence, Italy

^fDipartimento di Bioscienze e Territorio, Università degli Studi del Molise, 86090 Pesche (Isernia), Italy

^gDipartimento di Scienze della Terra, Università Sapienza, 00185 Rome, Italy

^hSoprintendenza Archeologia della Toscana, 50121 Florence, Italy

ⁱDipartimento di Scienze, Università Roma TRE, 00146 Rome, Italy

^jIstituto Italiano di Preistoria e Protostoria, 50121 Florence, Italy

^kDipartimento di Chimica, Università degli Studi di Torino, 10125 Turin, Italy

^lCNR -IGAG, 00015 Rome, Italy

(RECEIVED December 1, 2016; ACCEPTED June 8, 2017)

Abstract

Work on thermal pools at Poggetti Vecchi in Grosseto, Italy, exposed an up to 3-meter-thick succession of seven sedimentary units. Unit 2 in the lower portion of the succession contained vertebrate bones, mostly of the straight-tusked elephant, *Palaeoloxodon antiquus*, commingled with stone, bone, and wooden tools. Thermal carbonates overlying Unit 2 are radiometrically dated to the latter part of the middle Pleistocene. This time span indicates that early Neanderthals produced the human artifacts from Poggetti Vecchi. The elephant bones belong to seven individuals of different ages. Sedimentary facies analysis and paleoecological evidence suggest a narrow lacustrine-palustrine embayment affected by water-level fluctuations and, at times, by hydrothermal water. Cyclic lake-level variations were predominantly forced by the rapid climatic fluctuations that occurred at Marine Isotope Stage (MIS) 6–7 transition and throughout the MIS 6. Possibly an abrupt, intense, and protracted cold episode during the onset of MIS 6 led to the sudden death of the elephants, which formed an unexpected food resource for the humans of the area. The Poggetti Vecchi site adds new information on the behavioral plasticity and food procurement strategies that early Neanderthals were able to develop in Italy during the middle to the late Pleistocene transition.

Keywords: Paleoenvironment; Paleoecology; Early Neanderthals; Late middle Pleistocene; Central Italy

INTRODUCTION

Increased collaboration between natural sciences, archeology, and humanities has been bridging conceptual and methodological gaps over the last four decades; this has led to the creation of geoarcheology (Rapp and Hill, 1998; Ghilardi and Desruelles, 2009). Geoarcheology is the most effective means for revealing how past human populations dealt with the impact on

ecosystems of interacting geological, climatic, and biological factors. A Paleolithic site discovered in Grosseto in Italy during the spring of 2012 illustrates the value of detailed geoarchaeological studies. The site is located at Poggetti Vecchi that is a few kilometers north of Grosseto, and is an open-air, stratified, Paleolithic site that was unexpectedly brought to light at a depth of around 2.5 m while digging for a new 160 m² thermal swimming pool located northward of other preexisting Paleolithic sites. Emergency excavations in a 60 m² portion of the pool led to the unearthing of human artifacts and vertebrate bones of various mammal species, mostly from the straight-tusked elephant *Palaeoloxodon antiquus*. Researchers from the

*Corresponding author at: Dipartimento di Scienze della Terra, Università di Firenze, 50121 Florence, Italy. E-mail address: ma.benvenuti@unifi.it. (M. Benvenuti).

Ministry of Cultural Heritage, Activities, and Tourism conducted the stratigraphic excavation, carefully recording the position of all the finds in order to produce GIS maps of each level.

The Poggetti Vecchi assemblage of faunal remains and artifacts is radiometrically dated to the latter part of the middle Pleistocene, which indicates that the tools found were made by early Neanderthals. At transition from the middle to the late Pleistocene, the only evidence of human presence in Italy is the human skeleton from Altamura, which is dated to the Marine Isotope Stage (MIS) 6–7 boundary (Lari et al., 2015). In fact, most of the Italian sites with evidence of human activity on bones of *Paleoloxodon antiquus* are assigned to the Lower Paleolithic, e.g., Notarchirico (Piperno and Tagliacozzo, 2001), Castel di Guido (Boschian and Sacca, 2014), Atella (Abruzzese et al., 2015), Ficoncella (Aureli et al., 2015), and La Polledrara (Santucci et al., 2015).

The Poggetti Vecchi site is particularly interesting from the geoarchaeological perspective, because it provides snapshots of the local environment at a time when early Neanderthals occupied the area. The site is especially valuable because it demonstrates the considerable skills of Neanderthals to opportunistically reconfigure and vary their activities according to their circumstances and resource availability. The present study is a part of a wider, multidisciplinary research project, which aims to reconstruct the behavior and ways of life of the early Neanderthal populations in the region. In particular, this paper focuses on the environmental conditions under which middle Pleistocene humans lived in the area around Poggetti Vecchi.

GEOLOGICAL BACKGROUND AND ARCHEOLOGY OF THE SITE

Geomorphic setting

The Poggetti Vecchi site is located on the northeastern side of Grosseto's plain in southern Tuscany, Italy (Fig. 1A). This wide, coastal lowland is surrounded by low elevations composed of Triassic–Neogene clastic and carbonate deposits. The lowland was a lake, known as *Lacus Prilis*, through Etruscan and Roman times, before it became a wetland reclaimed by the nineteenth century (Stea and Tenerini, 1996). Its long-lasting lacustrine-palustrine system resulted in the sandy-muddy surface sediments that extend for a few hundred meters underground, forming the thick Quaternary coastal basin infill (Bravetti and Pranzini, 1987; Censini and Costantini, 2002). Poggetti Vecchi stands at the foot of a hill some 11 m above the plain that has developed on Mesozoic carbonate bedrock, which is extensively exposed on the slopes leading to the town of Roselle to the east (Fig. 1B). The lowland is affected by diffuse karstification that results in catastrophic subsoil collapses; one of these sinkholes formed in January 1999 at Bottegone, about 2 km north of Poggetti Vecchi (Censini and Costantini, 2002). The area has also many thermal springs (Bencini et al., 1977), which suggests a local geothermal anomaly. Small magmatic Neogene-Quaternary intrusions are

widespread in southern Tuscany and generate a high geothermal gradient (Baldi et al., 1995).

Data description

This section reports the results of the stratigraphic, paleontological, and dating analyses. For the methods applied, see Supplement Item 1.

Stratigraphy of the site

The east–west trending, 20-m-long swimming pool excavation (Fig. 1C and 2) exposed vertebrate bones and stone artifacts (Fig. 3A) embedded in a few meters of largely muddy sediments of the plain. Several hydrothermal springs were found at the bottom of the excavation. The abundant discharge of the springs had to be drained with water pumps to keep the sections clear and to recover the specimens. Seven lithostratigraphic units were encountered in the excavated section; they will be described here, starting from the lowest (Figs. 2 and 3).

Unit 1

Unit 1 consists of about 0.5 m of massive, dark grayish mudstone (Fig. 3B). The fossils present in this unit comprise abundant mollusks, ostracods, micro-vertebrates (mammals, amphibians, fishes), and plant remains, the latter including either unaltered (seeds, carophytes, pollen grains) or charred elements. The fossils were found uniformly dispersed in the sediment matrix.

Unit 2

The lower boundary of this bone bed is marked by an erosional contact. The unit is from 20 to 40 cm thick and mostly yielded remains of *Palaeoloxodon antiquus* mixed with bone and stone artifacts, scattered lithic production waste, but also wooden rods, which are presumably tools (Fig. 3A). Unit 2 is starved of sediment from the marginal source areas, and the skeletal remains accumulated to form a condensed layer of fauna. The top of the bone bed is an irregular surface formed by the assemblage of large bones and wooden remains.

Unit 3

Unit 3 is a lithologically composite unit, up to 20 cm thick, including two distinct divisions (Fig. 2): a lower one, indicated as 3a, made up of dark grayish mudstone with gastropod shells dispersed at the bottom; and an upper portion, called 3b, which consists of a few centimeters of laterally discontinuous, whitish, carbonate mudstone.

Unit 4

Unit 4 lays on an erosive surface and consists of millimeter- to centimeter-sized, clast-supported, coated, carbonate particles known as pisoliths, with scattered gastropod shells (Fig. 3C). Pisoliths are typical particles that grow by accretion of biochemical precipitates in stagnant thermal water; they still form

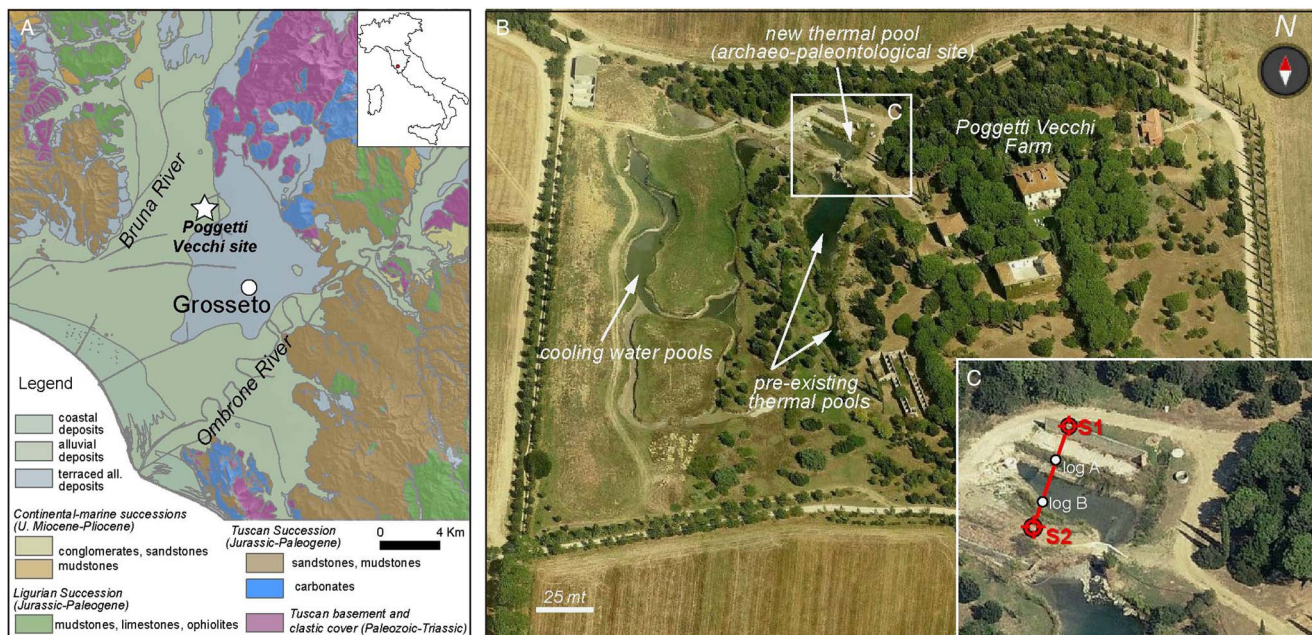


Figure 1. (color online) (A) Location of the study area and schematic geological map of the Grosseto plain and surrounding elevations. (B) Oblique aerial view of the Poggetti Vecchi site from Bing Map (<https://www.bing.com/maps/?cc=it>). (C) Detailed oblique view of the excavation area, with annotated location of cores S1 and S2 and logs A and B reported in Figure 2.

in the artificial pools that were built at Poggetti Vecchi. Remains of *Palaeoloxodon antiquus* associated with stone tools were found at the base of this unit. Sediment samples also

yielded microfossils dominated by ostracod shells. These sediments form a lenticular body up to 30 cm thick, which tapers towards the northern end of the excavation.

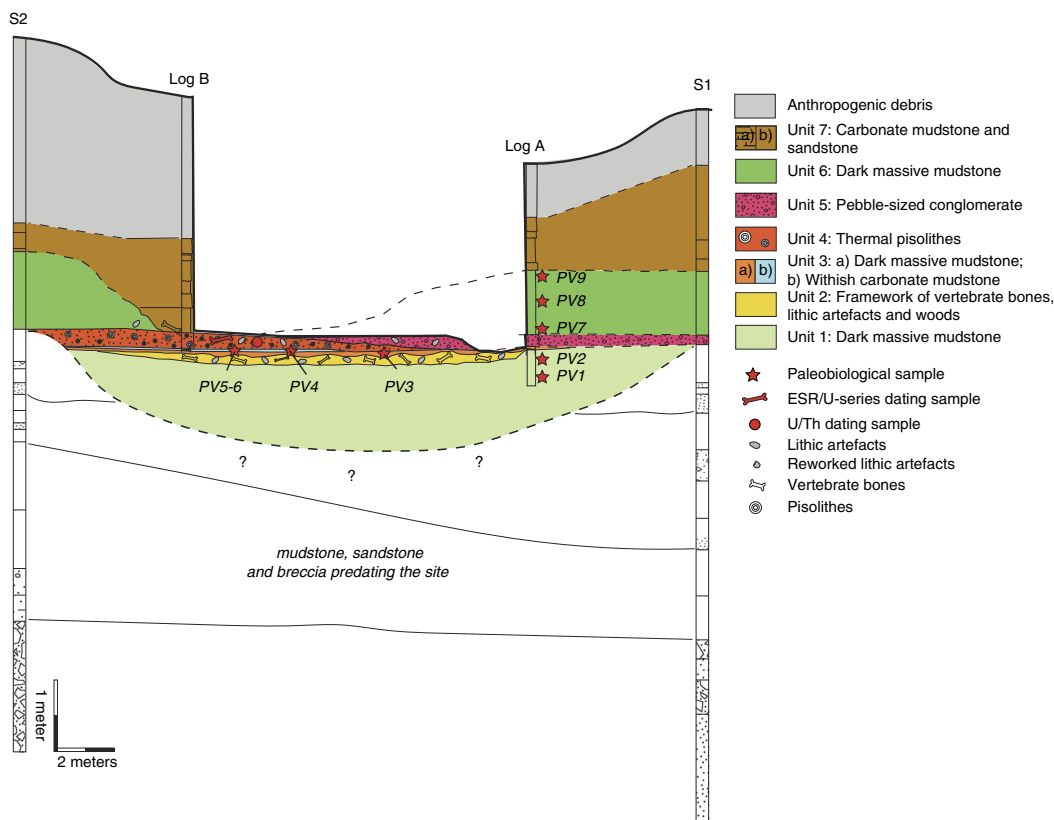


Figure 2. (color online) Correlation of stratigraphic data along the cross section indicated in Figure 1C. Samples analysed for mollusk and ostracod contents and for radiometric dating are shown.



Figure 3. (A) Plan view of Unit 2 during the archaeological excavation showing the framework of bones, stones (most of which artifacts), and wooden rods (indicated by red arrows). (B) Part of the section excavated along the northern side of the site where log A was measured. (C) The section excavated on the southern side (log B); note two molars and bones of *Palaeoloxodon antiquus* on top of Unit 4. Ten centimeters divisions for scale in all photographs. (For interpretation of the references to color in this figure legend, the reader is referred to the web version of this article.)

Unit 5

An erosional surface separates this unit from the underlying Unit 4. Unit 5 includes pebble-sized, clast-supported conglomerates with an intervening sandy-muddy matrix, arranged in a lenticular bed up to 25 cm thick (Fig. 3B). Clasts are subangular to sub-rounded and mostly composed of micritic grayish limestone with subordinate pisoliths and gastropod shells. Sparse vertebrate remains and stone tools were also recovered from this unit.

Unit 6

Unit 6 is up to 0.9 m thick and is a massive, dark, grayish mudstone similar to Unit 1 (Fig. 3B and C). The unit contains

abundant gastropod shells and plant remains, together with occasional stone implements at the base, associated with a small amount of wooden items, possibly tools.

Unit 7

Unit 7, up to 2 m thick, starts with an erosive base. This unit consists of two layers (Fig. 2): the lower one, called 7a, is 0.4 m of massive, whitish, calcareous mudstone (Fig. 3C), and contains the skull of a juvenile *Palaeoloxodon antiquus*; the upper one, 7b, consisting of a set of beds made up of massive/graded calcareous sandstone and mudstone, separated from one another by erosive surfaces (Fig. 3B).

An anthropogenic deposit up to 2 m thick, containing remains from the Roman Era, covers Unit 7 (Fig. 2, 3B–C).

The stratigraphic framework was constructed by correlating the stratigraphic logs recorded in the southern and northern portions of the excavation, and two shallow cores, S1 and S2, that were drilled just outside the excavated area (Fig. 2). This revealed that the site used to be in a small valley extending from the Poggetti Vecchi hill down to the plain. The seven lithological units are enclosed within a section, between cores S1 and S2, which widens a few meters north–south from the excavated area. Cores S1 and S2 were retrieved at depths up to 10 m. The sediments in the upper parts of the cores correspond to the deposits of Units 7 and 6, whereas the clastic succession beneath is dominated, from the top downwards, by massive mudstone with subordinate sandstone, which abruptly passes into reddish mudstone. The latter overlies a calcareous breccia present at the bottom of the cores. Both successions accumulated before the formation of Units 1–7. Summing up, our site consists of deposits piled up in a small valley carved at the side of a wide lacustrine area, whose water table repeatedly fluctuated, and which was ultimately affected by the geothermal heat flux.

Radiometric dating

Unit 4 contains pisoliths and vertebrate bones suitable for radiometric dating (see Supplement Item 1: Numerical dating). Pisoliths yield a U-series age of 171 ± 3 ka, and a left lower molar of *Bos primigenius* provided an ESR/U-series age of 170 ± 13 ka (Table 1). Based on these ages, the Poggetti Vecchi succession accumulated during a period spanning the latest MIS 7 interglacial and the whole MIS 6 glacial.

Archeological aspects of the site and their consequence

The open-air, stratified Paleolithic site of Poggetti Vecchi includes several anthropic layers: the oldest one is Unit 2, which yielded the richest collection of archaeological items. The excavated portion of this unit has an area of approximately 60 m². As explained above, Unit 2 developed upon the erosional surface that formed on top of Unit 1, when the lake level dropped. Animals (mostly elephants) and groups of hunter-gatherers visited the valley bottom during the short period that this unit represents. The presence of humans is demonstrated by the occurrence of numerous lithic tools and lithic manufacturing waste, obtained from siliceous fluvial pebbles or cobbles deriving from the erosion of various Apennine mountain geological formations. The most common raw materials used at the site are different types of chert, radiolarite, and quartzite. The stone tools are only broadly indicative of an early middle Paleolithic age. About 200 lithic objects (cores, flakes, and unworked raw material) and several waste materials (debris and fragments) have been recovered. Most of the lithic implements, mostly scrapers but also notches and choppers, had been retouched. Dozens of tiny flakes have also been found at the site: these are considered to be by-products of retouching that took place on site.

In virtually all the European middle Pleistocene sites where remains of *Palaeoloxodon antiquus* are associated with human artifacts, hunting or scavenging is normally suggested when just one individual elephant is present (e.g., Weber 2000; Villa et al., 2005; Wenban-Smith et al., 2006; Yravedra et al., 2010; Aureli et al., 2015; Santucci et al., 2015). In contrast, when many elephants are involved, they are generally assumed to have died due to natural causes (Gaudzinski, 1996; Villa et al., 2005; Boschian and Sacca, 2014; Santucci et al., 2015).

Table 1. (A) Activity ratios and age of the pisolite carbonatic fraction from Unit 4. All errors reported as 1σ. Age calculated using the Isoplot/EX 3.0 program proposed in Ludwig (2003). (B) ESR/U dating of Aurochs' tooth. A k-value ($D_{a\alpha}$ Internal (mGy/a)) of 0.13 ± 0.02 was used following the procedure outlined in Grün and Katzenberger-Apel (1994). The enamel thickness ($D_{a\beta}$ (μGy/a)) removed during preparation process was used to calculate the beta contribution. Cosmic dose ($D_{a\gamma}$ (γ+cosm) (μGy/a)) obtained using the formulae of Prescott and Hutton (1994). Uncertainties on the ESR/U-series datings (ESR/U-series ages (US or AU) (ka)) were calculated using Monte-Carlo approach following Shao et al. (2014).

A					
²³⁴ U/ ²³⁸ U	²³⁰ Th/ ²³⁴ U	²³⁰ Th/ ²³² Th	²³⁸ U	²³² Th	Age
(activity ratio)	(activity ratio)	(activity ratio)	(ppm)	(ppm)	(ka)
1.414 ± 0.014	0.841 ± 0.008	77 ± 5	1.48 ± 0.01	0.049 ± 0.003	171 ± 3

B									
Sample	Tissue	U (ppm)	Paleodose D_E (Gy)	U uptake p-parameter	$D_{a\alpha}$ Internal (μGy/a)	$D_{a\beta}$ (μGy/a)	$D_{a\gamma}$ (γ+cosm) (μGy/a)	D_a total (μGy/a)	ESR/U-series ages (US) (ka)
PGV1502 (c n°5485)	dentine enamel	1.84 ± 0.12 0.11 ± 0.01	91.41 ± 3.03	-0.84 ± 0.06 -0.53 ± 0.08	36 ± 37	69 ± 16	433 ± 20	538 ± 45	170 ± 13

Table 2. List of mollusk species and abundance matrix of samples collected from the different layers of the Poggetti Vecchi archaeological site. Ecological classes (EC): AF, Aquatic freshwater; TH, terrestrial hygrophilous; TW, terrestrial woodland; TO, terrestrial openland; TC, terrestrial catholic; TU, terrestrial unassigned.

Mollusc species	Samples									
	EC	PV1	PV2	PV3	PV4	PV5	PV6	PV7	PV8	PV9
<i>Viviparus</i> sp.	AF	–	1	–	–	–	–	–	–	–
<i>Melanopsis etrusca</i>	AF	43	33	14	13	9	1	96	17	35
<i>Bithynia leachii</i>	AF	15	35	4	58	21	55	30	11	52
<i>Bithynia tentaculata</i>	AF	180	191	41	6	55	129	3	–	3
<i>Bithynia</i> sp.	AF	106	70	26	–	82	105	3	7	13
<i>Belgrandia thermalis</i>	AF	8	7	263	–	166	1	9	14	13
<i>Pseudamnicola moussonii</i>	AF	2021	1931	642	2485	458	327	1925	1200	1896
<i>Islamia</i> sp.	AF	–	–	–	–	–	–	–	1	–
<i>Valvata piscinalis</i>	AF	3	12	4	1	–	–	–	–	–
<i>Physa acuta</i>	AF	–	–	–	1	–	–	–	–	–
<i>Galba truncatula</i>	AF	2	–	–	–	–	–	–	–	1
<i>Radix peregra</i>	AF	3	2	6	4	–	2	–	–	7
<i>Stagnicola palustris</i>	AF	2	–	6	2	1	–	1	5	–
<i>Planorbis moquini</i>	AF	23	3	–	163	1	–	53	77	243
<i>Planorbis planorbis</i>	AF	7	14	15	48	10	19	15	–	5
<i>Gyraulus crista</i>	AF	–	1	3	–	1	–	–	–	–
<i>Acroloxus lacustris</i>	AF	13	4	13	–	59	58	–	–	1
<i>Pisidium</i> sp.	AF	1	–	–	–	–	1	–	–	–
<i>Oxyloma elegans</i>	TH	1	–	–	–	–	–	–	–	1
<i>Vertigo antivertigo</i>	TH	2	4	–	6	–	–	4	5	1
<i>Carychium tridentatum</i>	TH	–	–	9	–	2	–	4	7	8
<i>Vitrea subrimata</i>	TW	–	1	3	–	–	–	2	–	–
<i>Daudebardia rufa</i>	TW	–	1	–	–	–	–	–	–	–
<i>Vertigo pygmaea</i>	TO	–	1	–	–	–	–	–	–	–
<i>Pupilla muscorum</i>	TO	–	–	–	–	–	–	2	1	6
<i>Vallonia pulchella</i>	TO	3	2	3	–	1	–	1	3	2
<i>Punctum pygmaeum</i>	TC	–	–	–	–	–	–	–	1	2
<i>Euconulus fulvus</i>	TC	–	–	–	–	–	–	–	1	–
<i>Discus</i> sp.	TU	–	–	–	–	–	–	–	–	1
<i>Monacha</i> sp.	TU	–	–	–	–	–	–	–	–	2
Hygromiidae indet.	TU	3	4	–	10	–	–	15	7	24
Abundance		2436	2317	1052	2797	866	698	2163	1357	2316
Species Richness (S)		18	19	15	12	13	10	15	15	20

Unit 2 at Poggetti Vecchi is the only European site that is dated to the latter part of the middle Pleistocene (MIS 6–7 transition) that has yielded the remains of several individuals of *Palaeoloxodon antiquus* of different ontogenetic ages that were found together with stone, bone, and wooden artifacts, mostly concentrated in a relatively small area at the western end of the excavation. Some of the implements found were horizontally oriented and commingled with the elephant remains (Fig. 3A), whereas others were found under the bones. The wooden artifacts present unequivocal evidence of human modification, as in, for example, the removal of small lateral branches and the removal of bark, and are therefore of particular interest, as such finds are very rarely encountered in prehistoric deposits due to the low durability of this material (Schniewind, 1990; Blanchette, 2003; Schoch et al., 2015, and references therein). All the wooden remains of

Poggetti Vecchi were found in a poor state of preservation: their restoration and analysis are still under way.

In Unit 4 of the same site, on the other hand, in the small area (25 m²) that was excavated, stone implements were found associated with the tusk and other remains of *Palaeoloxodon antiquus*. This Unit is radiometrically dated to about 171 ka, the terminus ante quem for Unit 2. Based on this dating, the human evidence from the site can be confidently attributed to the early Neanderthal period.

Unit 5 also revealed stone implements and faunal remains. Yet, only part of the lithic industry is fresh; the remainder is polished and could, therefore, possibly derive from a secondary context.

In the case of Unit 6, the lithic industry found at the base of the unit was found scattered with faunal and wood remains. This suggests that the shores of the lake were visited at a time when the water levels were starting to rise. The recurrent

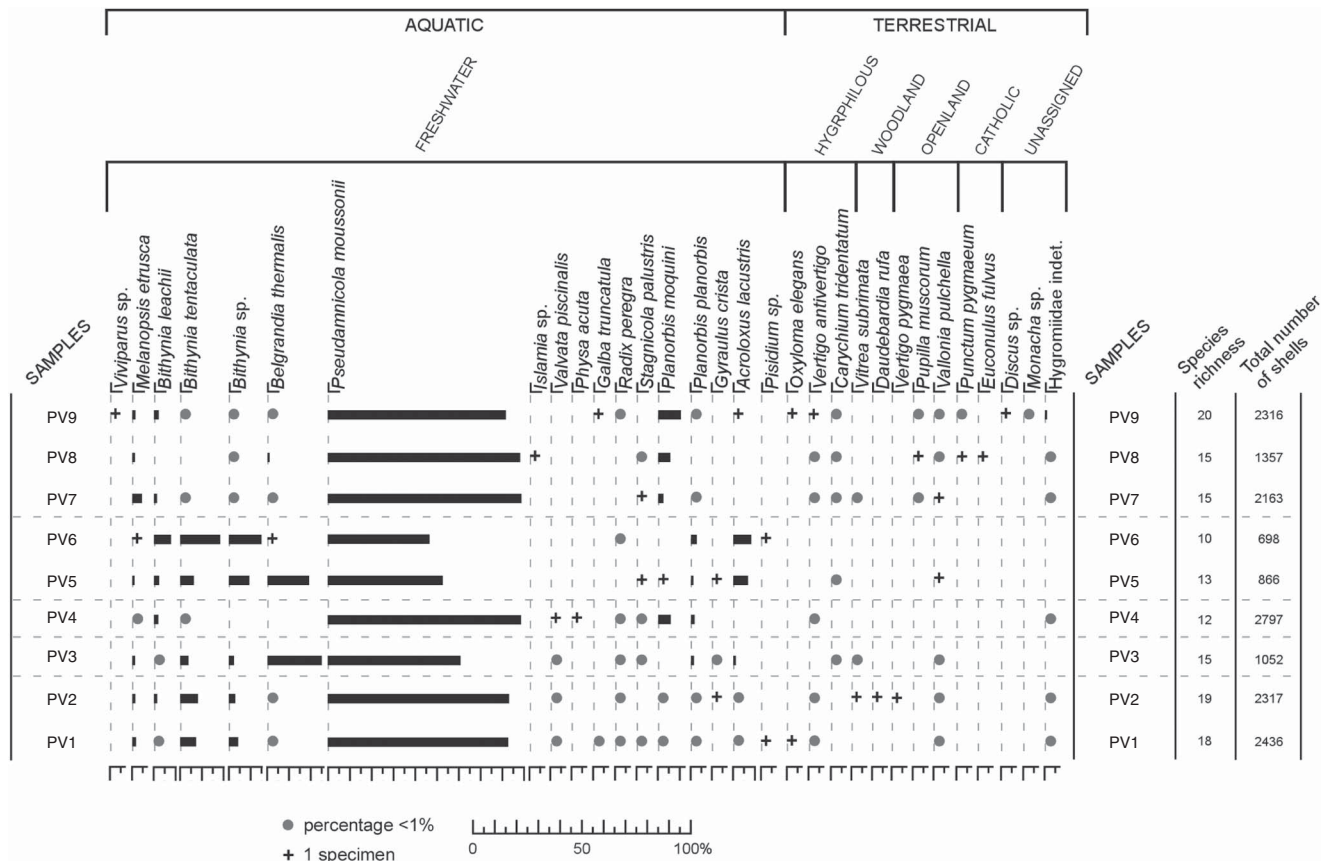


Figure 4. Malacological diagram (percentages of species) from the Poggetti Vecchi archeological site.

association of vertebrate remains and human implements in different layers (Units 2-4-5-6) of the Poggetti Vecchi stratigraphic succession indicates that humans visited the area on a regular basis, and were hunting and exploiting large mammals, especially *Palaeoloxodon antiquus*.

The microenvironment generated by the hot thermal springs at Poggetti Vecchi at a time when the climate was cooling on a global scale probably attracted both the local fauna and their human pursuers, and no doubt these circumstances helped create Poggetti Vecchi’s unusual and interesting co-occurrence of faunal remains and human implements. The site is undoubtedly important because it dates to the middle-late Pleistocene transition, which is very poorly studied in Europe owing to the lack of evidence found thus far. In Italy, following the recently revised dating of the remains from Saccopastore to around 250 ka (Marra et al., 2015), the only prehistoric evidence from the time of the MIS 6–7 transition is the human skeleton from Altamura (Lari et al., 2015). Sites from this period are also rare in other parts of Europe, probably because of the concurrent climate cooling (Sanchez Yustos and Diez Martin, 2015). In this context, therefore, the Poggetti Vecchi site offers a noteworthy chance of gaining new insights into early Neanderthal behavioral plasticity and food procurement strategies (cf., Binford, 1987; Weber, 2000; Surovell and Waguespack, 2008; Rabinovich et al., 2012; Yravedra et al., 2014; Scott et al., 2014).

Paleontological analyses

Mollusks

Overall, the samples analyzed for this study come from Units 1, 3, and 6. They have yielded rich and well-diversified assemblages of non-marine mollusks in a good state of preservation. A total of 29 freshwater and terrestrial gastropod species (17 aquatic prosobranchs and pulmonates plus 12 land pulmonates) and one bivalve have been identified. Moreover, a few undetermined species of land Hygromiidae were also recorded. In many cases, the species found at Poggetti Vecchi are still present today in Europe, Italy included. The complete list of species, together with the abundance matrix, is reported in Table 2. The aquatic gastropods dominate both in number of species (varying from 8 to 13) and specimens (up to 2781 in sample PV4), whereas the land gastropods are generally represented by lower species diversity (varying from 0 to 9) and especially by a lower number of specimens (up to 47 in sample PV9; Table 2). There is, therefore, a much higher number of aquatic than of terrestrial species in the excavated interval. The details of the molluscan assemblage from Units 1, 3, and 6 are given below. Starting from Unit 1 (PV1-2), the total number of shells ranges from 2317 to 2436, and species richness from 18 to 19. *Pseudamnicola moussonii* dominates among the aquatic species (ca. 83%), followed by *Bithynia tentaculata* (7–8%), and *Bithynia* sp. (3–4.5%; Fig. 4), whereas *Melanopsis*

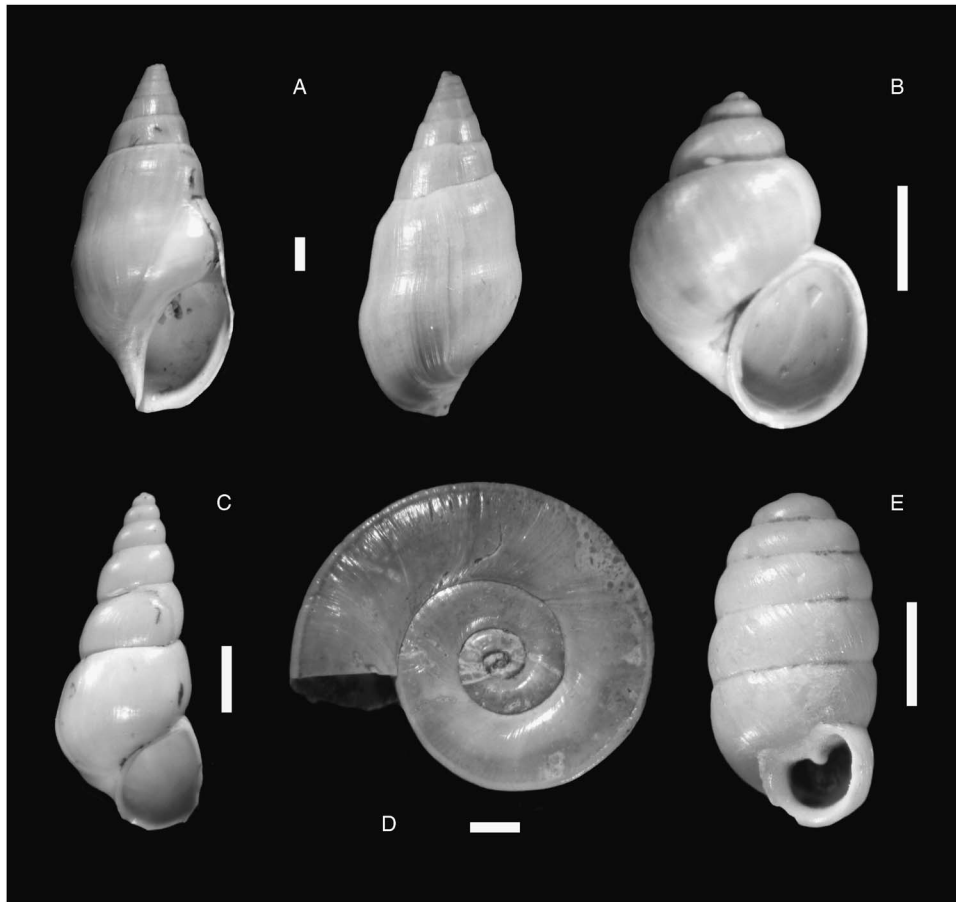


Figure 5. Selected examples of mollusc species from the sediment samples collected at Poggetti Vecchi archaeological site. Aquatic species: (A) *Melanopsis etrusca* Brot; (B) *Pseudamnicola moussonii* (Calcara); (C) *Heleobia stagnorum* (Gmelin); (D) *Planorbis planorbis* (Linnaeus). Land species: (E) *Pupilla muscorum* (Linnaeus). Scale bar = 1 mm.

etrusca (1.5–2%), *Bithynia leachii* (1–1.5%), *Belgrandia thermalis* (<1%), *Valvata piscinalis* (<1%), *Galba truncatula* (<1%), *Radix peregra* (<1%), *Stagnicola palustris* (<1%), *Planorbis moquini* (<1%), *P. planorbis* (<1%), and *Acroloxus lacustris* (<1%) are poorly represented. Freshwater bivalves include a single shell of *Pisidium* sp., and terrestrial gastropods consist of occasional hygrophilous taxa (*Oxyloma elegans* and *Vertigo antvertigo*), and very rare woodland species (*Vitrea subrimata* and *Daudebardia rufa*), and openland species (*Vertigo pygmaea* and *Vallonia pulchella*).

The total number of shells and species richness (1052 and 15, respectively) plummeted in Subunit 3a (PV3). *P. moussonii* still dominates, but at a lower percentage (61%) than in the previous samples. *B. thermalis* becomes proportionally more abundant (25%) than other aquatic species. Land gastropods include only occasional specimens of *Carychium tridentatum*, *V. subrimata*, and *V. pulchella*.

In Subunit 3b, the number of shells ranges from up to 2797 (PV5 sample) to 698–866 (PV7-9 samples), whereas species richness varies from 10 to 13. *P. moussonii* strongly dominates with a high percentage in PV4 (89%), just as in the PV1-2 samples. In contrast, its frequency declines abruptly in samples PV5–6 (47%–53%). Among the other aquatic taxa, Planorbidae are the best represented (7.5%), with the subordinate

occurrence of *B. thermalis* and *A. lacustris*. Land gastropods are very poorly represented occurring with only occasional specimens of *V. antvertigo* and *Hygromiidae* indet.

In Unit 6 (PV7-9 samples), the total number of shells ranges from 1357 to 2316, with species richness ranging from 15 to 20. *P. moussonii* continues to dominate, with very high percentages (82–89%), followed by *P. moquini*, which, in turn, shows an increasing upward trend within the unit (2.5–10.5%). The other aquatic taxa are found in much lower frequencies. The spring water species *Islamia* sp. was recorded (with only one specimen) for the first time in the succession in this unit. Terrestrial species show a higher shell abundance (25–47) and species richness (6–9) than in the other units. In particular, the open-landscape *Pupilla muscorum*, the catholic taxa *Punctum pygmaeum* and *Euconulus fulvus*, and the ecologically unassigned species, *Discus* sp. and *Monacha* sp., first appear in the succession here.

Summing up, the molluscan fauna recovered from the deposits exposed by the excavation, but also from cores S1-2, is characterized by the dominance of freshwater taxa (Fig. 5). The most common and abundant freshwater species, *P. moussonii* (from 30% to nearly 90% of abundance), colonizes not only spring water, or stream and river waters not far from the spring, but also rocky and sandy substrata (Giusti and Pezzoli, 1980; Giusti et al., 1995; Cianfanelli, 2009). Members

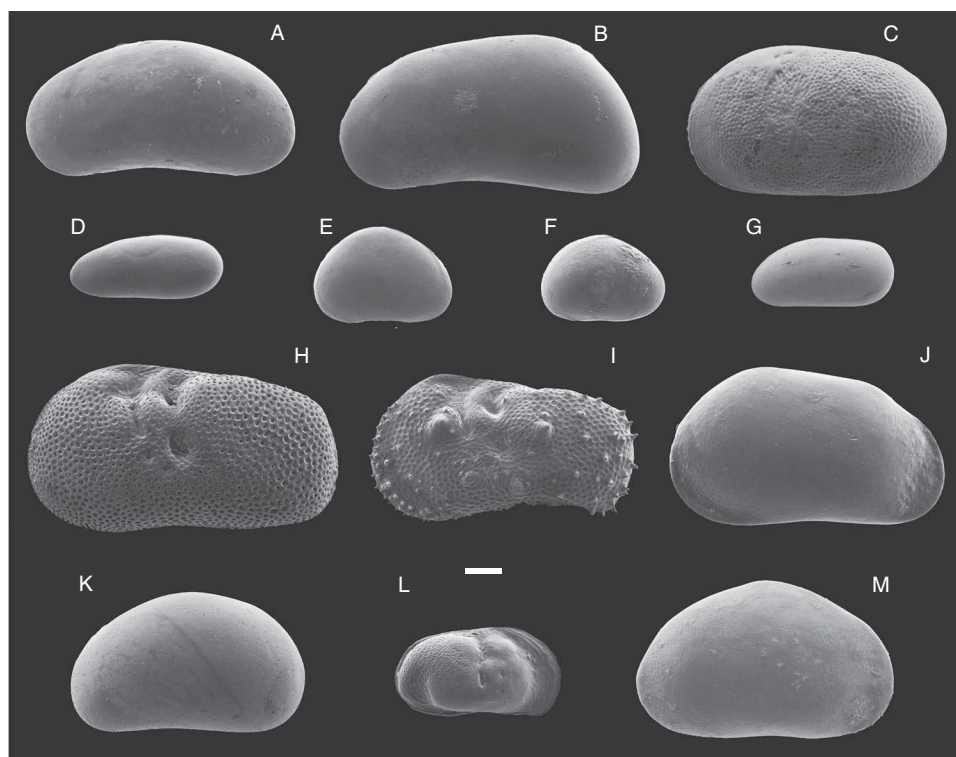


Figure 6. Scanning electron micrographs of fossil ostracod valves recovered in the sediments of Poggetti Vecchi archaeological site. (A) *Candona (Candona) improvisa* Ostermeyer. (B) *Candona (Neglecandona) neglecta* Sars. (C) *Cyprideis torosa* (Jones). (D) *Darwinula stevensoni* (Brady and Robertson). (E) *Cypria ophthalmica* (Jurine). (F) *Cyclocypris ovum* (Jurine). (G) *Vestalenula cylindrica* (Straub). (H) *Ilyocypris getica* Masi. (I) *Ilyocypris monstifrica* (Norman). (J) *Pseudocandona marchica* (Hartwig). (K) *Scottia pseudobrowniana* Kempf. (L) *Paralimnocythere messanai* Martens. (M) *Heterocypris salina* (Brady). White bar = 0.1 mm.

of Bithyniidae (*B. leachii* and *B. tentaculata*, and *Bithynia* sp.), Lymnaeidae (*R. peregra* and *S. palustris*), Planorbidae (*P. moquini* and *P. planorbis*), and Acroloxidae (*A. lacustris*), which are almost constantly present in the samples (Fig. 4), require slow moving or still, clear, shallow waters found in well-vegetated lakes and ponds (Ložek, 1964; Girod et al., 1980). Furthermore, two species typical of thermal spring waters and slow flowing waters, in this case, *M. etrusca* (Fig. 5) and *B. thermalis*, are frequent, with variable percentages in Units 1–4 and 6, as well as in core S2. These indicate the presence of thermal springs either nearby (Units 1 and 6) or at the site itself (Units 3 and 4). *M. etrusca* requires running water fed by thermal springs with a high mineral content, temperatures between 18° and 35°C, and an average pH of 6.8–7.2 (Bartolini et al., 2010). Population densities decrease moving away from the spring and with faster flowing water (Cianfanelli et al., 1991; Manganelli et al., 2000; Bartolini et al., 2010). *M. etrusca*, which is often associated with *T. fluviatilis*, *B. tentaculata*, *P. moussonii*, *B. thermalis*, *S. palustris*, *P. planorbis*, and *A. lacustris* (Giusti and Pezzoli, 1980; Cianfanelli et al., 1991, 2010; Manganelli et al., 2000; Bartolini et al., 2010), is endemic to Tuscany. Abundant populations of the species are still present today in 7 sites with thermal waters between Livorno and Grosseto. One of them is the Poggetti Vecchi spring. *M. etrusca* is currently an endangered species due to the overexploitation of thermal waters (Manganelli et al.,

2000; Cianfanelli, 2010). In addition, a single individual of the spring water genus *Islamia* (*Islamia* sp.) was recorded in PV7-9. The generally rare occurrence of land hygrophilous taxa, such as *C. tridentatum*, *V. antivertigo*, and the presence of one species of Succineidae (*O. elegans*), indicates restricted marshland surroundings. Instead, *P. muscorum* (Fig. 5) and *V. pulchella* in the PV7-9 samples denote an open landscapes such as dry grassland and exposed areas (Ložek, 1964; Kerney, 1999) in the later stages of the site.

Ostracods

All the ostracod valves are well preserved and, generally, each species includes both adults and juveniles. A population age structure of this type indicates an autochthonous thanatocoenosis typical of an environment with moderate energy (Boomer et al., 2003). Thirteen species of ostracods from eleven genera have been identified in the nine analyzed samples (Fig. 6, Table 3). These include: *Darwinula stevensoni* (Brady and Robertson), *Vestalenula cylindrica* (Straub), *Candona (Candona) improvisa* Ostermeyer, *Candona (Neglecandona) neglecta* Sars, *Pseudocandona marchica* (Hartwig), *Cypria ophthalmica* (Jurine), *Cyclocypris ovum* (Jurine), *Ilyocypris monstifrica* (Norman), *Ilyocypris getica* Masi, *Heterocypris salina* (Brady), *Scottia pseudobrowniana* Kempf, *Paralimnocythere messanai* Martens, and *Cyprideis torosa* (Jones).

Table 3. Percentage frequencies of the ostracod species recovered in the different units of the Poggetti Vecchi archaeological site.

Samples	<i>H. salina</i>	<i>C. torosa</i>	<i>P. marchica</i>	<i>C. neglecta</i>	<i>C. improvisa</i>	<i>C. ovum</i>	<i>C. ophthalmica</i>
PV9	43	8	40	0	0	4	4
PV8	46	7	17	22	0	2	2
PV7	69	20	0	0	0	0	3
PV6	79	5	12	0	0	0	3
PV5	83	0	7	4	0	0	0
PV4	72	0	9	4	0	2	0
PV3	4	6	8	0	77	2	0
PV2	22	19	7	22	0	4	4
PV1	23	15	5	28	0	15	3

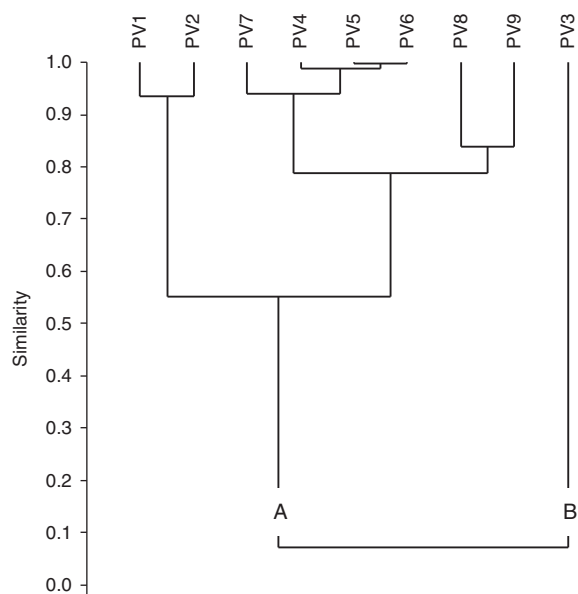
Samples	<i>I. monstifrica</i>	<i>I. getica</i>	<i>D. stevensoni</i>	<i>V. cylindrica</i>	<i>S. pseudobrowniana</i>	<i>P. messanai</i>
PV9	4	1	0	0	0	0
PV8	2	2	0	0	0	0
PV7	3	3	0	0	3	0
PV6	3	1	0	0	0	0
PV5	0	0	0	0	0	0
PV4	0	1	2	0	0	0
PV3	0	0	0	2	0	0
PV2	4	4	4	4	0	4
PV1	3	2	3	3	0	0

Almost all samples (except PV3) are dominated by *H. salina*, which is accompanied by *P. marchica* (particularly abundant in the upper part of the succession), with subordinated amounts of *C. torosa* and *C. (N.) neglecta*. All the other species show very low frequencies and are found scattered throughout the succession, except for *C. (C.) improvisa*, which is the dominant species (77%) in the low diversity assemblage recovered in sample PV3.

Cluster analysis was used to produce the dendrogram as illustrated in Figure 7, with a correlation coefficient of 0.98. Two clusters, A and B, emerge at the very low similarity value of about 0.07. Cluster A includes all samples from the archeological excavation site, except one from Unit 3a; these samples are mainly dominated by *H. salina* and include species typical of permanent shallow waters of ponds and lakes (Meisch, 2000; Fuhmann, 2012). The presence of *C. torosa* with both noded and smooth shells, combined with the predominance of *H. salina*, indicate slightly brackish waters, with salinity values below the osmoregulation threshold of *C. torosa* (8 psu; Keyser, 2005; Frenzel et al., 2012). The co-occurrence of *P. marchica* restricts the likely salinity range to a maximum of 4 psu (Griffiths and Holmes, 2000). Such a low salinity is testified also by the abundance of *Chara gyrogonites*. Cluster B, on the other hand, includes only sample PV3: it is dominated by *C. (C.) improvisa*, a species typical of seasonal pools (Meisch, 2000).

The Mutual Ostracod Temperature Range (MOTR) method was applied to the assemblages of cluster A in Figure 1 to estimate the paleotemperature ranges at the time of the deposition of the sediment. Horne (2007) and Horne et al. (2012) created this method for determining paleotemperature ranges by combining the Nonmarine Ostracod Distribution in

Europe Database (NODE; Horne et al., 1998) and WorldClim (version 1.3; Hijmans et al., 2005) datasets. The inferred paleotemperatures were then compared with today's mean July and January temperatures at Poggetti Vecchi. The results of the MOTR analysis are reported in Figure 8, and they show that July and January paleotemperatures of 15–22°C for July and and –1–4°C for January were both significantly below the present day mean values, which are 25°C and 7.6°C,

**Figure 7.** Dendrogram resulting from cluster analysis in Q-mode using the UPGMA method and the Morisita–Horn distance applied to the samples from the Poggetti Vecchi archeological site.

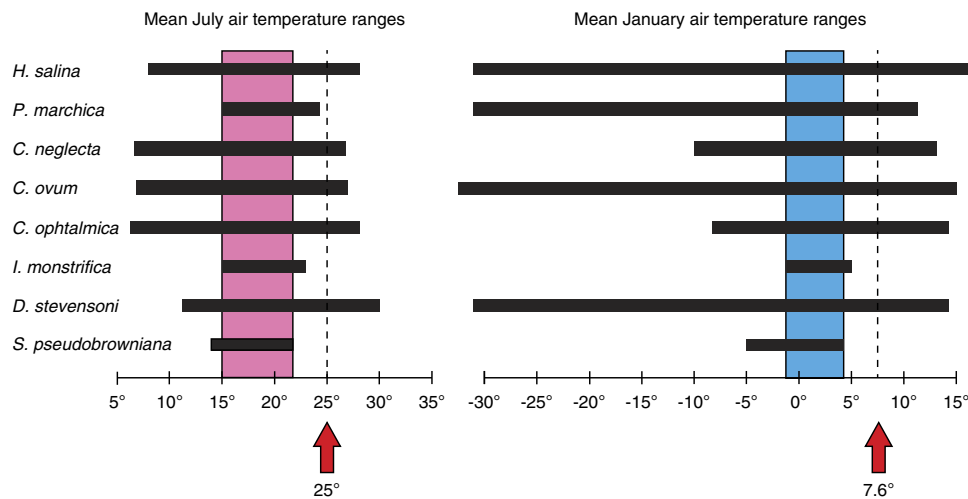


Figure 8. (color online) Estimated average air palaeotemperatures during the deposition of the sediments in the Poggetti Vecchi archaeological site based on the recovered fossil ostracods. Black lines indicate the tolerance temperature ranges for each species. The pink and light blue fields indicate the estimated July and January average temperature ranges in which the recovered ostracod species could coexist. The red arrows indicate the present July and January average temperatures for the Poggetti Vecchi area. (For interpretation of the references to color in this figure legend, the reader is referred to the web version of this article.)

respectively (these being the average values for the period 2005–2014; data retrieved from the hydrological station Grosseto -Servizio Idrologico Regionale Toscana).

Vertebrates

Unit 2 was particularly rich in vertebrate remains, whereas several isolated bones were found in Units 4 and 6. A total of 634 specimens were retrieved from Unit 2: 149 (23.5%) of them are undetermined. Table 4 and Figure 9 report the list of the species, with their relative frequencies and abundances expressed in Number of Identified Specimens (NISP) counts.

The remains of very large-sized grazers, i.e., the straight-tusked elephant (*Palaeoloxodon antiquus*) and the aurochs

(*Bos primigenius*), predominate in the excavation. Based on NISP 67% and 32.6% were found for the two species, respectively. Browsing herbivores, such as the red deer (*Cervus elaphus*), roe deer (*Capreolus capreolus*), and fallow deer (*Dama dama*) are much rarer. *Cervus elaphus*, for example, is the only middle-sized species present in the Unit 2 assemblage; whereas the remains of roe deer and fallow deer total 1.4% and 1.2% of the bones of the small-sized species, respectively. A very advanced *Ursus deningeri* (transitional to *U. spelaeus*; Auguste, 1992; García et al., 1997; Pacher and Stuart, 2008) is attested to by a right upper canine and a left m2. The mammal remains were accompanied by some scanty remains of the European pond turtle (*Emys orbicularis*), together with a vertebra of the European whip snake (*Hierophis viridiflavus*), and two fragmental bones of birds.

Only three specimens, in this case the lateral portion of diaphysis of a left humerus of *Bos primigenius* and the basal portion of a shed right antler and a fragmental diaphysis of a

Table 4. Vertebrate taxa from Poggetti Vecchi, with relative frequencies expressed in Number of Identified Specimens (NISP) counts.

Taxa	NISP	NISP %
<i>Palaeoloxodon antiquus</i>	283	39.70
<i>Bos primigenius</i>	138	19.35
<i>Capreolus capreolus</i>	12	1.70
<i>Dama dama</i>	1	0.14
<i>Cervus elaphus</i>	38	5.80
<i>Ursus deningeri-spelaeus</i>	2	0.28
<i>Arvicola terrestris</i>	62	8.70
<i>Terricola sp.</i>	2	0.28
<i>Microtus cf. arvalis</i>	1	0.14
Aves	2	0.28
<i>Emys orbicularis</i>	4	0.56
<i>Hierophis viridiflavus</i>	1	0.14
Doubtful attribution	74	10.37
Undetermined	93	13.04
Total	713	

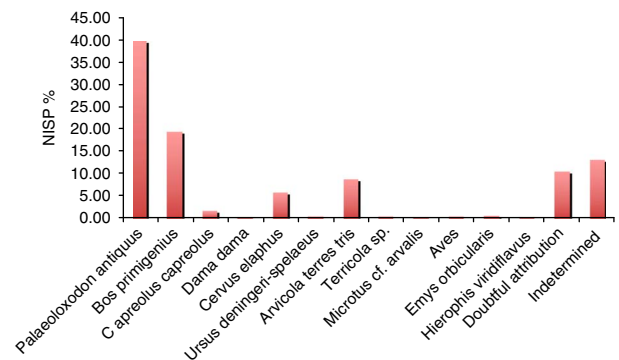


Figure 9. (color online) Relative frequencies of the vertebrate taxa of Poggetti Vecchi, expressed in Number of Identified Specimens (NISP) counts (data reported in Table 4).

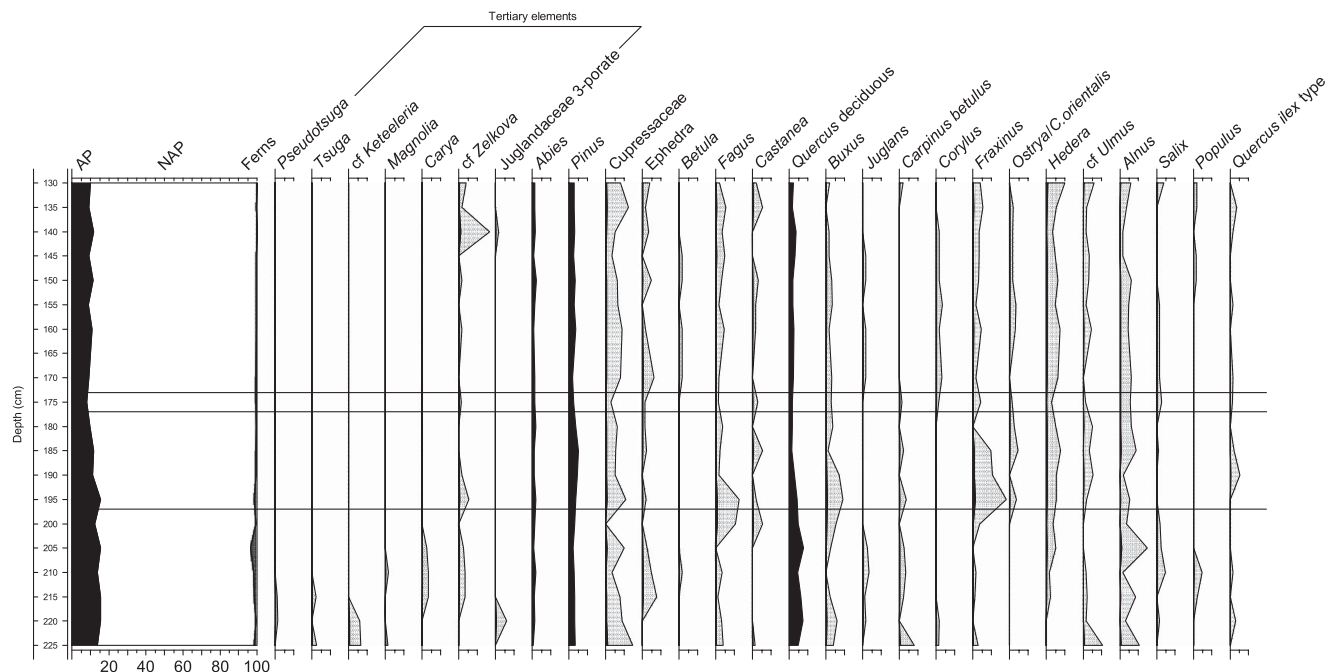


Figure 10. Pollen diagram of samples collected on the wall excavation of log A: selected taxa. Exaggeration 15×.

tibia of *Cervus elaphus*, show evidence of human modification. No such evidence has been observed on the elephant remains.

The terms of micromammals in Unit 2 (Table 4), these are dominated in NISP counts by the water vole *Arvicola amphibius*. This species, which is characterized by individuals with undifferentiated dental enamel (sensu Heinrich, 1978), is typical of waterside habitats. This water vole totals approximately 95% of the small mammal counts. The genus *Microtus*, on the other hand, is represented in Unit 2 by only three specimens: a fragmental left m1, attributed to *Microtus* cf. *arvalis*, a left m1 of *Microtus* (*Terricola*) ex gr. *savii*, and a right M1 ascribed to *Microtus* sp. The first lower molars found show a relatively short and wide anteroconid as well as a wide anterior cap, which are features suggesting a *Microtus* (*Terricola*) species of the *savii* group.

A cross examination of Units 4 and Unit 6 shows that they yielded fossil assemblages very similar to that found in Unit 2. Indeed, the relative frequencies in Unit 4 are virtually the same as those observed in Unit 2. In Unit 6, however, the frequency of *Arvicola amphibius* drops to 88%. *Microtus* spp. also grow progressively less abundant from Unit 6 to Unit 2. Although the cheek teeth (M3 and m1) diagnostic of *Microtus* cf. *arvalis* are missing in the arvicolid assemblages from Units 6 and 4, we cannot exclude its undetected presence in either unit. Worth noting is the occurrence of a fragmental mandible of *Crocidura* cf. *suaveolens* and a fragmental maxillary bone of *Oryctolagus* sp. in Unit 6.

In terms of large mammals, based on the evidence of the skull, mandible, molar, and tusk remains from Unit 2, *Palaeoloxodon antiquus* is represented by four juveniles in the range of 1–8 years of age, together with a 14–15 year-old subadult, and two 25–30 year-old adults. *Cervus elaphus* is also represented by at least four individuals, ranging from 3 to 12/13 years of age.

Particularly striking is the presence of at least nine left and three right shed antlers of this species. Also, remains of a single adult individual of *Capreolus capreolus* were found, alongside those of a fetus, a juvenile, and an adult of *Bos primigenius*. All the other taxa include one individual each.

Pollen

All the samples contained a fairly rich amount of well-preserved pollen grains, yielding a total of more than 100 taxa (Fig. 10). In all of the samples, herbaceous plants (NAP) dominate, whereas arboreal, shrubby and climbing plants (AP) never exceed 22%, indicating the persistence of an open environment throughout the whole time period under examination.

Noteworthy, among the arboreal taxa is the presence of Tertiary elements in the lowermost samples of Unit 1, such as *Tsuga*, cf. *Keteleeria*, and *Carya*. Two different morphotypes (i.e., with different exine thickness) of Ulmaceae suggest the possible presence of *Zelkova* in addition to *Ulmus*. These morphotypes occur throughout the sequence but always in low amounts. *Buxus* is always present in low concentrations throughout the succession. Its presence is unusual because *Buxus* grains are easily degraded.

Poaceae, on the other hand, are dominant and represented by different morphotypes, and this indicates the presence of extensive grasslands on the plain. The most frequent morphotype (A) is quite small, ranging from 22 to 28 µm, with a thick annulus measuring about 5 µm in diameter.

A noteworthy variety of pollen grains of hygrophytes and hydrophytes were recorded, indicating habitats with high biodiversity. They include *Poaceae* t. *Glyceria* type, Cyperaceae, Juncaceae, Alismataceae, *Lythrum*, cf. *Butomus*,

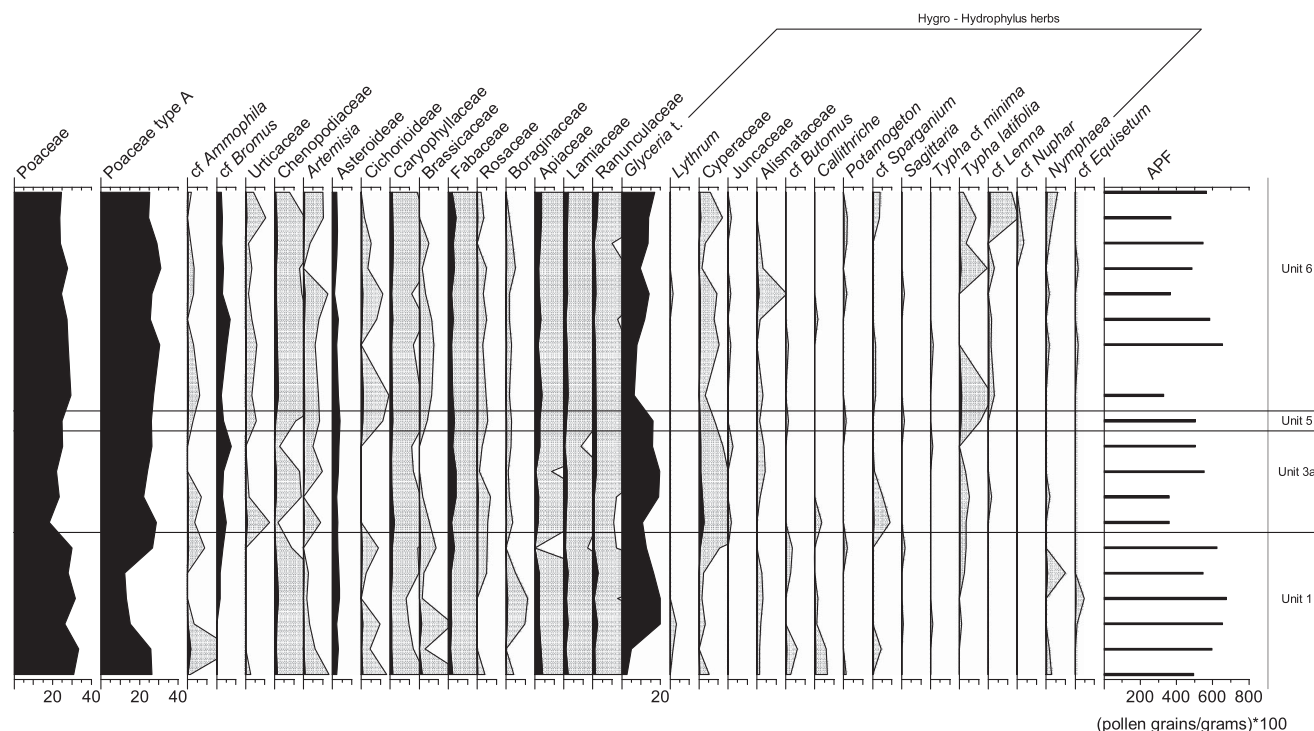


Figure 10. Continued.

Callitriche, *Potamogeton*, cf. *Sparganium t.*, *Sagittaria*, *Typha* spp., cf. *Lemna*, *Nymphaea*, and *Nuphar*. Their amounts change throughout the stratigraphic sequence.

Wood remains

An isolated fragment of *Ulmus* sp. (elm) was recovered from Unit 1, at the base of the stratigraphic succession. Unit 2 contained several horizontally oriented wood fragments interspersed with the elephant remains. Most of the wood items were concentrated in a relatively small area of the excavation. A few wood fragments were also found at the base of Unit 6.

Buxus sempervirens L. (boxwood) is dominant throughout the succession, whereas deciduous *Quercus* sp. (deciduous oak), *Fraxinus* sp. (ash), *Juniperus* sp. (juniper), and *Populus/Salix* (poplar/willow) are barely represented. The relative number of fragments for each of these trees is summarized in Table 5.

Table 5. Taxa identification of the wood fragments found in the succession of Poggetti Vecchi.

Lithological Unit	Taxa	No. of fragments
6	<i>Buxus sempervirens</i>	9
	Deciduous <i>Quercus</i>	1
	<i>Populus/Salix</i>	2
2-3	<i>Buxus sempervirens</i>	36
	Deciduous <i>Quercus</i>	2
	<i>Fraxinus</i> sp.	2
	<i>Juniperus</i> sp.	1
1	<i>Ulmus</i> sp.	1

The Boxwood remains above all consist of straight branches, most of whose surfaces of most of these branches are partially or entirely blackened. *Buxus* is a small, slow-growing evergreen tree or shrub. It usually lives in forests of larger trees, associated with *Juniperus*. It can also be found next to xero-thermophilus taxa, such as *Quercus*, in shrubs or thickets on well-drained calcareous substrates on plains to lower slopes. The high concentration of straight boxwood branches found in the Units 2 and 6 may indicate that they were intentionally selected by humans to make wooden implements. The study of these purported wooden tools is presently under way.

DISCUSSION

Paleoenvironmental reconstruction at the archeological site of Poggetti Vecchi

The integration of the multiproxy paleobiological data with the stratigraphy at the site has allowed for a detailed reconstruction of the landscape and an understanding of its evolution during the deposition of Units 1–6. The stratigraphic data together with the information provided by the fossil mollusk and ostracod assemblages indicate four different flooding events separated by regressions. During the flooding episodes, organic muds were deposited in a protected embayment of a shallow lake with rather homogeneous physicochemical characteristics. In contrast, concentrations of vertebrate remains and human artifacts accumulated on the erosive surfaces that formed during the regressions. The succession of the events is as follows.

A narrow valley was carved in the oldest deposits found in cores S1–S2, along the edge of a lake. A very shallow

bay formed in this valley during the first episode of lake-level rise, and subsequently lacustrine sediments started to accumulate. The deposits of Unit 1 record the infrequent sedimentation of lacustrine mud on a poorly oxygenated bottom that favored the preservation of organic matter. Abundant and diversified mollusk and ostracod assemblages, dominated by *P. moussonii* and *H. salina*, respectively, inhabited the bottom and this indicates fresh or slightly saline waters (<4 psu). When the bay dried up an erosive surface formed, separating Unit 1 from Unit 2. As the lake receded, elephant carcasses and various human artifacts accumulated on its now-exposed shores.

Unit 3 records a second lacustrine phase. A new rise in the water table initially created a shallow, mud-dominated pool in the small embayment (Unit 3a); the predominance of the ostracod *C. (C.) improvisa* in this particular horizon may reflect seasonal fluctuations of the water level. This event was then followed by the deposition of carbonate mud (3b), which is the first significant evidence of thermal activity at the site. The pisoliths of Unit 4 document the formation, during the late middle Pleistocene (MIS 6), of a thermal pool similar to the man-made ones that were built in modern times. This MIS 6 thermal pool was visited by both humans and large mammals, which included *Palaeoloxodon*. Although the invertebrate assemblages were still dominated by *P. moussonii* and *H. salina* at this point, *B. thermalis* and *M. etrusca* reach their highest frequency in Unit 3, confirming the thermal influence on the waterbody.

The second lacustrine phase ended with a new lake-level fall, and the older deposits were dissected by fluvial downcutting (Unit 5). In fact, a short creek flowing down from the Poggetti Vecchi hill drained the valley. In this stage, runoff flow over the valley floor was of sufficient energy to transport the calcareous pebbles that formed the channel lag of Unit 5.

A new flooding (third phase) once again restored the lake embayment, as attested to by the deposits of Unit 6. In this case, the depositional conditions were virtually identical to those when Unit 1 was formed.

Yet another drop in lake-level fall led to a new, deep incision of the valley floor. The erosive surface separating Unit 7 from older units remained exposed for a while, as indicated by the occurrence of the isolated skull of *Palaeoloxodon*, as well as the abundant presence of terrestrial gastropods.

Finally in the fourth phase, the valley floor was once again carved and infilled with calcareous mud (Subunit 7a). This recreated the lake bay, but this time most likely under thermal influence. The valley was infilled with calcareous sand and subordinate mud (Subunit 7b), these last reworked from thermal carbonates by the water flowing toward the lake. The carbonate composition of Unit 7 indirectly indicates that the thermal activity had finally stabilized.

Pollen, terrestrial mollusks, and vertebrate remains provide further information about the overall environmental conditions surrounding of the site. At the time when the fossiliferous site was formed, the Poggetti Vecchi area was dominated by extensive open grassland; *Palaeoloxodon antiquus* and *Bos primigenius* grazed the prairie, while the

red deer (*Cervus elaphus*) and the roe deer (*Capreolus capreolus*) browsed in sparse groves. The abundant frequency of freshwater fens, together with a high variety of wetland plants, denotes the presence of seeps and water bodies. Given the flux of wetland vegetation throughout the sedimentary succession, the bodies of water must have repeatedly expanded and contracted. Trees likely grew on the hills but also in well-drained areas of the plain; the predominance of *Buxus*, in particular, indicates well-drained, calcareous soils. It is often associated with travertines.

Chronological and paleoclimatic implications

The paleontological information reported above, but also the radiometric dating, indicates that the Poggetti Vecchi site developed during the late Quaternary, a period characterized by frequent climate fluctuations. Although infrequent, the presence of Tertiary pollen grains in the lowermost samples of Unit 1 is striking because these plants were thought to have disappeared from central Italy during the early-middle Pleistocene. Specifically, *Tsuga* and *Carya* had a marked decline in northern and Central Italy during the early middle Pleistocene, disappearing between 0.75 and 0.45 Ma, although they may have survived longer in Southern Italy (Corrado and Magri, 2011; Orain et al., 2013). *Zelkova* rapidly reduced in cold-arid periods and expanded again in warm-moist periods and finally became extinct in peninsular Italy before the latest glacial maximum (Follieri et al., 1986). Based on these data, the lower part of Unit 1 could not be younger than 0.4 Ma. We cannot exclude the possibility that the Tertiary pollen grains are actually allochthonous elements that have been reworked from older stratigraphic levels and that they may have migrated into higher beds via the capillary rise of mud.

The numerical ages of 171 ± 3 ka and 170 ± 13 ka obtained, respectively, from the pisoliths and Auroch's tooth found in Unit 4 locate the studied succession within an interval bracketing the transition between the latest MIS 7 and the whole of MIS 6. The physical stratigraphy of the transgressive and regressive deposits that formed during the time interval indicated by the age determination of Unit 4 suggests the following tentative calibration (Fig. 11).

Unit 1 transgression: lake highstand during the warm substage MIS 7a or during the following interstadial at the transition to MIS 6 (between 200–191 ka). Under either of these hypotheses, the Tertiary flora recorded in the lower part of Unit 1 would have survived in this area more than 0.4 Ma.

Unit 2 regression: lake lowstand and subaerial erosion at the onset of MIS 6.

Units 3 and 4: lake transgression and activation of the thermal system in the first interstadial of MIS 6 (around 170 ka).

Unit 5 regression: lake lowstand at the successive stadial.

Unit 6 transgression: lake highstand during the second interstadial.

Unit 7 regression: lake lowstand at the acme of MIS6 (around 130 ka). Deposition of Unit 7 may have occurred during the climatic rise in temperatures culminating with the peak interglacial interval MIS5e.

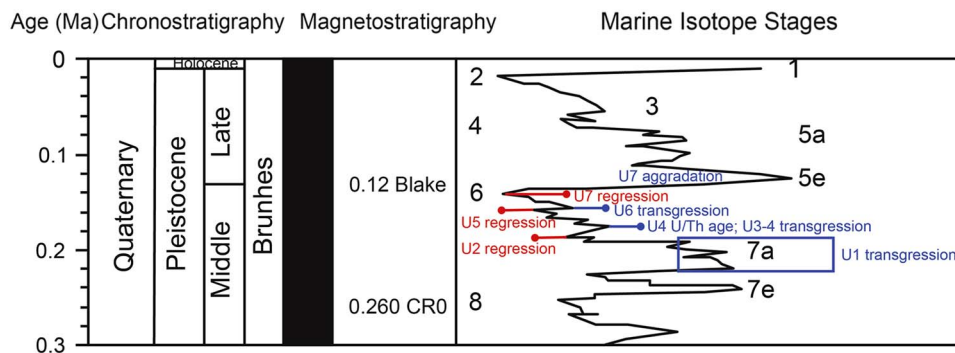


Figure 11. (color online) Tentative correlation of the Poggetti Vecchi Stratigraphy, calibrated for Unit 4 with radiometric datings to the Late Quaternary Marine Isotope Stages.

The paleobiological inferences based upon the Poggetti Vecchi small mammal remains provide further information supporting the tentative synchronization of the succession with the main climatic events of the associated time period. The dominant *Arvicola amphibius* is a typical inhabitant of moist environments. The presence of *Microtus cf. arvalis* in Unit 2, the decreasing abundances of *M. (Terricola) ex gr. savii* and the absence of *Crocidura* and *Oryctolagus* in the following units, might indicate cooler conditions moving upwards in the succession. Modern Italian populations of *Microtus cf. arvalis* are confined to the northern regions of the peninsula and are absent from the central Apennine further south. Therefore, its presence in southern Tuscany at very low altitudes is indicative of colder conditions at the time of Unit 2 than those existing today. In contrast the occurrence of *Crocidura cf. suaveolens*, *Oryctolagus sp.*, and *Microtus (Terricola) savii* in Unit 6 is indicative of warmer habitats.

The large mammal assemblage and the herpetofauna from Unit 2 including thermophilic taxa, such as the roe deer *Capreolus capreolus*, the European pond turtle *Emys orbicularis*, and the European whip snake *Hierophis viridiflavus*, show a wide distribution ranging from the warm peri-Mediterranean area, all the way into the much cooler northern European contexts (Lelièvre et al., 2010a, 2010b). The European pond turtles are usually only active above 5°C and so are another indicator of temperatures across the region (Novotný et al., 2004). *Palaeoloxodon antiquus* is typical of temperate contexts but also occurred in cooler conditions (Mazza et al., 2006).

On the whole, the fauna of Unit 2 comprises of species with varied climatic distributions that seem to be well-tuned with the fluctuations that occurred within the relatively short period between the onset of MIS 6 (lake regression and erosion at the top of Unit 1), and the next interstadial (lake transgression and deposition of Units 3 and 4). Intense seasonal oscillations can reasonably be expected to have occurred during the time span recorded by the Poggetti Vecchi succession. The occurrence of *Microtus cf. arvalis* is not at odds with the hypothesis that perhaps a cold snap occurred during the time of the deposition of Unit 2, which might have caused the sudden death of the elephant clan.

The molluscan fauna discloses relevant information that may assist in defining the climate regime during the deposition. The recorded presence of open-landscape species, such

as *P. muscorum* and *V. pulchella* from Unit 6, indicates that this Unit formed under cool climatic conditions (Rousseau, 1989; D’Amico et al., 2014). These conditions are compatible with the global cooling trend that culminated in the glacial maximum of MIS 6.

The ostracod fauna that was collected from Units 1–6 and analyzed with the MOTR method suggest there were mean annual temperatures about 6°C lower than today, which is in line with the temperatures at the onset of MIS 6 based on estimates from the Vostok Ice core in Antarctica, which indicates 7.5°C lower than today (Petit et al., 1999). In light of Ayalon et al.’s (2002) study, the humid period dated at 171 ka, which is also the calculated age of Unit 4, was likely the first interstadial of the glacial interval MIS 6.

CONCLUSIONS

The radiometric dating of about 171 ka obtained from the pisoliths and third lower molar of *Bos primigenius* of Unit 4 places the Poggetti Vecchi archaeo-paleontological site in a very crucial time span. This time period tells us that early Neanderthal populations produced the implements. Archaeo-paleontological sites attesting to the middle to late Pleistocene transition are scarcely documented in Europe. Poggetti Vecchi therefore offers the chance of obtaining an unprecedented amount of information on the behavior of early Neanderthals under the circumstances that have been documented through from this study.

Our analysis shows that at the time when the bone accumulation was formed the area consisted of widespread, open, wet grassland, scattered with water bodies, woods, and, perhaps, riverine belts of trees. The hot thermal springs in one of these water bodies located in a small embayment, probably created an attractive recess for the resident fauna, especially in a time period when the climate was globally deteriorating. It would appear from the artifacts found that the area could have been routinely patrolled by early Neanderthal hunter-gatherers who were monitoring the movements of the fauna that tended habitually to congregate in the warmer valley of Poggetti Vecchi. We can speculate that during a cold snap, large amounts of game animals would gather in the recess. Many of them were possibly debilitated by the harsh, inhospitable circumstances, or most

probably already lay dead, as perhaps happened in the case of the elephants. Their concentrated presence represented a valuable resource that could have attracted the local human pursuers. If this reconstruction is correct, the collected evidence indicates that these early Neanderthals were particularly skilled at modifying their survival strategies to take advantage of the particular environmental circumstances and opportunities presented to them in a changing environment.

ACKNOWLEDGMENTS

We are particularly indebted to the owner of the site A. Ceccarelli, who funded the excavation. We wish to thank A. Pessina and G. Poggesi for their support during the completion of this study, S. Pozzi, S. Caloni and S. Caramiello for the restoration of the fossil bones. We are very grateful to M.-H. Moncel, D. Bridgland, and C. Marean for significantly improving the manuscript. We thank K. Eadie and J. A. Thonn for the language editing. This study was financially supported by the Italian Ministry of Cultural Heritage, the “Fondazione Banca Federico del Vecchio” and the “Ente Cassa di Risparmio di Firenze”. Additional funding for the research was provided by Italian MIUR (the Italian Ministry of Education, University and Research) ex60% grants to the Department of Earth Sciences and to the Department of Biology, both of the University of Florence, and by Italian Mibact (Ministry of Cultural Heritage and Activities and Tourism).

SUPPLEMENTARY MATERIAL

To view supplementary material for this article, please visit <https://doi.org/10.1017/qua.2017.51>

REFERENCES

- Abruzzese, C., Aureli, D., Rocca, R., 2015. Assessment of the Acheulean in Southern Italy: New study on the Atella site (Basilicata, Italy). *Quaternary International* 393, 158–168.
- Auguste, P., 1992. Etude Archeozoologique des grands mammifères du site Pleistocène Moyen de Biache-Saint-Vaast (Pas-de-Calais, France): apports Biostratigraphiques et Paléthrographiques. *L'Anthropologie* 96, 49–70.
- Aureli, D., Contardi, A., Giaccio, B., Jich, B., Lemorini, C., Madonna, S., Magri, D., et al. 2015. *Palaeoloxodon* and human interaction: depositional setting, chronology and archaeology at the Middle Pleistocene Ficoncella Site (Tarquinia, Italy). *PLOS ONE* 10: e0124498. <http://dx.doi.org/10.1371/journal.pone.0124498>.
- Ayalon, A., Bar-Matthews, M., Kaufman, A., 2002. Climatic conditions during marine oxygen isotope stage 6 in the eastern Mediterranean region from the isotopic composition of speleothems of Soreq Cave, Israel. *Geology* 30, 303–306.
- Baldi, P., Bellani, S., Ceccarelli, A., Fiordelisi, A., Squarci, P., Taffi, L., 1995. Geothermal anomalies and structural features of southern Tuscany. *World Geothermal Congress Proceedings, Florence*, 1287–1291.
- Bartolini, F., Aquiloni, L., Lori, E., Cianfanelli, S., 2010. Countdown 2010, azioni concrete per ridurre la perdita di biodiversità: il caso del gasteropode endemico della Toscana meridionale *Melanopsis etrusca* Brot, 1862 (Gastropoda, Prosobranchia). In: Lenzi, A., Leoni, L., Baldacci, C., Brizzi, B., De Santi, C., Domenici, V., Feri, E., Lenzi, P., Montesarchio, E., Piombanti, P.P., Santinelli, M. (Eds.), *Codice Armonico, Terzo Congresso di Scienze Naturali, Ambiente toscano, Castiglioncello (LI), sezione Scientifica*. Edizioni ETS, Pisa, Italy, pp. 63–70.
- Bencini, A., Duchi, V., Martini, M., 1977. Geochemistry of thermal springs of Tuscany (Italy). *Chemical Geology* 19, 229–252.
- Binford, L.R., 1987. Data, relativism and archaeological science. *Man* 22, 391–404.
- Bischoff, J., Rosenbauer, R., Tavoso, A., de Lumley, H., 1988. A test of uranium-series dating of fossil tooth enamel: results from Tournal Cave, France. *Applied Geochemistry* 3, 145–151.
- Blanchette, R.A., 2003. Deterioration in Historic and Archaeological Woods from Terrestrial Sites. In: Koestler, R.J., Koestler, V.R., Charola, A.E., Nieto-Fernandez, F.E. (Eds.), *Art, Biology and Conservation: Biodeterioration of Works of Art*. The Metropolitan Museum of Art, New York, pp. 328–347.
- Boomer, I., Horne, D.J., Slipper, I.J., 2003. The use of ostracods in palaeoenvironmental studies, or what can you do with an ostracod shell? In: Park, L.E., Smith, A.J. (Eds.), *Bridging the Gap: Trends in the Ostracode Biological and Geological sciences*. The Paleontological Society Papers 9, Boulder, pp. 153–180.
- Boschian, G., Sacca, D., 2014. In the elephant, everything is good: carcass use and reuse at Castel di Guido (Italy). *Quaternary International* 361, 288–296.
- Bravetti, L., Pranzini, G., 1987. L'evoluzione quaternaria della pianura di Grosseto (Toscana): prima interpretazione dei dati del sottosuolo. *Geografia Fisica e Dinamica Quaternaria* 10, 85–92.
- Censini, G., Costantini, A., 2002. Il sottosuolo della pianura tra Grosseto e Ribolla: ipotesi sul suo assetto strutturale. Le voragini catastrofiche: un nuovo problema per la Toscana. Atti del Convegno di Grosseto del 31 Marzo 2000, Edizioni Regione Toscana, Firenze.
- Cianfanelli, S., 2009. I Molluschi della Provincia di Pistoia: le specie da tutelare e quelle da combattere. *Quaderni del Padule di Fucecchio* 6, 1–112.
- Cianfanelli, S., 2010. *Melanopsis etrusca*. The IUCN Red List of Threatened Species. Version 2014.3 (accessed May 18, 2015). <http://www.iucnredlist.org>.
- Cianfanelli, S., Bodon, M., Giusti, F., Manganelli, G., 2010. *Belgrandia thermalis*. The IUCN Red List of Threatened Species. Version 2014.3 (accessed May 18, 2015). <http://www.iucnredlist.org>.
- Cianfanelli, S., Talenti, E., Calcagno, M., 1991. Le stazioni di *Melanopsis dufouri* Ferrussac 1823 (Gastropoda, Prosobranchia) in Italia. *Quaderni del Museo di Storia Naturale di Livorno* 10, 59–76.
- Corrado, P., Magri, D., 2011. A late Early Pleistocene pollen record from Fontana Ranuccio (central Italy). *Journal of Quaternary Science* 26, 335–344.
- D'Amico, C., Esu, D., Magnatti, M., 2014. Land mollusc palaeocommunity dynamics related to palaeoclimatic changes in the Upper Pleistocene alluvial deposits of Marche Apennines (central Italy). *Italian Journal of Geoscience* 133, 235–248.
- Follieri, M., Magri, D., Sadori, L., 1986. Late Pleistocene *Zelkova* extinction in Central Italy. *New Phytologist* 103, 269–273.
- Frenzel, P., Schulze, I., Pint, A., 2012. Noding of *Cyprideis torosa* valves (Ostracoda) – a proxy for salinity? New data from field observations and a long-term microcosm experiment. *International Review of Hydrobiology* 97, 314–329.
- García, N., Arsuaga, J.L., Torres, T., 1997. The carnivore remains from the Sima de los Huesos Middle Pleistocene site (Sierra de Atapuerca, Spain). *Journal of Human Evolution* 33, 155–174.
- Gaudzinski, S., 1996. Karlich-Seeufer: Untersuchungen zu einer Altpaläolithischen Fundstelle in neuwieder Becken (Rheinland-Platz). *Jahrbuch des Römisch-Deutschen Zentralmuseums Mainz* 43, 1–242.

- Ghilardi, M., Desruelles, S., 2009. Geoarchaeology: where human, social and earth sciences meet with technology. *Surveys and Perspectives Integrating Environment and Society (S.A.P.I.E.N.S.)* 2.2., 1–9.
- Girod, A., Bianchi, I., Mariani, M., 1980. Gasteropodi, 1. Guide per il riconoscimento delle specie animali delle acque interne italiane, AQ/1/44, Vol. 7. Consiglio Nazionale delle Ricerche, Verona.
- Giusti, F., Pezzoli, E., 1980. Gasteropodi, 2. Guide per il riconoscimento delle specie animali delle acque interne italiane AQ/1/47, Vol. 8. Consiglio Nazionale delle Ricerche, Verona.
- Giusti, F., Manganelli, G., Schembri, P.J., 1995. The non-marine molluscs of the Maltese Islands. *Monografie Museo Regionale di Scienze Naturali di Torino* 15, 1–608.
- Griffiths, H.I., Holmes, J.A., 2000. Non-marine ostracods and Quaternary palaeoenvironments. *Quaternary Research Association Technical Guide* 8, 1–179.
- Grimm, E.C., 1994. Tilia and tiliagraph Pollen Diagramming Program. Illinois State Museum, Springfield, Illinois.
- Grimm, E.C., 2004. Tilia and TG View Version 2.0.2. Illinois State Museum, Research and Collector Center, Springfield, Illinois.
- Grün, R., Katzenberger-Apel, O., 1994. An alpha irradiator for ESR dating. *Ancient TL* 12, 35–38.
- Grün, R., Schwarcz, H., Chadam, J., 1988. ESR dating of tooth enamel: Coupled correction for U-uptake and U-series disequilibrium. *Nuclear Tracks and Radiation Measurements* 14, 237–241.
- Heinrich, W.-D., 1978. Zur biometrischen Erfassung eines Evolutionstrends bei *Arvicola* (Rodentia, Mammalia) aus dem Pleistozän Thüringens. *Säugetierkundliche Informationen* 2, 3–21.
- Hijmans, R.J., Cameron, S.E., Parra, J.L., Jones, P.G., Jarvis, A., 2005. Very high resolution interpolated climate surfaces for global land areas. *International Journal of Climatology* 25, 1965–1978.
- Horne, D.J., 2007. A Mutual Temperature Range method for Quaternary palaeoclimatic analysis using European nonmarine Ostracoda. *Quaternary Science Reviews* 26, 1398–1415.
- Horne, D.J., Baltanas, A., Paris, G., 1998. Geographical distribution of reproductive modes in living non-marine ostracods. In: Martens, K. (Ed.), *Sex and Parthenogenesis: Evolutionary Ecology of Reproductive Modes in Non-marine Ostracods*. Backhuys, Leiden, pp. 77–99.
- Horne, D.J., Curry, B.B., Mesquita-Joanes, F., 2012. Mutual climatic range methods for Quaternary ostracods. *Developments in Quaternary Science* 17, 65–84.
- Kerney, M.P., 1999. *Atlas of the land and freshwater molluscs of Britain and Ireland*. Harley Books, Cambridge, UK.
- Keyser, D., 2005. Histological peculiarities of the nodin process in *Cyprideis torosa* (Jones) (Crustacea, Ostracoda). *Hydrobiologia* 538, 95–106.
- Lari, M., Di Vincenzo, F., Borsato, A., Ghirotto, S., Micheli, M., Balsamo, C., Collina, C., et al. 2015. The Neanderthal in the karst: first dating, morphometric, and paleogenetic data on the fossil skeleton from Altamura (Italy). *Journal of Human Evolution* 82, 88–94.
- Lelièvre, H., Blouin-Demers, G., Bonnet, X., Lourdaï, O., 2010a. Thermal benefits of artificial shelters in snakes: A radiotelemetric study of two sympatric colubrids. *Journal of Thermal Biology* 35, 324–331.
- Lelièvre, H., Le Hénanff, M., Blouin-Demers, G., Naulleau, G., Lourdaï, O., 2010b. Thermal strategies and energetics in two sympatric colubrid snakes with contrasted exposure. *Journal of Comparative Physiology B* 180, 415–425.
- Ložek, V., 1964. Quartärmollusken der Tschechoslowakei. Rozpravi Ústředního Ústavu. *Geologického* 31, 1–374.
- Ludwig, K.R., 2003. Users Manual for Isoplot/Ex Version 3.0: a Geochronological Toolkit for Microsoft Excel. Special Publication 3. Berkeley Geochronology Centre, Berkeley.
- Manganelli, G., Bodon, M., Cianfanelli, S., Favilli, L., Giusti, F., 2000. Conoscenza e conservazione dei molluschi non marini italiani: lo stato delle ricerche. *Bollettino Malacologico* 36, 5–42.
- Marra, F., Ceruleo, P., Jicha, B., Salari, L., 2015. A new age within MIS 7 for the Homo neanderthalensis of Saccopastore in the glacio-eustatically forced sedimentary successions of the Aniene River Valley, Rome. *Quaternary Science Reviews* 129, 260–274.
- Mazza, P.P.A., Martini, F., Sala, B., Magi, M., Colombini, M.P., Giachi, G., Landucci, F., Lemorini, C., Modugno, F., Ribechini, E., 2006. A new Palaeolithic discovery: tar-hafted stone tools in a European mid-Pleistocene bone-bearing bed. *Journal of Archaeological Science* 33, 1310–1318.
- Meisch, C.K., 2000. *Freshwater ostracoda of western and central Europe*. Spektrum Akademischer Verlag, Heidelberg.
- Novotný, M., Danko, S., Havaš, P., 2004. Activity cycle and reproductive characteristics of the European pond turtle (*Emys orbicularis*) in the Tajba National Nature Reserve, Slovakia. In: Fritz, U., Havaš, P. (Eds.), Proceedings of the 3rd International Symposium on *Emys orbicularis*, Košice 2002. *Biologia* 59 (Suppl. 14). Slovak Academic Press, Bratislava, pp. 113–121.
- Orain, R., Lebreton, V., Ermolli, E.R., Combourieu-Nebout, N., Sémah, A.M., 2013. *Carya* as marker for tree refuges in southern Italy (Boiano basin) at the Middle Pleistocene. *Palaeogeography, Palaeoclimatology, Palaeoecology* 369, 295–302.
- Pacher, M., Stuart, A.J., 2008. Extinction chronology and palaeobiology of the cave bear (*Ursus spelaeus*). *Boreas* 38, 189–206.
- Petit, J.R., Jouzel, J., Raynaud, D., Barkov, N.I., Barnola, J.M., Basile, I., Bender, M., et al. 1999. Climate and atmospheric history of the past 420,000 years from the Vostok ice core, Antarctica. *Nature* 399, 429–436.
- Piperno, M., Tagliacozzo, A., 2001. The elephant butchery area at the middle Pleistocene site of Notarchirico (Venosa, Basilicata, Italy). In: Cavarretta, G., Gioia, P., Mussi, M., Palombo, M.R. (Eds.), *The World of Elephants*. Consiglio Nazionale delle Ricerche, Rome, pp. 230–236.
- Prescott, J., Hutton, J., 1994. Cosmic ray contributions to dose rates for luminescence and ESR dating: Large depths and long-term time variations. *Radiation Measurements* 23, 497–500.
- Rabinovich, R., Ackermann, O., Aladjem, E., Barkai, R., Biton, R., Milevski, I., Solodenko, N., Marder, O., 2012. Elephants at the Middle Pleistocene Acheulian open-air site of Revadim Quarry, Israel. *Quaternary International* 276–277, 183–197.
- Rapp, Jr. G.R., Hill, C.L., 1998. *Geoarchaeology: the Earth-science approach to archaeological interpretation*. Yale University Press, New Haven.
- Rousseau, D.-D., 1989. Réponses des malacofaunes terrestres quaternaires aux contraintes climatiques en Europe septentrionale. *Palaeogeography, Palaeoclimatology, Palaeoecology* 69, 113–124.
- Sanchez Yustos, P., Diez Martin, F., 2015. Dancing to the rhythms of the Pleistocene? Early Middle Paleolithic population dynamics in NW Iberia (Duero Basin and Cantabrian Region). *Quaternary Science Reviews* 121, 75–88.
- Santucci, E., Marano, F., Cerilli, E., Fiore, I., Lemorini, C., Palombo, M.R., Anzidei, A.P., Bulgarelli, G.M., 2015. *Palaeoloxodon* exploitation at the middle Pleistocene site of La Polledrara di Cecanibbio (Rome, Italy). *Quaternary International* 406, 169–182.

- Schniewind, A.P., 1990. Physical and mechanical properties of archaeological wood. In: Rowell, R.M., Barbour, R.J. (Eds.), *Archaeological wood: properties, chemistry, and preservation*. Advances in Chemistry Series 225, American Chemical Society, Washington, DC. pp. 87–109.
- Schoch, W.H., Bigga, G., Böhner, U., Richter, P., Terberger, T., 2015. New insights on the wooden weapons from the Paololithic site of Schöningen. *Journal of Human Evolution* 89, 214–225.
- Scott, B., Bates, M., Bates, R., Conneller, C.H., Pope, M., Shaw, A., Smith, G., 2014. A new view from La Cotte de St. Brelade, Jersey. *Antiquity* 88, 13–29.
- Shao, Q., Bahain, J.-J., Dolo, J.-M., Falguères, C., 2014. Monte Carlo approach to calculate US-ESR ages and their uncertainties. *Quaternary Geochronology* 22, 99–106.
- Stea, B., Tenerini, I., 1996. L'ambiente naturale della pianura grossetana e la sua evoluzione dalla preistoria alla cartografia rinascimentale. In: Citter, C. (Ed.), *Grosseto, Roselle e il Prile*. Società Archeologica, Mantua, Italy, pp. 12–24.
- Surovell, T.A., Waguespack, N.M., 2008. How many elephant kills are 14? Clovis mammoth and mastodon kills in context. *Quaternary International* 191, 82–97.
- Villa, P., Soto, E., Santonja, M., Perez-Gonzalez, A., Mora, R., Parcerisas, J., Sesé, C., 2005. New data from Ambrona: closing the hunting versus scavenging debate. *Quaternary International* 126–128, 223–250.
- Wenban-Smith, F.F., Allen, P., Bates, M.R., Parfitt, S.A., Preece, R.C., Stewart, J.R., Turner, C., Whittaker, J.E., 2006. The Clactonian elephant butchery site at Southfleet Road, Ebbsfleet, UK. *Journal of Quaternary Science* 21, 471–483.
- Weber, T., 2000. The Eemian *Elephas antiquus* finds with artifacts from Lehringen and Grobern: are they really killing sites? *Anthropologie et Préhistoire* 111, 177–185.
- Yravedra, J., Domínguez-Rodrigo, M., Santonja, M., Pérez-González, A., Panera, J., Rubio-Jara, S., Baquedano, E., 2010. Cut marks on the Middle Pleistocene elephant carcass of Áridos 2 (Madrid, Spain). *Journal of Archaeological Science* 37, 2469–2476.
- Yravedra, J., Panera, J., Rubio-Jara, S., Manzano, I., Expósito, A., Pérez-González, A., Soto, E., López-Recio, M., 2014. Neanderthal and *Mammuthus* interactions at EDAR Culebro 1 (Madrid, Spain). *Journal of Archaeological Science* 42, 500–508.